Heat transfer to a resonant pulsating air stream in a pipe

Hirst, S. L.

HEAT TRANSFER TO A RESONANT PULSATING AIR STREAM IN A PIPE

by

S.L. HIRST B.Sc. (Dunelm)

Thesis submitted for the
degree of Doctor of Philosophy
in the University of Durham

Department of Engineering Science
The University
Durham

October 1974

Abstract

The effect on convective heat transfer of resonant, longitudinal oscillations superimposed on a turbulent mean flow in a pipe has been investigated relative to the equivalent steady flow.

Theoretically it is shown that the effect of acoustic streaming velocities is negligible for the range of pulsation parameters, but that the oscillating velocity can generate changes in the time-mean flow diffusivity - the change in mean diffusivity can only be predicted if quasi-steady pulsations are assumed. Heat transfer coefficients for the mean flow are evaluated from the Energy equation, for fully established conditions, assuming quasi-steady oscillations. It is proposed that a frequency factor can be derived to relate experimental heat transfer to the quasi-steady predictions, and that the factor would be a function of Strouhal number only.

Local heat transfer coefficients were measured for a constant heat flux supply to an oscillating air flow in a pipe. The pulsations were generated by a siren. It was shown that the centre-line velocity amplitudes could be predicted from inviscid flow theory using a mean velocity of sound. The range of the major parameters was:

Dimensionless pulsation velocity	$0.3 < B < 5$
Strouhal number	$0.5 < S < 10$
Reynolds number	$14,300 < \overline{Re_d} < 31,250$

For fully developed flow, the experimental results were related to the corresponding quasi-steady predictions by a function of Strouhal number. It was shown that the changes in heat transfer were due to changes in the mean diffusivity generated by the acoustic velocity.

For a defined range of pulsation parameters, it is possible to predict local heat transfer coefficients under fully established conditions for a pulsating flow from the empirical frequency correction factor applied to the theoretical quasi-steady predictions.

Acknowledgements

I would like to acknowledge the encouragement given by my supervisor, Dr. P.H. Clarke, throughout this project.

Thanks are due also to Mr. 'Sam' Beale for many long discussions.

I wish to thank the technical staff of the Department of Engineering Science, especially Mr. L. Fleet, Mr. A. Harker and Mr. W. Johnson, for their assistance with the experimental work.

I would like to thank Mrs. E.A. Wood for typing the thesis.

I am indebted to Shell International Petroleum Co. Ltd. for providing the financial support for the research.

Table of Contents

List of Figures

Nomenclature

Symbol		S.I. unit
a	Half channel width	m
b	$b = \frac{1}{2}\sqrt{(4\omega^2 - M^2)}$	1/s
B	Dimensionless pulsation velocity, $B = \hat{U}/\bar{U}_m$	1
B_A	Dimensionless pulsation velocity at V.A., $B_A = \hat{U}_A/\bar{U}_m$	1
$\bar{c}$	Velocity of sound	m/s
C_p	Specific heat at constant pressure	KJ/Kg°K
C_v	Specific heat at constant volume	KJ/Kg°K
d	Pipe diameter	m
d_J	Diameter of siren input jet	m
f	Frequency of acoustic oscillations	1/s
f_e	Eddy frequency of turbulence fluctuations	1/s
$f_{e_{AVE}}$	Eddy frequency at y = 0.05 R	1/s
F_c	$F_c = 1 - (R_A - R_{A_{HF}})/(R_{A_{QS}} - R_{A_{HF}})$	1
h	Heat transfer coefficient	KW/m²°K
$\bar{h}$	Time-independent heat transfer coefficient	KW/m²°K
I	Current to heating tape	Amperes
K	Thermal conductivity	KW/m°K
K_I	Thermal conductivity of pipe insulation	KW/m°K
ℓ	Prandtl Mixing Length	m
L	Test section length	m
L_A	Acoustic length	m
$L_{\frac{1}{4}}$	Quarter-wavelength	m

Symbol		S.I. unit
$\dot{m}$	Mass flowrate	Kg/s
$\overline{\dot{m}}$	Time-independent mass flowrate	Kg/s
$\dot{m}_s$	Mass flowrate supply to siren	Kg/s
M	Rate of change of velocity of sound for linear variation	1/s
M_A	Mach number, $M_A = U_m/\bar{c}$	1
$\overline{M}_A$	Time-independent Mach number, $\overline{M}_A = \overline{U}_m/\bar{c}$	1
n	Integer n = 1, 2, 3	1
N	Velocity of sound at x = 0	m/s
Nu_d	Nusselt number, $Nu_d = hd/K$	1
$\overline{Nu}_d$	Time-independent Nusselt number, $\overline{Nu}_d = \overline{h}d/K$	1
Nu_{de}	Nusselt number of equivalent steady flow	1
p	Pressure	N/m^2
$\bar{p}$	Time-independent pressure	N/m^2
p_1	Time-varying acoustic pressure	N/m^2
p'	$p' = p/\bar{\rho}\,\hat{U}_A^2$	1
$\bar{p}'$	$\bar{p}' = \bar{p}/\bar{\rho}\,\hat{U}_A^2$	1
p_1'	$p_1' = p_1/\bar{\rho}\,\hat{U}_A^2$	1
$\hat{P}$	Pressure amplitude	N/m^2
$\hat{P}_A$	Pressure amplitude at V.N.	N/m^2
$\hat{P}_N$	Pressure amplitude at V.A.	N/m^2
PO	Pressure amplitude at x = 0	N/m^2
P_r	Prandtl number, $Pr = \mu\, Cp/K$	1
$\dot{q}_V$	Energy input per second per unit area	KW/m^2
$\dot{q}_{V_m}$	Energy input per second per unit mass	KW/Kg
$\dot{q}_{V_E}$	Energy output per second of heating tape per unit area	KW/m^2

Symbol		S.I. Unit
$\dot{q}_L$	Energy loss through pipe insulation per second per unit area	KW/m^2
$\dot{Q}_E$	Energy output per second of heating tape	KW
$\dot{Q}_{\delta x}$	Energy input per second over length δx	KW
r	Co-ordinate direction	m
r_1	Inner radius of pipe insulation	m
r_2	Outer radius of pipe insulation	m
R	Pipe radius	m
R_A	Improvement ratio, $R_A = \overline{W}/W_e$	1
$R_{A_{QS}}$	Improvement ratio for quasi-steady oscillations, $R_{A_{QS}} = \overline{Nu}_d / Nu_{de}$	1
$R_{A_{HF}}$	Improvement ratio at high frequency	1
Re_a	Reynolds number for channel flow, $Re_a = 2U_m a/\upsilon$	1
$\overline{Re}_a$	Time-independent Reynolds number for channel flow, $\overline{Re}_a = 2\overline{U}_m a/\overline{\upsilon}$	1
Re_d	Reynolds number for pipeflow, $Re_d = U_m d/\upsilon$	1
$\overline{Re}_d$	Time-independent Reynolds number for pipe flow, $\overline{Re}_d = \overline{U}_m d/\overline{\upsilon}$	1
S	Strouhal number	1
S_c	Critical Strouhal number	1
t	Time	s
t'	$t' = t\,\hat{U}_A/\lambda$	1
T	Temperature	°K
T_m	Bulk temperature	°K
T_c	Centre-line temperature	°K
T_w	Wall temperature	°K

Symbol		S.I. unit
$\overline{T}$	Time-independent temperature	°K
$\overline{T}_m$	Time-independent bulk temperature	°K
$\overline{T}_c$	Time-independent centre line temperature	°K
$\overline{T}_w$	Time-independent wall temperature	°K
T_{RT}	Ambient temperature in the laboratory	°K
u	Velocity co-ordinate direction x	m/s
$\bar{u}$	Time-independent valocity (x)	m/s
u_1	Time-varying acoustic velocity (x)	m/s
$\textcircled{u}$	Turbulence fluctuations (x)	m/s
$\tilde{u}$	$\tilde{u} = \bar{u} + u_1$	m/s
u'	$u' = u / \hat{u}_A$	1
$\bar{u}'$	$\bar{u}' = \bar{u} / \hat{u}_A$	1
u_1'	$u_1' = u_1 / \hat{u}_A$	1
u_s	Velocity of equivalent steady flow for quasi-steady analysis	m/s
$\hat{u}$	Velocity amplitude	m/s
$\hat{u}_A$	Velocity amplitude at V.A.	m/s
$\hat{u}_N$	Velocity amplitude at V.N.	m/s
$\hat{u}_I$	Velocity amplitude of incident wave	m/s
$\hat{u}_R$	Velocity amplitude of reflected wave	m/s
$\hat{u}_c$	Velocity amplitude constant	m/s
u_m	Bulk velocity	m/s
$\bar{u}_m$	Time-independent bulk velocity	m/s
u_c	Centre-line velocity	m/s
$\bar{u}_c$	Time-independent centre line velocity	m/s
$\lvert u \rvert_{(t)}$	$\lvert u \rvert_{(t)} = \lvert u_m + \hat{u} \cos(\omega t) \rvert$	m/s
$\overline{\lvert u \rvert}$	$\overline{\lvert u \rvert} = \overline{\lvert u_m + \hat{u} \cos(\omega t) \rvert}$	m/s

Symbol		S.I. unit
v	Velocity co-ordinate direction y	m/s
$\bar{v}$	Time-independent velocity (y)	m/s
v_1	Time-varying acoustic velocity (y)	m/s
$\textcircled{v}$	Turbulence fluctuations (y)	m/s
v'	$v' = v / \hat{u}_A$	1
$\bar{v}'$	$\bar{v}' = \bar{v} / \hat{u}_A$	1
v_1'	$v_1' = v_1 / \hat{u}_A$	1
$\tilde{v}$	$\tilde{v} = \bar{v} + v_1$	m/s
V	Voltage to heating tape	volts
W	Flow independent, $W = Nu_d / \left(Re_d^{0.8} P_r^{0.4} (T_m/T_w)^{0.5} \right)$ Nusselt number	1
$\overline{W}$	Mean flow independent, $\overline{W} = \overline{Nu}_d / \left(\overline{Re}_d^{0.8} P_r^{0.4} (\overline{T}_m/\overline{T}_w)^{0.5} \right)$ Nusselt number	1
W_e	Flow independent Nusselt number for the equivalent steady flow	1
x	Co-ordinate direction	m
x'	$x' = x/\lambda$	1
y	Co-ordinate direction	m
y'	$y' = y/\lambda$	1
y_β	Limiting viscous layer	m
Z	$Z = \frac{1}{M} \log_e \left(\frac{M}{N} x + 1 \right)$	s
Z_L	$Z_L = \frac{1}{M} \log_e \left(\frac{M}{N} L_A + 1 \right)$	s
α	$\alpha = K / \rho C_p$	m^2/s
$\bar{\alpha}$	$\bar{\alpha} = K / \bar{\rho} C_p$	m^2/s
α_A	Phase angle	1

Symbol		S.I. unit
β	$\beta = \sqrt{(\omega / 2\bar{\upsilon}_T)}$	1/m
β_L	$\beta_L = \sqrt{(\omega / 2\upsilon)}$	1/m
γ	Ratio of specific heats, $\gamma = C_p / C_v$	1
δ_{SL}	Laminar sub-layer thickness	m
δ_E	Equivalent laminar sub-layer thickness	m
ε_M	Momentum diffusivity	m^2/s
$(\varepsilon)_M$	Equivalent momentum diffusivity	m^2/s
$\overline{(\varepsilon)}_M$	Mean equivalent momentum diffusivity	m^2/s
$\overline{\varepsilon}_{M_c}$	Mean core momentum diffusivity	m^2/s
$\overline{\varepsilon}_M$	Mean momentum diffusivity	m^2/s
ε_H	Thermal diffusivity	m^2/s
$\overline{\varepsilon}_H$	Mean thermal diffusivity	m^2/s
$\Delta\overline{\varepsilon}_{M_c}$	Increase in mean momentum diffusivity for turbulent core	m^2/s
ε_{M_s}	Momentum diffusivity for equivalent steady flow	m^2/s
λ	Wavelength	m
μ	Dynamic viscosity	Kg/ms
μ_T	Turbulent dynamic viscosity	Kg/ms
υ	Kinematic viscosity	m^2/s
$\bar{\upsilon}$	Mean kinematic viscosity	m^2/s
$\bar{\upsilon}_T$	Turbulent kinematic viscosity	m^2/s
ρ	Density	Kg/m^3
$\bar{\rho}$	Time-independent density	Kg/m^3
ρ_1	Time-varying acoustic density	Kg/m^3

Symbol		S.I. unit
e'	$e' = e/\bar{e}$	1
$\bar{e}'$	$\bar{e}' = 1$	1
e_1'	$e_1' = e_1/\bar{e}$	1
ψ	Dimensionless stream function	1
ω	Angular frequency	1/s

Abreviations

E	:	Error
ID	:	Internal diameter
NPL	:	National Physical Laboratory
QS	:	Quasi-steady
SPL	:	Sound pressure level
VA	:	Velocity antinode
VN	:	Velocity node

CHAPTER 1

Introduction

1. Introduction

Combustion-driven acoustic oscillations occur in many different systems and under many types of conditions. They are only part of general combustion instability. Resonant acoustic oscillations of the chamber volume are generated - the frequencies are closely related to the combustion chamber dimensions and the velocity of sound in the combustion gases. For a cylindrical volume, three basic types are possible

A. Longitudinal

The gases move back and forth along the axis of the chamber (often referred to as 'organ-pipe' oscillation).

B. Radial

The gases oscillate between the axis of the chamber and the wall.

C. Tangential

The gases oscillate around the perimeter.

- in addition combined modes are possible.

Great interest has been and still is being shown in acoustic instability. The reason is twofold - one, that the oscillations can be harmful by increasing the rate of erosion, or by generating large amplitude mechanical vibrations. Secondly, it has been found that the instabilities can increase both the combustion intensity and the overall energy transfer coefficient between the combustion gases and the wall of the exhaust pipe.

The first reference to this type of instability was made by Byron Higgins, in 1777, who reported the production of a musical tone when a hydrogen flame was placed in an open-ended pipe. No major work in the field, though, was carried out until the beginning of the 20th century and this early work is recorded in a number of German, Swiss and French patents dating from 1900 to 1910. Only from 1930 were there any thoughts towards practical applications of the phenomenon and in this sense the term "pulsating combustion" came into use. These resulted from independant work by Schmidt in Germany, and Reynst in Germany and France. From these basic ideas, designs have been produced for the use of pulsating combustion in aeronautical engines (Schmidt pulse jet engine in V.1 rocket), car and space heaters, boilers, insecticide spraying, domestic heating and grain drying. In most cases, the instability was of the longitudinal mode - the majority of the work has been experimental with few theoretical analyses of the phenomenon. The field has been reviewed recently by Putnam (1) and Beale (2). The most unusual application is that a musical instrument, the pyrophone, has been made based upon combustion-driven acoustic oscillations. It consists of small gas jets in tubes of varying length and when a key is pressed the jet is ignited producing a clear note. The instrument is on display at the Science Museum, London. Further information on combustion-driven acoustic oscillations can be found in references 3, 4 and 5.

Great claims have been made for increases in time-mean convective heat transfer coefficient in the exhaust pipe of pulse combustors, due to the unsteady motion. Reynst (3), for example, talks of "vast increases in heat transfer due to a thinning of the thermal resistance layer due to the pulsating flow" - many similar statements can be found in the literature, but there is a lack of extensive quantitative work. Zartman and Churchill (6), in 1961, experimentally investigated heat transfer in a cylindrical burner with resonant longitudinal (350 Hz) and tangential (4000 Hz) oscillations (this was a continuation of the work of Sundstrom and Churchill (7)) - using a ram jet type burner, a maximum increase of 100% in local heat transfer coefficient was measured, and was independant of mode of oscillation. The mean flow was turbulent with Reynolds numbers of the range 35,000 - 48,000. The results were correlated by a linear function of sound pressure level, but no calculations of velocity amplitude in the chamber were possible. In 1963, Francis (8) made a general investigation into the practicability of gas-fired pulsating combustors. Using both a Schmidt and Helmholtz combustor, resonating in the longitudinal mode, local and overall heat transfer were measured using a water calorimeter. Correlation with local fluctuating velocities was not possible but results indicated maximum heat transfer at velocity antinodes and minimum at velocity nodes - increases of the order of 100% were found. The major work in the field was by Hanby in 1968 (9). Using a Schmidt combustor, Hanby investigated the effect of longitudinal oscillations in the fundamental mode (frequency of 100 Hz) on convective heat transfer in the exhaust pipe. By using quarter-wavelength damping tubes, the pressure amplitudes were independantly controlled and, with maximum attenuation, steady flow results were obtained. From measurements of pressure amplitude along the pipe, the velocity amplitudes were calculated by simple one-dimensional sound theory using a mean velocity of sound. It was found that maximum increases of 120% were obtained for local heat transfer, with the major parameter being the ratio of local velocity amplitude to mean bulk velocity (defined as Dimensionless pulsation velocity, B) - the greater the value of B, the greater the heat transfer coefficient. For B = 1, a small decrease of 10% was measured. The results were correlated by a quasi - steady method - see Appendix I. This method gave good agreement with the experimental results, despite the relatively high frequency of 100 Hz.

From the limited information, it is difficult to draw any definite conclusion, but it appears that large increases (of the order 100%) and decreases can be obtained in local heat transfer. If pulsating combustors are to be developed for practical applications, the heat transfer coefficients must be predictable in terms of the pulsation variables - this is not possible from existing information. But experimental work with pulsating combustors is difficult due to the limited control of the main variables, and in many cases the combustors can not be operated under steady conditions to give a direct comparison of heat transfer.

The aim of the project was to consider the effect of the unsteady motion on convective heat transfer relative to the exhaust pipe of a pulsating combustor. It was hoped to explain the reported changes in local heat transfer, and to develop a method of predicting heat transfer coefficients from the pulsation parameters. Due to the problems of controlled experimental work with pulsating combustors, it was decided to investigate the heat transfer from the pulsating flow by modelling the

combustor exhaust pipe i.e. consider energy transfer to a resonant oscillating turbulent air stream of the longitudinal mode in a pipe. 'Organ-pipe' oscillation was defined for investigation since it is the most common mode of operation for pulsating combustors. By the appropriate choice of pulsation generator, wide range and control of frequency and amplitude can be obtained. For simplification of the experimental system, energy transfer from the pipe wall to the air was to be measured. The project was interested in energy transfer to the mean flowrate only i.e. the heat transfer coefficients for the mean flowrate in comparison to the equivalent steady flowrate.

CHAPTER 2

Literature Survey

- the effect of oscillations on convective heat transfer

2.1 Free Convection

2.2 Forced Convection

2.3 Summary

2. Literature Survey

- the effect of oscillations on convective heat transfer.

The modelling of the exhaust pipe of pulsating combustors in terms of the effect of flow oscillations on time-mean convective heat transfer is not a new idea. With the claims of large increases in heat transfer, a great amount of work has been done over a wide range of conditions - the effect of flow oscillations and surface vibration, of many modes, frequencies and amplitudes, on free and forced convection (laminar and turbulent flow) have been investigated. The reported survey covered the general field, but concentrated on resonant longitudinal oscillation, with turbulent mean flow, in ducts.

2.1 Free convection

There has been extensive work on the effect of sound fields on free convection, and similarly with vibrating bodies in a stationary fluid. Although, in general, not directly related to conditions in pulsating combustors, these projects give an insight into the mechanisms affecting heat transfer in unsteady conditions.

In 1938 Martinelli and Boetler (10) vertically vibrated a horizontal cylinder in water with sinusoidal oscillations in the range 0 - 40 Hz, and measured overall heat transfer. At maximum amplitude, an increase of 400% was measured. Kubanskii (11), in 1953, investigated the influence of a longitudinal sound field upon free convection from a heated horizontal cylinder in air - increase of 75% was measured. Shadowgraph techniques indicated circulation cells near the hot surface with outward flow at the nodes and inward flow at the antinodes. Lemlich (12), in 1955, considered the effect of transverse vibration of electrically heated wires in air. For frequencies of 39 - 122 Hz, an increase of 300% was measured at maximum amplitude. These early experimental investigations demonstrated that acoustic oscillation and body vibration could produce large increases in heat transfer, and stimulated further work.

In 1960 Holman (13) proposed a mechanism to explain the increases - this involved an interaction between the acoustic streaming velocities and the free convection velocities, with the definition of a critical sound pressure level above which the inner streaming boundary layer is destroyed creating turbulent mixing. Large increases were predicted as a result of the turbulence generation. Acoustic streaming is the flow field of time independant velocities created by a sound field around an object (or vibrating body in stationary fluid). Reynolds' stresses due to the time mean values of the oscillating components give rise to the steady streaming velocities. The analysis is well established for an adiabatic cylinder in a sound field (14). Fand (15), in 1962, attempted to correlate both sound field and body vibration experimental results but, with the wide range of conditions and the complexity of the problem, little progress was made. In 1967 Richardson (16) published an excellent review of the progress in this field and gave full discussion of the effects of acoustic streaming (paper also contained discussion of effects with forced convection).

Work has continued to extend the studies over a wide range of frequency and amplitude.

See Bibliography References 1 to 15

2.2 Forced convection

The majority of work has involved longitudinal oscillations of a flow in a duct. The field can be considered in two sections - studies of convection to non-steady water flow, relative to low frequency reciprocating pumps, and, secondly, heat transfer to oscillating compressible fluids (with reference to pulsating combustors).

The first section will be considered briefly - in all cases the overall heat transfer was measured for a pulsating water flow in a steam jacket. The first published work was by Martinelli (17) in 1943. For a turbulent mean flow, the change in heat transfer was measured for oscillating flow of frequency 0 - 4 Hz. A small decrease of 10% was found. This paper first introudced the idea of the basic quasi-steady analysis (see Appendix I). In 1952, West and Taylor (18) considered a pulsating flow of 1.67 Hz, produced by a reciprocating pump, for a turbulent mean flow with Reynolds numbers of 30,000 to 85,000. A maximum increase of 70% was measured, but the velocity amplitudes could not be predicted. In this project no measurement of steady flow conditions was made and consequently the improvement ratios must be regarded with some doubt. Darling (19), in 1955, considered changes in overall heat transfer for a mean turbulent flowrate for frequencies between 0.25 - 15.0 Hz, produced by a motor driven interrupter valve. An increase was measured for the valve positioned just upstream from the heat exchanger - this was due to induced cavitation (no change if valve was moved from entrance). Similar effects were found by Lemlich (20) and Morgan (21). In 1965, Baird (22) measured the change in heat transfer due to flow pulsations for a turbulent mean flow (Reynolds number 5,000 to 16,000). Pulsations, over the frequency range 0.8 - 1.7 Hz, were produced by an air pulser - the design was such that the displacement amplitude was measured directly. A maximum improvement of 40% was found and the results were correlated by simple quasi-steady theory. Further work can be found in the Bibliography - references 16, 17, 18.

The major interest was in heat transfer to oscillating compressible fluids. Havemann (23, 24), in 1956, considered overall heat transfer to a turbulent mean flow of air, through a horizontal pipe, from a steam jacket. The flow was pulsated using a poppet valve for frequencies 5 to 40 Hz, and using different driving cams the waveform could be varied, but no amplitude measurements in the test section were possible. The changes in heat transfer coefficient were complex and no correlation was achieved. Similar work was carried out by Mueller (25), Romie (26) and Chalitbtan (27).

In 1961 Lemlich and Hwu (28) considered overall heat transfer from a steam jacket to an air flow with superimposed resonant oscillations produced by a horn (frequencies of 198, 256 and 322 Hz corresponding to 3rd, 4th, 5th harmonics). Both laminar and turbulent flow conditions were considered. For laminar flow, a maximum increase of 57% was measured, and for turbulent flow a maximum increase of 27%. But no measurements of pressure amplitude were made, and consequently no correlation was possible in terms of unsteady flow parameters.

Both theoretical and experimental aspects of the effect of resonant pulsating flow on laminar and turbulent mean flows were investigated by Jackson from 1955 to 1967 - references 29 to 36. The experimental work was summarised in reference 34. A resonant sound field was produced in a pipe 0.097 m I.D. and 3.05 m length by an electro-magnetic horn. The air blower gave a range of Reynolds number of 2,000 to 200,000. Pressure amplitude was measured close to the driver by a microphone, and velocity amplitudes were calculated using one dimensional sound theory with a mean value of velocity of sound. Heat transfer was measured from a steam jacket to the air flow - local heat transfer coefficients were found by using 21 separate condensate chambers along the pipe. Results were given in the paper (34) for a frequency of 221 Hz (3rd harmonic). No hydrodynamic or thermal entrance lengths were used in the rig, and consequently for higher Reynolds numbers the flow conditions were not developed. The rig was modified (36) to include an entrance length and results taken using 90 Hz frequency.

See Figure 1 page 7

The graphs show two conflicting cases. For lower turbulent Reynolds numbers, maximum increases occur at velocity antinodes and maximum decreases at velocity nodes - the greater the amplitude, the greater the increases and decreases. But for the higher flowrates, maximum decrease was at velocity antinodes and no change at the nodes. For laminar flow, the results were difficult to interpret due to free convection effects.

Theoretically Jackson and Purdy (32, 33) investigated the interaction between a resonant oscillating field and a laminar mean flow. It was shown that the acoustic streaming velocities could produce standing vortices in the pipe.

See Figure 2 page 8

Purdy (35) extended this work and solved the energy equation for resonant laminar flow in a channel. It was shown that the local heat transfer coefficient was significantly altered by the vortex formation but with no change in overall heat transfer.

See Figure 3 page 8

The theoretical predictions for laminar flow were of a similar form as the experimental results for local heat transfer found for the lower turbulent flowrates (Figure 1a page 7). Jackson proposed that a similar vortex formation existed for the turbulent flow, with Dimensionless pulsation velocity a controlling factor (vortex formation if $B > 1$). But this could not explain the results for higher flowrates, and no other mechanism was suggested.

From 1959 to 1967, Harrje investigated heat transfer to pulsating turbulent pipe flow (37 to 43). The aim of the project was to determine the cause of the increases in heat transfer in the exhaust pipe of pulse combustors. The major part of the work is found in the report by Bogdanoff (42). Assuming heat transfer to be dependant on local pulsation variables, Bogdanoff showed by dimensional analysis that the major pulsation parameters were Dimensionless pulsation velocity and Strouhal number.

Fig. 1.a

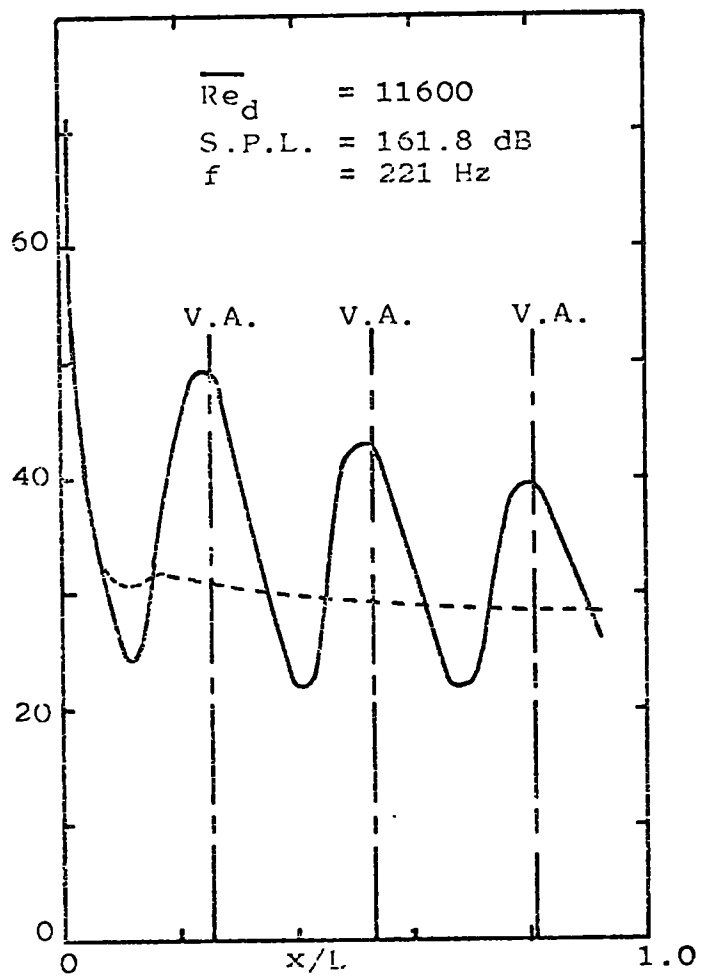

Fig. 1.b

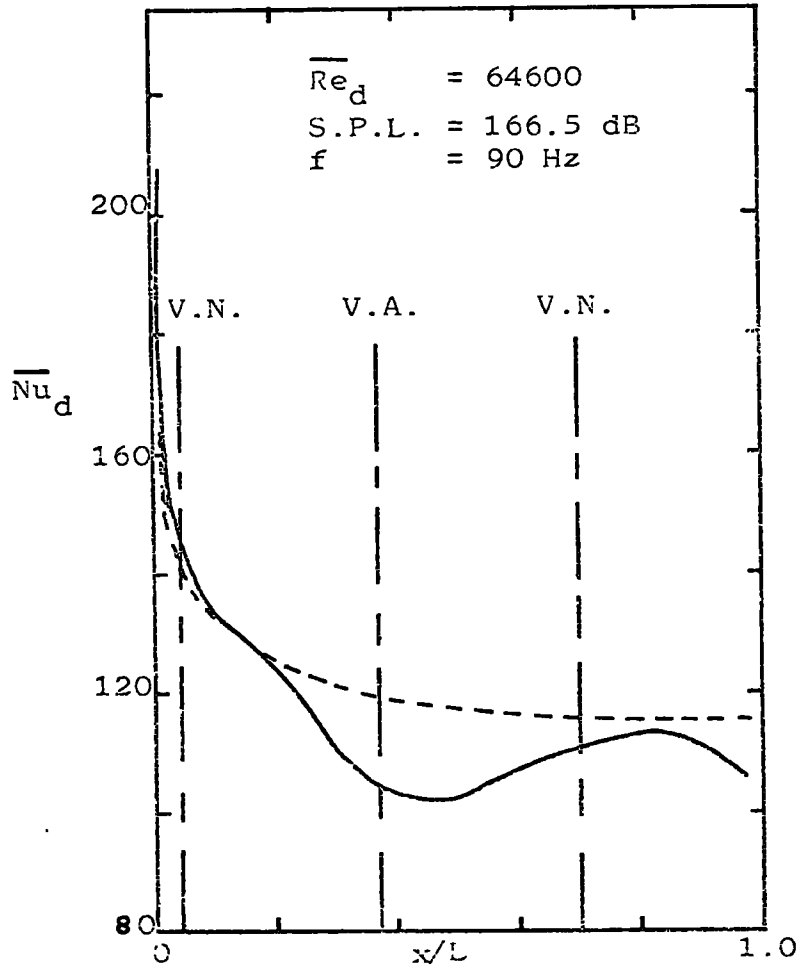

Fig.1 Nusselt Number against position in heat exchanger

Experimental Data - Jackson

– – – – Equivalent steady flow

Fig.2 Standing Vortex Formation - Stream Function

$(\hat{U}_A/\bar{U}_M)^2\bar{M}_A = 13.3$

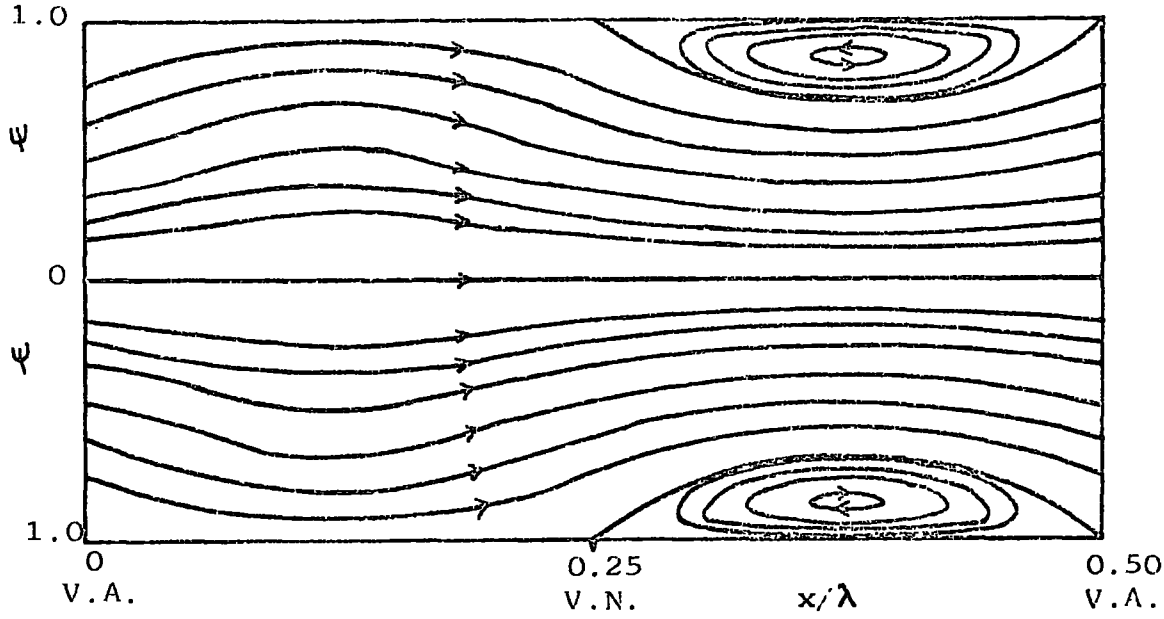

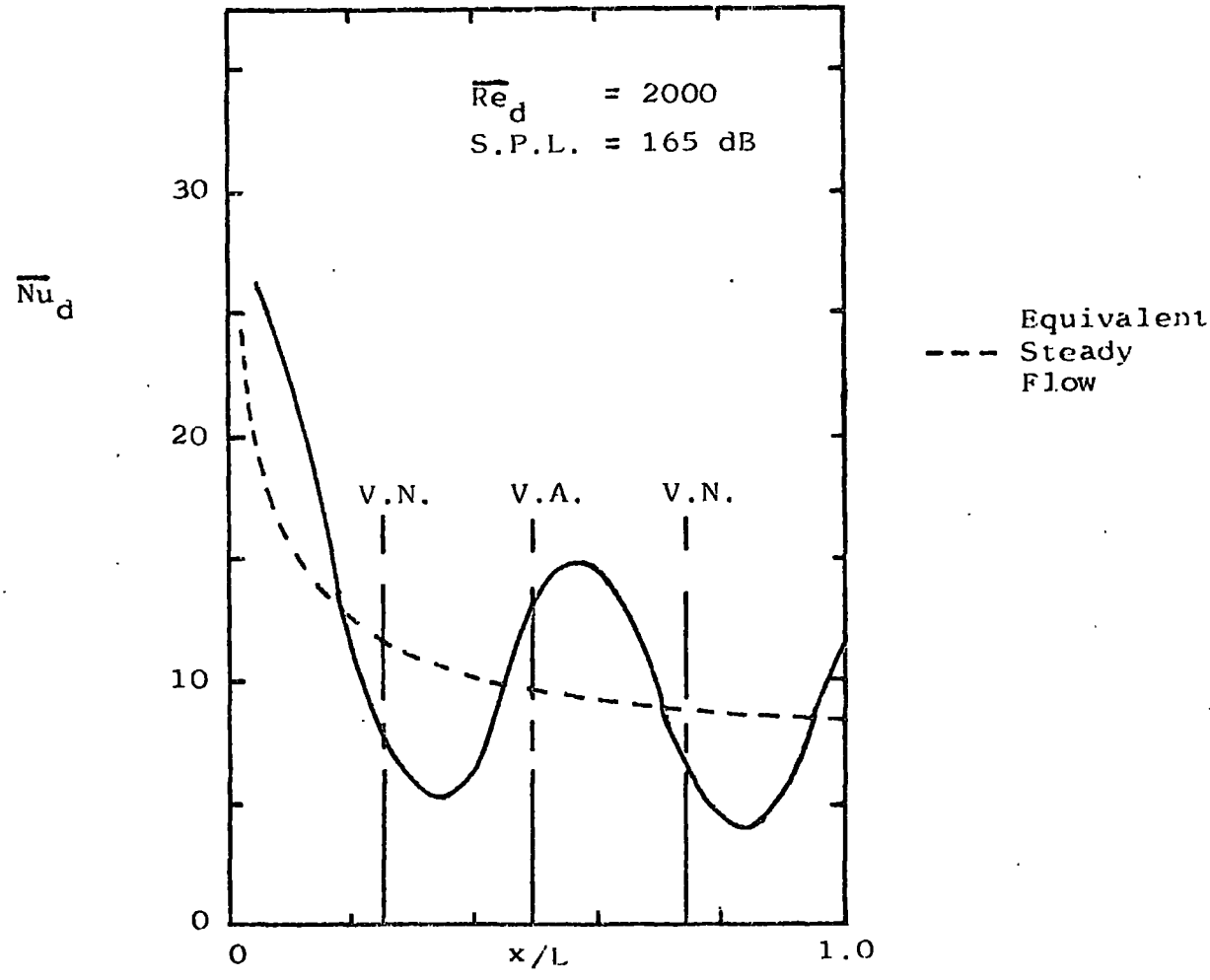

Fig.3 Effect of Vortex Flow on Heat Transfer

Nusselt number, $\overline{Nu}_d \approx f(\overline{Re}_d, B, S)$

for $\overline{Re}_d$, Reynolds number

B, Dimensionless pulsation velocity

S, Strouhal number

Heat transfer was measured between a steam jacket and a turbulent air stream in a pipe, 0.038 m I.D., and 1.15 m length. The condensate was collected in 20 separate chambers to give local heat transfer. A resonant oscillating field was produced by a siren of frequency range 5 to 5,000 Hz, with the amplitude controlled by varying the air gap between the siren wheel and the outlet nozzle. Pressure amplitude was measured close to the siren wheel (pressure antinode) using a strain-gauge type transducer. Velocity amplitudes were calculated from one-dimensional sound theory using a mean value for the velocity of sound. Results were recorded for only one frequency (270 Hz - 6th harmonic) and one mean flowrate (Reynolds number 100,000).

See Figure 4 page 10

The graphs indicate that local heat transfer was dependant on local pulsation characteristics (cf. Hanby (9)).

Bogdanoff also investigated the velocity profiles in the pipe using a hot-wire anemometer, measuring both instantaneous and mean velocities. The results showed no evidence of the acoustic streaming mechanism proposed by Jackson, but the mean velocity measurements indicated an increase in the turbulent diffusivity close to the wall. The heat transfer results also gave no indication of acoustic streaming effects. Bogdanoff proposed that the changes in heat transfer at a point were due to changes in the diffusivity generated by the oscillating velocity at the point. Bogdanoff also attempted to correlate the various experimental projects but with little success - the importance of the local dimensionless pulsation velocity was suggested, especially the condition of 'reverse flow' ($B > 1$).

An extensive experimental investigation was conducted by Galitseyskiy from 1967 to 1970 (44 to 47). Local heat transfer coefficients were measured for an air flow with a constant heat flux input (direct electrical heating of the pipe). The pipe was 0.0084 m I.D. and 1.885 m length. Reynolds numbers were from 10,000 to 100,000. Resonant oscillations were produced by a rotating valve with frequency range 50 to 500 Hz. The pressure amplitude was controlled, for a given flowrate, by varying the orifice diameter at outlet, and was measured at the inlet and outlet of the test section. Frequencies used were the fundamental to 4th harmonic (90, 180, 270, 360 and 450 Hz). The results showed maximum heat transfer coefficient at velocity antinodes and minimum at velocity nodes, with a maximum increase of 120%. But it was obvious from the results that the standing wave decayed along the pipe due to frictional dissipation. Despite the extensive work, the results are so recorded as to make interpretation in terms of pulsation variables very difficult.

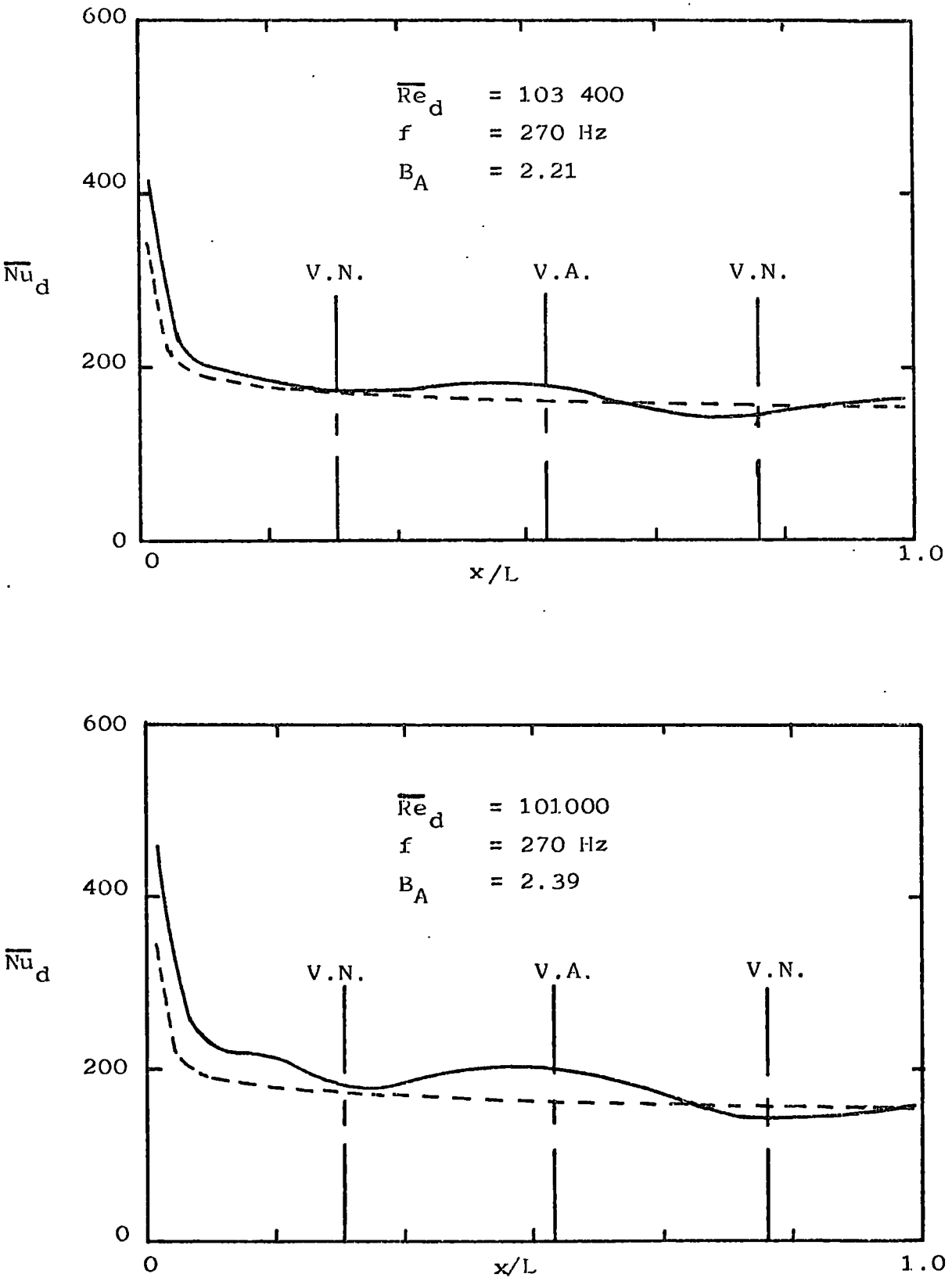

Fig.4 Nusselt number against position in heat exchanger

Experimental Data - Bogdanoff

— — — — Equivalent steady flow

Work has not been limited to duct flow - flow over flat plates and around cylinders has also been considered. In 1961 Bayley (48) measured heat transfer coefficient from a flat plate to a pulsating flow. The pulsations were produced by a rotating valve with frequency range 10 to 100 Hz. Increases of 70% were found at maximum amplitude and the effect of frequency was negligible. It was proposed that the increases were caused by a change in the point of separation of the boundary layer. Feiler (49, 50) considered large amplitude oscillations, generated by a siren, on a flat plate and increases of 65% were measured. The mechanism of change was given as transition to turbulent conditions at a lower Reynolds number. Similar findings were reported by Miller (51). Investigations for forced convection around cylinders are limited. No correlation has been achieved between the various projects - see references 19 to 23 in Bibliography. Richardson (52) proposed that an interaction can occur between the oscillation frequency and the instability frequency of the wake to give large increases.

Further references for the effect of flow oscillations (and surface vibration) on forced convective heat transfer are given in the Bibliography - references 24 to 47.

2.3 Summary

The work considered demonstrates the complexity of the problem - no single mechanism has been shown to be the controlling factor, but various possible causes have been proposed. The problem is further complicated by the vast range of conditions of the projects i.e. extremes of frequency, amplitude, waveform and mode of vibration. But the investigations have confirmed that oscillation can affect heat transfer.

The time-independant velocity field of acoustic streaming is the major factor in the effect of oscillations on free convection. Similarly it has been shown theoretically that acoustic streaming can generate increases and decreases in local heat transfer for a resonant laminar gas flow in a pipe. But the effect of flow pulsations on Transitional Reynolds number for laminar to turbulent flow has not been investigated.

For the majority of pulsating combustors, the most important case is that of the effect of longitudinal oscillations of a turbulent mean flow in a pipe.

The experimental investigations for low frequency pulsations of a water flow were described by quasi-steady considerations (except for the effects of induced cavitation).

For resonant pulsations, the work of Jackson, Harrje and Galitseyskiy showed the critical dependance of local heat transfer on the resonant field distribution - consequently investigations which did not consider local heat transfer and local velocity amplitude are of little use in predicting the heat transfer characteristics of a pulse combustor. The three investigations, although conflicting in parts, gave some general indications. Local heat transfer can be both increased or decreased by resonant longitudinal oscillations. The most important

parameter is the Dimensionless pulsation velocity (B) especially the case of 'reverse flow' ($B > 1$), but no conclusion on the effect of frequency can be drawn. It is not possible to define a general mechanism of action for the flow pulsations, but two possible modes have been proposed to explain the changes in heat transfer - vortex formation (Jackson) and changes in mean diffusivity (Harrje). Despite the extensive investigations, prediction of local heat transfer is not possible from the pulsation parameters.

From the literature review, the basic criteria for the project were formed relative to the original aims. An experimental investigation over a wide range of pulsation parameters was required to characterise the effect of flow oscillations. Local heat transfer was to be measured for resonant longitudinal oscillations of a turbulent air flow in a pipe. The experimental rig had to be capable of measurements for the equivalent steady flowrate. The pulsation generator had to generate high pressure amplitudes (to give 'reverse flow', $B>1$) over a wide frequency range (to investigate a number of harmonics). A sinusoidal waveform was desirable to simplify any theoretical predictions (applicable to any other time variation by Fourier analysis). It was important that the velocity amplitude distribution along the heat exchanger could be found to compare to local heat transfer measurements. To investigate possible mechanisms of action of the flow pulsations on heat transfer, it was hoped to theoretically determine the acoustic streaming velocity field for a turbulent flow (relative to vortex formation), and consider the effect of the oscillating velocity on the mean flow diffusivity. From the proposed experimental and theoretical investigations, it was hoped to explain the changes in heat transfer and derive a method of predicting local heat transfer coefficients from the pulsation parameters.

CHAPTER 3

Prediction of Velocity Amplitude

3.1 Adiabatic

3.2 Energy transfer

3.3 Summary

3. Prediction of velocity amplitudes

It has been shown that the velocity amplitude of the longitudinal oscillations was an important parameter for the investigation. Experimentally it is difficult to measure the velocity fluctuations, but relatively easy to measure pressure amplitude. It was intended to measure pressure amplitude and from the measurements derive velocity amplitude.

It can be assumed that except for close to the pipe wall the unsteady motion can be considered inviscid (59, 60). The flow is analysed for an inviscid fluid to evaluate a relationship between pressure amplitude and velocity amplitude - the experimental heat transfer results were related to this measure of velocity amplitude.

Wave propagation in an adiabatic flow and in a flow with energy transfer, for an inviscid fluid, are considered in the following sections.

3.1 Adiabatic

Consider longitudinal oscillations of a gas flow in a constant diameter pipe. It is assumed that the fluid is inviscid and can be considered a perfect gas. The analysis for one-dimensional adiabatic unsteady motion is well established (53).

Consider motion as a steady flow, having mean properties $\bar{u}, \bar{\rho}$, and $\bar{p}$, on which is superimposed incremental time-varying properties u_1, ρ_1, p_1.

i.e. Velocity, $u = \bar{u} + u_1$

Density, $\rho = \bar{\rho} + \rho_1$

Pressure, $p = \bar{p} + p_1$

The incremental properties are such that their squares and products can be considered negligible.

- Small Pertubation Theory

The Small Pertubation Theory limits the solutions to waves of small amplitude. It can be shown that if

$$\left(1 + (\gamma - 1) \frac{u_1}{2\bar{c}} \right)^{-(\gamma+1)/(\gamma-1)} \ll 1$$

for γ, ratio of specific heats

$\bar{c}$, velocity of sound

then the theory is applicable (54).

Applying the incremental approximations to the appropriate control volume, the following set of equations can be derived from the basic laws of Continuity, Momentum and Energy.

$$\frac{\partial \rho_1}{\partial t} + \bar{u}\frac{\partial \rho_1}{\partial x} + \bar{\rho}\frac{\partial u_1}{\partial x} = 0$$

$$\frac{\partial u_1}{\partial t} + \bar{u}\frac{\partial u_1}{\partial x} = -\frac{1}{\bar{\rho}}\frac{\partial p_1}{\partial x}$$

$$\frac{1}{\bar{\rho}}\frac{\partial p_1}{\partial x} = \frac{\bar{c}^2}{\bar{\rho}}\frac{\partial \rho_1}{\partial x}$$

for t, time

x, co-ordinate distance along the pipe

From the three equations, the following differential equation can be formed (53).

$$(\bar{c}^2 - \bar{u}^2)\frac{\partial^2 u_1}{\partial x^2} - 2\bar{u}\frac{\partial}{\partial x}\left(\frac{\partial u_1}{\partial t}\right) - \frac{\partial^2 u_1}{\partial t^2} = 0$$

..... 1

If $\bar{u} = 0$,

$$\frac{\partial^2 u_1}{\partial x^2} = \frac{1}{\bar{c}^2}\frac{\partial^2 u_1}{\partial t^2}$$

- this is the one-dimensional Wave equation which describes the propagation of plane sound waves.

Consider the flow to occur in the following acoustic system

Closed/open pipe

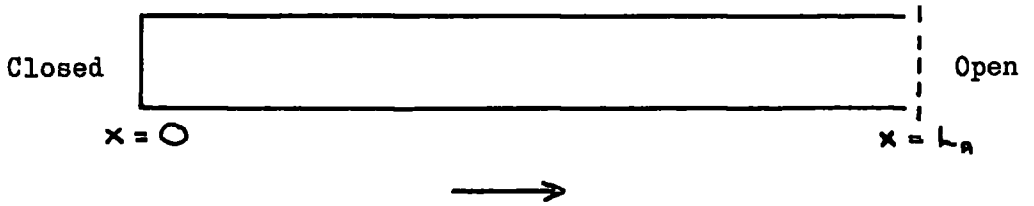

where L_A = acoustic length

Assume a sinusoidal pressure oscillation of angular frequency ω is generated at x = 0. At resonance a standing wave is produced in the pipe due to wave reflection from the open end

i.e. $u_1 = 0$ at $x = 0$

$p_1 = 0$ at $x = L_A$

assuming perfect reflection

For a full discussion of resonance see references 55, 56.

General solution of equation 1 is

$$u_1 = A \sin \omega\left(t - \frac{x}{\bar{c} + \bar{u}}\right) + B \sin \omega\left(t + \frac{x}{\bar{c} - \bar{u}}\right)$$

where A, B are constants

This equation can be physically interpreted as two waves, of angular frequency ω, superimposed - one with a propagation velocity of $(\bar{c} + \bar{u})$ in the direction of the flow and the other with a velocity of $(\bar{c} - \bar{u})$ opposing the flow.

Boundary condition

$$u_1 = 0 \quad \text{at} \quad x = 0$$

By substitution

$$u_1 = \hat{U}_A \sin\left(\omega x \frac{\bar{c}}{\bar{c}^2 - \bar{u}^2}\right) \cos\left(\omega t + \frac{\omega x \bar{u}}{\bar{c}^2 - \bar{u}^2}\right)$$

..... 2

where $\hat{U}_A = -2A$

From Momentum equation

$$\frac{\partial p_1}{\partial x} = -\bar{\rho}\left(\frac{\partial u_1}{\partial t} + \bar{u}\frac{\partial u_1}{\partial x}\right)$$

Substitution and integration gives

$$p_1 = \hat{P}_A \cos\left(\omega x \frac{\bar{c}}{\bar{c}^2 - \bar{u}^2}\right) \sin\left(\omega t + \frac{\omega x \bar{u}}{\bar{c}^2 - \bar{u}^2}\right)$$

..... 3

where $\hat{P}_A = 2\bar{\rho}\bar{c}A$

Boundary condition

$$p_1 = 0 \quad \text{at} \quad x = L_A$$

Substitution gives the resonant frequencies, f

$$f = (2n-1)\frac{1}{4L_A}\frac{(\bar{c}^2 - \bar{u}^2)}{\bar{c}}$$

..... 4

where n = 1, 2, 3

Assume the effect of the mean velocity can be neglected

i.e. assuming $\bar{u} \ll \bar{c}$

Substitute in equations 2, 3, 4

$$u_1 = \hat{U}_A \sin\left(\omega \frac{x}{\bar{c}}\right) \cos\left(\omega t\right)$$

where $\hat{U}_A$ is velocity amplitude at a velocity antinode

$$p_1 = \hat{P}_A \cos\left(\omega \frac{x}{\bar{c}}\right) \sin\left(\omega t\right)$$

where $\hat{P}_A$ is pressure amplitude at a pressure antinode

for $F = (2n-1)\frac{\bar{c}}{4L_A}$

for n = 1, 2, 3

From the equations it can be shown that

$$\hat{U}_A = -\frac{\bar{c}}{\gamma \bar{p}} \cdot \hat{P}_A$$

i.e. from a measurement of pressure amplitude at an antinode velocity amplitude distribution can be evaluated

Modulus of pressure and velocity amplitudes for the fundamental and 1st harmonic of the system are shown in Figure 5 page 18.

But in the derivation of the equations it is assumed that perfect reflection occurs from the open end - in practice this is not correct, and some sound radiation occurs at the pipe exit. (56)

Assume velocity amplitude of incident wave = $\hat{U}_I$

and velocity amplitude of reflected wave = $\hat{U}_R$

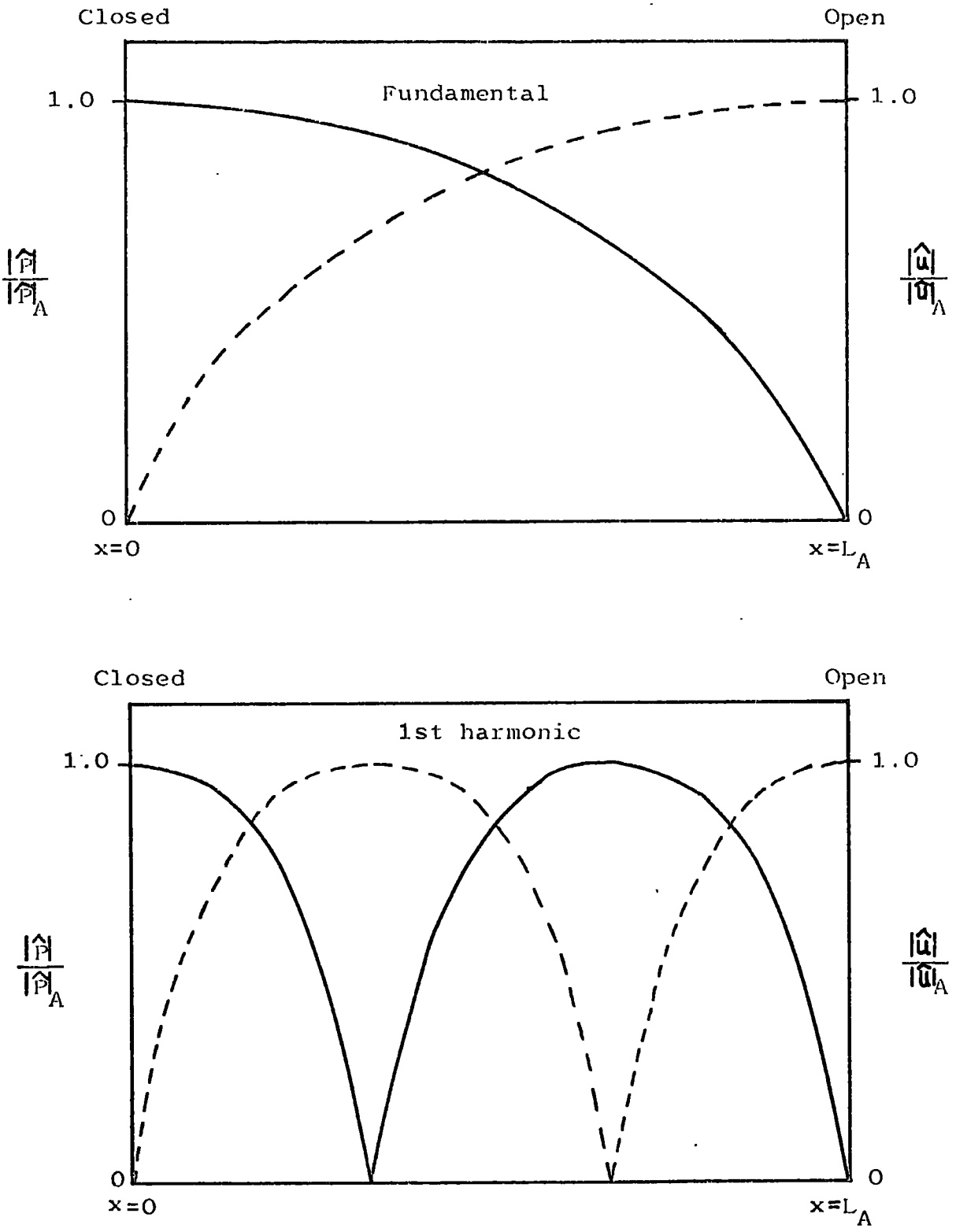

Fig.5 Modulus Pressure/Velocity Amplitude against Position in Pipe

——— Pressure

- - - - - Velocity

It can be shown (55) that

$$u_1 = -\sqrt{\left(\left(\hat{u}_I + \hat{u}_R\right)^2 \sin^2\left(\omega\frac{x}{\bar{c}}\right) + \left(\hat{u}_I - \hat{u}_R\right)^2 \cos^2\left(\omega\frac{x}{\bar{c}}\right)\right)} \cos\left(\omega t + \alpha_a\right)$$

where $$\tan\alpha_a = \frac{\left(\hat{u}_I - \hat{u}_R\right)}{\left(\hat{u}_I + \hat{u}_R\right)} \cot\left(\omega\frac{x}{\bar{c}}\right)$$

$$p_1 = \bar{\rho}\bar{c}\sqrt{\left(\left(\hat{u}_I + \hat{u}_R\right)^2 \cos^2\left(\omega\frac{x}{\bar{c}}\right) + \left(\hat{u}_I - \hat{u}_R\right)^2 \sin^2\left(\omega\frac{x}{\bar{c}}\right)\right)} \sin\left(\omega t + \alpha_a\right)$$

where $$\tan\alpha_a = -\frac{\left(\hat{u}_I - \hat{u}_R\right)}{\left(\hat{u}_I + \hat{u}_R\right)} \tan\left(\omega\frac{x}{\bar{c}}\right)$$

If the wavelength of the oscillations is large compared to the pipe diameter, the travelling wave component is small, and the phase angle can be considered negligible.

The equations can be written as

$$u_1 = \sqrt{\left(\hat{u}_A^2 \sin^2\left(\omega\frac{x}{\bar{c}}\right) + \hat{u}_N^2 \cos^2\left(\omega\frac{x}{\bar{c}}\right)\right)} \cos\left(\omega t\right)$$

$$p_1 = \sqrt{\left(\hat{p}_A^2 \cos^2\left(\omega\frac{x}{\bar{c}}\right) + \hat{p}_N^2 \sin^2\left(\omega\frac{x}{\bar{c}}\right)\right)} \sin\left(\omega t\right)$$

where $\hat{U}_N$ = velocity amplitude at velocity node

$\hat{P}_N$ = pressure amplitude at pressure node

for the resonant frequencies defined by

$$F = (2n-1)\frac{\bar{c}}{4L_A}$$

for $n = 1, 2, 3$

and $$\hat{U}_A = -\frac{\bar{c}}{\gamma \bar{p}}\hat{p}_A$$

$$\hat{U}_N = -\frac{\bar{c}}{\gamma \bar{p}}\hat{p}_N$$

For an inviscid perfect gas, under adiabatic conditions, unsteady periodic motion has been analysed for longitudinal oscillations in a closed/open acoustical pipe - the main assumptions are that of small amplitude, and that the effect of the mean velocity is negligible. The resonant frequencies and the pressure amplitude and velocity amplitude distributions have been derived for both perfect and imperfect reflection from the open end. For the experimental investigation a simple relationship has been found to calculate the velocity amplitude distribution from measurements of pressure amplitude at a node and antinode.

3.2 Energy transfer

In the exhaust pipe of a pulsating combustor (or in the proposed rig for the project) conditions are not adiabatic but energy transfer occurs between the pipe walls and the mean flow. To predict the velocity amplitudes under these conditions, the effect of the energy transfer must be analysed. In previous investigations the heat transfer effects on wave propagation were not considered.

It is assumed that the fluid is inviscid and a perfect gas. Consider the following control volume for the longitudinal oscillations

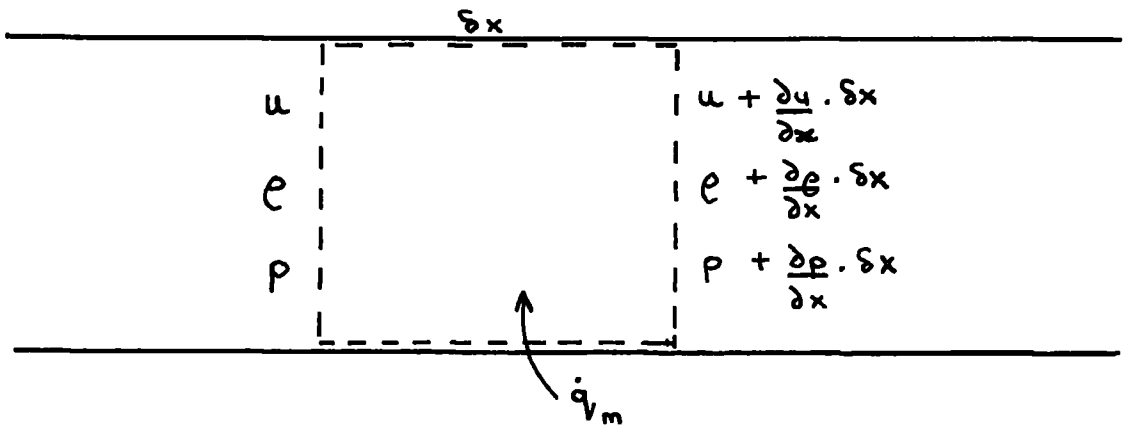

where $\dot{q}_m$ = energy transfer per unit time per unit mass

Apply fundamental equations to Control volume

Continuity

$$\frac{\partial \rho}{\partial t} + \rho \frac{\partial u}{\partial x} + u \frac{\partial \rho}{\partial x} = 0$$

Navier - Stokes

$$\frac{\partial u}{\partial t} + u \frac{\partial u}{\partial x} + \frac{1}{\rho} \frac{\partial p}{\partial x} = 0$$

Energy

It can be shown (53) that

$$\frac{\partial p}{\partial t} + u \frac{\partial p}{\partial x} - c^2 \left(\frac{\partial \rho}{\partial t} + u \frac{\partial \rho}{\partial x} \right) = \dot{q}_m \rho (\gamma - 1)$$

For the adiabatic analysis it is found that the effect of mean velocity could be neglected if $\bar{u} << \bar{c}$. Similarly assume $\bar{u} << \bar{c}$ and consequently that the effect of convective terms is negligible.

i.e. assume $\bar{u} = 0$ and $\dot{q}_m = 0$

The problem reduces to that of wave propagation in a stratified medium due to the temperature gradient (continuously varying physical properties along the pipe).

Assume that Small Pertubation Theory is applicable

$$u = \bar{u} + u_1$$

$$p = \bar{p} + p_1$$

$$\rho = \bar{\rho} + \rho_1$$

But, due to the temperature gradient along the pipe,

$$\bar{u} = f(x)$$

$$\bar{\rho} = g(x)$$

$$\bar{c} = h(x)$$

Substitute into basic equations and approximate to give

Continuity

$$\frac{\partial \rho_1}{\partial t} + \bar{\rho} \frac{\partial u_1}{\partial x} + u_1 \frac{\partial \bar{\rho}}{\partial x} = 0$$

Navier - Stokes

$$\frac{\partial u_1}{\partial t} + \frac{1}{\bar{\rho}} \frac{\partial p_1}{\partial x} = 0$$

Energy equation

$$\frac{\partial p_1}{\partial t} - \bar{c}^2 \left(\frac{\partial \rho_1}{\partial t} + u_1 \frac{\partial \bar{\rho}}{\partial x} \right) = 0$$

By substitution from equations

$$\frac{\partial^2 u_1}{\partial x^2} - \frac{1}{\bar{c}^2} \frac{\partial^2 u_1}{\partial t^2} = 0$$

..... 5

and

$$\frac{\partial p_1}{\partial t} = - \bar{c}^2 \bar{\rho} \frac{\partial u_1}{\partial x}$$

Similar analysis has been applied by Kapur (57).

Consider the gas flow in a pipe which is closed/open acoustically, and with an axial temperature gradient such that the change in the velocity of sound is linear.

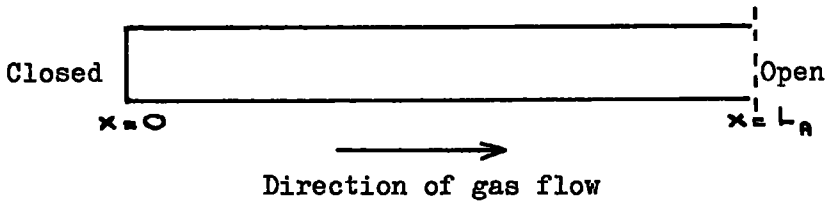

Direction of gas flow

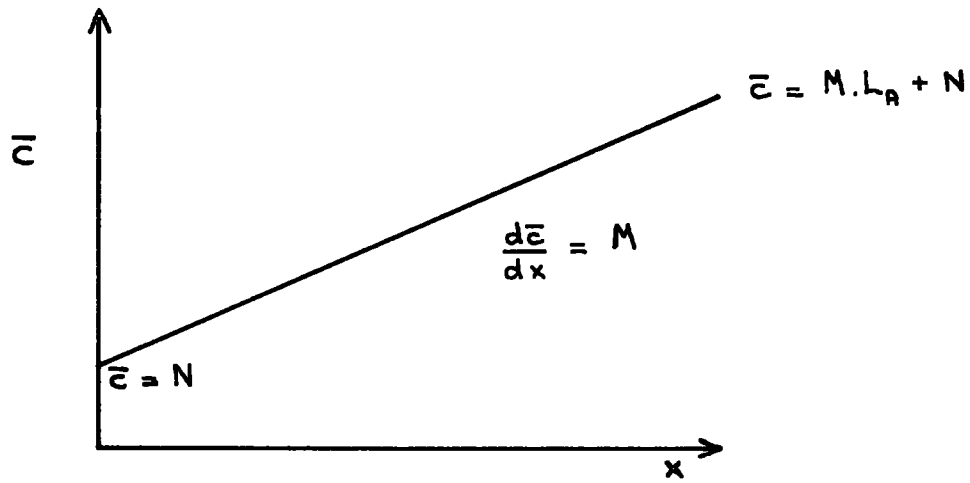

where N = velocity of sound at x = o

M = rate of change of velocity of sound along the pipe

Boundary conditions at resonance

$$u_1 = 0 \text{ at } x = 0$$

$$p_1 = 0 \text{ at } x = L_A$$

for perfect reflection.

From equation 5

$$\frac{\partial^2 u_1}{\partial t^2} = (Mx + N)^2 \frac{\partial^2 u_1}{\partial x^2}$$

The differential equation can be solved analytically - see Appendix II.

Governing equations for resonance in the defined system.

Resonant frequencies are given by

$$\frac{M}{2}\sin(bz_L) + b\cos(bz_L) = 0 \qquad \ldots\ldots 6$$

where $b = \frac{1}{2}\sqrt{(4\omega^2 - M^2)}$

$$u_1 = -\frac{\omega}{b}\frac{N}{\gamma\bar{p}} PO\, e^{Mz/2}\sin(bz)\cos(\omega t) \qquad \ldots\ldots 7$$

$$p_1 = \frac{N}{b}\frac{1}{(Mx+N)} PO\, e^{Mz/2}\left(\frac{M}{2}\sin(bz) + b\cos(bz)\right)\sin(\omega t) \qquad \ldots\ldots 8$$

for $z = \frac{1}{M}\log_e\left(\frac{M}{N}x + 1\right)$

where PO is pressure amplitude at x = 0

From the equations it can be seen that a standing wave is produced at resonance. The effect of a linear variation in speed of sound along the pipe was investigated numerically for a given system. A comparison was made between the given theory and from using an average value for velocity of sound with the adiabatic theory (this has been the method used, in the past, in pulse combustor analysis cf. Hanby (9)).

Consider a closed/open pipe of acoustic length 2.0 m - define a linear rise in velocity of sound over a temperature change of 1000 °C, and assume a pressure amplitude of 6900.0 N/m^2 at x = 0. Resonant frequencies, found by solving equation 6 by Newton - Raphson iteration technique (58), are

	Fundamental	1st Harmonic	2nd Harmonic	
Predicted	71.9	191.2	314.9	Hz
Adiabatic Theory	70.6	211.7	352.9	Hz
% difference	1.8	10.7	12.1	%

Substitution in equations 7 and 8 gives the pressure and velocity amplitude distributions. Results are given for the 1st harmonic.

See Figure 6 page 26

The following conclusions can be drawn on the effect of the temperature rise on the resonance characteristics of the given system.

A. Resonant frequency is increased relative to ambient conditions.

B. Wavelength increases along the pipe.

C. Nodes and antinodes are displaced towards $x = 0$ relative to ambient conditions.

D. Pressure amplitude at pressure antinodes decreases from $x = 0$ to $x = L_A$.

E. Velocity amplitude at velocity antinodes increases from $x = 0$ to $x = L_A$.

The adiabatic theory using an average velocity of sound gives a good estimate of resonant frequency, but large errors in the prediction of standing wave distributions (see Figure 6).

One cannot assume a linear decrease in velocity of sound for pulse combustors, but the analysis should give an indication of the effect of the temperature gradient on the acoustic characteristics of the exhaust pipe. The results show that the use of the adiabatic theory with mean velocity of sound gives large errors in the prediction of velocity amplitudes - this gives rise to doubts on the correlation of heat transfer obtained by Hanby (9).

The given system was also analysed numerically for a temperature rise of 40°C. The results show that for a small temperature change in the test section the resonance characteristics can be predicted accurately by adiabatic theory using a mean velocity of sound.

3.4 Summary

The resonant unsteady motion of an inviscid, perfect gas has been analysed for small amplitude periodic oscillations in a stratified medium. Assuming convective terms to be negligible, the analysis applies to wave propagation in a pipe with energy transfer to a mean flow. An analytical solution has been found for a linear change in velocity of sound. The results indicate that, for a small change in temperature, adiabatic theory, using an average velocity of sound, can be used to predict velocity amplitude. But, for pulsating combustors, adiabatic approximation could give large errors in predicted velocity amplitude due to the large temperature gradients.

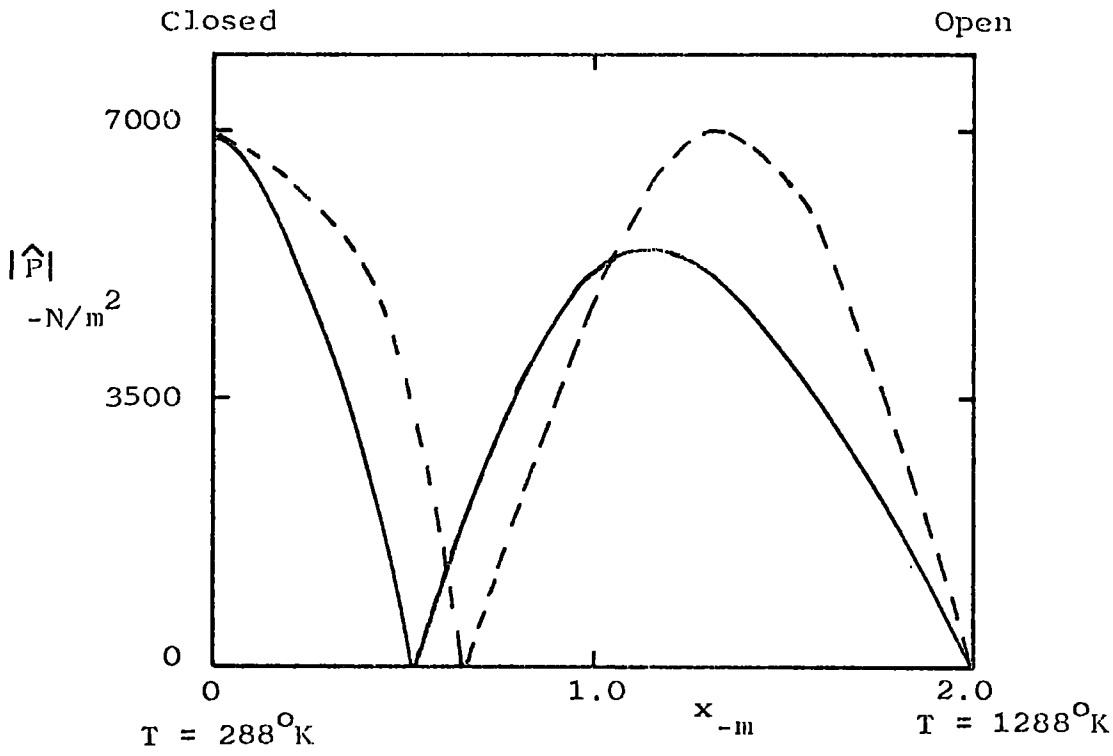

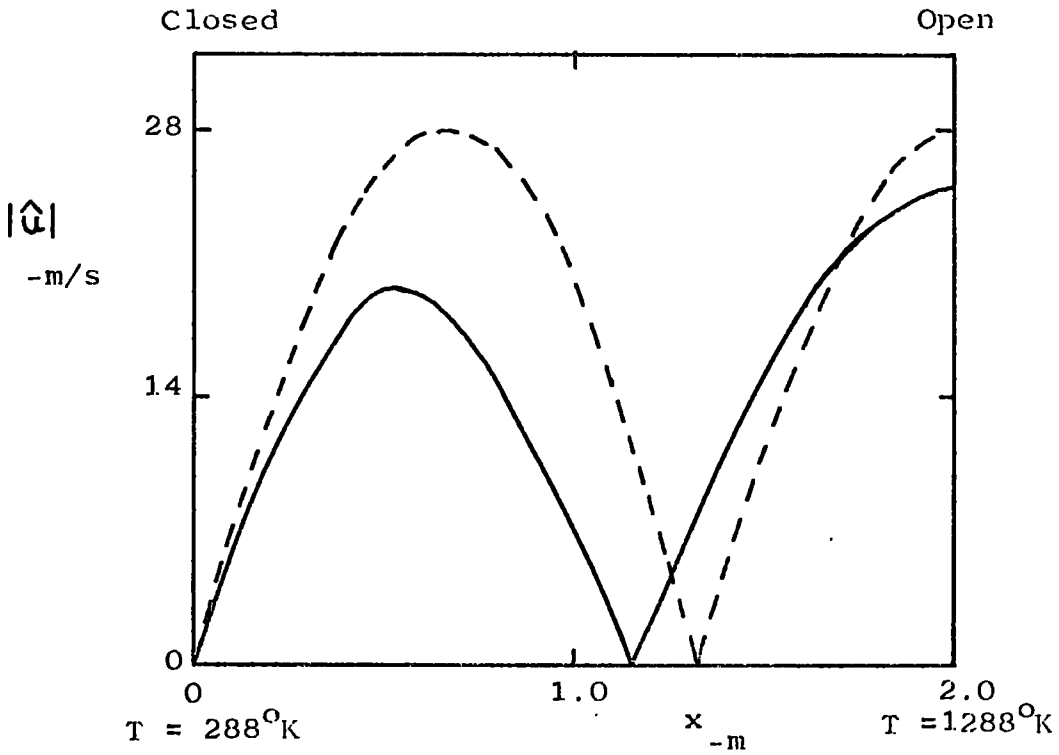

Fig.6 Modulus of Pressure/Velocity amplitude against position for 1000°C Temperature Rise

- 1st harmonic f = 191 Hz

---- Mean velocity of sound prediction

CHAPTER 4

Theory

4.1 Turbulent flow between parallel infinite plates with a resonant acoustic field

- 4.1.1 Basic System
- 4.1.2 Basic Equations
- 4.1.3 Acoustic time-varying velocity
- 4.1.4 Time mean differential equations
- 4.1.5 Time mean diffusivity
- 4.1.6 Time mean velocity
- 4.1.7 Summary

4.2 Convective heat transfer to a pulsating turbulent flow in a pipe

- 4.2.1 Steady flow
- 4.2.2 Quasi-steady flow
- 4.2.3 Frequency factor
- 4.2.4 Summary

4. Theory

4.1 Turbulent flow between parallel infinite plates with a resonant acoustic field

Two possible mechanisms have been proposed to explain the measured heat transfer coefficients in oscillating turbulent flow - first, acoustic streaming and, second, changes in the mean flow diffusivity. A survey of the literature gave little information on pulsating turbulent flow (general information on unsteady flow is reported in the Bibliography - references 48 to 59). It was proposed to investigate the turbulent flow of a perfect gas between parallel infinite walls with a resonant acoustic field - this system is used instead of pipe flow to simplify the equations.

It is assumed that the viscous effects on the acoustic velocity occur in a 'thin' region close to the walls, and apart from this area the oscillating conditions are given by inviscid flow theory. This has been shown experimentally and theoretically for laminar flow (59,60). To find the oscillating velocity profile and the time-independant acoustic streaming velocities, the method of analysis originated by Lin (61), and developed by Purdy (59), is used. By a rigorous order of magnitude analysis, independant time-dependant and time-independant differential equations are derived. It is assumed that the flow is fully developed for the analysis. To estimate the acoustic velocity profile an equivalent viscosity is defined to approximate the turbulent conditions to a laminar flow (in order to solve the basic equations). From the derived acoustic velocity profile, the possible effect of the pulsations on the mean flow diffusivity is considered. To evaluate the mean velocity profile, it is assumed that no periodic turbulence fluctuations are generated by the acoustic oscillations i.e. the time variations of the acoustic flow and of the turbulence variations are independant. The justification of this assumption for the project is discussed in Section 4.2.3. It was hoped to show from the mean velocity profile whether or not vortex formation (as derived for resonant laminar flow by Purdy (59)) is a major factor affecting heat transfer for turbulent flow.

4.1.1 Basic system

Consider the flow of a perfect gas between two infinite parallel plates separated by distance 2a.

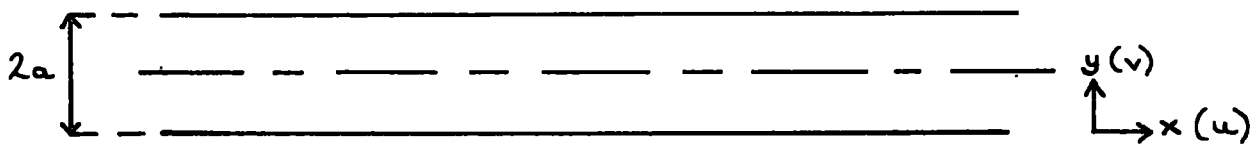

⟶ Direction of flow

Velocity field

$$u_{(x,y,t)} = \bar{u}_{(x,y)} + u_{1(x,y,t)} + \textcircled{u}_{(x,y,t)}$$

$$v_{(x,y,t)} = \bar{v}_{(x,y)} + v_{1(x,y,t)} + \textcircled{v}_{(x,y,t)}$$

where u_1, v_1 are the acoustic velocities

$\textcircled{u}$, $\textcircled{v}$ are random fluctuations of turbulent flow

By definition of the time mean values

$$\overline{u_1} = \overline{v_1} = 0$$

$$\overline{\omega} = \overline{v} = 0$$

The following boundary conditions are applicable

$$u = v = 0 \qquad \text{at} \quad y = 0,\ y = 2a$$

$$\frac{\partial \bar{u}}{\partial y} = \frac{\partial u_1}{\partial y} = 0 \qquad \text{at} \quad y = a$$

$$\bar{v} = v_1 = 0 \qquad \text{at} \quad y = a$$

From mean flow continuity,

$$\bar{U}_m = \frac{1}{a} \int_0^a \bar{u}\, dy$$

It is assumed that inviscid flow theory is applicable away from the channel walls - resonance field is defined for a velocity antinode at x = 0.

Away from wall

$$u_{1(x,t)} = -\hat{U}_A \cos\left(\omega \frac{x}{\bar{c}}\right) e^{-i\omega t}$$

Similarly for the acoustic oscillations

$$p_{1(x,t)} = -i\gamma \bar{p} \frac{\hat{U}_A}{\bar{c}} \sin\left(\omega \frac{x}{\bar{c}}\right) e^{-i\omega t}$$

$$\rho_{1(x,t)} = -i \bar{\rho} \frac{\hat{U}_A}{\bar{c}} \sin\left(\omega \frac{x}{\bar{c}}\right) e^{-i\omega t}$$

for $\bar{U}_m \ll \bar{c}$ assuming perfect reflection

(see section 3.1)

Pressure field

$$P_{(x,y,t)} = \bar{P}_{(x,y)} + P_{1\,(x,t)}$$

- it is assumed that the acoustic pressure is independant of the y co-ordinate, and that the turbulence pressure fluctuations are negligible since ⓤ and ⓥ are small.

Similarly for the density field

$$\rho_{(x,y,t)} = \bar{\rho} + \rho_{1\,(x,t)}$$

assuming mean density is independant of spatial variations

By definition

$$\bar{P}_1 = \bar{\rho}_1 = 0$$

4.1.2 Basic equations

The system is analysed using the two-dimensional equations of fluid motion expressed in cartesian co-ordinates.

Continuity

$$\frac{\partial \rho}{\partial t} + \frac{\partial}{\partial x}(\rho u) + \frac{\partial}{\partial y}(\rho v) = 0$$

Navier-Stokes

- no body forces

$$\rho\left(\frac{\partial u}{\partial t} + u\frac{\partial u}{\partial x} + v\frac{\partial u}{\partial y}\right) = -\frac{\partial p}{\partial x} + \frac{\partial}{\partial y}\left(\mu\left(\frac{\partial u}{\partial y} + \frac{\partial v}{\partial x}\right)\right) + \frac{\partial}{\partial x}\left(\mu\left(2\frac{\partial u}{\partial x} - \frac{2}{3}\left(\frac{\partial u}{\partial x} + \frac{\partial v}{\partial y}\right)\right)\right)$$

$$\rho\left(\frac{\partial v}{\partial t} + u\frac{\partial v}{\partial x} + v\frac{\partial v}{\partial y}\right) = -\frac{\partial p}{\partial y} + \frac{\partial}{\partial x}\left(\mu\left(\frac{\partial u}{\partial y} + \frac{\partial v}{\partial x}\right)\right) + \frac{\partial}{\partial y}\left(\mu\left(2\frac{\partial v}{\partial y} - \frac{2}{3}\left(\frac{\partial u}{\partial x} + \frac{\partial v}{\partial y}\right)\right)\right)$$

for derivation see reference 62

4.1.3 Acoustic time-varying velocity

To solve the basic equations, it is assumed that the resistance to wave propagation, relative to the boundary walls, of the turbulent flow can be defined by an equivalent viscosity i.e. the model is analysed as for laminar flow.

Define 'turbulent' dynamic viscosity, μ_T

By definition of the viscosity

$$\textcircled{u} = \textcircled{v} = 0$$

$$\therefore \quad u_{(x,y,t)} = \bar{u}_{(x,y)} + u_{1(x,y,t)}$$

$$v_{(x,y,t)} = \bar{v}_{(x,y)} + v_{1(x,y,t)}$$

Define the following non-dimensionals

$$u' = u/\hat{u}_A = \bar{u}' + u_1'$$
$$v' = v/\hat{u}_A = \bar{v}' + v_1'$$
$$x' = x/\lambda$$
$$y' = y/\lambda$$
$$p' = p/\bar{\rho}\hat{u}_A^2 = \bar{p}' + p_1'$$
$$\rho' = \rho/\bar{\rho} = 1 + \rho_1'$$
$$t' = t\hat{u}_A/\lambda$$

The following order of magnitudes can be derived for the non-dimensional variables, with the main constraint that $\hat{U}_A \gg \bar{U}_m$ i.e. the oscillating velocity is an order of magnitude greater than the mean velocity.

Let δ be of small order

$$x' = 1 \qquad y' = \delta$$
$$\bar{u}' = \delta \qquad u_1' = 1$$
$$\bar{v}' = \delta^2 \qquad v_1' = \delta$$
$$\rho_1' = \delta \qquad p_1' = \delta$$

The method of determining the non-dimensionals and their orders of magnitude was described by Hirbar and Purdy (63).

Express the Continuity and Navier-Stokes equations in terms of the non-dimensionals.

Continuity

$$\bar{\rho}\frac{\hat{U}_A}{\lambda}\left(\frac{\partial \rho_1'}{\partial t'} + (1+\rho_1')\frac{\partial}{\partial x'}(\bar{u}'+u_1') + (\bar{u}'+u_1')\frac{\partial \rho_1'}{\partial x'} + (1+\rho_1')\frac{\partial}{\partial y'}(\bar{v}'+v_1')\right) = 0$$

By order of magnitude analysis retaining terms ≥ 1

$$\frac{\partial \rho_1}{\partial t} + \bar{\rho}\frac{\partial u_1}{\partial x} + \bar{\rho}\frac{\partial v_1}{\partial y} = 0 \qquad \ldots\ldots 1$$

Navier-Stokes

Similar procedure gives

$$\bar{\rho}\left(\frac{\partial u_1}{\partial t} + u_1\frac{\partial u_1}{\partial x} + v_1\frac{\partial u_1}{\partial y}\right) = -\frac{\partial p_1}{\partial x} + \frac{\partial}{\partial y}\left(\mu_T\frac{\partial u_1}{\partial y}\right) \qquad \ldots\ldots 2$$

assuming $\mu_T / \bar{\rho}\hat{U}_A\lambda = \delta^2$

The equations can be solved by the method of successive approximations (58).

Let $u_1 = u_{10} + u_{11}$

$v_1 = v_{10} + v_{11}$

where $u_{11} << u_{10}$

$v_{11} << v_{10}$

Substitute into 1 and 2 to give

$$\frac{\partial u_{10}}{\partial x} + \frac{\partial v_{10}}{\partial y} = -\frac{1}{\bar{\rho}}\left(\frac{\partial \rho_1}{\partial t}\right)$$

..... 3

$$\frac{\partial u_{11}}{\partial x} + \frac{\partial v_{11}}{\partial y} = 0$$

..... 4

$$\frac{\partial p_1}{\partial x} + \bar{\rho}\frac{\partial u_{10}}{\partial t} = \frac{\partial^2}{\partial y^2}\left(\mu_T \frac{\partial u_{10}}{\partial y}\right)$$

..... 5

$$\bar{\rho}\left(\frac{\partial u_{11}}{\partial t} + u_{10}\frac{\partial u_{10}}{\partial x} + v_{10}\frac{\partial u_{10}}{\partial y}\right) = \frac{\partial^2}{\partial y^2}\left(\mu_T \frac{\partial u_{11}}{\partial y}\right)$$

..... 6

Define

$$u_{10} = \hat{U}_A \cos\left(\omega \frac{x}{\bar{c}}\right) \cdot F_{(y)} \cdot e^{-i\omega t}$$

from inviscid flow theory

Substitute into 5 to find $F_{(y)}$

$$\therefore \quad \frac{\mu_T}{\bar{e}} \cdot F''_{(y)} + i\omega F_{(y)} + i\omega = 0$$

since $$p_1 = -i\gamma \bar{p} \frac{\hat{U}_A}{\bar{c}} \sin\left(\omega \frac{x}{\bar{c}}\right) e^{-i\omega t}$$

General solution

$$F_{(y)} = -1 + A e^{\beta(1-i)y} + B e^{-\beta(1-i)y}$$

where A, B are constants

for $$\beta = \sqrt{(\omega / 2\bar{\upsilon}_T)}$$

with $$\bar{\upsilon}_T = \mu_T / \bar{e}$$

From the boundary conditions and equation 3 the velocity components are

$$u_{10} = -\hat{U}_A \cos\left(\omega \frac{x}{\bar{c}}\right)\left(\cos(\omega t) - e^{-\beta y}\cos(\omega t - \beta y)\right)$$

$$v_{10} = \frac{\hat{U}_A}{\sqrt{2}\beta\bar{c}} \omega \sin\left(\omega \frac{x}{\bar{c}}\right)\left(\cos(\omega t - \frac{\pi}{4}) - e^{-\beta y}\cos(\omega t - \frac{\pi}{4} - \beta y)\right)$$

From equations 4 and 6, the second approximations (u_{11}, v_{11}) can be calculated - it can be shown that they are negligible relative to the first approximations.

$$\therefore \quad u_1 = u_{10}$$

$$v_1 = v_{10}$$

The equation shows that the acoustic velocity, u_1, approaches inviscid conditions as $e^{-\beta y} \rightarrow 0$. It is assumed that flow can be considered inviscid at position y_β from the walls when $e^{-\beta y} = 0.01$.

Let y_β be defined as limiting viscous layer

$$\therefore \quad y_\beta = 4.61 / \beta$$

It should be noted that the velocity, v_1, must tend to zero as $y \rightarrow a$ to satisfy the boundary condition. The error in the derived expression is due to neglecting the contribution of the y - momentum equation.

The oscillating velocities have been derived assuming laminar flow with an equivalent viscosity. The definition of this approximate viscosity will now be considered.

For turbulent flow, Boussinesq proposed in 1877 the concept of a mixing coefficient such that

$$\text{Shear stress} = \rho(\upsilon + \varepsilon_M)\frac{du}{dy} \qquad (64)$$

where ε_M is the momentum eddy diffusivity (mixing coefficient)

The diffusivity is a function of the flow and position. Turbulent flow is of such complexity that the mixing coefficient cannot be described exactly, but, in 1925, Prandtl proposed the Mixing Length hypothesis (65).

$$\varepsilon_M = l^2 \left| \frac{du}{dy} \right|$$

where $l = 0.4\ y$

From this semi-empirical approach, a universal velocity profile can be derived which is in good agreement with experimental results (66). Using the velocity profile and experimental measurements of friction factor, the following expression can be derived for the turbulent core

$$\varepsilon_M = \upsilon\left(\frac{0.04}{a^2}\, Re_a^{\frac{7}{8}}\,(a-y)y - 1\right)$$

..... 7

(66)

As defined above the total diffusivity goes to zero at the centreline (y = a). This is not physically realistic, and it has been shown (66) that a better representation is to use equation 7 for $y \leq a/2$, and assume a constant diffusivity, equal to that at $y = \frac{a}{2}$, for the central region. It must be stressed that the Mixing Length hypothesis is only a simple approach to describe turbulent flow, and is only one of many analyses.

The 'equivalent' viscosity, $\bar{\upsilon}_T$, is defined, for a point in the flow, as the average diffusivity between that point and the channel wall calculated from the eddy diffusivity of an equivalent turbulent flow with the same mean flowrate - this can be considered as an approximation of the resistance to acoustic wave propagation.

For point distance y from the wall

$$\bar{\upsilon}_T = 0{\cdot}04\,\upsilon\,\overline{Re}_a^{\frac{7}{8}}\,\frac{y}{2}\left(a - \frac{2}{3}y\right)\frac{1}{a^2}$$

for $y \leq a/2$

$$\bar{\upsilon}_T = 0{\cdot}04\,\upsilon\,\overline{Re}_a^{\frac{7}{8}}\left(\frac{a}{12} + \left(y - \frac{a}{2}\right)\frac{1}{4}\right)\frac{1}{y}$$

for $a/2 < y \leq a$

A simple iteration process is used to evaluate the limiting viscous layer, y_β.

$$y_\beta = 4{\cdot}61/\beta$$

for $\beta = \sqrt{(\omega/2\bar{\upsilon}_T)}$

The starting value is given by using $\bar{\upsilon}_T = \upsilon$ (laminar flow conditions), and the iteration is convergent within a maximum of 30 steps.

For the turbulent flow, the oscillating velocity profile is not only a function of frequency and fluid property (as for laminar flow), but also a function of mean Reynolds number - see the above equations.

The equivalent channel flow to the experimental pipe flow system of the project was analysed to determine the decay constant, β, relative to laminar theory predictions (i.e. $\beta_L = \sqrt{(\omega/2\upsilon)}$). A turbulent air flow at 30°C in a channel of 0.04 m width was considered for a frequency range of 25 to 225Hz.

$\overline{Re}_a$ = 13,500

Frequency - Hz	β - 1/m	β_L - 1/m
25.0	405.68	2185.0
125.0	1416.55	4890.0
225.0	2427.28	6560.0

$\overline{Re}_a$ = 29,600

Frequency - Hz	β - 1/m	β_L - 1/m
25.0	269.84	2185.0
125.0	790.09	4890.0
225.0	1299.66	6560.0

The decay constant is decreased for the turbulent conditions relative to the laminar flow predictions. But the profile is dependant on the mean Reynolds number - as $\overline{Re}_a \longrightarrow 2000$, $\beta \longrightarrow \beta_L$.

The experimental work of Bogdanoff (42) provided a limited check. Using a hot-wire anemometer, the acoustic velocity profile was found for a frequency of 270 Hz with Reynolds number 100,000 in a pipe of diameter 0.04 m. The criterion for comparison was the decay distance, y_β .

From experimental graph, y_β = 0.00280 m

Predicted decay distance, y_β = 0.00243 m

% Difference = -13%

For this very limited comparison, good agreement was obtained between theory and experiment. No other experimental work could be found in the literature for comparison.

It must be stressed that the derived acoustic velocity profiles can only be regarded as approximate with the lack of experimental comparison.

4.1.4 Time mean differential equations

The equivalent viscosity approximation is not used to evaluate the time mean velocity profile.

Let $u = \tilde{u} + \textcircled{u}$

i.e. $\tilde{u} = \bar{u} + u_1$

$v = \tilde{v} + \textcircled{v}$

i.e. $\tilde{v} = \bar{v} + v_1$

Substitute into the Continuity and Navier-Stokes equations

Continuity

Time average equation

$$\frac{\partial}{\partial x}\overline{(\rho\tilde{u})} + \frac{\partial}{\partial y}\overline{(\rho\tilde{v})} + \frac{\partial}{\partial x}\overline{(\rho\omega)} + \frac{\partial}{\partial y}\overline{(\rho\omega)} = 0$$

From mean value theorems (62)

$$\frac{\partial}{\partial x}\overline{(\rho\omega)} = \frac{\partial}{\partial x}\overline{(\bar{\rho} + \rho_1)\omega}$$

$$= \frac{\partial}{\partial x}\overline{(\bar{\rho}\omega)} + \frac{\partial}{\partial x}\overline{(\rho_1\omega)}$$

$$= \frac{\partial}{\partial x}\overline{(\rho_1\omega)}$$

since $\bar{\rho}\,\frac{\partial}{\partial x}\overline{(\omega)} = 0$

To evaluate the above expression, the relationship between the oscillating components and random turbulence fluctuations must be known. It is assumed that the time-variations are independant.

For independant variables, X & Y

$$\overline{X.Y} = \overline{X}.\overline{Y} \qquad (67)$$

$$\therefore \frac{\partial}{\partial x}\overline{(\rho_1\omega)} = 0$$

Similarly

$$\frac{\partial}{\partial y}\overline{(\rho \textcircled{v})} = 0$$

$$\therefore \frac{\partial}{\partial x}\overline{(\rho \tilde{u})} + \frac{\partial}{\partial y}\overline{(\rho \tilde{v})} = 0$$

..... 8

Navier-Stokes

X-direction

Consider system as boundary layer flow

$$\therefore \rho\left(\frac{\partial u}{\partial t} + u\frac{\partial u}{\partial x} + v\frac{\partial u}{\partial y}\right) = -\frac{\partial p}{\partial x} + \frac{\partial}{\partial y}\left(\mu\left(\frac{\partial u}{\partial y}\right)\right)$$

Substitute and time average

$$\therefore \overline{\rho\frac{\partial}{\partial t}(\tilde{u}+\textcircled{u})} + \overline{\rho(\tilde{u}+\textcircled{u})\frac{\partial}{\partial x}(\tilde{u}+\textcircled{u})}$$

$$+ \overline{\rho(\tilde{v}+\textcircled{v})\frac{\partial}{\partial y}(\tilde{u}+\textcircled{u})} = -\frac{\partial \bar{p}}{\partial x} + \frac{\partial}{\partial y}\left(\mu\frac{\partial \bar{u}}{\partial y}\right)$$

Similar analysis as for Continuity

$$\therefore \overline{\rho\frac{\partial \tilde{u}}{\partial t}} + \overline{\rho\tilde{u}\frac{\partial \tilde{u}}{\partial x}} + \overline{\rho\tilde{v}\frac{\partial \tilde{u}}{\partial y}}$$

$$= \frac{\partial}{\partial y}\left(\mu\frac{\partial \bar{u}}{\partial y}\right) - \frac{\partial \bar{p}}{\partial x} - \bar{\rho}\left(\overline{\textcircled{u}\frac{\partial \textcircled{u}}{\partial x}} + \overline{\textcircled{v}\frac{\partial \textcircled{u}}{\partial y}}\right)$$

Consider terms

$$\bar{\rho}\,\overline{u}\,\frac{\partial \overline{u}}{\partial x}\ ,\quad \bar{\rho}\,\overline{v}\,\frac{\partial \overline{u}}{\partial y}$$

- these are not zero since $\overline{u}$ and $\overline{v}$ are dependant (68)

Write as

$$\bar{\rho}\left(\frac{\partial}{\partial x}\overline{(u^2)} + \frac{\partial}{\partial y}\overline{(uv)} - \overline{u}\left(\frac{\partial \overline{u}}{\partial x} + \frac{\partial \overline{v}}{\partial y}\right)\right)$$

From the Continuity equation it can be shown that

$$\overline{\bar{\rho}\left(u\frac{\partial u}{\partial x} + u\frac{\partial v}{\partial y}\right)} = 0$$

$$\therefore\ \bar{\rho}\left(\overline{u\frac{\partial u}{\partial x}} + \overline{v\frac{\partial u}{\partial y}}\right) = \bar{\rho}\left(\frac{\partial}{\partial x}\overline{(u^2)} + \frac{\partial}{\partial y}\overline{(uv)}\right)$$

Terms on R.H.S. are Reynolds Stresses differentials

$\bar{\rho}\,\overline{u}^2$ = direct stress x plane

$\bar{\rho}\,\overline{u}\,\overline{v}$ = Shear stress x-y plate

(62)

Since boundary layer flow

$$\frac{\partial}{\partial x}\overline{(u^2)} \ll \frac{\partial}{\partial y}\overline{(uv)}$$

Equation becomes

$$\overline{\rho \frac{\partial \tilde{u}}{\partial t}} + \overline{\rho \tilde{u} \frac{\partial \tilde{u}}{\partial x}} + \overline{\rho \tilde{v} \frac{\partial \tilde{u}}{\partial y}}$$

$$= -\frac{\partial \bar{p}}{\partial x} + \frac{\partial}{\partial y}\left(\mu \frac{\partial \bar{u}}{\partial y}\right) - \bar{\rho} \overline{\frac{\partial}{\partial y}(\omega v)} \qquad \ldots\ldots 9$$

The equations 8 and 9 are expressed as non-dimensionals, and order of magnitude analysis used to retain major terms - as for the analysis of oscillating velocity components.

The following equations are derived

Continuity

$$\frac{\partial \bar{u}}{\partial x} + \frac{\partial \bar{v}}{\partial y} = -\frac{1}{\bar{\rho}} \overline{\left(u_1 \frac{\partial \rho}{\partial x} + \rho_1 \frac{\partial u_1}{\partial x} + \rho_1 \frac{\partial v_1}{\partial y}\right)} \qquad \ldots\ldots 10$$

Navier-Stokes

$$\frac{\partial}{\partial y}\left(\mu \frac{\partial \bar{u}}{\partial y}\right) - \bar{\rho} \overline{\frac{\partial}{\partial y}(\omega v)} - \frac{\partial \bar{p}}{\partial x}$$

$$= \overline{\bar{\rho}\left(u_1 \frac{\partial u_1}{\partial x} + v_1 \frac{\partial u_1}{\partial y} + \frac{\rho_1}{\bar{\rho}} \frac{\partial u_1}{\partial t}\right)} \qquad \ldots\ldots 11$$

- to solve the differential equations the Reynolds Stress $\bar{\rho}\overline{\omega v}$ must be known.

4.1.5 Time mean diffusivity

The effect of the oscillating velocity on the momentum diffusivity of the flow, at a point, is considered.

For pulsating flow, the generated turbulence stresses are very complex and cannot be predicted in general - hot wire anenometry would have to be used to investigate the turbulence properties. It is assumed that there is no resonance interaction between the oscillating frequency and the turbulence fluctuations, but the magnitude of the Reynolds stress may depend on the acoustic velocity gradient. There are two extremes which can be considered theoretically. If the acoustic frequency is very high ($\omega \rightarrow \infty$), the rate of change of flow conditions is such that the diffusivity can be considered to depend only on the mean flow. If the frequency is very small ($\omega \rightarrow 0$), a quasi-steady analysis is applicable i.e. the rate of change is such that the diffusivity, at an instance of the cycle, is dependant on the instantaneous velocity gradient. For the frequency range of the project, the conditions were between the two extremes as would be expected for most practical situations. The position of a system relative to the extremes is discussed in Section 4.2.3.

It was decided to investigate quasi-steady conditions, and evaluate a time-independant diffusivity. It is assumed in the analysis that the turbulent properties of a point along the channel are only dependant on the mean flowrate and the acoustic velocity (u_1) at that point. The velocity, v_1 , is defined to have negligible effect on the mean diffusivity - the oscillations are considered to occur in the laminar sub-layer regime ($v_1 \longrightarrow 0$ as $y \longrightarrow y_\beta$). From the analysis of oscillating velocity profile, assuming phase angle effects to be negligible,

$$u_1 = \hat{U} \cos(\omega t)(1 - e^{-\beta y})$$

for a point of velocity amplitude $\hat{U}$.

To allow for the diffusivity of the mean flowrate let

$$u_s = \bar{U}_m (1 - e^{-\beta y})$$

- this is an approximation to simplify calculation of total diffusivity.

Define flow conditions by a laminar sub-layer and turbulent core (no buffer layer).

For the turbulent core,

Diffusivity at any, instance of time $\varepsilon_{M(t)} = \ell^2 \left| \frac{\partial u_s}{\partial y} + \frac{\partial u_1}{\partial y} \right|$

by Prandtl Mixing Length hypothesis

$$\therefore \varepsilon_{M(t)} = \ell^2 \beta e^{-\beta y} \left| \bar{U}_m + \hat{U} \cos(\omega t) \right|$$

For the laminar sub-layer, $\varepsilon_{M_{(t)}} = 0$

For steady flow,

Sub-layer, $\delta_{SL} = 120\, a \Big/ Re_a^{\frac{7}{8}}$

thickness

(66)

for $4000 \leqslant Re_a \leqslant 100{,}000$

$\delta_{SL} = a$ if $Re_a \leqslant 2000$

- for $2000 < Re_a < 4000$ calculate the sub-layer thickness by linear interpolation from the above limits

Define

Sub-layer thickness, at any instance of time $\delta_{SL_{(t)}} = 120\, a \Big/ Re_{a_{(t)}}^{\frac{7}{8}}$

where $Re_{a_{(t)}} = \frac{2a}{\bar{\upsilon}} \left| \bar{u}_M + \hat{u} \cos(\omega t) \right|$

for the defined limits

To evaluate time-mean diffusivity define an equivalent viscosity, $\varepsilon_{M_{(t)}}$, for any instance of time

$$\varepsilon_{M_{(t)}} = \frac{1}{a}\left(\bar{\upsilon} \cdot \delta_{SL_{(t)}} + A_{(y)} \left| \bar{u}_m + \hat{u} \cos(\omega t) \right| (a - \delta_{SL_{(t)}}) \right)$$

where $A_{(y)}$ is a factor to allow for y variation of diffusivity in the turbulent core.

It is assumed that the factor $A_{(y)}$ is approximately constant for all conditions.

Evaluate mean value over period

$$\therefore \overline{\varepsilon}_M = \frac{1}{a}\left(\bar{\upsilon} \cdot \overline{\delta_{SL_{(t)}}} + A_{(y)} \cdot a \overline{\left| \bar{u}_m + \hat{u} \cos(\omega t) \right|} - A_{(y)}\, \delta_{SL_{(t)}} \left| \bar{u}_m + \hat{u} \cos(\omega t) \right| \right)$$

$$\therefore \overline{\textcircled{\varepsilon}}_M = \frac{\bar{v}}{a} \cdot \overline{\delta_{SL}} + A_{(y)} \overline{|\bar{u}|} - \frac{B_{(y)}}{a} \overline{\delta_{SL_{(t)}} |u|_{(t)}}$$

where $$|u|_{(t)} = |\bar{u}_M + \hat{u} \cos(\omega t)|$$

$$\overline{|u|} = \overline{|\bar{u}_M + \hat{u} \cos(\omega t)|}$$

The equivalent time-mean diffusivity must be equal to the above expression. It is assumed that the mean diffusivity can be expressed as an equivalent laminer sub-layer, thickness δ_E, with turbulent core given by

$$\bar{\varepsilon}_{M_c} = \ell^2 \beta e^{-\beta y} \overline{|\bar{u}_M + \hat{u} \cos(\omega t)|}$$

this assumption simplifies the mathematical evaluation.

$$\therefore \overline{\textcircled{\varepsilon}}_M = \frac{1}{a} \left(\bar{v} \cdot \delta_E + A_{(y)} \overline{|\bar{u}|} (a - \delta_E) \right)$$

Evaluate δ_E

$$\bar{v} \cdot \delta_E + A_{(y)} \overline{|\bar{u}|} (a - \delta_E)$$

$$= \bar{v} \cdot \overline{\delta_{SL}} + A_{(y)} a \overline{|\bar{u}|} - A_{(y)} \overline{\delta_{SL_{(t)}} |u|_{(t)}}$$

But $$\bar{v} << A_{(y)} \cdot \overline{|\bar{u}|}$$

$$\bar{v} \cdot \overline{\delta_{SL}} << A_{(y)} \overline{\delta_{SL_{(t)}} |u|_{(t)}}$$

$$\therefore \delta_E = \frac{\overline{\delta_{SL_{(t)}} \cdot |u|_{(t)}}}{\overline{|\bar{u}|}}$$

This analysis has approximated for <u>quasi-steady conditions</u> the time-mean diffusivity in terms of a laminar sub-layer thickness, δ_E and turbulent core diffusivity, $\bar{\varepsilon}_{M_c}$

It can be shown that

$$\overline{\varepsilon}_{M_c} = 0.16\, y^2\, \bar{u}_m\, \beta\, e^{-\beta y}\left(\pi + 2B\sin(XX) - 2XX\right)/\pi$$

where $XX = \cos^{-1}(1/B)$ For $B > 1$

$XX = 0$ For $B \leq 1$

$$\delta_E = \frac{\overline{\delta_{sl(\omega)} \cdot |u|_{(\omega)}}}{|\bar{u}|}$$

where $$|\bar{u}| = \frac{\bar{u}_m}{\pi}\left(\pi + 2B\sin(XX) - 2XX\right)$$

It can be seen from the equations that the core diffusivity is a function of Dimensionless pulsation velocity (B), frequency ($\beta = g$ (Frequency)) and mean flowrate - the sub-layer thickness is independant of frequency. For $B < 1$, for a given flowrate and frequency, the core diffusivity is unchanged but the sub-layer thickness is increased, with a maximum at $B = 1$, relative to steady flow. For $B > 1$ the diffusivity of the core is increased.

Although only quasi-steady analysis has been considered, one can assume that changes in diffusivity can occur for higher frequencies - at the other extreme, as $\omega \rightarrow \infty$, the diffusivity is as for the equivalent steady flow. Bogdanoff (42) showed experimentally, from measurements of mean velocity profile, changes in mean diffusivity for a frequency of 270 Hz.

4.1.6 Time-mean velocity

Equation 11 can be written as

$$\frac{\partial}{\partial y}\left((\mu + \bar{\rho}\,\overline{\varepsilon}_M)\frac{\partial \bar{u}}{\partial y}\right) - \frac{\partial \bar{p}}{\partial x} = \overline{\bar{\rho}\left(u_1\frac{\partial u_1}{\partial x} + v_1\frac{\partial u_1}{\partial y} + \frac{\rho_1}{\bar{\rho}}\frac{\partial u_1}{\partial t}\right)} = Q$$

assuming that the turbulence stress can be expressed in terms of a mean diffusivity ε_M.

R.H.S. of the equation can be evaluated from the derived equations.

Substitution and integration gives

$$Q = -\frac{\omega}{4\bar{c}}\hat{U}_A^2 \sin\left(2\omega\frac{x}{\bar{c}}\right)\left(2 - e^{-\beta y}\left(3\cos(\beta y) - \sin(\beta y) - e^{-\beta y}\right)\right)$$

Equation can be written as

$$\frac{\partial}{\partial y}\left((\bar{\upsilon} + \bar{\varepsilon}_M)\frac{\partial \bar{u}}{\partial y}\right) = X + \frac{\omega}{4\bar{c}}\hat{U}_A^2 \sin\left(2\omega\frac{x}{\bar{c}}\right)e^{-\beta y}\left(3\cos(\beta y) - \sin(\beta y) - e^{-\beta y}\right)$$

where $X = g(x)$

Integrate

Boundary condition

$$\frac{\partial \bar{u}}{\partial y} = 0 \quad \text{at} \quad y = a$$

$$\therefore \quad (\bar{\upsilon} + \bar{\varepsilon}_M)\frac{\partial \bar{u}}{\partial y} = X(y - a) + G_{cx}\left(\frac{e^{-\beta y}}{2\beta}\left(4\sin(\beta y) - 2\cos(\beta y) + e^{-\beta y}\right)\right)$$

where $G_{cx} = \frac{\omega}{4\bar{c}}\hat{U}_A^2 \sin\left(2\omega\frac{x}{\bar{c}}\right)$

To evaluate mean velocity profile

Integrate

$$\bar{u} = X \int_0^y \frac{(y-a)}{(\bar{\upsilon}+\bar{E}_M)} dy + G_{(x)} \int_0^y \frac{e^{-\beta y}}{2\beta} \frac{1}{(\bar{\upsilon}+\bar{E}_M)} \left(4\sin(\beta y) - 2\cos(\beta y) + e^{-\beta y}\right) dy$$

To evaluate X

$$X \int_0^a \int_0^y \frac{(y-a)}{(\bar{\upsilon}+\bar{E}_M)} dy\,dy = a\,\bar{u}_M - G_{(x)} \int_0^a \int_0^y \frac{e^{-\beta y}}{2\beta} \frac{1}{(\bar{\upsilon}+\bar{E}_M)} \left(4\sin(\beta y) - 2\cos(\beta y) + e^{-\beta y}\right) dy\,dy$$

To solve the equations and evaluate the velocity profile, the mean diffusivity must be known. An estimate of the profile can be made by considering the two possible extremes of the system i.e. assuming quasi-steady conditions (as derived in Section 4.1.5), and unchanged diffusivity, relative to the equivalent steady flow, as defined for high frequency oscillation ($\omega \longrightarrow \infty$). The results of these two conditions would give an indication to the magnitude of the acoustic streaming velocities. It is not possible to define the overall acoustic streaming effects for turbulent flow due to the complexity of the equations and the lack of an analytical solution - the integrals can only be solved numerically (use Trapezoidal rule (58)). From the solution of the integral equations the mean velocity $\bar{v}$ can be found by substitution in equation 10. By comparison of relative amplitudes, it was shown that the component $\bar{v}$ could be neglected.

Relative to the work of the project, the equivalent channel flow to the experimental pipe flow system was analysed to find the mean velocity profile i.e. air flow, at 30°C, in a channel of width 0.04 m with Reynolds number range 10,000 to 35,000, maximum Dimensionless pulsation velocity 6.0 and frequency range 25 Hz to 225 Hz. The system was analysed for both the extremes i.e. quasi-steady and steady flow diffusivity. In both cases, the acoustic streaming velocities were small (15% maximum in the turbulent core), and the standing vortex formation was not predicted. It was considered that, for the experimental investigation, acoustic streaming would not be a major factor defining convective heat transfer.

The integrals can be approximated to give an analytical solution - this is to give an insight into general effects of acoustic streaming for turbulent flow. For the field of interest, the range of pulsation variables can be limited from the literature survey - resonant frequencies from 0 to 500 Hz, and maximum Dimensionless pulsation velocity 6. It is assumed that the diffusivity is dependant on mean flowrate only.

It has been shown that

$$\bar{u} = X \int_0^y \frac{(y-a)}{(\bar{\upsilon}+\bar{E}_M)}\, dy + G_{(x)} \int_0^y \frac{e^{-\beta y}}{2\beta} \frac{1}{(\bar{\upsilon}+\bar{E}_M)} \left(4\sin(\beta y) - 2\cos(\beta y) + e^{-\beta y} \right) dy$$

$$= I_A + I_B$$

Assume for the integral I_B that the diffusivity can be approximated to the equivalent viscosity $\bar{\upsilon}_T$, as defined in the evaluation of the acoustic velocity profile (since $e^{-\beta y} \longrightarrow 0$ as $y \longrightarrow y_\beta$)

$$\therefore I_B = \frac{G_{(x)}}{\bar{\upsilon}_T} \cdot \frac{1}{4\beta^2} \left(3 - e^{-\beta y} \left(6\sin(\beta y) + 2\cos(\beta y) + e^{-\beta y} \right) \right)$$

But $\beta^2 = \omega / 2\bar{\upsilon}_T$

Substituting for $G_{(x)}$ gives

$$I_B \approx \frac{\hat{U}_A^2}{8\bar{c}} \sin\left(2\omega \frac{x}{\bar{c}}\right) \left(3 - e^{-\beta y} \left(6\sin(\beta y) + 2\cos(\beta y) + e^{-\beta y} \right) \right)$$

By similar assumption

$$I_A = \left(a\bar{U}_m - \frac{G_{(x)}}{\upsilon_T} \left(\frac{3a}{2\beta} - \frac{9}{4\beta^2} \right) \right) \frac{\int_0^y \frac{(y-a)}{(\bar{\upsilon}+\bar{E}_M)}\, dy}{\int_0^a \int_0^y \frac{(y-a)}{(\bar{\upsilon}+\bar{E}_M)}\, dy\, dy}$$

For the equivalent steady flow

i.e. assuming the acoustic streaming components to be negligible

$$u = a\,\bar{U}_m \int_0^y \frac{(y-a)}{(\bar{\nu}+\bar{\varepsilon}_M)}\,dy \Big/ \int_0^a \int_0^y \frac{(y-a)}{(\bar{\nu}+\bar{\varepsilon}_m)}\,dy\,dy .$$

Assume that the velocity profile of the equivalent steady flow can be described by the 1/7th power law.

$$u = U_c (y/a)^{1/7}$$

where U_c is the centre - line velocity

By substitution

$$I_A = U_c (y/a)^{1/7} - \frac{3}{8}\,\frac{\hat{U}_A^2}{\bar{c}}\,\frac{1}{\bar{U}_m}\sin\left(\frac{2\omega x}{\bar{c}}\right)\left(1-\frac{3}{2a\beta}\right)U_c\left(\frac{y}{a}\right)^{1/7}$$

For the range of variables, the expression can be approximated to

$$I_A \approx U_c (y/a)^{1/7}$$

since $\frac{3}{8}\,\frac{\hat{U}_A^2}{\bar{c}}\,\frac{1}{\bar{U}_m}\left(1-\frac{3}{2a\beta}\right) \ll 1$

$$\bar{u} = I_A + I_B$$

$$\therefore \bar{u} = U_c (y/a)^{1/7} + \frac{\hat{U}_A^2}{8\bar{c}}\sin\left(\frac{2\omega x}{\bar{c}}\right)\left(3 - e^{-\beta y}\left(2\cos(\beta y) + 6\sin(\beta y) + e^{-\beta y}\right)\right)$$

Compare to laminar flow

$$\bar{u} = \frac{3}{2}\bar{U}_m\left(2ay - y^2\right) + \frac{\hat{U}_A^2}{8\bar{c}}\sin\left(\frac{2\omega x}{\bar{c}}\right)\left(3 - e^{-\beta y}\left(2\cos(\beta y) + 6\sin(\beta y) + e^{-\beta y}\right)\right)$$

For laminar flow, the limiting viscous layer is close to the channel wall

i.e. $e^{-\beta y} \approx 0$ except for close to the wall

$$\therefore \bar{u} \approx \frac{3}{2}\bar{U}_m\left(2ay - y^2\right) + \frac{3}{8}\frac{\hat{U}_A^2}{\bar{c}}\sin\left(\frac{2\omega x}{\bar{c}}\right)$$

Maximum size of vortex at $x = 3\lambda/8$

i.e. $\sin\left(\frac{2\omega x}{\bar{c}}\right) = -1$

$$\therefore \bar{u} \approx \frac{3}{2}\bar{U}_m\left(2ay - y^2\right) - \frac{3}{8}\frac{\hat{U}_A^2}{\bar{c}}$$

For $x = 3\lambda/8$

Vortex formation if

$$\frac{3}{8}\frac{\hat{U}_A^2}{\bar{c}} > \frac{3}{2}\left(2ay - y^2\right)\bar{U}_m$$

for $y_\beta \leq y \leq a$

The exact equations for predicting vortex size in laminar channel flow are given by Purdy (59).

For turbulent flow, by definition of the velocity profile by the 1/7th power law, the velocity gradients are greater in comparison to the laminar profile close to the wall. Consequently, for the same relative conditions, the size of vortex would be decreased i.e. reverse flow occurs closer to the channel wall. But, for turbulent flow, the limiting viscous layer is increased compared to laminar conditions - the effect on vortex formation cannot be neglected.

Consequently, for $x = \frac{3\lambda}{8}$ vortex formation is defined by

$$\frac{\hat{U}_A^2}{8\bar{\varepsilon}}\left(3 - e^{-\beta y}\left(2\cos(\beta y) + 6\sin(\beta y)\right) + e^{-\beta y}\right) > U_c\left(y/a\right)^{\frac{1}{7}}$$

- it can be seen that for $y < y_\beta$, $\bar{u} \longrightarrow U_c(y/a)^{\frac{1}{7}}$ as $y \longrightarrow 0$.

The increased velocity gradients and the increased limiting viscous layer indicate that vortex formation would be limited to high amplitude oscillations - for the defined range of pulsation parameters, it would appear that acoustic streaming was not a major factor in defining heat transfer.

But, to find the mean velocity profile, the derived integrals must be numerically integrated for each set of conditions.

4.1.7 Summary

The analysis derives the acoustic velocity profile by approximating the flow to laminar conditions using an equivalent viscosity - for very limited experimental comparison, good agreement was obtained.

It is assumed that the time variations of the pulsations and the turbulence are independant, but the time-mean diffusivity can be increased or decreased due to the oscillating velocity - it is only possible to predict theoretically for quasi-steady conditions. For very high frequencies ($\omega \longrightarrow \infty$) the transport properties would be unchanged.

Assuming quasi-steady or steady-state diffusivity, the mean velocity profile can be found by numerical integration. Relative to the experimental investigation, an analysis of the equivalent channel flow showed negligible acoustic streaming velocities - no vortex formation. An approximate analytical solution indicated that the effect of acoustic streaming on heat transfer, for the defined range of variables, would be minimal for turbulent flowrates.

4.2 Convective heat transfer to a pulsating turbulent flow in a pipe

It was decided to investigate the effect of the changes in mean diffusivity, generated by the acoustic velocity, on heat transfer coefficient - acoustic streaming effects are assumed negligible. But, theoretically, it is only possible to derive the diffusivity for quasi-steady conditions. For high frequency ($\omega \longrightarrow \infty$) steady-state diffusivity is defined and thus, relative to the equivalent steady flow, heat transfer characteristics are unchanged.

For practical systems, the conditions are between the two extremes. If all oscillations are considered quasi-steady in order to give a prediction of heat transfer, a frequency correction factor could be derived from a comparison of experimental measurements and the predicted coefficients. The factor would define the actual flow diffusivity, in terms of heat transfer, relative to the quasi-steady diffusivity. By definition of the changes in mixing coefficient, quasi-steady pulsations would represent the maximum possible variation in heat transfer i.e. the measured heat transfer changes would be less than the theoretical predictions.

The aim of the project was to investigate time independant energy transfer i.e. consider convective heat transfer to the mean flow. The pulsations are defined to affect the mixing coefficient only i.e. analyse as a steady flow with diffusivity dependant on the pulsation parameters.

4.2.1 Steady flow

Consider a steady flow of air, at bulk velocity U_m, in a pipe of diameter d (radius R) with a constant heat flux input along the pipe ($\dot{q}$)

Co-ordinate system

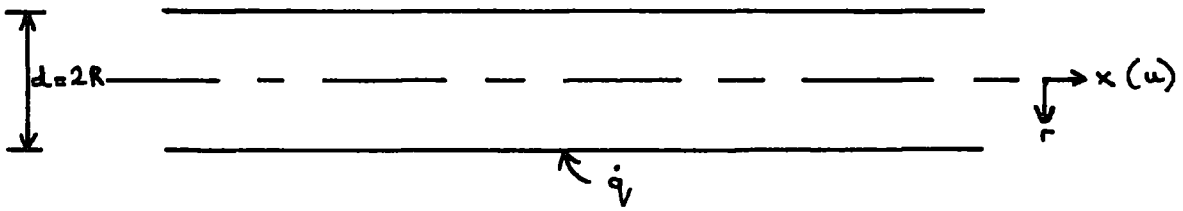

Energy equation

The following assumptions are made

(a) Low velocities

(b) Negligible pressure gradient

(c) Symmetrical heat transfer

(d) Negligible axial conduction

(e) Perfect gas

(f) Constant properties

For fully developed conditions,

$$u \frac{\partial T}{\partial x} = \frac{1}{r} \frac{\partial}{\partial r}\left(r(\alpha + \varepsilon_H) \frac{\partial T}{\partial r} \right)$$

where $\alpha = k / \rho C_p$

(66)

- the effect of the random turbulence fluctuations is considered by defining a thermal diffusivity, ε_H, similar to the momentum diffusivity, ε_M.

By energy balance for the mean flowrate

$$\frac{dT_m}{dx} = \frac{2\dot{q}}{\rho C_p R U_m}$$

where bulk air, temperature $T_m = \frac{2}{R^2 U_m} \int_0^R r u T \, dr$

For fully developed flow with constant heat flux along the pipe,

$$\frac{\partial T}{\partial x} = \frac{dT_m}{dx}$$

(66)

To simplify the integration methods assume $u = U_m$

Energy equation becomes

$$\frac{2\dot{q}}{\rho C_p R} = \frac{1}{r} \frac{\partial}{\partial r}\left(r(\alpha + \varepsilon_M) \frac{\partial T}{\partial r} \right)$$

Integrate

$$\therefore \quad T - T_c = \frac{\dot{q}}{\rho C_p R} \int_0^R \frac{r \, dr}{(\alpha + \varepsilon_H)}$$

from boundary conditions

$$\frac{\partial T}{\partial r} = 0 \quad \text{at } r = 0$$

$$T = T_c \quad \text{at } r = 0$$

At $r = R$, $T = T_w$

$$\therefore \quad T_w - T_c = \frac{\dot{q}}{\rho C_p R} \int_0^R \frac{r\,dr}{(\alpha + \varepsilon_H)}$$

Velocity profile can be approximated to

$$u = u_c \left((R-r)/R\right)^{\frac{1}{7}}$$

By similarity assuming Prandtl number is close to unity

$$\frac{T - T_w}{T_c - T_w} = \left((R-r)/R\right)^{\frac{1}{7}}$$

From definition of bulk air temperature

$$\frac{T_m - T_w}{T_c - T_w} = 0.833$$

By substitution

$$T_w - T_m = 0.833 \frac{\dot{q}}{\rho C_p R} \int_0^R \frac{r\,dr}{(\alpha + \varepsilon_H)}$$

Karman-Boelter-Martinelli analogy (66)

Assume $\varepsilon_H = \varepsilon_M$ - the momentum diffusivity can be calculated from shear stress and velocity measurements. This has been shown to be a reasonable assumption if Prandtl number is close to 1.

The momentum diffusivity is defined by a laminar sub-layer and turbulent core.

Laminar sub-layer

For $r \geq R - 120\,R\,(Re_d)^{-\frac{7}{8}}$

for $4{,}000 \leq Re_d \leq 100{,}000$

$$\varepsilon_M = \varepsilon_H = 0$$

Turbulent core

$$\text{for} \quad 0 \leq r < R - 120\,R\left(Re_d\right)^{-\frac{7}{8}}$$

$$\varepsilon_M = \varepsilon_H = \upsilon\left(\frac{0.04}{R^2}\left(Re_d\right)^{+\frac{7}{8}} r\left(R-r\right) - 1\right)$$

(66)

By definition

Heat transfer, coefficient $\quad h = \dfrac{\dot{q}}{T_w - T_m}$

Nusselt number, $\quad Nu_d = \dfrac{hd}{k} = \dfrac{\dot{q}}{\left(T_w - T_m\right)} \cdot \dfrac{d}{k}$

By substitution for the flow diffusivity, the Nusselt number can be evaluated by numerical intergration - use Trapezoidal rule (58).

From the theoretical derivation, it is shown that, for fully developed conditions, local Nusselt number is a constant for a given Reynolds number i.e. independant of position along the pipe.

4.2.2 Quasi-steady flow

Consider a resonant oscillating air flow, bulk mean velocity $\overline{U}_m$, in a pipe of diameter d (radius R) with constant heat flux input along the pipe ($\dot{q}$).

The oscillating flow is analysed for the mean flowrate i.e. the flow is defined as steady with the thermal diffusivity dependant on the pulsation parameters. It is assumed that the hydrodynamic and thermal boundary layers are fully established.

It is assumed that

$$\frac{\partial \overline{T}}{\partial x} \approx \frac{d\overline{T}_m}{dx}$$

- if the rate of change of velocity amplitude along the pipe is small, the local mean diffusivity can be considered to be the governing factor.

For a point along the pipe,

$$\overline{T}_w - \overline{T}_c = \frac{\dot{q}}{\overline{\varrho}\, C_p R} \int_0^R \frac{r\,dr}{\left(\overline{\alpha} + \overline{\varepsilon}_H\right)}$$

where $\overline{\alpha} = K / \overline{\varrho}\, C_p$

- see previous section for assumptions and derivation

It is assumed that the mean velocity profile can be approximated by

$$\bar{u} = \bar{U}_c \left((R-r)/R\right)^{\frac{1}{7}}$$

By similarity

$$\frac{\bar{T} - \bar{T}_w}{\bar{T}_c - \bar{T}_w} = \left((R-r)/R\right)^{\frac{1}{7}}$$

From definition of bulk air temperature

$$\frac{\bar{T}_m - \bar{T}_w}{\bar{T}_c - \bar{T}_w} = 0.833$$

By substitution

$$\bar{T}_w - \bar{T}_m = 0.833 \frac{\dot{q}}{\bar{\rho} c_p R} \int_0^R \frac{r\,dr}{(\bar{\alpha} + \bar{\varepsilon}_H)}$$

Time mean Nusselt number

$$\overline{Nu}_d = \frac{\dot{q}}{(\bar{T}_w - \bar{T}_m)} \cdot \frac{d}{k}$$

To evaluate the mean Nusselt number the time mean diffusivity at the point must be known. It is defined that the pulsations can be considered quasi-steady. Consequently the diffusivity can be predicted theoretically - assuming the Karman-Boelter-Martinelli analogy, the mixing coefficient can be defined by a laminar sub-layer and core diffusivity (see Section 4.1.5). For the derivation of mean diffusivity for a quasi-steady pulsating flow, it is assumed that the transport properties are dependant on the acoustic velocity and the mean flow - acoustic streaming effects are considered negligible relative to convective heat transfer.

Laminar sub-layer, $r \geq R - \delta_E$

where $$\delta_E = \frac{\overline{\delta_{sub}|U|}}{|\bar{u}|}$$

$$\bar{\varepsilon}_M = \bar{\varepsilon}_H = 0$$

Turbulent core, $0 \leq r \leq R - \delta_E$

$$\bar{\varepsilon}_M = \bar{\varepsilon}_H = \Delta\bar{\varepsilon}_{M_c} + \varepsilon_{M_s}$$

where $$\Delta\bar{\varepsilon}_{M_c} = 0.16(R-r)^2\bar{u}_m\beta\frac{2}{\pi}(B\sin(XX) - XX)$$

$$XX = \cos^{-1}(1/B) \quad \text{For } B > 1$$

$$XX = 0 \quad \text{For } B \leq 1$$

$$\varepsilon_{M_s} = \bar{\upsilon}\left(\frac{0.04}{R^2}(\overline{Re_d})^{\frac{7}{8}}r(R-r) - 1\right)$$

The equations can only be solved numerically - use Trapezoidal rule (58).

The analysis is rigorously applicable to a non-resonant pulsating flow i.e. $\partial\bar{u}/\partial x = 0$. By defining the rate of change of velocity amplitude to be small, resonant oscillating flow can be analysed. Consequently, by definition of this assumption, for a resonant flow Nusselt number at a point, for fully developed conditions, is dependant only on the mean diffusivity at that point i.e. for a given frequency and mean flowrate, the heat transfer coefficient is a function of Dimensionless pulsation velocity only.

The experimental investigation of the project was analysed to give local heat transfer assuming quasi-steady pulsations. The following system was analysed - air flow in a pipe of 0.04 m I.D. with mean Reynolds number 10,000 to 30,000 for frequency range 25 to 225 Hz with a maximum Dimensionless pulsation velocity 4 for fluid properties defined at a temperature of 30°C. For a given flowrate and frequency, Nusselt number was compared to the equivalent steady flow heat transfer over a range of pulsation velocity (from B = 0 to B = 4). The results were compared to the quasi-steady theory used by Hanby - see Appendix I. The theory is a simplification of the derived method - the instantaneous diffusivity is described by the steady flow function, using the instantaneous velocity, for all frequencies (change in heat transfer is independant of frequency of oscillation and mean flowrate).

Define Improvement ratio, R_A

$$R_A = \overline{Nu}_d / Nu_{d_e}$$

where Nu_{d_e} is the Nusselt number of the equivalent steady slow

See Figure 7 Page 58

The analysis shows that large increases in heat transfer occur at high velocity amplitudes (in the reverse flow regime), but at lower amplitudes Nusselt number is decreased with a minimum at B = 1. The minimum is dependant on mean flowrate - the lower the flowrate, the greater the decrease. The effect of frequency is more pronounced at lower flowrates - the higher the frequency, the smaller the change in heat transfer (for $B > 1$). The functions are similar in variation to that given by the simple quasi-steady method (as used by Hanby).

It is possible by the analysis to estimate local heat transfer for an oscillating flow in a given system, under fully developed conditions, from mean flowrate, frequency and velocity amplitude assuming quasi-steady pulsations.

4.2.3 Frequency factor

The degree to which an oscillating flow can be considered quasi-steady is dependant on the rate of change on the acoustic velocity relative to the turbulence fluctuations of the equivalent steady flow.

The turbulence fluctuations can be described by an eddy frequency

Prandtl eddy frequency, $f_e = \frac{u}{\ell}$

for velocity fluctuations, u

Prandtl mixing length, ℓ

(69)

The parameter is the reciprocal of the time for which any particular eddy exists as an entity.

For the flow in a pipe

$$\ell = f(y)$$

where $y = R - r$

$$u \approx 0.05 \, \overline{U}_m$$

except for very close to the pipe wall

$$\therefore \quad f_e \propto \frac{\overline{U}_m}{y}$$

(69)

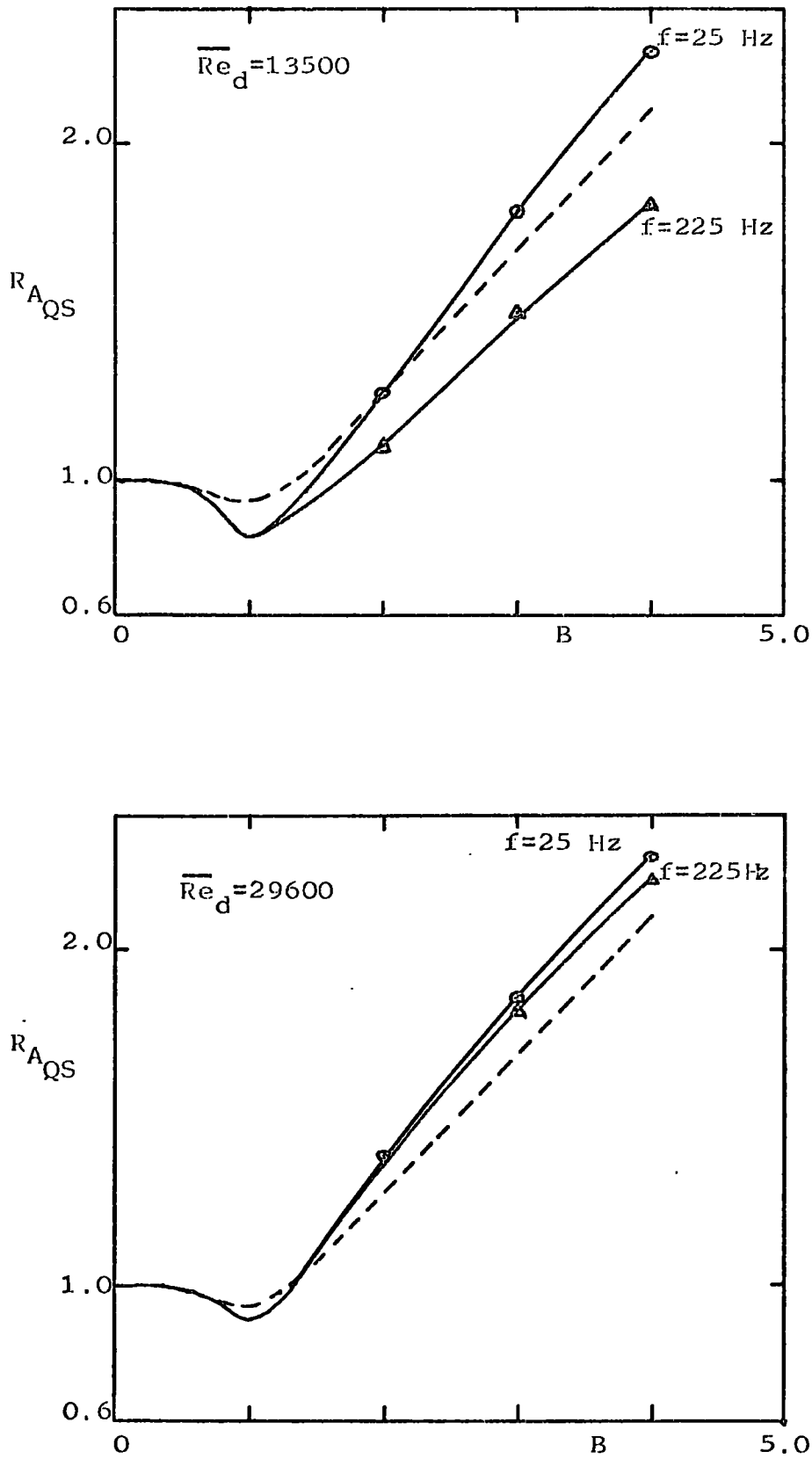

Fig.7 Improvement Ratio against Pulsation Velocity for quasi-steady flow

---- Hanby Theory

For the range of Reynolds number $4{,}000 < Re_d < 100{,}000$ the velocity profiles are similar ($u/\overline{U}_m = f(y)$), and the majority of thermal resistance is close to the wall

e.g. for $y = 0.1\ R$, $u/U_c \approx 75\%$

Consequently, relative to convective heat transfer, this area close to the wall is of primary interest. From the definition of eddy frequency, it can be seen that the turbulence frequency is high in this regime. For the range of acoustic frequency of interest (0 to 300 Hz), it would appear that resonance interaction between the oscillations and the turbulence fluctuations is not a major factor for the defined region (see derivation of acoustic streaming velocities - Section 4.1.4).

It is defined that the turbulence fluctuations can be represented by the eddy frequency at $y = 0.1\ R$ ($u/U_c \approx 75\%$). Consequently for the definition of heat transfer

$$f_e \propto \frac{\overline{U}_m}{d}$$

for the given Reynolds number range

Consider the acoustic velocity profile at a point along the pipe

$$u_1 \approx \hat{U} \cos(\omega t)\left(1 - e^{-\beta(R-r)}\right)$$

- see Section 4.1.5

$$\therefore \quad \frac{\partial u_1}{\partial t} = -\hat{U}\,\omega \sin(\omega t)\left(1 - e^{-\beta(R-r)}\right)$$

For the important regime close to the wall the frequency of oscillation can be considered the dominant factor in comparison to local velocity amplitude relative to the rate of change of the oscillating velocity gradient.

The degree to which an oscillating flow can be considered quasi-steady is dependant on the rate of change of the acoustic velocity gradient relative to rate of change of the turbulence eddies. Consequently, relative to convective heat transfer, the relation to quasi-steady can be defined by the ratio of the angular frequency of pulsation to the eddy frequency of the equivalent mean flow

$$\text{i.e.} \quad S = \frac{\omega}{\frac{\overline{U}_m}{d}} = \frac{\omega d}{\overline{U}_m}$$

- as $S \longrightarrow 0$, the flow tends towards quasi-steady oscillations. The non-dimensional parameter is defined as the Strouhal number.

It was hoped to derive a frequency correction factor from a comparison of experimental results to the theoretical quasi-steady predictions. From the discussion of this section, it was proposed that the frequency factor would be a function of Strouhal number. But with the non-linear interaction of laminar sub-layer and core diffusivity, the correction factor was envisaged to be a complex function of Strouhal number.

4.2.4 Summary

The theoretical investigation proposes that the acoustic velocity can produce changes in the time-mean diffusivity assuming quasi-steady pulsations. Assuming quasi-steady oscillations, large increases in heat transfer, for fully-developed conditions, are predicted for high velocity amplitudes ($B \geq 1$), but Nusselt number is also dependant on the frequency and the mean flowrate. For a point, under given frequency and mean flowrate conditions, the heat transfer coefficient is dependant only on the dimensionless pulsation velocity at that point.

The assumption of quasi-steady pulsations predicts the maximum possible changes in heat transfer - at the other extreme, for high frequency oscillations ($\omega \longrightarrow \infty$), no change in heat transfer is predicted. It was proposed that from a comparison of experimental results and predicted time-mean Nusselt numbers, assuming quasi-steady conditions, a frequency factor could be derived - it was considered that the factor would be a function of Strouhal number.

CHAPTER 5

Pulsation Generator

5.1 Design

5.1.1 Air supply

5.1.2 Siren

5.1.3 Amplitude control

5.1.4 Test section

5.1.5 Silencing chamber

5.2 Characteristics

5.3 Summary

5. Pulsation generator

The first step in the experimental investigation was to develop the pulsation generator. It was defined that the device was to produce sinusoidal, resonant longitudinal oscillations, over a frequency range of 5 - 500 Hz, superimposed on a turbulent flow in a pipe. Large amplitude pulsations were required to produce momentary reversal of the air flow ($B > 1$). It was hoped to produce approximately sinusoidal waveform since, by Fourier Analysis, all other functions could be predicted from the results.

It was decided to use a siren for the project since it is a simple device capable of producing high intensities. The siren is based on a wheel which periodically interrupts an air jet - it is a fluid regulator i.e. fluid flow is regulated by a time-varying orifice. As the orifice rapidly opens, high pressure fluid is forced into contact with fluid downstream of the modulator. The resulting strain on the low pressure fluid produces an acoustic wave. As the orifice closes a rarefaction is created, and consequently a periodic pressure wave is generated. Little work has been published on the design of sirens, despite the wide usage - see references 70 - 75. It was obvious that the design of the siren to the project specifications would be mostly an experimental approach and not theoretical.

The basic format for the system was chosen - a known flowrate of air was to be supplied from a compressor to the siren. By enclosing the siren wheel in a sealed plenum chamber, the driving air supply was to be used as the mean flowrate for the heat transfer measurements. The flowrate was to be measured between the compressor and siren, and consequently no pulsations must be transmitted back along the inlet line to the flowmeter. A silencing chamber was to be used to decrease the laboratory noise level.

See Figure 8 Page 62

5.1 Design

5.1.1 Air supply

A two-stage, reciprocating compressor, with a receiver pressure of 10.5 bars gauge, supplied air to the siren (model 15T type 30 manufactured by Ingersoll Rand Ltd.). A water-cooled, counter-flow heat exchanger was designed for the outlet line of the compressor to maintain constant temperature supply to the flowmeters - maximum variation + 4°C over a 4 hr. test. The supply flowrate was measured by two Gapmeters in parallel (Types IGU/29F and IGU/15F manufactured by G.A. Platon Ltd.). The combined range was 0.1×10^{-2} to 6.0×10^{-2} Kg/s at 7 bar gauge and 15°C. The Gapmeters were calibrated by the manufacturers to an accuracy of $\pm$ 1¼% of full scale deflection. The calibration pressure was maintained by a pressure regulator, and any temperature variation was corrected from a measurement of air temperature in the plenum chamber. The flow was controlled by two parallel gate valves downsteam of the flowmeters. A maximum flowrate of 2.2×10^{-2} Kg/s was available to the siren. Transducer measurements for pressure oscillations close to the flowmeters showed no variation in pressure over the frequency range - steady flow supply could be assumed.

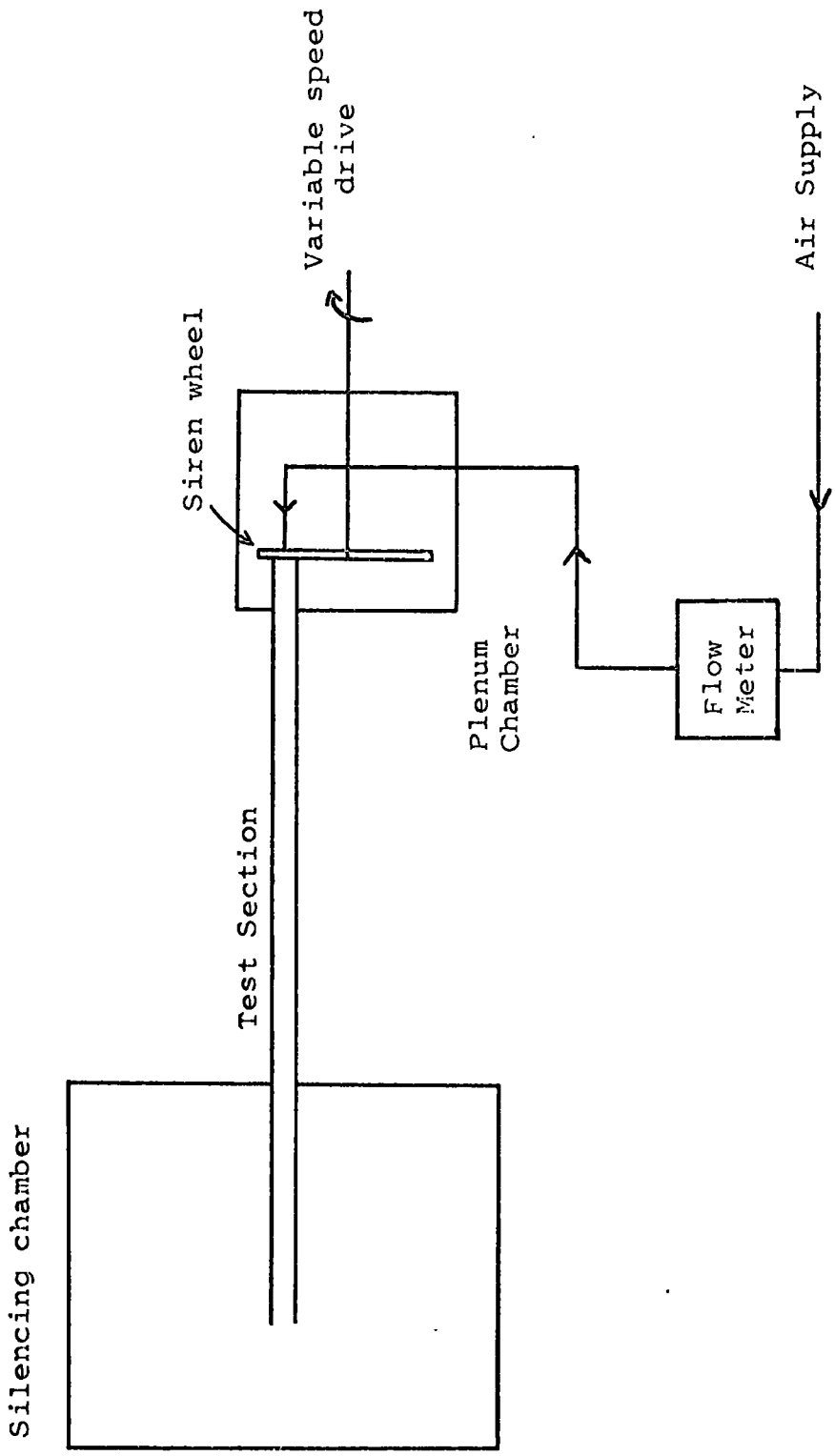

Fig.8 Basic Experimental System

5.1.2 Siren

The siren rotor was a 0.178 m diameter disc of mild steel, with 20 orifices of 9.54 mm diameter symmetrically placed around the circumference - see Figure 9 Page 64. The drive shaft (31.8 mm diameter) was belt driven from a variable speed D.C. motor. The motor was a $\frac{1}{2}$ h.p. 110 V D.C. shunt interpole machine, with maximum speed of 2,100 r.p.m. - a rectified mains driver circuit was designed. The speed could be controlled by a 10 amp. variac on the A.C. supply line. Shaft speed (from which acoustic frequency was calculated) was measured from a disc on the shaft by an electro-magnetic transducer - frequency range was 20 to 450 Hz.

The seal between the rotor and test section was produced by a P.T.F.E. faced flange - the stator. The stator orifice was of the same diameter as a rotor orifice.

The necessary pressure rise on closing of the stator orifice was generated by using a high speed flow of the supply air directed onto the rotor (by using small diameter nozzles). Various jet diameters were used - in the range 3.17 mm to 9.54 mm. The gap between the nozzle outlet and rotor face was approximately 12.7 mm.

The rotor and stator were enclosed in a plenum chamber to provide a seal - the chamber also acted as an expansion volume to prevent pressure oscillations in the air inlet system. The plenum chamber volume was approximately 0.018 m^3. Transducer measurements in the chamber showed that the oscillation amplitudes, for all frequencies, were negligible - conditions in the plenum volume could be considered steady. A spring-loaded lip seal was used between the drive shaft and the chamber, but under test it was found to leak. Since it had been shown that flow in the chamber could be considered steady, the leakage flowrate was calibrated against mean pressure of the plenum chamber, which was measured by a water manometer - maximum loss of 10%.

In order to increase pressure amplitudes for low flowrates, a by-pass line was fitted to the plenum chamber. The amplitude generated by the device was dependant on the mass flowrate in the supply nozzle and not on the flowrate in the test section. The by-pass line allowed a known flowrate to be bled from the chamber and discharged to the atmosphere. Consequently, a higher Dimensionless pulsation velocity (B) was produced for the decreased flow in the test section. The bleed air flow was controlled by a gate valve and measured by a low pressure rotameter (Type 35G, produced by Rotameter Co. Ltd., range 0.1×10^{-2} to 1.0×10^{-2} Kg/s at atmospheric pressure and 20°C - the rotameter was calibrated against the supply flowrate Gapmeters). This method could only be used because the conditions in the chamber could be regarded as steady.

See Figure 11 Page 67

5.1.3 Amplitude control

A requirement for the heat transfer investigation was that the oscillation amplitude could be independantly controlled relative to the mean flowrate for a given harmonic - quarter-wavelength damping pipes were used i.e. variable length side-branches perpendicular to the test section.

All Dimensions in millimetres

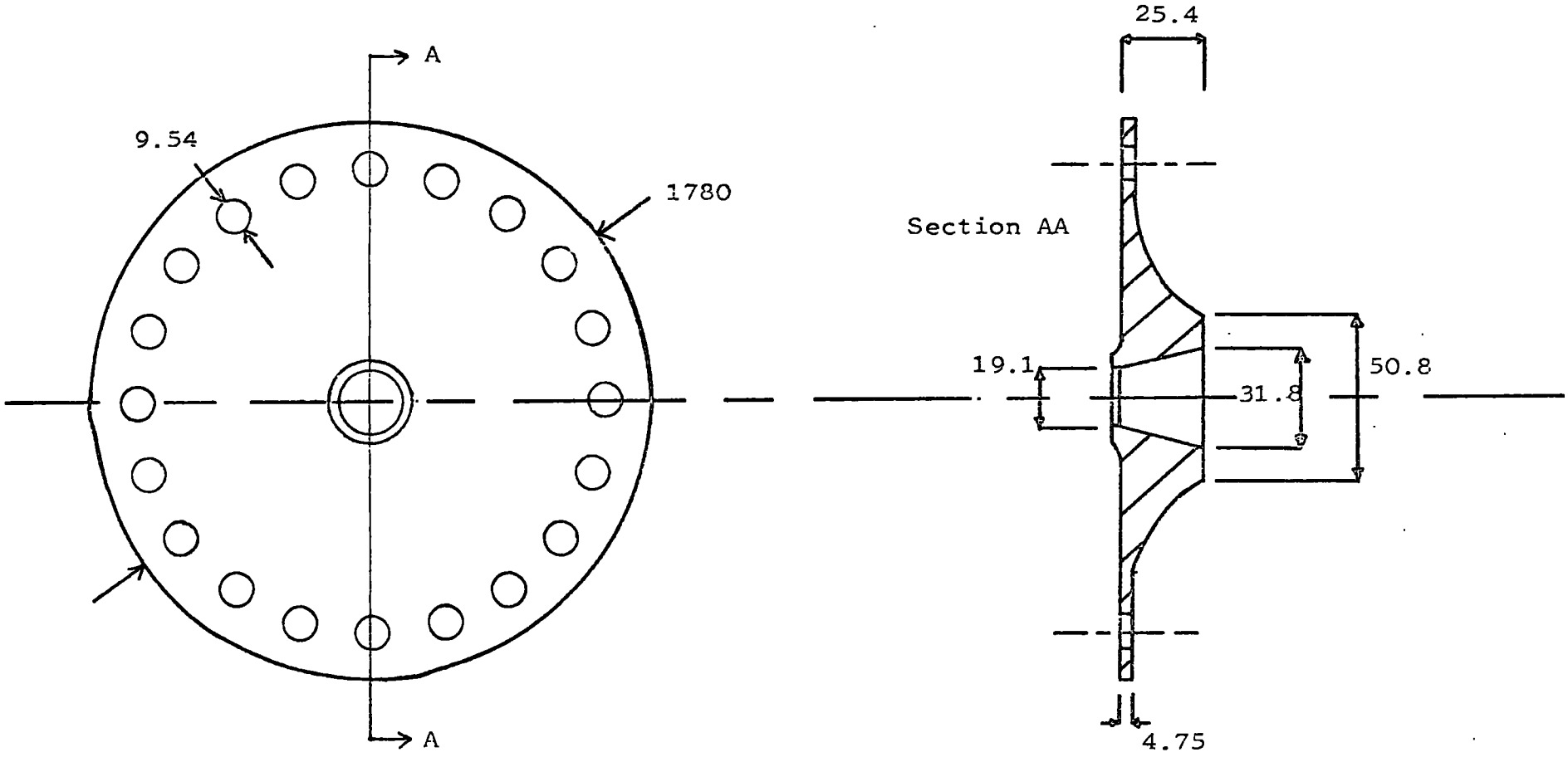

Fig.9 Siren Rotor

Scale 1:2

Fig.10 Diagrammatic representation of Siren

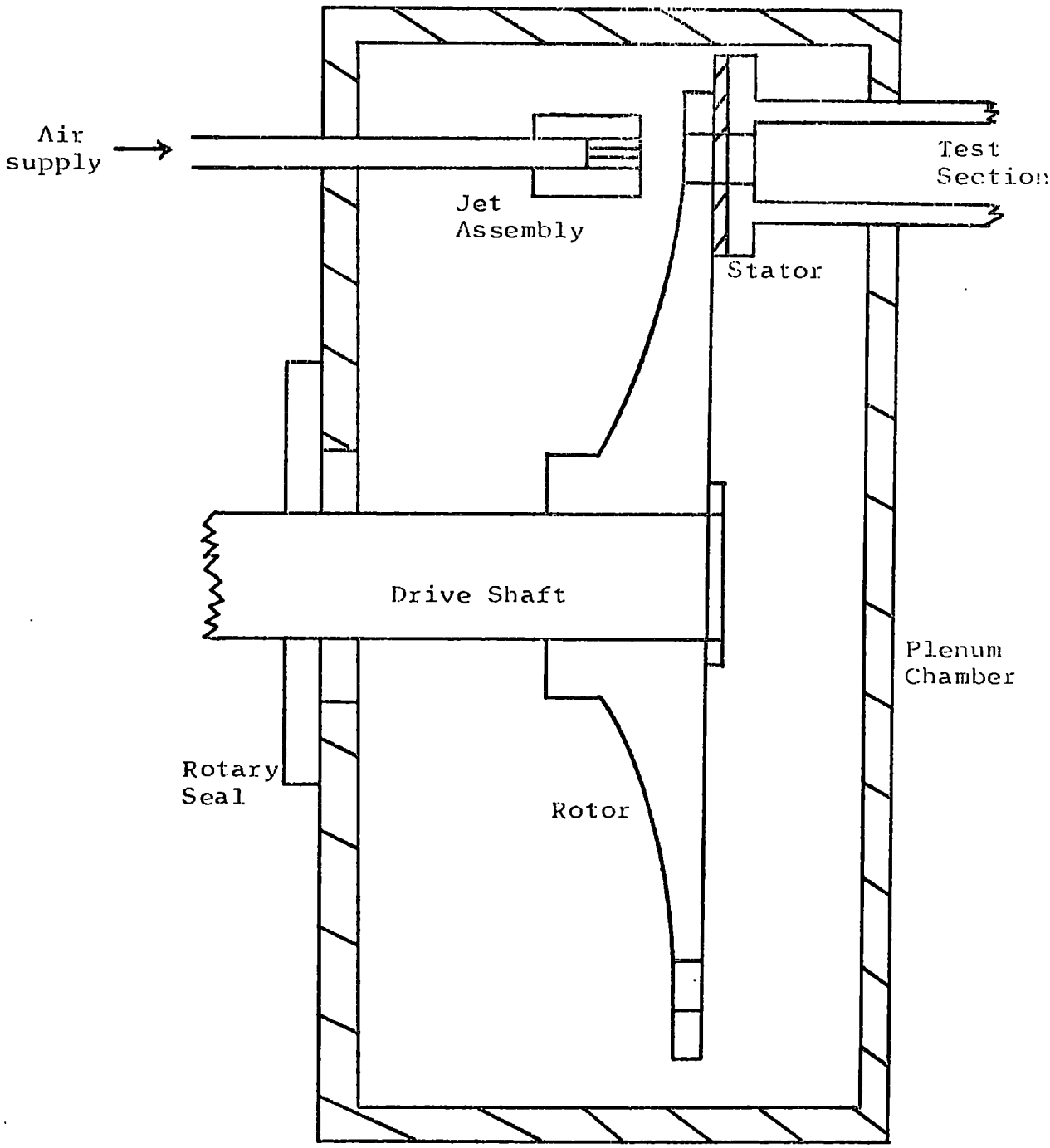

Bearings are
not shown

Not to Scale

Side branches have been used as acoustical dampers for combustors and for the exhaust pipes of I.C. engines - see References 5, 76-78. Hanby (9) used similar devices in an investigation of heat transfer from pulsating flow. Basically the length of the side pipe is adjusted, by a movable piston, to give a distance equivalent to the quarter wave-length of the frequency ($L_{\frac{1}{4}} = \bar{c}/4f$). Wave reflection generates a standing wave with a node at the junction of the pipes - consequently a large attenuation in the pressure amplitude in the downstream test section is produced. Maximum decreases of 95% have been measured using this method (78). By using positions offset from the quarter-wavelength, the amplitude could be varied between the maximum and minimum. The side branches must be placed close to a pressure antinode for greatest efficiency.

For the project two side branches of 25.4 mm I.D., were placed between the siren outlet and the test section. The maximum available length for each pipe was 1.0 m - the side branch length was controlled by a wood piston.

5.1.4 Test section

To investigate the system performance a test section was designed to enable the measurement of the resonance characteristics i.e. harmonic frequencies and pressure amplitude distribution - this was replaced by the heat transfer section after the development of the generator.

A pipe of internal diameter 40.0 mm and acoustic length of 2.0 m was modified to enable pressure amplitude to be measured at 15 points along the pipe. The maximum possible mean flowrate in the pipe was 2.0×10^{-2} Kg/s - equivalent to Reynolds number (Re_d) 35,800 at 15°C.

In the project, pressure amplitudes were measured using quartz crystal piezoelectric transducers (Kistler type 601A). The measuring range was 0 to 250 bars with a scale linearity of 0.25%. The output from the transducer was displayed on an oscilloscope using a charge amplifier - the amplitude was measured from the screen. The frequency of the oscillation could also be found from the trace and compared to the shaft speed measurement.

5.1.5 Silencing chamber

A chamber was constructed to give a volume of approximately 3 m^3 - it exhausted directly to the atmosphere. The sides were lined with fibre-glass insulation and acoustic tiles. Over the range of operation an average decrease of 50% in room sound level was measured.

See Figure 11 Page 67

5.2 Characteristics

The resonance characteristics of the test section were investigated to measure the siren output.

The pipe was tuned to resonance by varying the frequency of oscillation to give maximum pressure amplitude at $x = 0$, and a standing wave distribution i.e. a system of nodes and antinodes along the pipe, with a phase change of 180° at nodes. It was found that resonance also corresponded to maximum sound level in the room.

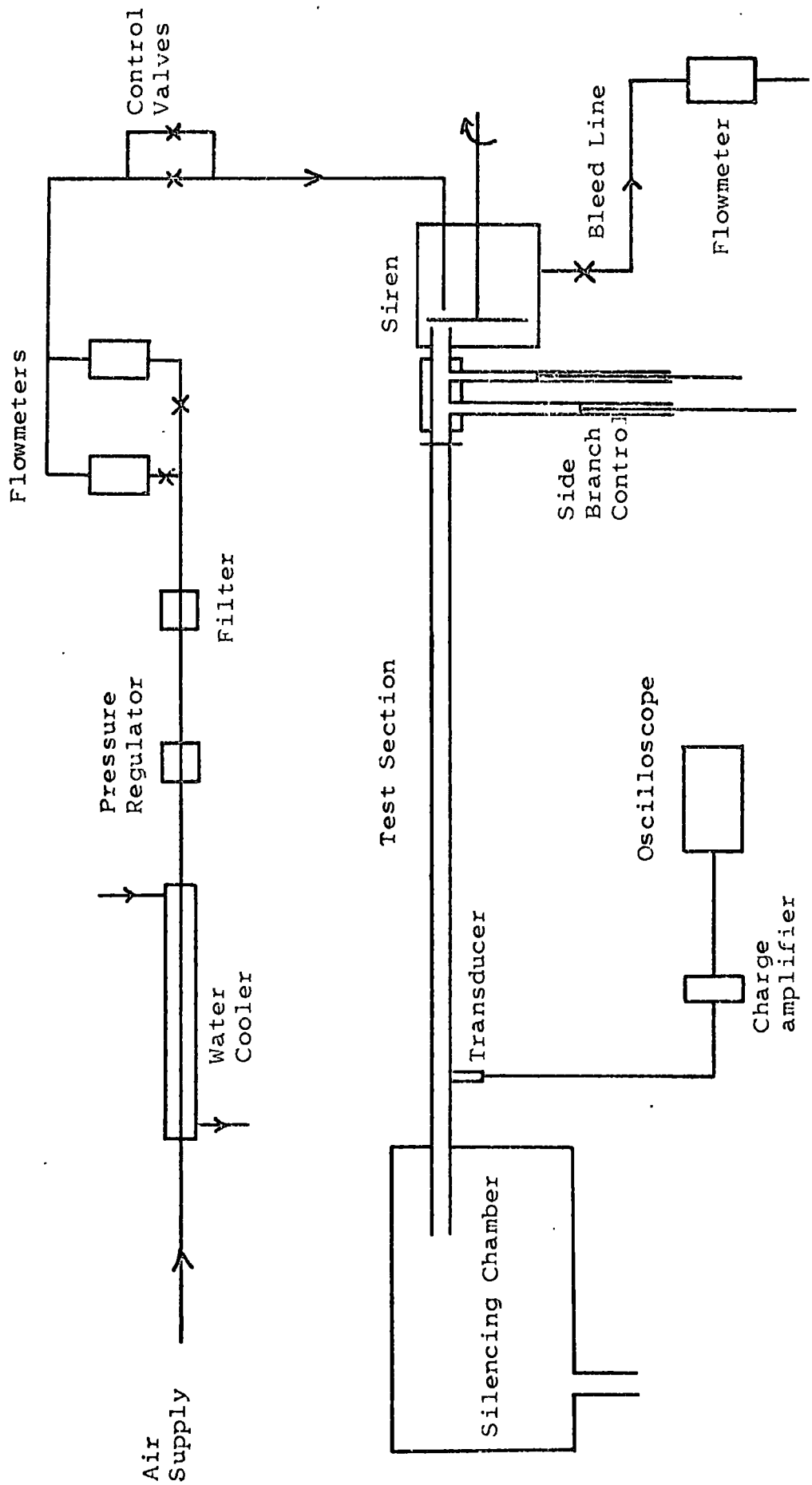

Fig.11 Pulsation Generator System

From inviscid flow theory (see Chapter 3), the resonant frequencies for a closed/open pipe are given by

$$f = (2n - 1)\ \frac{\bar{c}}{4L_A}$$

for $n = 1,2,3$ .....

- for air temperature 288°K, $\bar{c}$ = 340.0 m/s

Since L_A = 2.0 m, the following comparisons could be made between experimental and theoretical values.

	Experimental	Theoretical
Fundamental	40.2	42.5 Hz
1st harmonic	122.3	127.5 Hz
2nd harmonic	206.0	212.0 Hz
3rd harmonic	280.8	298.0 Hz

The standing wave distributions were as expected i.e. the position of the nodes and antinodes, and phase changes of approximately 180° across the nodes. Node amplitude was not zero due to imperfect wave reflection. Experimental and theoretical pressure amplitude modulus are shown in comparison for the fundamental and 1st harmonic.

See Figure 12 Page 69

The theoretical variations were derived from inviscid flow theory using the measured values of pressure amplitude at a node and antinode. For higher harmonics (f > 280 Hz) there was a reduction in maximum pressure amplitude due to a decrease in wave reflection from the open end.

The waveform of the oscillation was analysed using a wave analyser i.e. Fourier analysis into harmonic components by electrical filters (A.F. Analyser type 1461A manufactured by Dawe Ltd.). For all conditions, the main harmonic was 3 x the frequency with maximum distortion, given by a comparison of harmonic amplitude to main frequency amplitude, of 15%.

The experimental results justified the use of the small pertubation, inviscid flow theory to predict resonant frequencies and pressure amplitude distribution. The theory was used to predict velocity amplitudes from pressure amplitude measurements.

Velocity amplitude distribution

$$u_1 = \sqrt{\left(\hat{U}_A^2 \sin^2\left(\omega \frac{x}{\bar{c}}\right) + \hat{U}_N^2 \cos^2\left(\omega \frac{x}{\bar{c}}\right)\right)} \cos(\omega t)$$

where $\hat{U}_A = -\frac{\bar{c}}{\gamma \bar{p}} \cdot \hat{p}_A$

$\hat{U}_N = -\frac{\bar{c}}{\gamma \bar{p}} \cdot \hat{p}_N$

- see Chapter 3

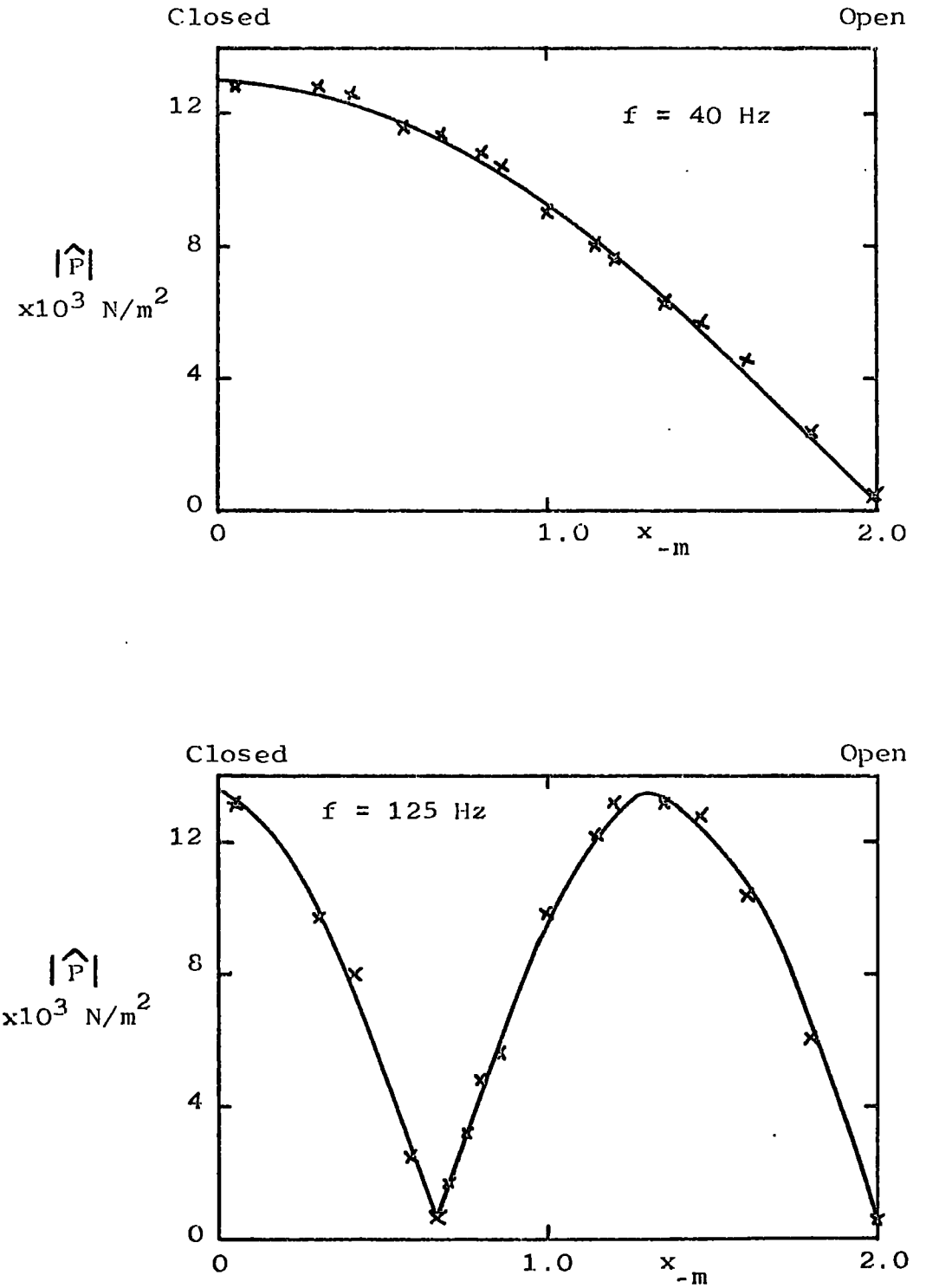

Fig.12 Comparison between experiment and theory for pressure amplitude modulus

——— Theory

× Experiment

No measurements of velocity amplitude were made but Bogdanoff (42) showed, under similar conditions, that predicted values from the given method agreed within 5% of the measured centre-line velocity amplitude.

The velocity amplitudes at an antinode are shown against air supply flowrate, for two jet sizes, for the 2nd harmonic (f = 200 Hz).

See Figure 13 Page 71

For a given frequency, the amplitude was a function of flowrate and jet size only. It had been shown that an important parameter for the investigation was the Dimensionless pulsation velocity (B). The maximum values of this velocity are shown as a function of mass flowrate in the test section.

See Figure 14 Page 71

The complex variation was due to the use of the by-pass line from the plenum chamber. The results showed that 'reverse flow' could be obtained under all conditions with a maximum of 500% (B = 6) at the lower flowrates.

The amplitude control system had a maximum attenuation of 84% at the lower harmonics (defined by the reduction in amplitude at a pressure antinode). The effect of length of side branch on pressure amplitude is shown for the 1st and 2nd harmonics (f = 125 Hz and f = 200 Hz).

See Figure 15 Page 72

The table below shows a comparison between the length for maximum attenuation from the experiment and theory

Frequency	Experimental length -cm	Theoretical length -cm
125 Hz	69.5	67.9
200 Hz	43.0	42.4
280 Hz	31.0	30.4

where Theoretical length, $L_{\frac{1}{4}} = \frac{\bar{c}}{4f}$

High attenuation for the fundamental frequency was not possible due to the limited length of the side branches - this was later modified by using a flexible hose to extend the tuning pipe. For higher harmonics (f > 280 Hz) the efficiency of attenuation was decreased due to the position of the side pipes relative to pressure nodes. Two side branches had been included in the original design so as to enable both amplitude control and harmonic control i.e. to give a pure sinusoidal oscillation. It was found that waveform control was unnecessary - see earlier discussion of harmonic content.

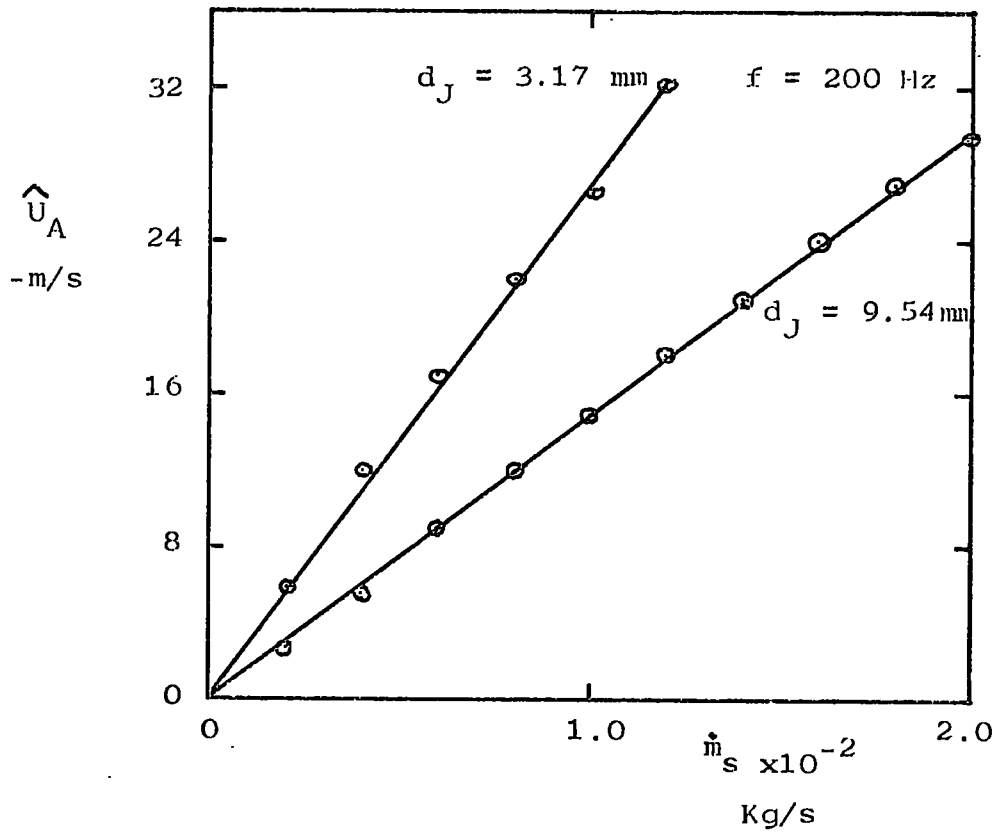

Fig.13 Velocity amplitude $\hat{U}_A$ against supply air flowrate for different jet sizes

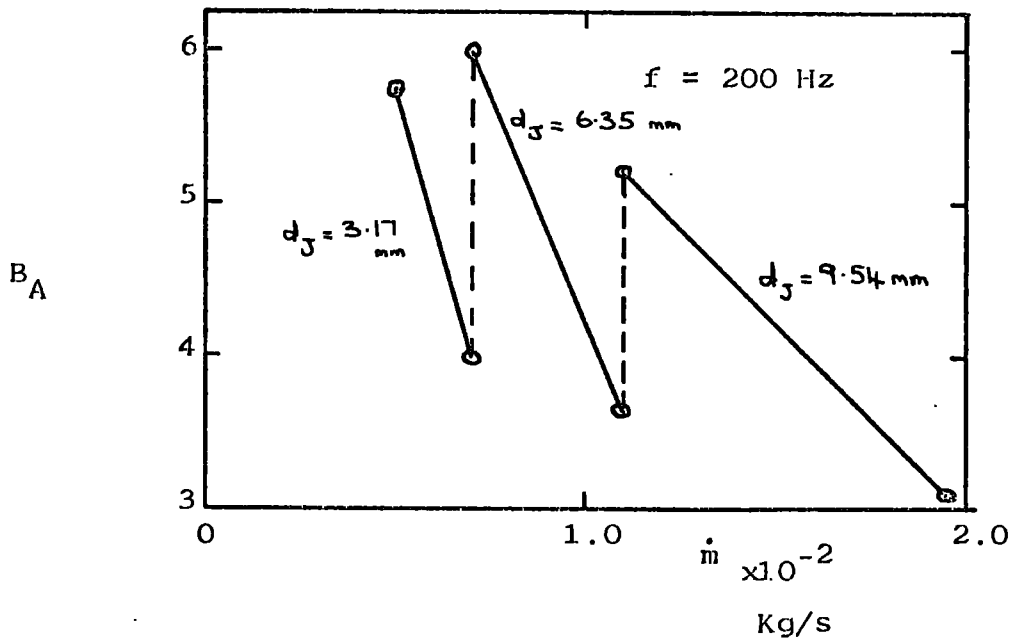

Fig.14 Pulsation velocity B_A against pipe air flowrate with bleed system

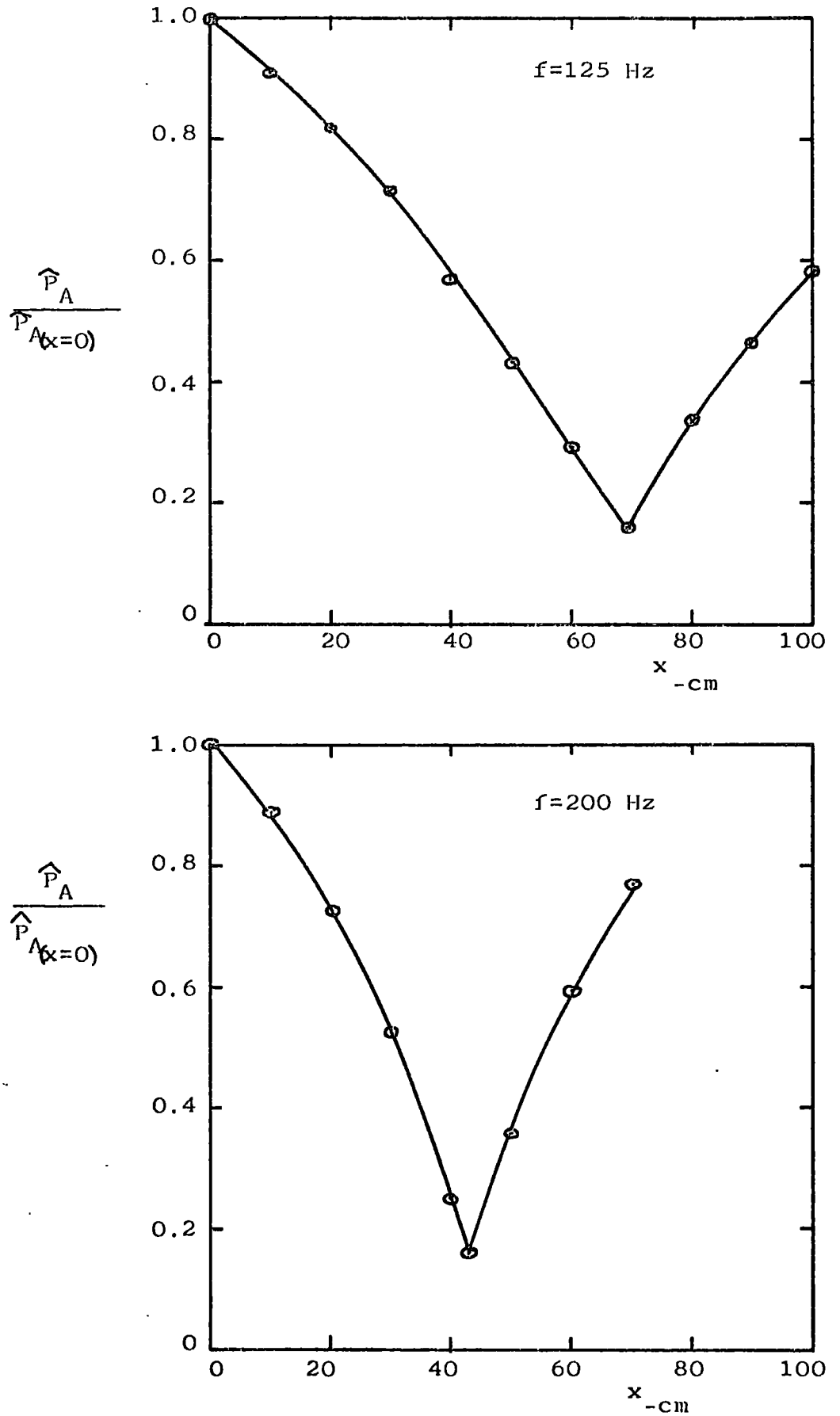

Fig.15 Pressure amplitude attenuation relative to side branch length

5.3 Summary

The siren had a frequency range of 20 to 450 Hz, and was capable of producing large amplitude oscillations. The pipe acted closed/open acoustically, and the resonant frequencies and standing wave distribution could be accurately predicted from inviscid flow theory. Under resonant conditions, a maximum Dimensionless pulsation velocity of 6 was possible and, for all flowrates, the maximum amplitude at velocity antinodes was such to give momentary flow reversal. The waveform could be assumed to be sinusoidal - maximum distortion of 15%. Independant amplitude control was possible with the variable length side branch - maximum attenuation of 84%. But for higher harmonics ($f > 280$ Hz) the amplitudes were decreased, and amplitude control was poor with the maximum attenuation level decreased.

CHAPTER 6

Experimental heat transfer

6.1 Design

- 6.1.1 Heat exchanger
- 6.1.2 Wall temperature measurement
- 6.1.3 Air temperature measurement
- 6.1.4 Measurement of pulsation variables

6.2 Experimental Programme

6.3 Test Procedure

6.4 Data Reduction

6.5 Error analysis

6.6 Results

6. Experimental Heat Transfer

The requirements for the experimental investigation have been stated - a comparison of time-independant local heat transfer of a resonant, oscillating turbulent air flow, of known frequency and amplitude, to the heat transfer coefficients of a steady flow of the same mean flowrate. The pulsation generator has been designed and evaluated, and the acoustic test section had to be replaced by the experimental heat exchanger.

It was decided that the energy source would supply a constant heat flux along the pipe. Assuming no energy loss, from measurements of the bulk air temperature at the inlet to the heat exchanger and the heat flux, the bulk air temperature at any point along the pipe could be calculated by a simple energy balance - a constant heat flux input would give a linear rise in air temperature along the pipe. Heat transfer coefficients (and Nusselt Numbers) could be calculated from measurements of local wall temperature. Heat transfer coefficients for a constant heat flux system can be predicted theoretically for fully developed conditions for a steady flow (see Section 4.2.1).

For the investigation of energy transfer to the oscillating flow, time-mean coefficients only were calculated - no provision was made for the measurement of instantaneous temperatures. With the same mean flowrate and energy flux, the increase in time-mean bulk air temperature would be the same as for the equivalent steady flow (assuming the same energy loss). Any change in the mean heat transfer coefficient at a point, due to the oscillations, would be shown by a change in the average wall temperature at that point.

Acoustic wave propagation in a mean flow of an inviscid fluid with energy transfer has been investigated. For a defined linear change in velocity of sound along a pipe, the resonant characteristics can be predicted theoretically. The velocity of sound variation for a linear rise in temperature (as given by constant heat flux input) can be approximated to linear function of velocity of sound if the change in temperature is small. It was decided to define a maximum temperature rise of 40°C along the test section. But it has been shown for a small change in temperature that adiabatic theory with a mean velocity of sound can be used to predict velocity amplitudes - see Section 3.2.

6.1 Design

6.1.1 Heat exchanger

The test section was a thin-walled copper pipe of 40.0 mm I.D., 0.794 mm wall thickness and length 1.71 m. The constant heat flux source was produced along the pipe by electric surface heating using a flat element heating tape (type G100-180 produced by Hotfoil Ltd.). The tape was closely wrapped around the pipe, on top of the wall thermocouples with no longitudinal spacing in order to prevent 'ripple' input. (Surface temperature measured by thermocouples - see Section 6.1.2). Aluminium foil was used as a thermal mass between the thermocouples and the heating tape - preliminary work showed that the heating tape produced 'hot spots' which gave a large deviation in wall temperature distribution. The heating

elements were insulated from the pipe surface and the thermocouples by a woven glass-cloth covering. The tape had a maximum loading of 2.8 KW from a 240V A.C. supply, and a safe surface operating temperature up to 450°C - it had a length of 9.0 m width 25.0 mm and thickness 1.5 mm. The supply was controlled by a 15 amp variac, and the energy input was measured by an ammeter (range 0 - 10 amp) and voltmeter (range 0 - 150V). The system was insulated by moulded pipe sections of a calcium silicate insulant, Newtherm 800 (produced by Newalls Insulation Co. Ltd.). The thermal conductivity, at a mean temperature of 50°C, was 0.0515 W/m°C, and the maximum allowable hot face temperature was 800°C. The thickness of insulation was 75.0 mm.

To produce fully developed hydrodynamic flow at the inlet of the heat exchanger, an inlet section (length 0.5 m, 40.0 mm I.D.) was placed between the pulsation generator and the heat exchanger. Preliminary work showed that, for pulsating flow, vast increases in heat transfer were found at the exit of the heat exchanger - this was due to cold air drawn into the pipe. But the effect was not a representation of the conditions in the exhaust pipe of a pulsating combustor, and an outlet section (length 1.0 m, 40.0 mm I.D.) was placed at the exit of the heat exchanger. Both inlet and outlet pipes were used to mount pressure transducers (see Section 6.1.4).

6.1.2 Wall temperature measurement

Wall surface temperatures were measured by Copper/Constantan thermocouples. It was assumed that the temperature drop across the thin wall of the copper pipe was negligible, and the thermocouples were mounted on the outer wall of the pipe.

The junctions were formed by twisting the two constituent wires together, and silver soldering for good electrical contact. The junctions were electrically insulated by applying a thin covering of araldite.

The thermocouple wire was calibrated against N.P.L. calibrated thermometers ($\pm$ 0.1°C) using a constant temperature oil bath. The bath was thermostatically controlled with a maximum operating temperature of 200°C. The results agreed with the standard calibration curves (79) to within 0.5%.

The positions of the nodes and antinodes in the heat exchanger for the first five resonant frequencies (fundamental to 4th harmonic inclusive) were calculated, and thermocouples were placed at these points. Allowance was made for the thermal entrance length by a high density of thermocouples close to the heat exchanger inlet - a total of 29 wall thermocouples were used. The thermocouples were sellotaped into position on the pipe wall - the heating tape and aluminium foil held the thermocouples in position. The measuring system for the thermocouples is shown.

See Figure 16 Page 76

The reference zone was an insulated box containing the junctions of the thermocouple wires and the copper connecting wires - the temperature of the zone was measured with a calibrated thermometer ($\pm$ 0.5°C). The generated voltages were measured by a digital voltmeter using a data logging system

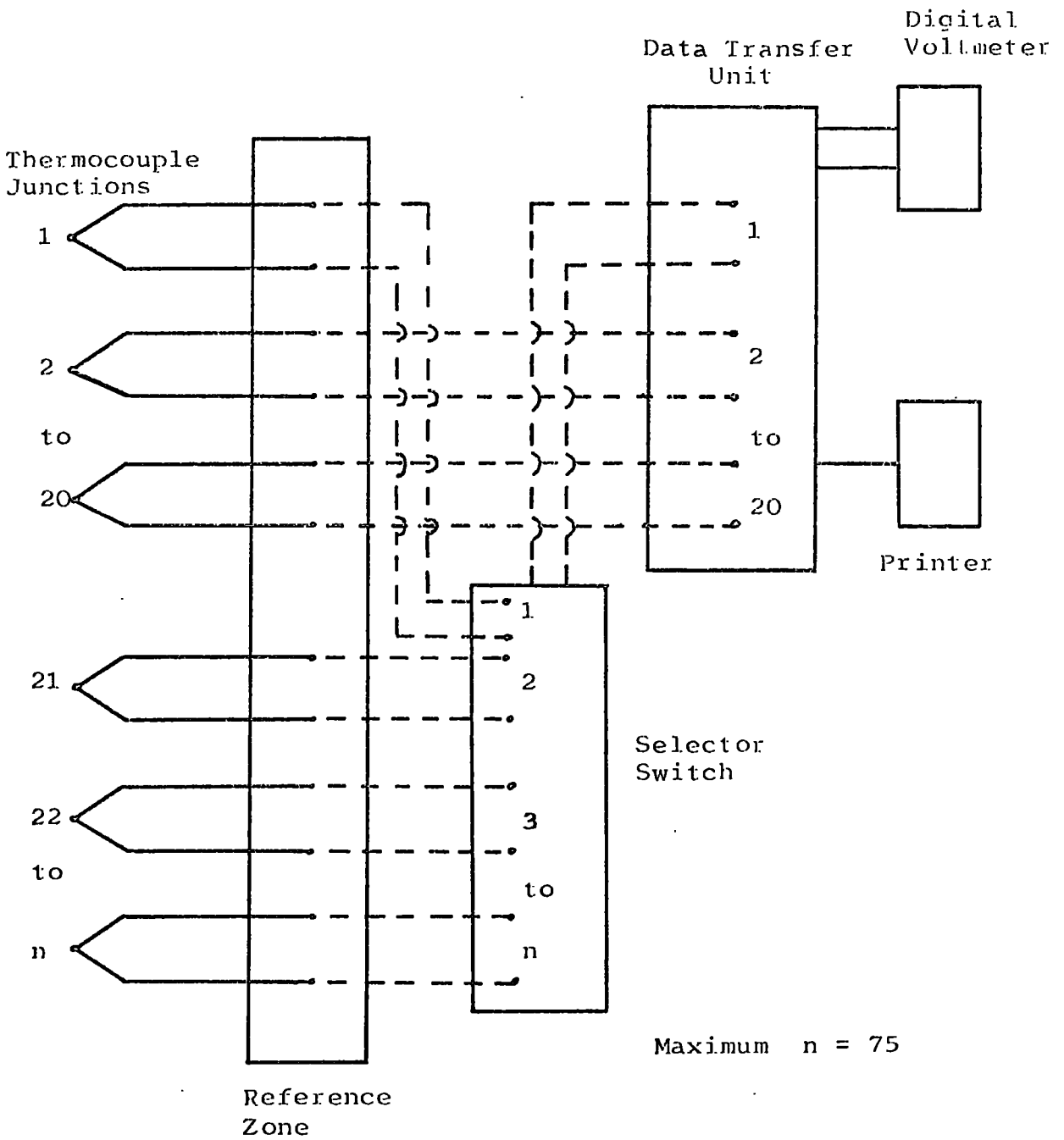

Fig.16 Thermocouple System

(Data Transfer Unit type 320 and voltmeter type LM 1604, manufactured by Solatron Ltd.) - the output was printed on a paper tape (Addmaster type 35 manufactured by Addmaster Co. Ltd.). But, due to limited input channels to the transfer unit, a selector switch had to be incorporated in the design. The arrangement enabled all wall temperatures to be measured relative to a reference temperature, and the equivalent voltages recorded on a paper tape print out.

6.1.3 Air temperature measurement

Air inlet temperature was measured by three copper/constantan thermocouples in the plenum chamber of the siren. The thermocouple wire and the measuring system were as for the wall thermocouples.

It was required to measure the bulk air temperature at the outlet of the heat exchanger in order to check the method of calculating temperature distribution along the pipe (by mean flow energy balance with correction for insulation losses). By the definition of bulk temperature, it is a difficult quantity to measure in fluid flow (see Section 4.2.1 for definition). But, under steady conditions, for fully developed turbulent flow, a direct relationship exists between bulk temperature, wall temperature and centre-line temperature.

$$\frac{T_w - T_m}{T_w - T_c} = 0.833 \qquad (66)$$

A stand was designed to mount a copper-constantan thermocouple at the centre line of the outlet of the heat exchanger. The measuring system was as for the air inlet thermocouples. Stagnation effects due to the air velocity were negligible. The above equation cannot be assumed for oscillating flow - results of temperature measurements in pulsating flow are given in Section 6.6

6.1.4 Measurement of pulsation variables

The acoustic length of the pipe system was 3.5 m - assuming closed/open acoustic properties, for ambient conditions of 15°C, the fundamental frequency was 24.3 Hz. The resonance characteristics were investigated under ambient conditions - the results were as expected relative to the previous work in the testing of the pulsation generator (see Section 5.2).

It was decided that the maximum temperature rise of the air would be limited to 40°C to enable the use of adiabatic wave propagation theory. Preliminary work with the heat exchanger showed that the assumption was correct by measuring pressure amplitude distributions with a transducer probe. For the experimental investigation, the energy input of the heating tape was adjusted to give the same temperature rise for all mean flowrates in order to give the same resonant frequencies.

Transducer tappings were made, in the inlet and outlet sections of the test pipe, corresponding to the predicted positions of nodes and anti-nodes for the first five harmonics (fundamental to 4th harmonic). From measurement of pressure amplitude at a node and antinode, the velocity amplitude distribution could be calculated. The frequency of oscillation was measured from the siren drive shaft by an electro-magnetic transducer.

See Figure 17 Page 79

6.2 Experimental Programme

Due to the available compressor and chamber leakage, the maximum possible flowrate in the test section was 2.0×10^{-2} Kg/s - this gave an upper limit of Reynolds number 35,750 for ambient conditions of 15°C. The minimum flowrate, for the full frequency range, was defined as 0.6×10^{-2} Kg/s due to non-equilibrium air temperature in the plenum chamber produced by friction heating in the drive shaft seal - this gave a lower limit Reynolds number of 10,700 at 15°C. The following mean flowrates were used in the project

Mass flowrate $\dot{m}$ - Kg/s	Reynolds No. - R_{e_d}
0.0080	14,300
0.0115	20,550
0.0145	25,900
0.0175	31,250

for fluid properties defined at 15°C.

From the evaluation of the pulse generator, the upper frequency limit was defined at 250 Hz due to decreased amplitudes and inefficient wave attenuation by the side branch control. For a temperature rise of 40°C in the heat exchanger, the resonant frequencies were found to be 25.0 Hz, 75.0 Hz, 125.0 Hz, 175.0 Hz and 225.0 Hz within the defined frequency range. It was not possible to control the oscillation amplitude for the fundamental frequency (25.0 Hz) due to the limited length of the side branch.

For a given mean flowrate, heat transfer measurements were made for each of the defined harmonics for different pressure amplitudes. For comparison, heat transfer coefficients were measured for the equivalent steady flow. The pulsation amplitude was controlled by the quarter-wavelength side branch - results for the condition of maximum attenuation were important in that a direct comparison could be made to the equivalent steady flow. For a given flowrate and frequency, measurements were made over the complete range of possible amplitudes i.e. from zero to maximum attenuation.

6.3 Test Procedure

Equilibrium conditions were defined as constant wall temperature i.e. maximum variation of $\pm$ 1°C. It was found that the approximate time to reach equilibrium from cold start was 1 hour, and half an hour for every subsequent change in conditions.

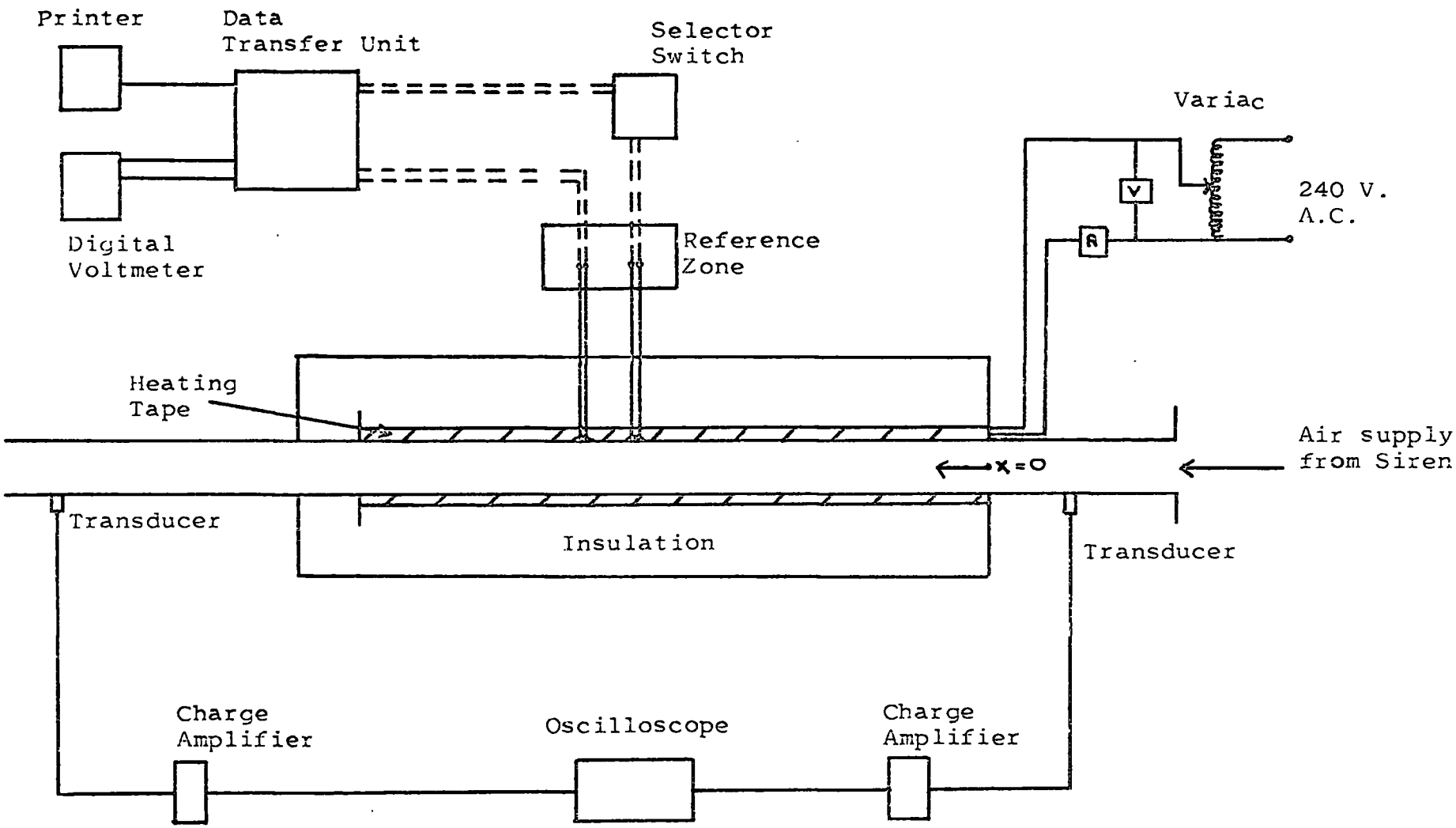

Fig.17 Heat Transfer Rig

For each test the following measurements were taken for the equilibrium state

Mean air flowrate

- Gapmeter
- Bleed rotameter
- Plenum chamber pressure

Energy input to heating tape

- Voltmeter
- Ammeter

Air inlet temperature

- Thermocouples in plenum chamber (3)

Air outlet temperature

- Centre-line thermocouple at heat exchanger outlet

Wall temperatures

- Thermocouples (29)

Reference zone temperature

- Thermometer

Room temperature

- Thermometer

For unsteady flow, the following additional parameters were noted

Frequency

- Siren shaft transducer

Pressure amplitudes at node and antinode

- Pressure transducer

From the experimental measurements, local Nusselt number was calculated for positions along the heat exchanger

- See Section 6.4

6.4 Data Reduction

- to calculate local Nusselt number.

For the heating tape,

Let voltmeter reading = V volts

ammeter reading = I amps

$\therefore$ Energy output from heating tape per sec, $\dot{Q}_E = V \cdot I$ watts

Surface area of heat exchanger $= \pi d L \ m^2$

where $d = 0.04$ m

$L = 1.71$ m

$\therefore$ Energy output/unit area per sec, $\dot{q}_E = \frac{\dot{Q}_E}{\pi d L} \cdot 10^{-3} \ KW/m^2$

Consider inlet to heat exchanger ($x = o$)

Bulk air temperature $= Tm_{(o)}$ °K

(measured in plenum chamber of siren)

Measured wall temperature $= T_{w(o)}$ °K

Consider point x incremental distance δx from inlet,

Measured wall temperature $= T_{w(x)}$ °K

By linear interpolation,

Average wall temperature over distance, $= \frac{1}{2} (T_{w(x)} + T_{w(o)})$ °K

$= T_{w(\delta x)}$ °K

- assuming the distance δx to be small

$$\text{Energy loss over length } \delta x = \frac{-2\pi K_I \delta x}{\log_e(\frac{r_2}{r_1})} (T_{w(\delta x)} - T_{R.T.}) \quad \text{KW}$$

where K_I = thermal conductivity of insulation
= 0.0515 x 10^{-3} KW/m °K

$r_2 - r_1$ = thickness of insulation
= 75.0 mm

r_2 = 99.0 mm

r_1 = 24.0 mm

$T_{R.T.}$ = ambient temperature of laboratory °K

(62)

- the outer surface temperature of the insulation could be approximated to room temperature.

$$\therefore \quad \text{Energy input, over distance } \delta x, \text{ per sec } \dot{Q}_{\delta x} = \frac{\dot{Q}_E}{L} \cdot \delta x \cdot 10^{-3}$$

$$\frac{-2\pi K_I \delta x}{\log_e(\frac{r_2}{r_1})} (T_{w(\delta x)} - T_{R.T.}) \quad \text{KW.}$$

Apply steady flow energy equation to mean flow of air

$$\therefore \quad \dot{Q}_{\delta x} = \dot{m} C_p (T_{m(x)} - T_{m(o)}) \quad \text{KW}$$

where $\dot{m}$ = mean mass flowrate Kg/s

C_p = specific heat at constant pressure
= 1.00 KJ/Kg °K
over temperature range.

$$\therefore \quad T_{m(x)} = T_{m(o)} + \frac{\dot{Q}_{\delta x}}{\dot{m} C_p} \quad °K$$

By similar method, the bulk air temperature was calculated along the pipe by successive calculations - the accuracy of the predictions is dependant on the step length δx .

For point x

$$\text{Energy loss/unit area per sec, } \dot{q}_{L(x)} = \frac{-2K_I}{d\log_e(\frac{r_2}{r_1})} (T_{w(x)} - T_{R.T.}) \text{ KW/m}^2$$

$$\therefore \text{ Energy input to air flow/unit area/sec} = \dot{q}_E - \dot{q}_{L(x)} \text{ KW/m}^2$$

By definition

$$\text{Heat transfer coefficient, } h_{(x)} = \frac{\dot{q}_E - \dot{q}_{L(x)}}{(T_{w(x)} - T_{m(x)})} \text{ KW/m}^2\text{°K}$$

$$\therefore \text{ Nusselt number, } Nu_{d(x)} = h_{(x)} \cdot \frac{d}{k}$$

where k = thermal conductivity of air

- all fluid properties used in the experimental calculations were defined at local bulk air temperature. The property tables are given in reference 80.

Similarly the local Nusselt number was calculated for positions along the pipe from measurements of local wall temperature.

For pulsating flow, the velocity amplitude distribution was calculated from measurements of pressure amplitude at a node and antinode from inviscid flow theory - see Section 3.1. The frequency of oscillation was calculated from a measurement of the siren drive shaft speed. From these calculations, the Dimensionless pulsation velocity (B) and the Strouhal number (S) were found for points along the heat exchanger.

$$B = \hat{U}/\overline{U}_m$$

$$S = \omega d/\overline{U}_m$$

It can be shown by dimensional analysis that for fully developed turbulent flow in a pipe

$$Nu_d = f \ (Re_d, \ Pr, \ T_m/T_w)$$

(62)

Previous experimental investigations have been correlated in terms of the non-dimensional parameters - the following expression can be used to predict heat transfer coefficient for a constant heat flux source for $3{,}000 < R_{e_d} < 100{,}000$.

$$Nu_d = 0.023 \ (Re_d)^{0.8}(Pr)^{0.4}(T_m/T_w)^{0.5}$$

(66)

It was decided to express the experimental heat transfer characteristics in terms of the non-dimensional W where

$$W = N_{u_d}/((R_{e_d})^{0.8}(Pr)^{0.4}(T_m/T_w)^{0.5})$$

- define W as the flow independant Nusselt number

For the experimental results for steady flow, the function should be a constant for fully-established conditions, and approximately equal to 0.023 - the given equation is a derived function to approximate previous experimental results over the defined range of Reynolds number, and a better estimate can be found from the solution of the energy equation for a given flowrate (see Section 4.2.1).

For a pulsating flow, it has been shown for local heat transfer, with fully developed boundary layer, that

$$\overline{N_{u_d}} \approx g\ (\overline{R_{e_d}}, Pr, \overline{T_m}/\overline{T_w}, B, S)$$

assuming dependance on local pulsation parameters only

(42)

It was assumed that the following expression could be defined

$$\overline{N_{u_d}} = (\overline{R_{e_d}})^{0.8}(Pr)^{0.4}(\overline{T_m}/\overline{T_w})^{0.5} g'(\overline{Re}_d, B, S)$$

i.e. the effect of fluid properties and transverse temperature gradient were assumed similar as for steady flow. The effect on pulsation parameters was considered negligible

$$\therefore \quad \overline{W} = g'(\overline{R_{e_d}}, B, S)$$

A comparison between the flow-independant Nusselt numbers was made between the pulsating flow and the equivalent steady flow.

See Section 6.6

6.5 Error analysis

The maximum possible experimental errors in the parameters of the investigation are considered.

It is assumed that

a) No personal error

b) No environmental error

c) No computational error

The error is considered relative to the instrumentation i.e. consider the maximum errors in the derived parameters from the possible errors of the measuring instruments. The estimations of the errors are shown in algebraic form to demonstrate the method of prediction.

- for Laws of Propagation of Errors see reference 81

Consider the major variables of the project i.e. Nusselt number, Reynolds number, Dimensionless pulsation velocity and Strouhal number.

Nusselt number

$$Nu_d = \frac{hd}{k} = \frac{\dot{q}}{(T_w - T_m)} \cdot \frac{d}{k}$$

But

$$T_{m(x)} = T_{m(o)} + \frac{\dot{q}}{\dot{m}} \cdot \frac{\pi d}{C_p} \cdot x$$

- see Section 6.4 for method of data reduction

The following assumptions are made

a) Negligible error in scale measurements e.g. pipe diameter, length

b) Relative to the errors in bulk temperature, the physical properties of the air can be considered to have negligible error

$\therefore$ Error in bulk air temperature $E_{T_{m(x)}} = E_{T_{m(o)}} + \left(\frac{E_{\dot{q}}}{\dot{q}} - \frac{E_{\dot{m}}}{\dot{m}}\right)\frac{\dot{q}}{\dot{m}} \cdot \frac{\pi d}{C_p} \cdot x$

$\therefore$ Error in temperature difference $E_{(T_{w(x)} - T_{m(x)})} = E_{T_{w(x)}} - E_{T_{m(o)}} - \left(\frac{E_{\dot{q}}}{\dot{q}} - \frac{E_{\dot{m}}}{\dot{m}}\right)\frac{\dot{q}}{\dot{m}} \cdot \frac{\pi d}{C_p} \cdot x$

But $h_{(x)} = \frac{\dot{q}}{T_{w(x)} - T_{m(x)}}$

$\therefore$ Fractional error in heat transfer coefficient

$$\frac{E_{h(x)}}{h(x)} = \frac{E_{\dot{q}}}{\dot{q}} - \frac{\left(E_{T_{w(x)}} - E_{T_{m(o)}}\right)}{\left(T_{w(x)} - T_{m(x)}\right)} + \frac{1}{\left(T_{w(x)} - T_{m(x)}\right)}\left(\frac{E_{\dot{q}}}{\dot{q}} - \frac{E_{\dot{m}}}{\dot{m}}\right)\frac{\dot{q}}{\dot{m}}\frac{\pi d}{C_p} x$$

$$Nu_{d(x)} = h_{(x)} \frac{d}{k}$$

$\therefore$

$$\frac{E_{Nu_{d(x)}}}{Nu_{d(x)}} = \frac{E_{h_{(x)}}}{h_{(x)}}$$

Reynolds number

$$Re_d = U_m \frac{d}{\nu}$$

$$= \frac{4}{\pi d} \cdot \frac{\dot{m}}{\mu}$$

$$\therefore \quad \frac{E_{Re_{d(x)}}}{Re_{d(x)}} = \frac{E_{\dot{m}}}{\dot{m}}$$

Flow independant Nusselt number

$$W = Nu_d/((Re_d)^{0.8}(Pr)^{0.4}(T_m/T_w)^{0.5})$$

The experimental results were expressed in terms of the non-dimensional W - see Section 6.4.

$$\therefore \quad \frac{E_{W(x)}}{W(x)} = \frac{E_{Nu_{d(x)}}}{Nu_{d(x)}} - \frac{0.8E_{Re_{d(x)}}}{Re_{d_{(x)}}} - 0.5\left(\frac{E_{T_m(x)}}{T_{m(x)}} - \frac{E_{T_W(x)}}{T_{W(x)}}\right)$$

Dimensionless pulsation velocity

$$B_{(x)} = \hat{U}_{(x)}/\bar{U}_{m(x)}$$

The velocity amplitude, $\hat{U}$, along the pipe is calculated from pressure amplitude measurements

$$\therefore \quad \frac{E\hat{U}_{(x)}}{\hat{U}(x)} \approx \frac{E\hat{P}_A}{\hat{P}_A}$$

$$\bar{U}_m = \frac{4}{\pi d^2} \cdot \frac{\dot{m}}{\bar{\rho}}$$

$$\therefore \quad \frac{E\bar{U}_{m(x)}}{\bar{U}_{m(x)}} = \frac{E_{\dot{m}}}{\dot{m}}$$

$\therefore$ Fractional error of, the dimensionless pulsation velocity

$$\frac{E_{B(x)}}{B_{(x)}} = \frac{E\hat{P}_A}{\hat{P}_A} - \frac{E_{\dot{m}}}{\dot{m}}$$

Strouhal number

$$S = \omega d/\bar{U}_{m(x)}$$

$$w = 2\pi f$$

$\therefore$ Fractional error of Strouhal number

$$\frac{E_{S(x)}}{S(x)} = \frac{E_f}{f} - \frac{E_{\dot{m}}}{\dot{m}}$$

The relevant instrument accuracies can be defined.

Mass flowrate

Gapmeter accuracy ± 1.25% F.S.D.

- it is assumed that the chamber loss and the bleed system have negligible errors relative to the supply flowmeters

Energy flux

Heating tape

Voltmeter resolution ± 0.7% F.S.D.

Ammeter resolution ± 1.0% F.S.D.

- the possible error of the heat flux calculations is assumed negligible relative to the heating tape errors.

Temperature

Calibration error of thermocouple wire ± 0.1°C

Resolution of digital voltmeter ± 0.25°C

Pulsation parameters

Pressure amplitude measurement

Oscilloscope resolution ± 3%

- it is assumed that possible errors of the transducers and charge amplifiers are negligible relative to the oscilloscope resolution.

Frequency measurement

Counter resolution ± 2%

For the flow-independant Nusselt number, the maximum possible error is a complex combination of the measurement errors. The error can only be defined for individual positions along the heat exchanger, and due to the interaction of the measuring errors, a wide range of possible errors is predicted. From a consideration of the range of parameters, it is proposed that, for approximation, an average error of 20% for flow-independant Nusselt number can be defined. The errors for the other parameters can be predicted directly from the relevant instrument errors.

The analysis can only be considered to give an indication of the possible maximum errors. Since the convective heat transfer for a fully-developed turbulent flow can be predicted theoretically for a constant heat flux input (see Section 4.2.1), an estimate of the performance of the experimental system can be found from a comparison of the theory to steady flow results.

6.6 Results

It was found that an energy loss occurred at the exit of the heat exchanger to the outlet section. This loss could not be allowed for in the calculations, and consequently results in the last 10 cm of the heat exchanger were not considered. Due to this loss, the measurements of outlet air temperature for steady flow had limited meaning. But the maximum difference between measured and predicted bulk air temperature was 14.8%. The difference was accepted considering the unknown energy loss.

The experimental results are recorded graphically in terms of flow-independant Nusselt number (W) against position in heat exchanger (x) - the results for mean flowrate 0.0115 Kg/s are reported in this section.

See Figure 18 Page 90 to 95

The majority of the results for the other flowrates are given in Appendix III.

The thermal entrance length for all the flowrates under steady conditions was approximated to 50 cm - see graphs. The flow-independant Nusselt number can be predicted from the energy equation for fully-developed conditions (see Section 4.2.2) - approximately equal to 0.023 as discussed in Section 6.4. The following table gives a comparison between experimental and theoretical determinations. The experimental result was found from the appropriate graph.

Re_d	W exp.	W theory	% difference
14,300	0.0250	0.0240	+ 4.16
20,550	0.0230	0.0232	- 0.86
25,900	0.0230	0.0227	+ 1.32
31,250	0.0220	0.0224	- 1.79

for Re_d defined at air temperature of 15°C.

The agreement between theory and experiment justified the experimental system and the methods of analysis (compare to maximum error limits - see Section 6.5). The repeatability for the experimental results was within 3% - all tests were repeated to check the limits of variation.

The results for pulsating flow are shown in comparison to the fully-developed flow-independant Nusselt number of the equivalent steady flow, and also relative to the positions of the velocity nodes and anti-nodes. It was obvious that large increases in heat transfer occurred relative to the equivalent steady flow e.g. local increase of 100% for the fundamental frequency (25 Hz) - see Figure 18b Page 91 . But decreases in Nusselt number were also measured e.g. local decrease of 17.5% for the 1st harmonic (75 Hz) - see Figure 18c Page 92.

The general indications were that the effect of oscillations on local heat transfer were complex, and dependant on both frequency and local velocity amplitude. Measurements for conditions of maximum attenuation showed that any change in heat transfer was due to the acoustic oscillations - the results agreed with the equivalent steady flow to within $\pm$ 3%.

No indication was given by the experimental results that acoustic streaming flow patterns were influencing the heat transfer - characteristic streaming effects are given in Section 2.2. Theoretical predictions of mean velocity profiles indicated that acoustic streaming would have a negligible effect for the range of parameters in the experimental programme - see Section 4.1.6.

Centre-line temperature was measured at the outlet of the heat exchanger under pulsating conditions. It was found that the thermocouple reading was dependant on the velocity amplitude at that point. Further tests, under ambient conditions, showed that errors of the order of -20% were given from thermocouples in the oscillating air stream - the larger the velocity amplitude at the point, the greater the error. These limited results showed that simple temperature measurements in an oscillating flow must be regarded with some doubt.

The experimental results were analysed in terms of local heat transfer relative to local Dimensionless pulsation velocity.

- see Chapter 7

Figure 18 a/j Experimental heat transfer

- Local flow-independant Nusselt number against position in heat exchanger

Mean air flowrate $\bar{\dot{m}}$ = 0.0115 Kg/s

Reynolds number, $\overline{Re}_d$ = 20550
at bulk air temperature 15°C

Results are shown for five frequencies

f = 25, 75, 125, 175, 225 Hz

for different pressure amplitudes relative to the equivalent steady flow (compared to the fully-developed flow-independant Nusselt number)

Results for the other mean flowrates are given in Appendix III.

Fig.18a Steady Flow

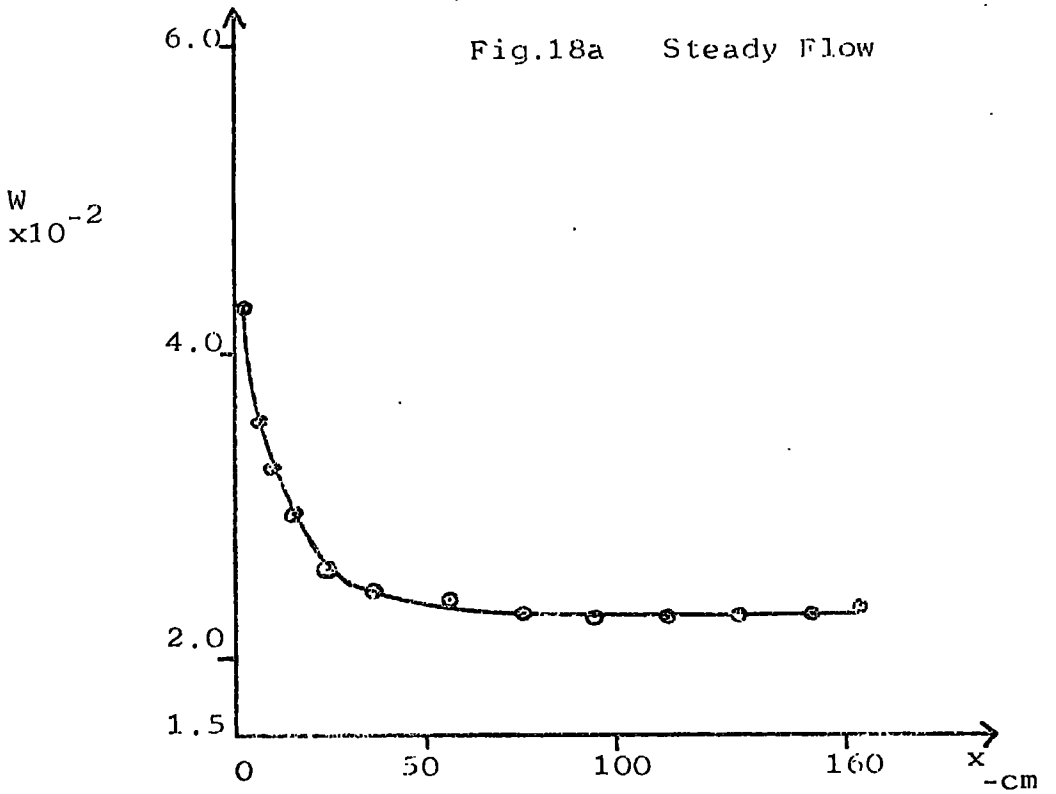

Fig.18b

f = 25 Hz
$\hat{P}$ = 15900 N/m^2
$\hat{P}_N$ = 2450 N/m^2

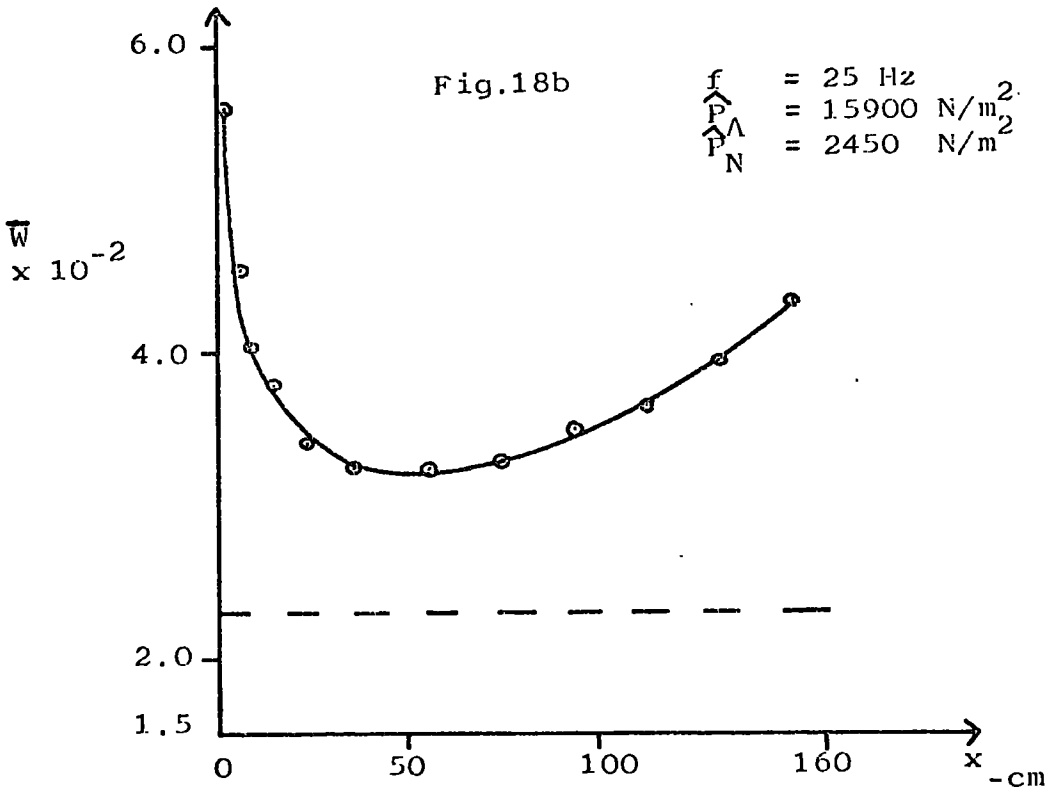

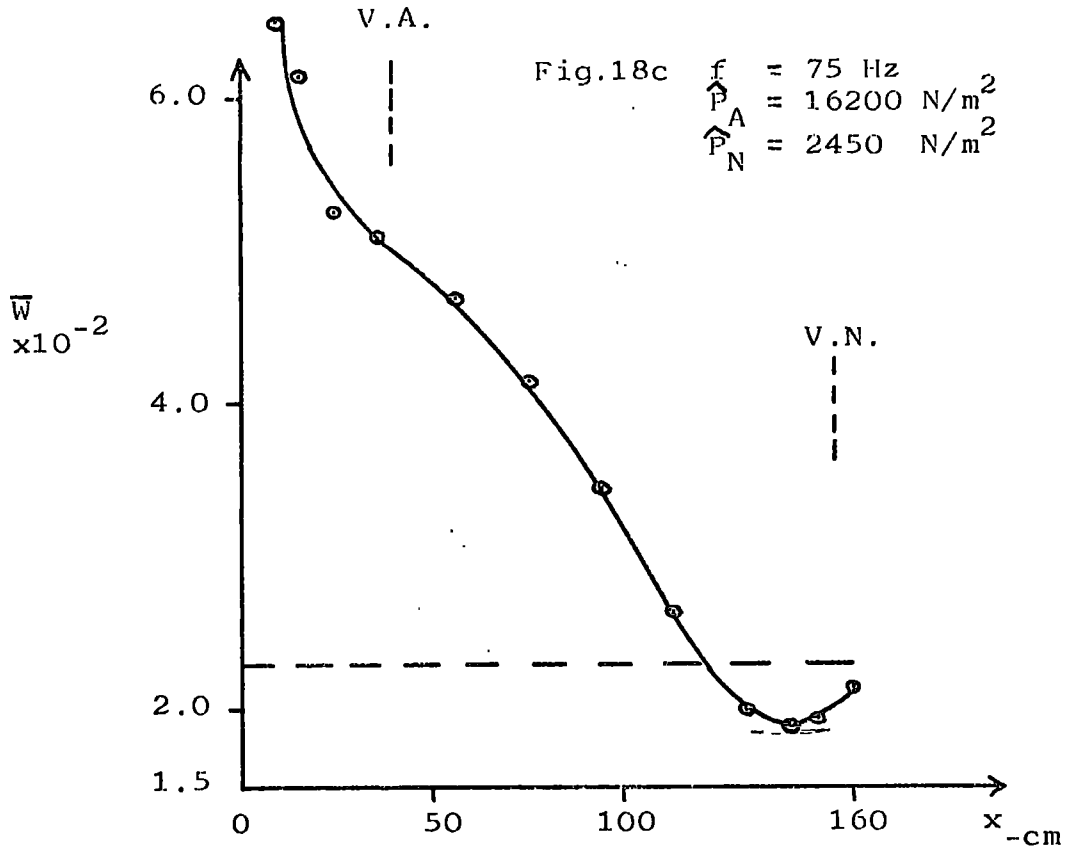

Fig.18c f = 75 Hz
$\hat{P}_A$ = 16200 N/m^2
$\hat{P}_N$ = 2450 N/m^2

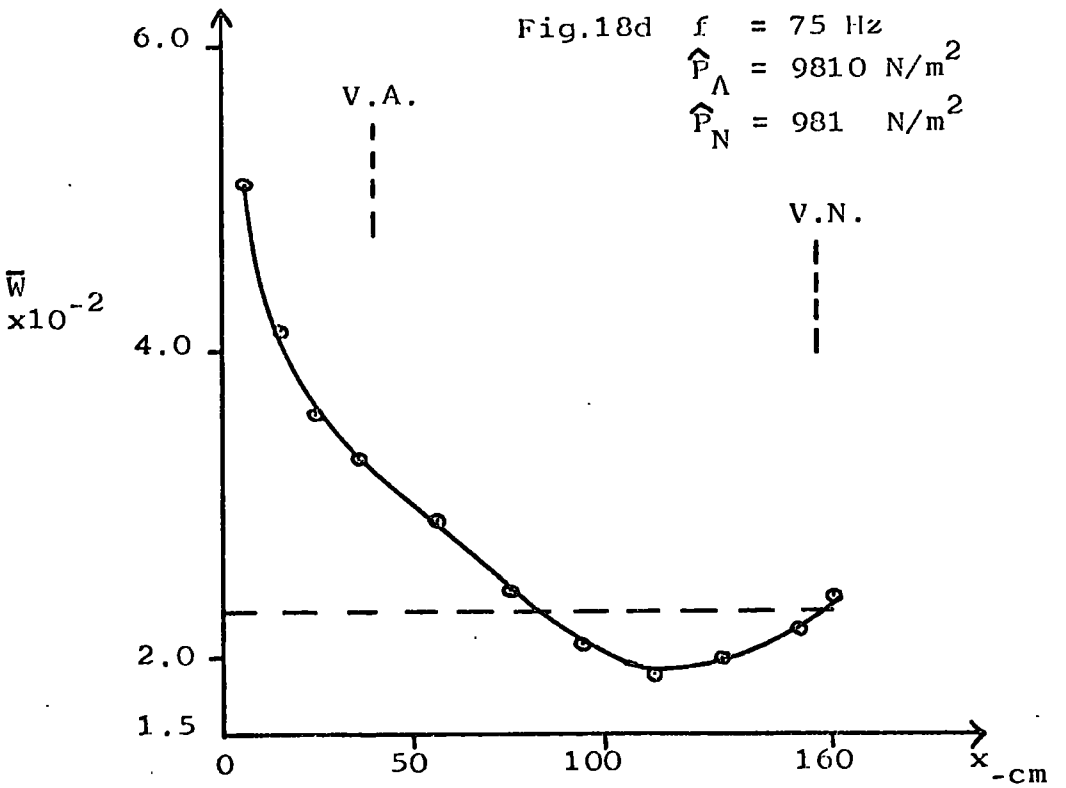

Fig.18d f = 75 Hz
$\hat{P}_A$ = 9810 N/m^2
$\hat{P}_N$ = 981 N/m^2

Fig.18e f = 125 Hz
$\hat{P}_A$ = 14500 N/m^2
$\hat{P}_N$ = 2450 N/m^2

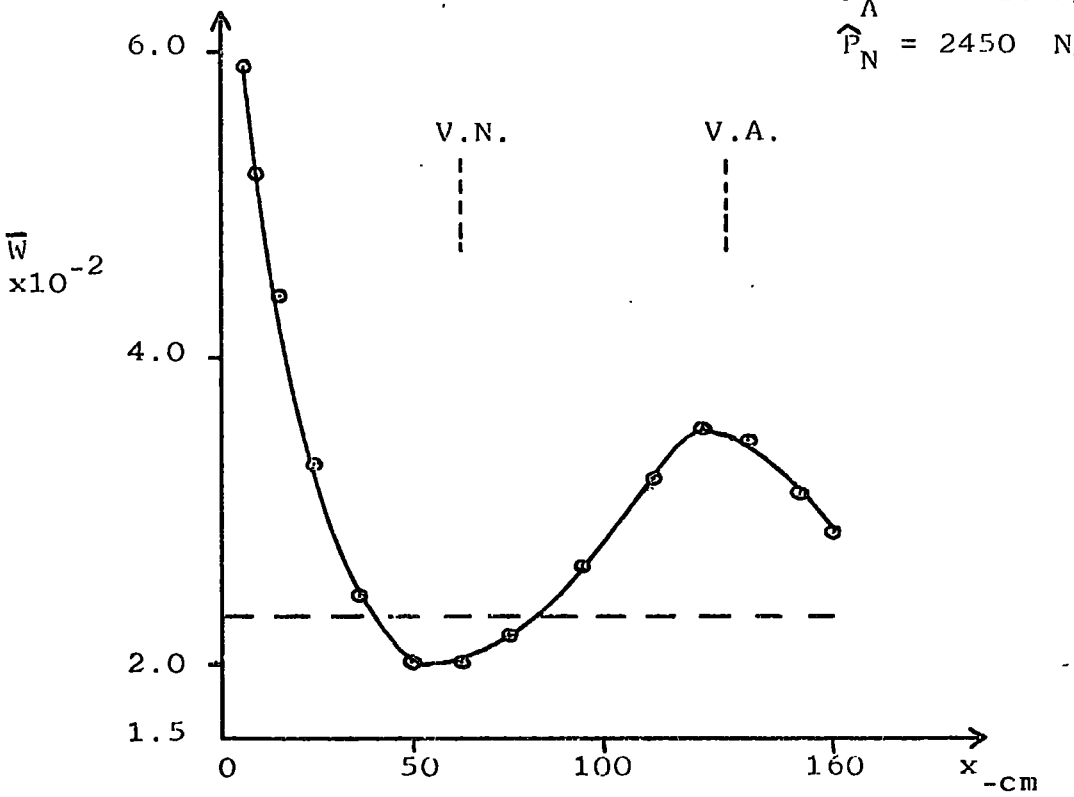

Fig.18f f = 125 Hz
$\hat{P}_A$ = 12730 N/m^2
$\hat{P}_N$ = 1960 N/m^2

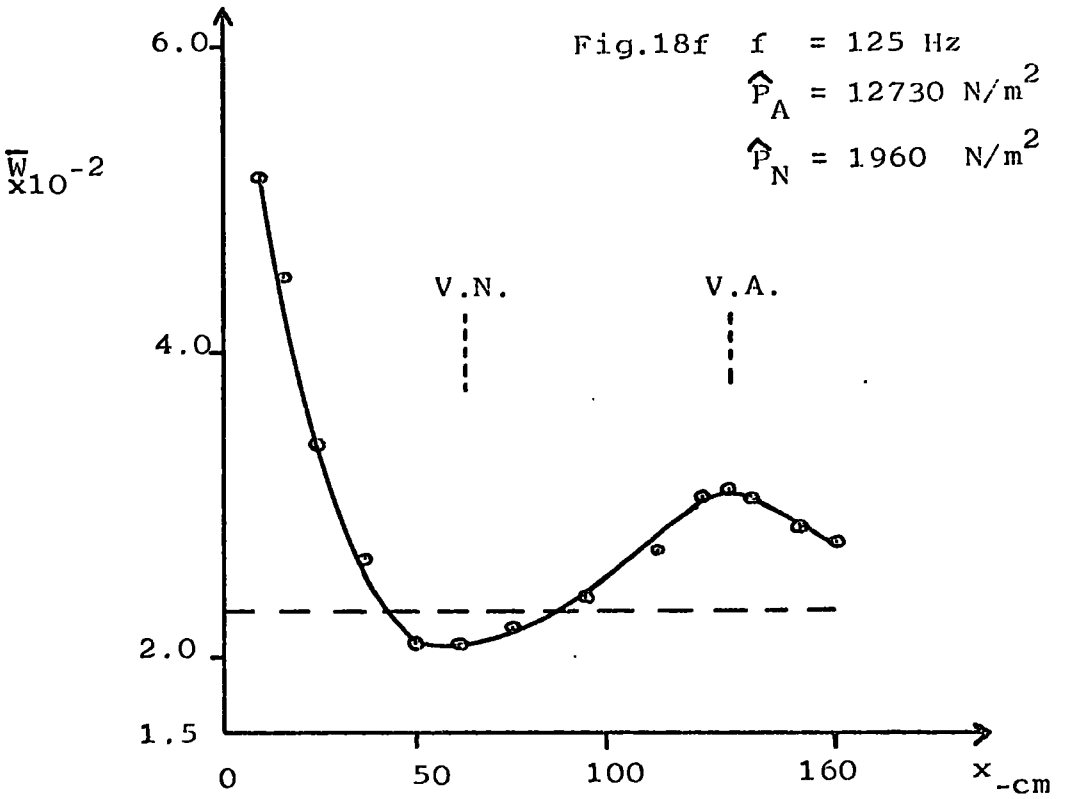

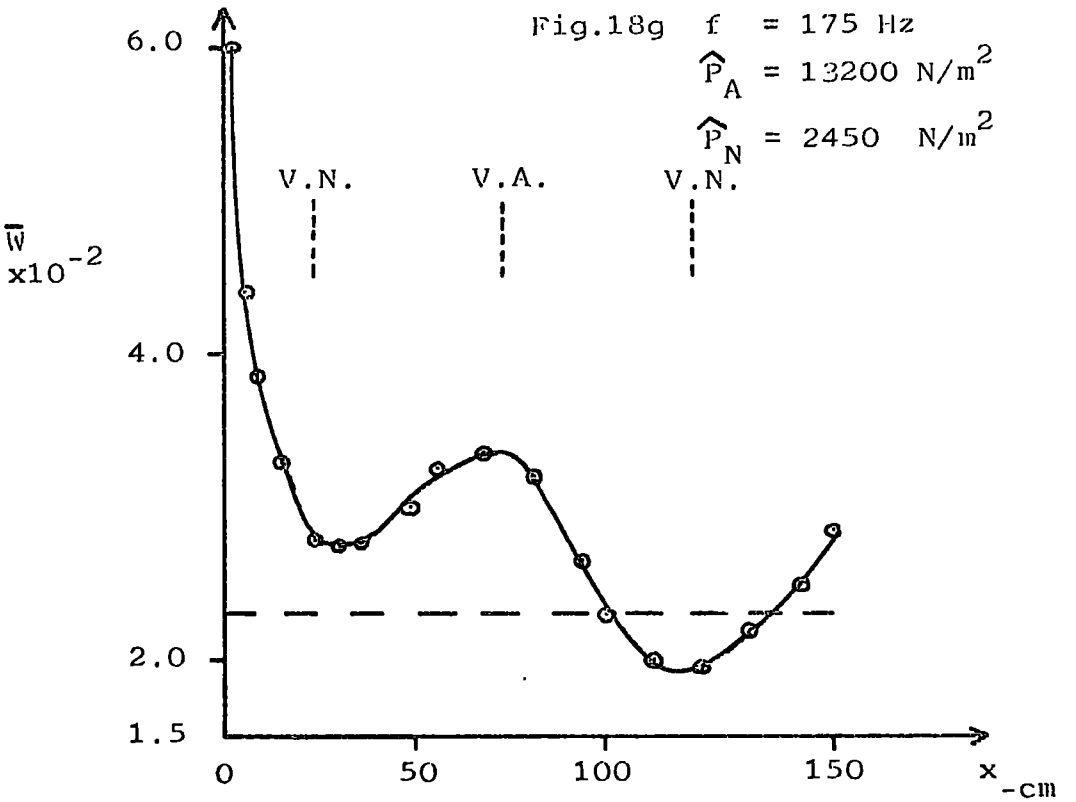

Fig.18g f = 175 Hz
$\hat{P}_A$ = 13200 N/m^2
$\hat{P}_N$ = 2450 N/m^2

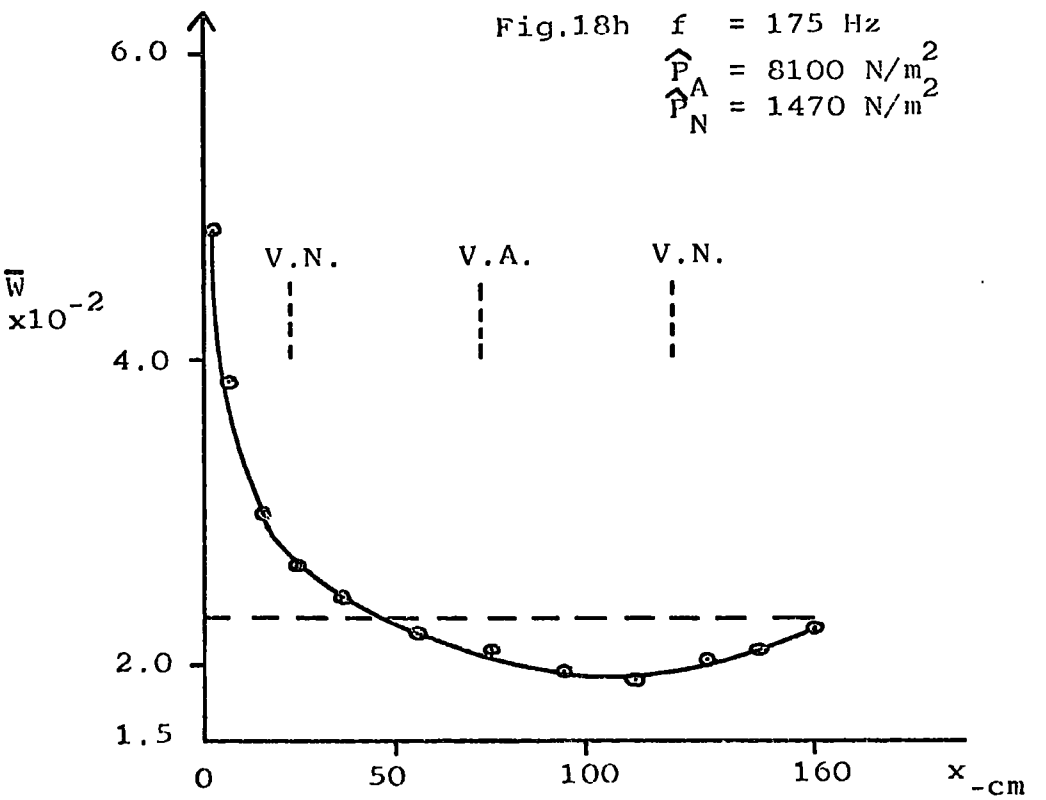

Fig.18h f = 175 Hz
$\hat{P}_A$ = 8100 N/m^2
$\hat{P}_N$ = 1470 N/m^2

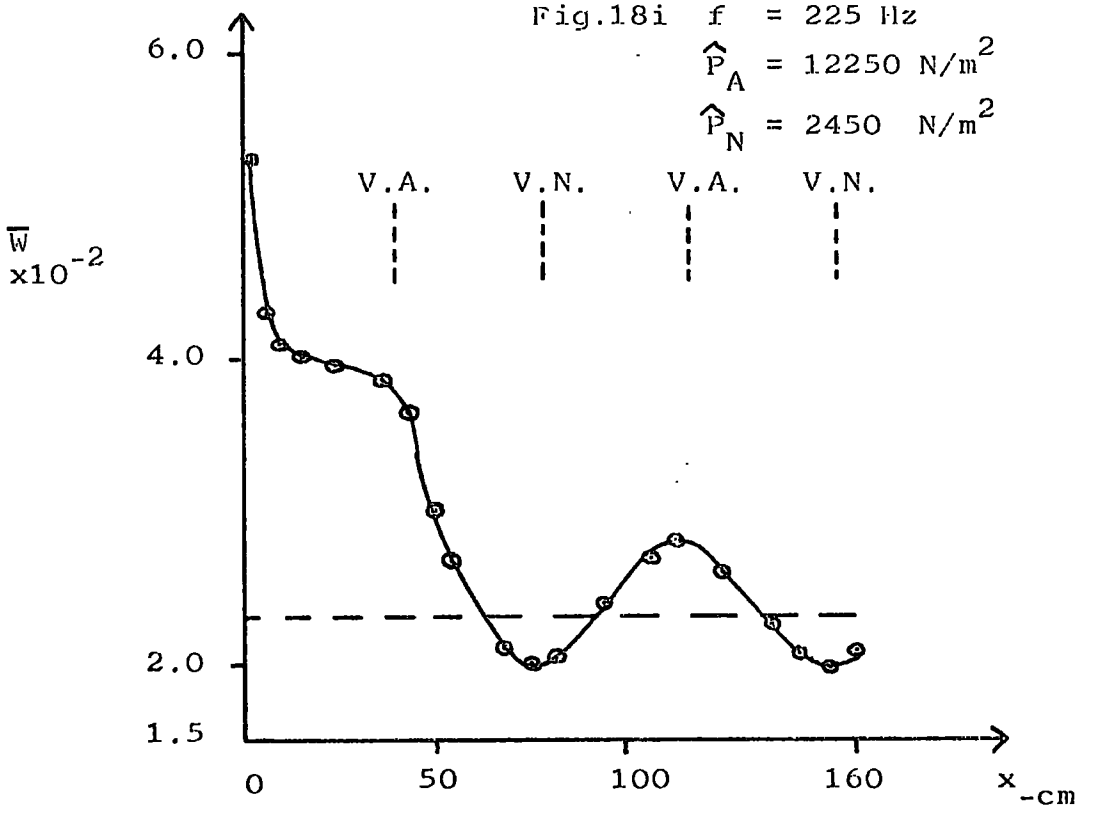
Fig.18i f = 225 Hz
$\hat{P}_A$ = 12250 N/m^2
$\hat{P}_N$ = 2450 N/m^2
V.A.
V.N.
V.A.
V.N.
$\overline{W}$ x10^{-2}
6.0
4.0
2.0
1.5
0
50
100
160
x -cm

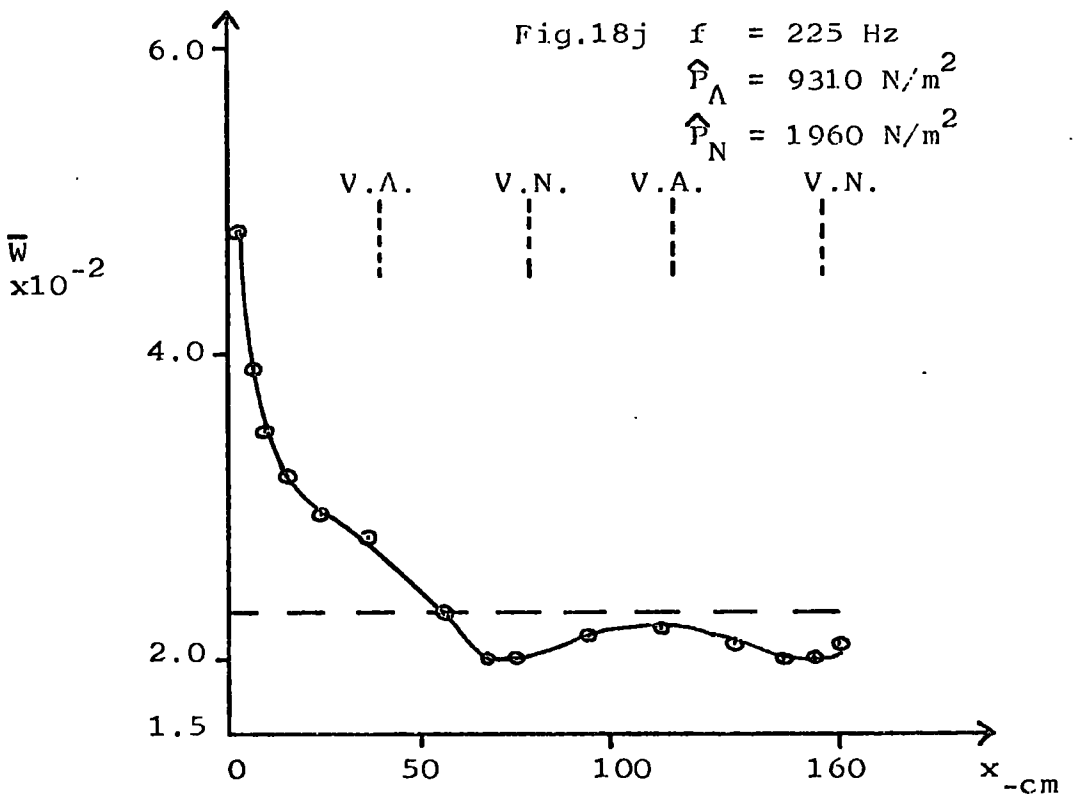
Fig.18j f = 225 Hz
$\hat{P}_A$ = 9310 N/m^2
$\hat{P}_N$ = 1960 N/m^2
V.A.
V.N.
V.A.
V.N.
$\overline{W}$ x10^{-2}
6.0
4.0
2.0
1.5
0
50
100
160
x -cm

CHAPTER 7

Frequency factor evaluation

7. Frequency factor evaluation

It has been proposed for pulsating flow that, for a given Reynolds number and Strouhal number for a system, the change in local heat transfer relative to the equivalent steady flow is dependent only on the local Dimensionless pulsation velocity for fully developed conditions - see Section 4.2. Since the change in air temperature along the pipe was small, Strouhal number and Reynolds number can be assumed to be constant for a given experimental condition of frequency and flowrate. For fully developed conditions, the improvement ratio R_A was calculated.

$$R_A = \frac{\overline{W}}{W_e}$$

where W_e is the flow independent Nusselt number for the equivalent steady flow

The thermal entrance length for pulsating conditions was assumed to be the same as for the equivalent steady flow. For fully developed conditions, local improvement ratio was plotted against the corresponding pulsation velocity for a given frequency and mean flowrate. The quasi-steady predictions are shown for comparison i.e. assuming, for the defined frequency and flowrate, that the pulsations can be considered quasi-steady - see Section 4.2.2. The analysis for mean flowrate 0.0115 Kg/s is recorded in this chapter.

See Figure 19 Page 97 to 99

Analysis for the other flowrates is shown in Appendix IV.

For the experimental range, the ratio was dependent only on local pulsation velocity for a given flowrate and frequency (within experimental error). The experimental functions were of a similar form as the variation given by quasi-steady theory - characteristic decrease at B = 1, and for higher values of pulsation velocity an approximately linear increase. In all cases any increase in heat transfer relative to the equivalent flow was less than the corresponding predicted quasi-steady change - as $\omega \longrightarrow 0$, $R_A \longrightarrow R_{AQS}$, and as $\omega \to \infty$, $R_A \longrightarrow 1.0$.* For a given frequency, an increase in mean flowrate showed $R_A \longrightarrow R_{AQS}$ relative to the lower flowrate i.e. if flowrate A was less than flowrate B, $(R_{AQS} - R_A)_A > (R_{AQS} - R_A)_B$ for the same pulsation velocity.

Relative to the proposed mechanism, it has been suggested that the degree to which conditions approach quasi-steady can be described by a function of Strouhal number, and it was hoped that a frequency factor, in terms of Strouhal number only, could be defined to relate measured local heat transfer to predicted quasi-steady coefficients - see Section 4.2.3. But, due to the non-linearity of the interaction of laminar sub-layer and core diffusivity a simple direct relationship, relative to Strouhal number, cannot be defined from a comparison of heat transfer. The effect of the non-linearity can be seen from the experimental results - at high frequency, for large pulsation velocity, $R_A \longrightarrow 1.0$ but for $B \approx 1$ the effect of frequency was less, relative to the quasi-steady variation, due to the dominance of the laminar sub-layer thickness.

* With limitations on velocity amplitude within small perturbation theory - not shock wave condition

Fig.19 a/e Local Improvement Ratio for fully developed flow against the corresponding local Dimensionless Pulsation velocity for a given frequency

Mean air flowrate $\overline{\dot{m}}$ = 0.0115 Kg/s

Reynolds number $\overline{Re}_d$ = 20550
at Bulk air temperature 15°C

Experimental data shown in comparison to the equivalent quasi-steady predictions.

x, Δ, □ Experimental data (each symbol representing different amplitude condition)

⊙ Quasi-steady theory

Correlations for the other mean flowrates are given in Appendix IV

Fig.19a f = 25 Hz
S = 0.78

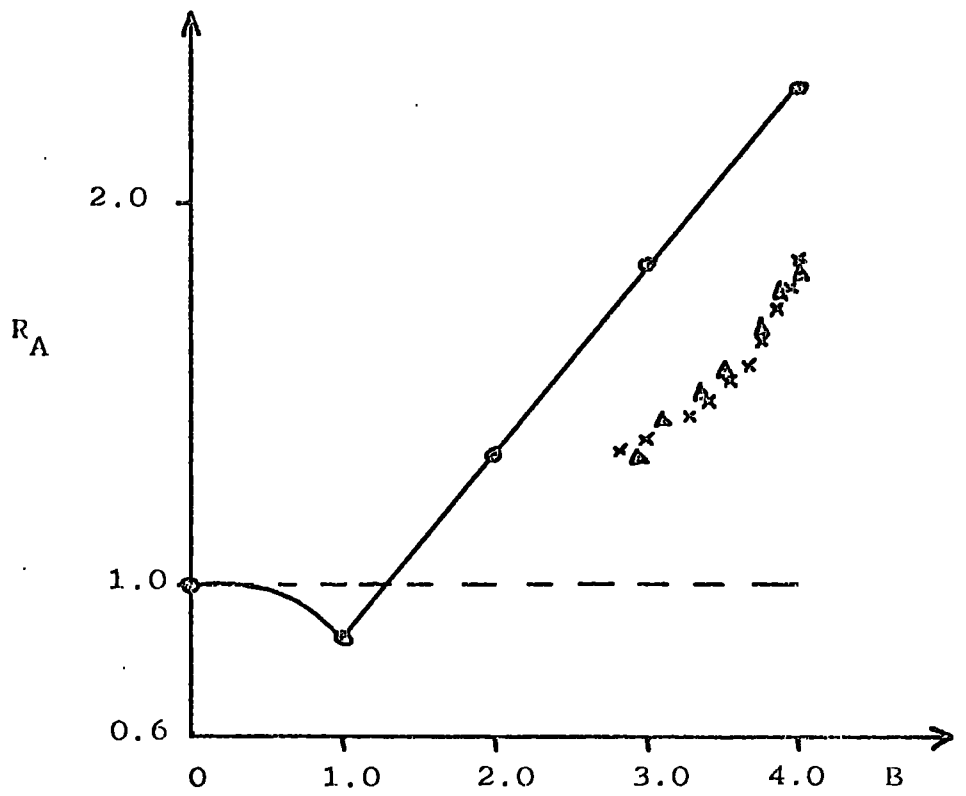

Fig.19b f = 75 Hz
S = 2.33

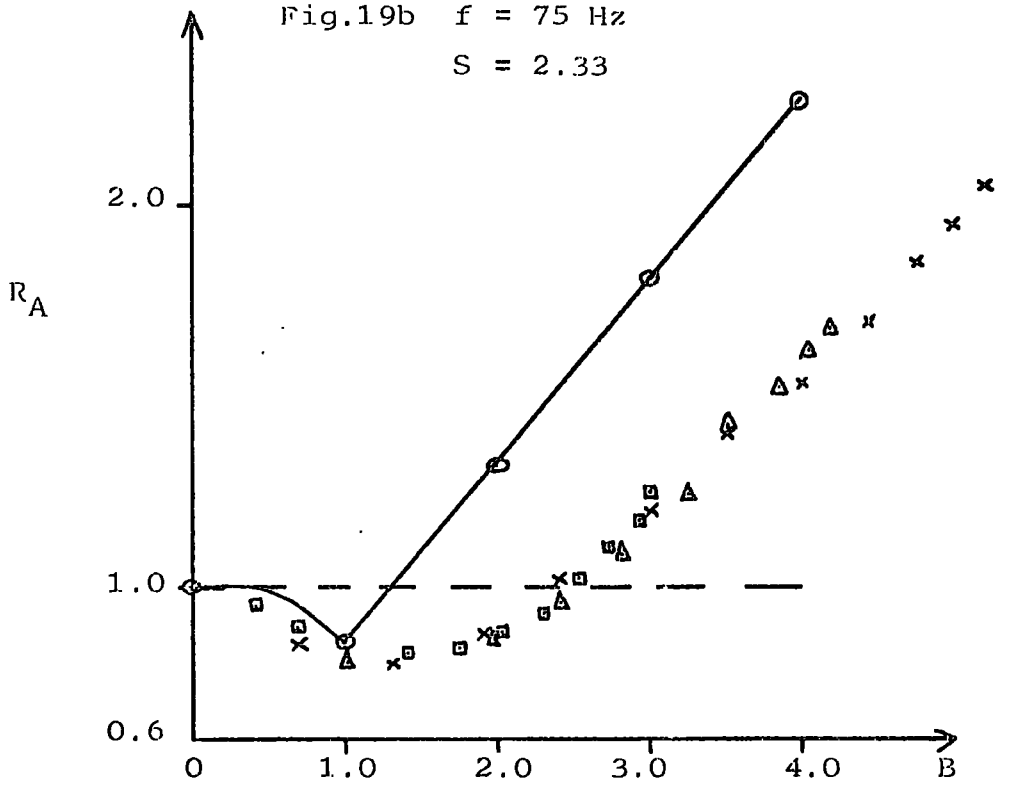

Fig.19c f = 125 Hz
S = 3.83

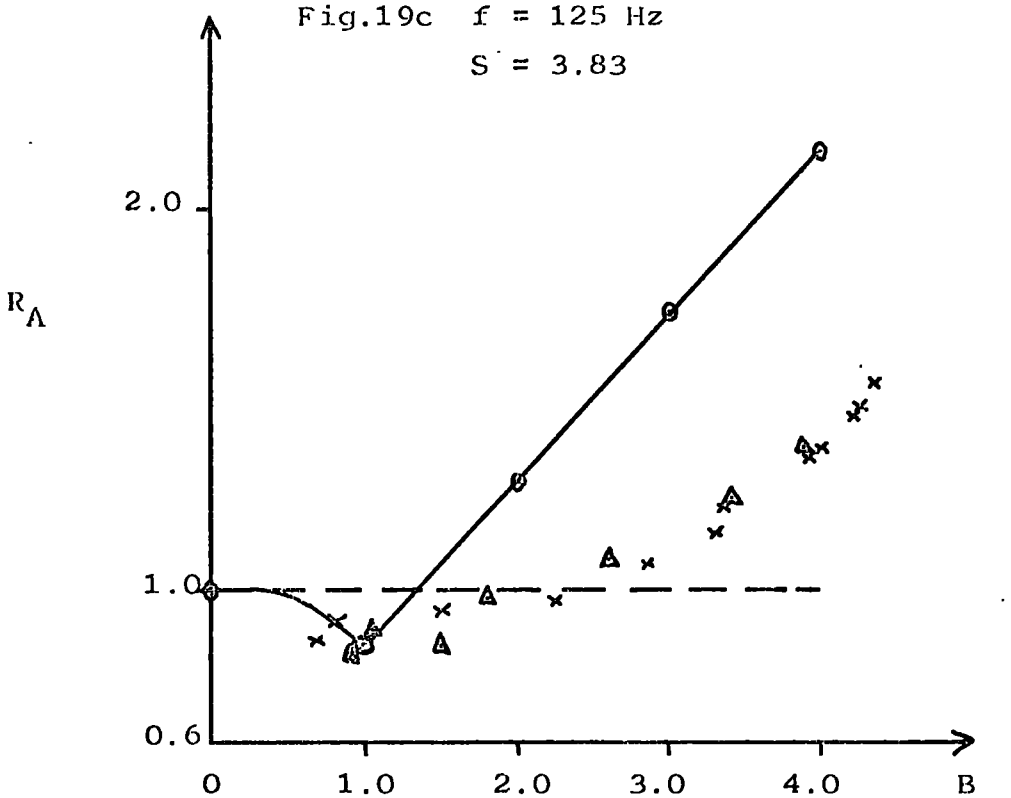

Fig.19d f = 175 Hz
S = 5.38

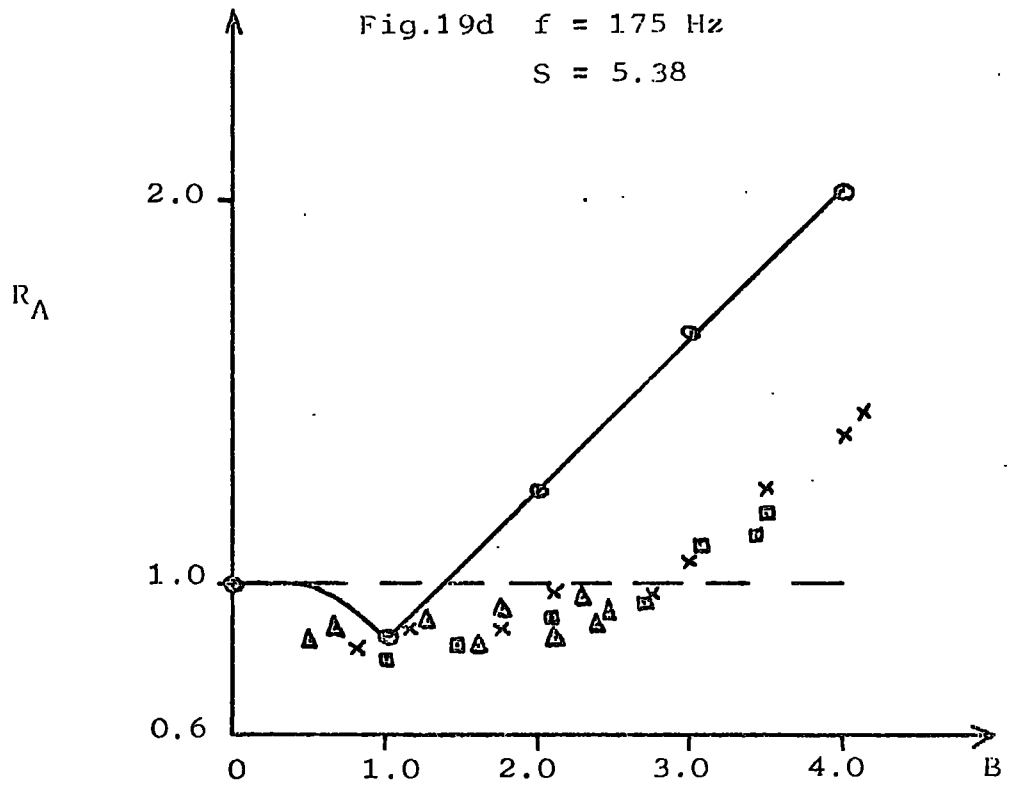

Fig.19e f = 225 Hz
S = 6.95

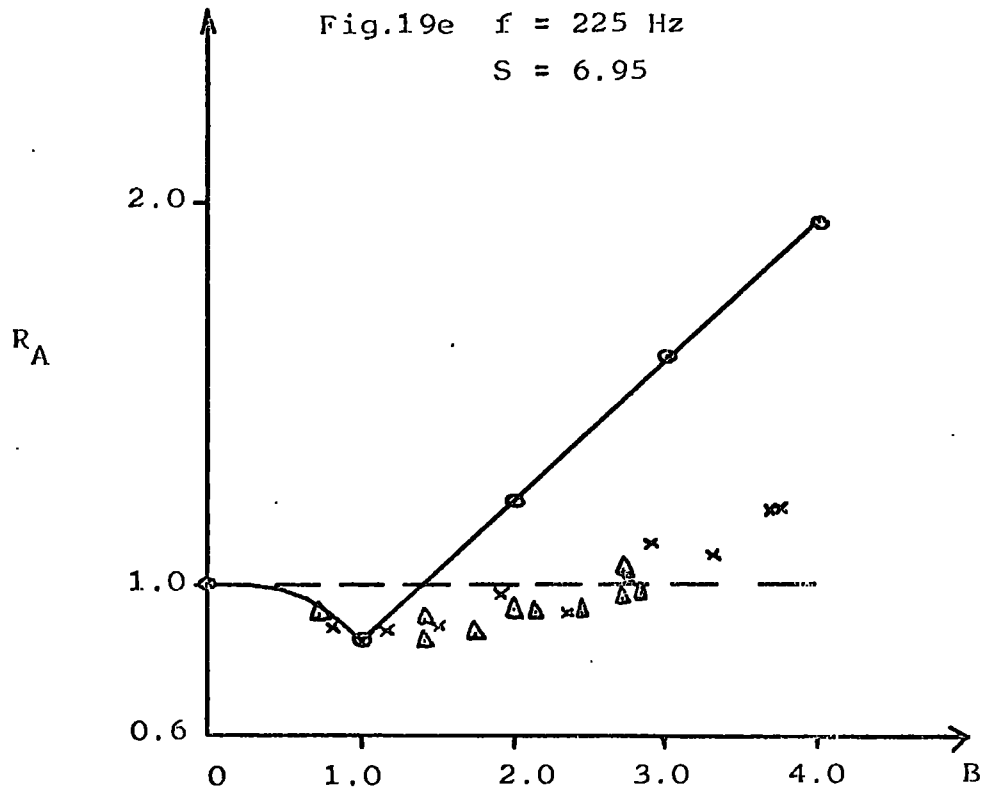

But to be able to predict heat transfer in a pulsating flow, a frequency correction factor must be defined to relate experimental results to the corresponding quasi-steady predictions. The following approximation was made - it was defined, from the experimental data, that the improvement ratios at high frequency were given by

$$R_{A_{HF}} = R_{A_{QS}} \quad \text{for} \quad B < 1$$

$$R_{A_{HF}} = 1.0 + 0.2\,(B - 6.0)\,(1.0 - R_{A_{QS_{B=1}}}) \quad \text{for} \quad 1 < B < 6$$

$$R_{A_{HF}} = 1.0 \quad \text{for} \quad B > 6$$

From the above definitions, the following relationship can now be considered

$$(R_A - R_{A_{HF}}) = (R_{A_{QS}} - R_{A_{HF}})\,(1.0 - A\,(\frac{\omega d}{U_m})^B)$$

where A and B are constants

- the flow was considered to be quasi-steady at zero frequency.

By defining the high frequency function, a simple relationship can be investigated to relate practical and theoretical data. For high Reynolds number ($\overline{Re_d} > 25000$) the error due to the approximation will be negligible since $R_{A_{QS}} \approx 1$ at $B = 1$ - at low Reynolds number, the function can be considered the lower limit for high frequency pulsation with an upper limit of $R_{A_{HF}} = 1.0$.

Define the function F_c

$$F_c = 1.0 - (R_A - R_{A_{HF}})/(R_{A_{QS}} - R_{A_{HF}})$$

The frequency factor equation can be rewritten as

$$F_c = A\,(\frac{\omega d}{U_m})^B$$

For a given flowrate and frequency, the function F_c was evaluated for various pulsation velocities for $B > 1$ - the derived parameters were averaged to give a mean value to represent that Strouhal number.

Plot $\log_{10}(F_c)$ against $\log_{10}(S)$ to calculate the constants A and B.

See Figure 20 Page 101

The graph shows that a relationship between measured heat transfer data and the quasi-steady theoretical predictions can be defined by a function of Strouhal number. Regression analysis, using the method of least squares (82), gives

$$\frac{R_A - R_{A_{HF}}}{R_{A_{QS}} - R_{A_{HF}}} = 1.0 - 0.43\,(\frac{\omega d}{U_m})^{0.306}$$

Fig.20 Derivation of Frequency Correction Factor

$$F_c = 1.0 - (R_A - R_{A_{HF}})/(R_{A_{QS}} - R_{A_{HF}})$$

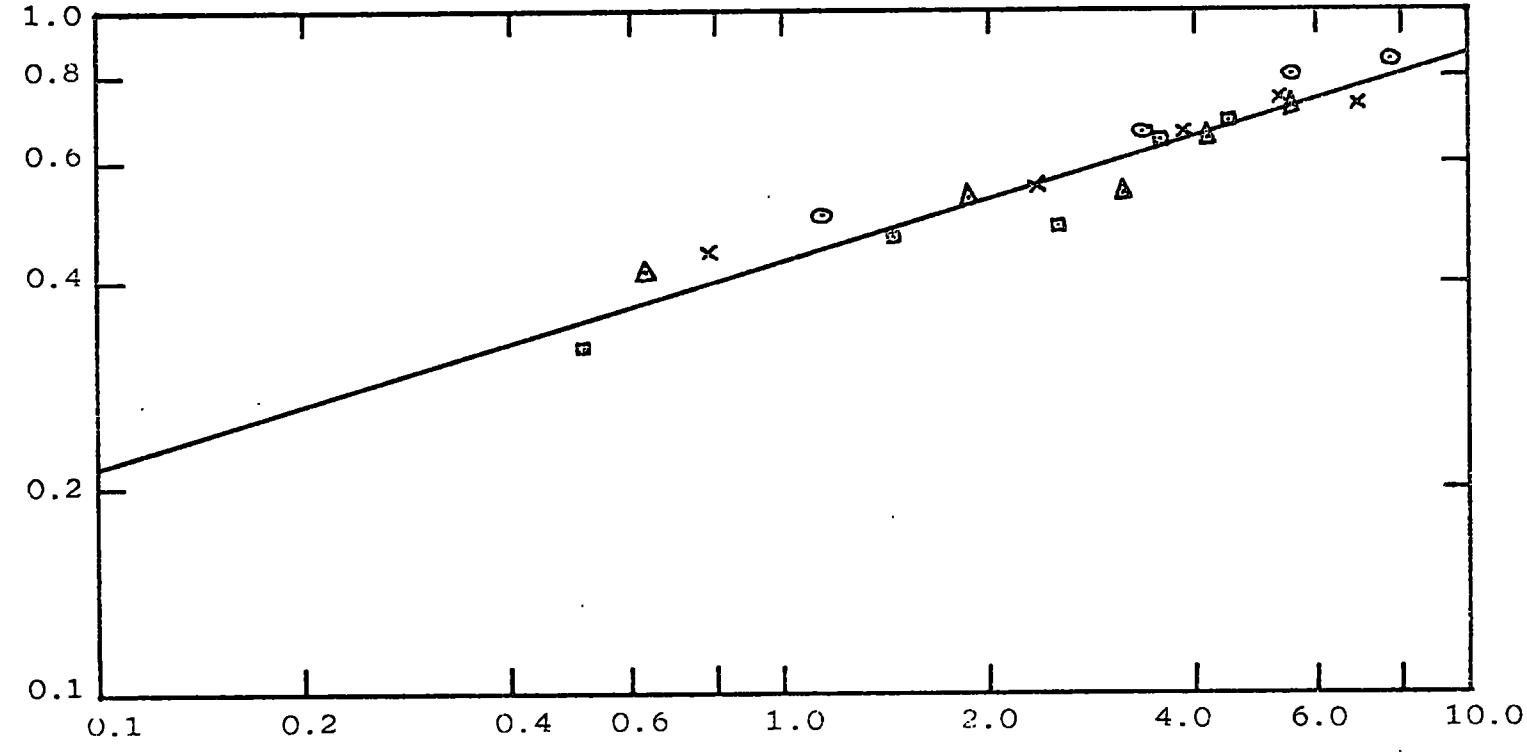

By Method of Least Squares,

$F_c = 0.43(S)^{0.306}$

The maximum value of Strouhal number is limited by the basic function

$$\text{i.e.} \quad \text{limit } 0.43 \left(\frac{\omega d}{\bar{U}_m}\right)^{0.306} = 1.0$$

$$\therefore \quad S = \frac{\omega d}{\bar{U}_m} = 16$$

It was assumed that the above equation was valid for $0 < S < 16$, and for $S \geqslant 16$ that $R_{A_{HF}} < R_A < 1.0$.

The derived frequency factor equation was used to predict actual heat transfer from the quasi-steady analysis for comparison with the experimental results - to check the method of averaging the improvement function for a given flowrate and frequency in the derivation of the Strouhal number relationship. The comparison showed an average mean modulus deviation for all flowrates 7% with maximum deviation 25% (compare to the estimated possible error - see Section 6.5). The agreement was acceptable and it was considered that the actual heat transfer was related to the corresponding quasi-steady prediction by a function of Strouhal number.

It was shown from the analysis that a frequency correction factor, a function of Strouhal number only, could be defined relating the experimental heat transfer to the theoretical quasi-steady predictions (using a high frequency approximation).

- the conclusions from the analysis of the experimental data are discussed in Chapter 8.

CHAPTER 8

Discussion

8. Discussion

From the analysis of the experimental data for heat transfer to a pulsating flow, it was shown that for fully established flow

(a) Local heat transfer was dependent only on the corresponding local Dimensionless pulsation velocity, B, for a given flow-rate and frequency.

(b) The functional relationship between Improvement ratio, R_A, and Dimensionless pulsation velocity, B, was of a similar form as for the quasi-steady theoretical predictions.

(c) For all experimental conditions, the changes in heat transfer were less than the equivalent quasi-steady predictions

$$- \text{ as } \quad \omega \longrightarrow 0, \; R_A \longrightarrow R_{AQS}$$

(d) The experimental Improvement ratio, R_A, was related to the quasi-steady Improvement ratio, R_{AQS}, by a function of Strouhal number, S (Frequency correction factor).

Relative to the theoretical analysis of convective heat transfer to a pulsating flow, the above derivations from the experimental data showed that the changes in heat transfer characteristics were due to changes in mean flow diffusivity generated by the oscillating velocity (compare the experimental findings to the theoretical predictions of the diffusivity hypothesis - see Section 4.2). The effect on heat transfer due to the diffusivity mechanism, for fully established flow, can be characterised by the following.

(a) Local heat transfer is dependent only on the corresponding local Dimensionless pulsation velocity, B, for a given Reynolds number, $\overline{Re_d}$, and Strouhal number, S.

(b) The optimum changes in heat transfer coefficients are given by quasi-steady pulsations.

(c) Experimental heat transfer can be related to the quasi-steady predictions by a function of Strouhal number, S.

The major parameters defining the effect on heat transfer, relative to the equivalent steady flow, are mean Reynolds number $\overline{Re_d}$, Dimensionless pulsation velocity B and Strouhal number S (compare to the non-dimensional analysis of Bogdanoff (42) - see Section 2.2).

The frequency correction factor (a relation between experimental heat transfer data and quasi-steady theory) was derived from a comparison of local heat transfer by approximating high frequency condition. It was necessary to make the approximation in order to derive a simple function due to the non-linear interaction of the laminar sub-layer and core diffusivity in the mechanism of convective heat transfer for a pulsating flow. But the induced error is small (especially for high Reynolds number flow) since $R_{AQS} \approx 1$ for B = 1 - see Chapter 7. Since the error from the approximation is small, the Strouhal number function, relating experimental and theoretical heat transfer, can be considered to show that the changes in heat transfer were due to changes in mean flow diffusivity.

It is possible to derive the mean heat transfer coefficients for a fully developed pulsating flow from the Energy equation on the assumption of quasi-steady oscillations - see Section 4.2.2. An empirical frequency factor was derived from a comparison of the practical heat transfer results to the corresponding quasi-steady predictions. Consequently it is possible to predict local heat transfer for a defined system from the theoretical quasi-steady prediction and the empirical correction factor. But the frequency correction factor was defined from a limited range of experimental variables. The range of the major parameters for the project is shown

Dimensionless pulsation velocity,	B	:	0.3 - 5.0
Strouhal number,	S	:	0.5 - 10.0
Reynolds number,	$\overline{Re_d}$	:	14,300 - 31,250 defined at bulk air temperature of 15°C

It was attempted to assess the applicability of the method by considering experimental conditions outside the given range.

For the experimental rig, a lower Reynolds number limit was defined due to friction heating from the shaft seal in the siren plenum chamber. But, for the fundamental and 1st harmonic resonant frequencies, local heat transfer could be measured for mean air flowrate 0.0035 Kg/s (R_{e_d} = 6,250 for bulk air temperature 15°C). For fully-developed conditions, local improvement ratio was plotted against local Dimensionless pulsation velocity for each frequency. For comparison, the improvement ratio was predicted from the corresponding quasi-steady analysis using the appropriate frequency correction factor.

See Figure 21 Page 105

For both resonant frequencies, good agreement was found between predicted and experimental heat transfer - maximum deviation 12.5%.

The derived method of prediction was considered relative to the experimental work of Jackson (29-36) and Bogdanoff (42). For the given conditions, local heat transfer was predicted, for fully established flow, assuming quasi-steady pulsations and corrected by the appropriate frequency factor. The estimated improvement ratios were compared to the reported experimental results by considering local Improvement ratio relative to local Dimensionless pulsation velocity. It was difficult to analyse the information due to a lack of data in the published reports, and the comparisons can only be regarded as approximate.

Jackson investigated experimentally local heat transfer to a resonant longitudinal oscillating air flow in a pipe over a wide range of Reynolds number - two conflicting cases were reported (see Section 2.2). For higher Reynolds numbers, no change in heat transfer at velocity nodes was found but a decrease was measured at velocity antinodes e.g. for R_{e_d} = 64,600, S = 4.66 and B = 1.27 at the velocity antinodes - see Figure 1b Page 7. For the comparison of predicted and experimental heat transfer

See Figure 22a Page 107

Fig.21 Comparison between experiment and Frequency Factor prediction at low Reynolds number

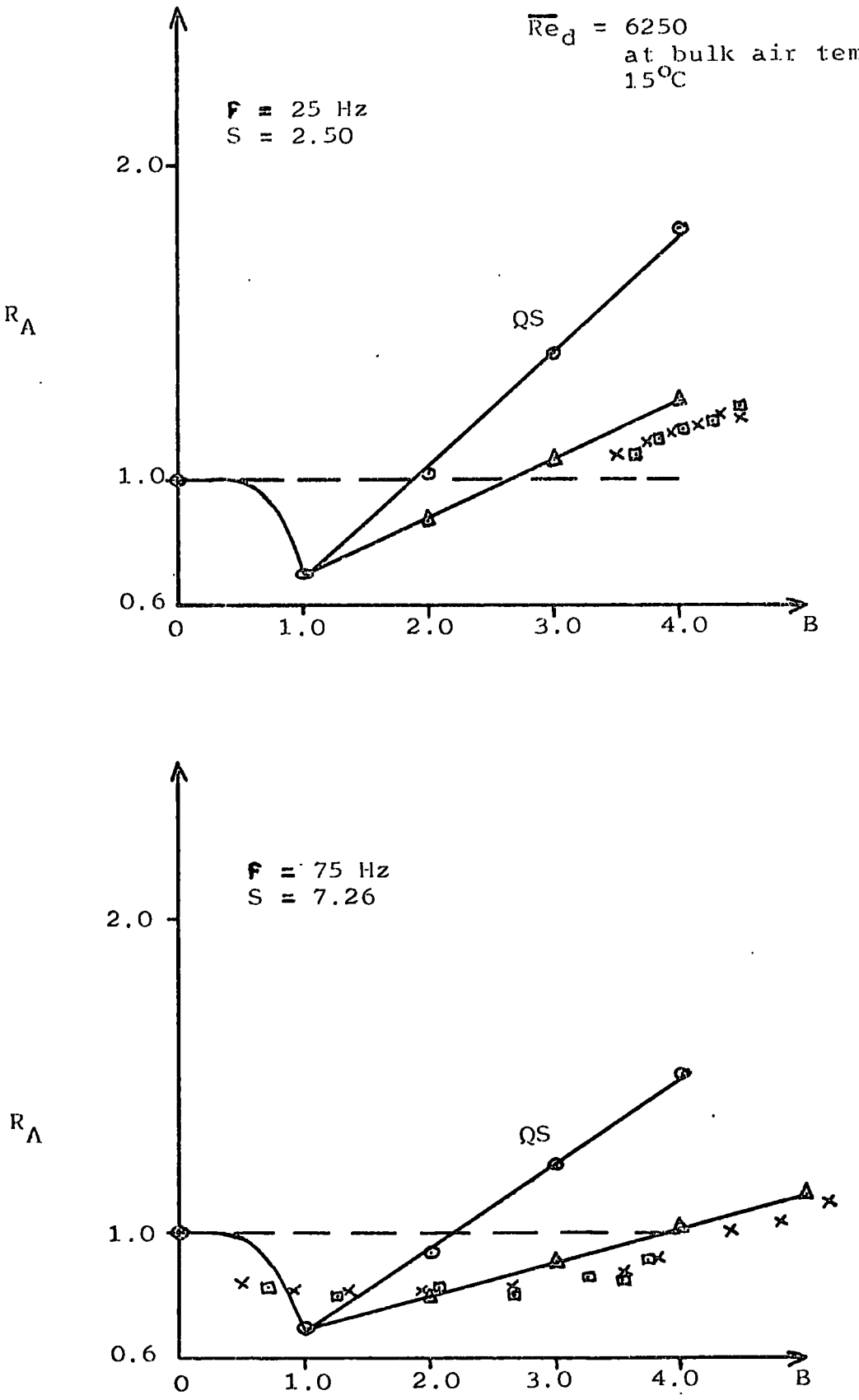

× , ⊡ Experiment

Δ Frequency Factor prediction

Due to the low velocity amplitude, the comparison was of limited value but good agreement was shown. For lower Reynolds numbers, large increases and decreases for local heat transfer were measured by Jackson e.g. for $\overline{Re_d}$ = 11,600, S = 63.4 and B = 4.25 at velocity antinodes - see Figure 1a Page 7 . But, since the Strouhal number was high (S $\gg$ 16), the derived diffusivity theory predicted negligible effect on local heat transfer at high pulsation velocity. Jackson proposed that acoustic streaming was the governing factor at the lower Reynolds numbers, but an analysis of the mean velocity profile showed negligible streaming effects (for method of analysis see Section 4.1.6).

Bogdanoff investigated local heat transfer for a resonant, turbulent mean air flow in a pipe with $\overline{Re_d}$ = 100,000, S = 5.62 and maximum Dimensionless pulsation velocity B = 3.4 (see Figure 4 Page 10). It was proposed by Bogdanoff that the changes in heat transfer were due to changes in mean diffusivity (see Section 2.2). For comparison of predicted and experimental heat transfer

See Figure 22b Page 107

For the given Reynolds number and Strouhal number, good agreement was shown between the predicted improvement ratios and the experimental measurements - maximum deviation 13.3%.

It had been hoped to consider the experimental work on heat transfer in a pulsating combustor by Hanby (9), but it was not possible to correlate the basic published information for comparison with the diffusivity theory.

The use of the frequency correction factor with the quasi-steady theoretical predictions has been justified to a limited extent for a wider range of parameters. It was shown that Strouhal number is a critical parameter - at high Strouhal numbers the possibility of another mechanism of action was indicated. The diffusivity theory was justified for an extended mean Reynolds number range, but no further limits could be claimed for Dimensionless pulsation velocity and Strouhal number. The following limitations on the parameters can be defined.

Dimensionless pulsation velocity,	B	:	0.3 - 5.0
Strouhal number,	S	:	0.5 - 10.0
Reynolds number,	$\overline{Re_d}$	:	6,250 - 100,000 defined at bulk air temperature of 15°C

The experimental work of Jackson indicated that, at high Strouhal numbers, heat transfer in a pulsating flow was not determined by the proposed diffusivity mechanism. For the definition of time-mean diffusivity in the theoretical analysis, it is assumed that the acoustic oscillations and the turbulent fluctuations are independent relative to time variation i.e. no resonance interaction. For the range of parameters in the project, this assumption was justified from a comparison of acoustic frequency to eddy frequency - see Section 4.2.3. Consider the relationship between the ratio acoustic frequency/eddy frequency to Strouhal number.

Fig.22a Jackson

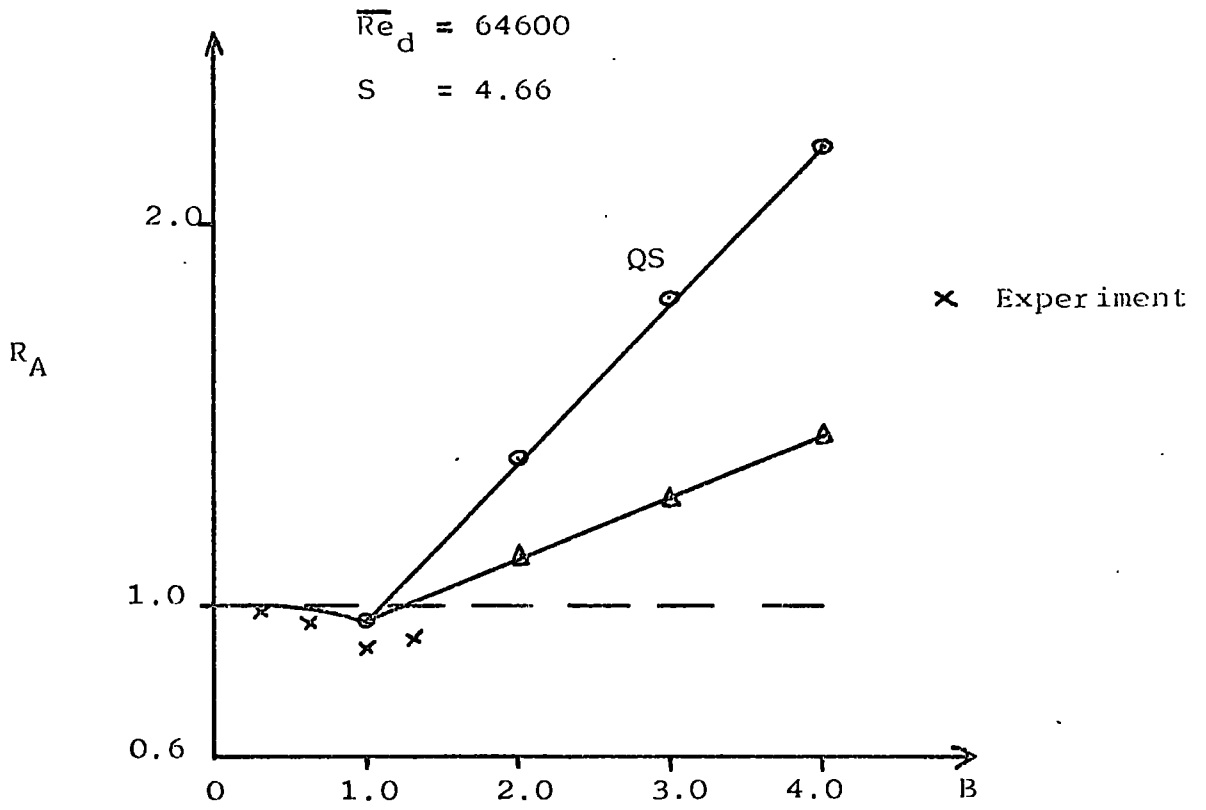

Fig.22b Bogdanoff

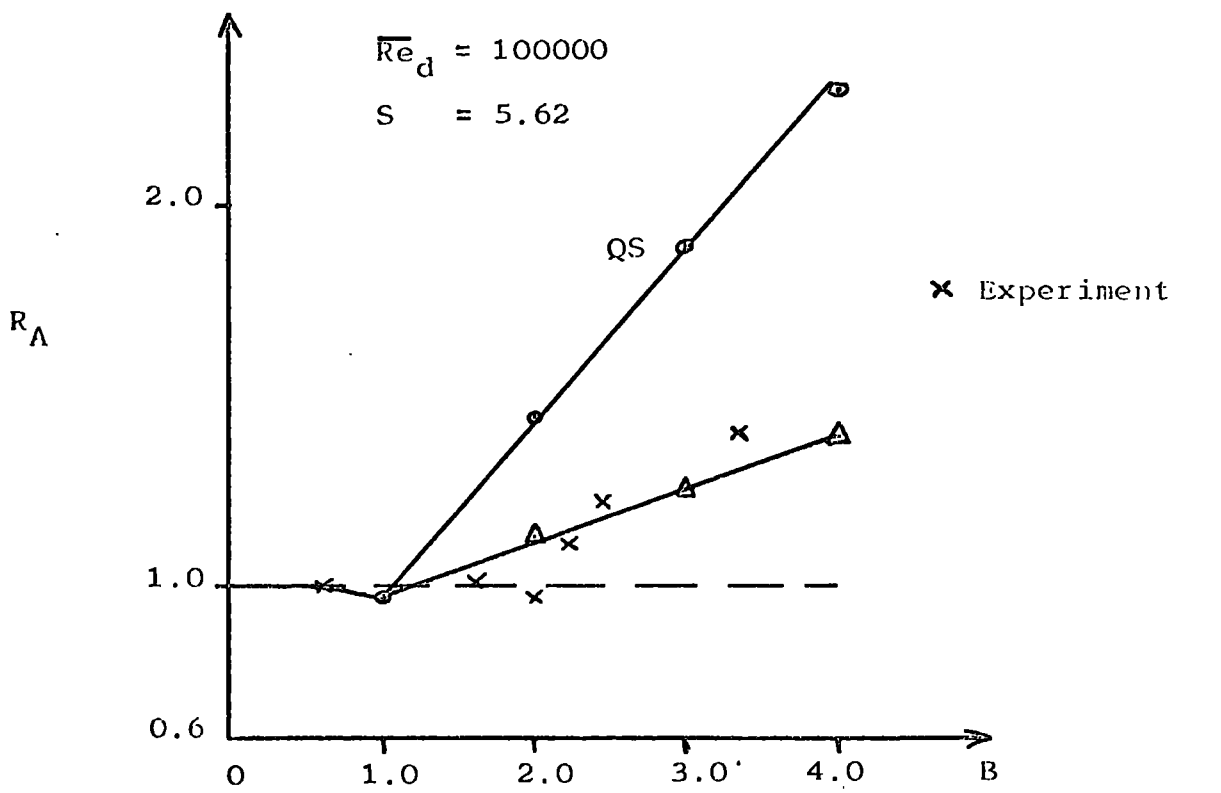

Fig.22 Comparison between Frequency Factor prediction and experimental work of Jackson and Bogdanoff

Δ Frequency Factor prediction

Relative to convective heat transfer, the critical flow regime was defined at $0 < y < 0.1$ R ($u / U_c \approx 75\%$ at $y = 0.1R$). Consider the point $y = 0.05R$ to approximately characterise the eddy frequency range of this regime.

Eddy frequency, $f_e = 0.125 \frac{\overline{U}_m}{y}$

- see Section 4.2.3

But $y = 0.025$ d

$\therefore \quad f_{e_{AVE}} = 5.0 \frac{\overline{U}_m}{d}$

$\therefore$ Ratio of frequencies $= \frac{f}{f_{e_{AVE}}}$

$= 0.2 \frac{fd}{\overline{U}_m}$

But Strouhal number, $S = \frac{\omega d}{\overline{U}_m} = 2\pi \frac{fd}{\overline{U}_m}$

$\therefore \quad \frac{f}{f_{e_{AVE}}} = 0.032S$

Assume the critical frequency defining significant resonant interaction between the acoustic oscillations and the turbulence fluctuations for the defined flow regime is given by

$f = f_{e_{AVE}}$

i.e. Critical Strouhal number, $S_c = 31.4$

Jackson experimentally measured large increases in heat transfer for the range of Strouhal number S = 30 to 70. Despite the approximate analysis to define the critical Strouhal number, the regime of operation of the experimental work indicates that a resonance interaction between the acoustic oscillations and the turbulence fluctuations may affect local heat transfer.

The entrance length regime of the heat exchanger was not analysed in terms of local pulsation variables. It can be seen from the experimental results that a similar pattern as for fully established flow was found but as $x \longrightarrow 0$, $R_A \longrightarrow 1.0$ (see Section 6.6). It was assumed that the thermal entrance length for a pulsating flow was the same as for the equivalent steady flow in the derivation of the frequency correction factor - the entrance length was approximately equal to 15 x pipe internal diameter (d) for the Reynolds number range of the project.

Relative to the theoretical analysis of a resonant pulsating turbulent gas stream, the following major assumptions were made

(a) the use of small perturbation, inviscid flow theory to predict centre-line velocity amplitudes.

(b) the use of an equivalent viscosity to determine the acoustic velocity profile.

(c) the assumption of no resonance interaction between the acoustic pulsations and the random turbulence fluctuations.

It was shown from the assumptions that, for the range of pulsation variables of interest, acoustic streaming velocities were negligible for a fully-established boundary layer. It must be noted that no direct measurement of velocity amplitudes, oscillating velocity profile or mean velocity profile were made to confirm the findings. It is only possible to define the mean diffusivity from the derived acoustic velocity profile if quasi-steady oscillations are assumed. But the reported analysis can only be regarded as approximate due to the limitations in predicting the laminar sub-layer thickness. Assuming the quasi-steady mean diffusivity, the Energy equation for the mean flow can be solved for a pulsating flow.

For the experimental heat transfer investigation, it was assumed that the centre-line velocity amplitude distribution could be predicted from pressure amplitude measurements by small perturbation, inviscid flow theory - finite amplitude effects were considered negligble. The effect of energy transfer was shown to be negligible - see Section 3.2.

Relative to the preceding discussion of the project, the following suggestions are made for future work in the investigation of convective heat transfer to a turbulent mean flow superimposed with longitudinal oscillations.

(a) Extension of the range of major parameters (Reynolds number, Dimensionless pulsation velocity, Strouhal number) to check the use of the frequency correction factor with quasi-steady predictions.

(b) Experimental investigation of local heat transfer at high Strouhal numbers ($S > 30$) to consider the possibility of a resonance mechanism (in comparison to the work of Jackson).

(c) Investigate the hydrodynamic and thermal entrance lengths for pulsating flows relative to the equivalent steady flows.

(d) Correlate the improvement ratios to local pulsation parameters for the thermal entrance length relative to a theoretical quasi-steady analysis.

(e) Experimentally investigate a resonant, pulsating turbulent flow in terms of the major flow parameters:

Velocity amplitudes at the pipe centre line

Acoustic velocity profile

Acoustic streaming effects

Mean turbulence levels

The basic ideas for the project were formed from the reported increases in heat transfer in the exhaust pipe of a pulsating combustor. The project has shown that the effect of the longitudinal oscillations, compared to the equivalent steady flow, is complex and local heat transfer can be both increased or decreased. Relative to the findings of the project, assuming the action of the diffusivity mechanism, the following conditions can be defined to give optimum overall heat transfer increase in the exhaust pipe for a given mean flowrate - high amplitude, low frequency oscillations in the fundamental mode

i.e. Maximum Dimensionless pulsation velocity ($B \gg 1$)

Minimum Strouhal number ($S \longrightarrow 0$)

It was not possible to correlate the available data from pulse combustors in terms of pulsation parameters. A major problem has been the prediction of velocity amplitudes in the exhaust pipe from measured pressure amplitudes. From the theory developed in the project (see Section 3.2), it should be possible to derive the velocity amplitude distribution from pressure measurements given the bulk gas temperature function - the analysis has not been verified by experiment for large temperature gradients. Experimental data for local heat transfer in pulsating combustors is very limited, and no comparison could be made to predictions from the mean diffusivity theory. Despite the possible improvements in heat transfer, the practical application of pulsating combustors is limited by the major problem of high environmental noise - extensive work would be required to design appropriate practical silencer systems. It must be stressed that only the longitudinal mode of oscillations has been considered in the project (tangential and radial modes were not investigated), and the discussion on future prospects of practical development of pulse combustors is limited to this mode of operation. But, with the other possible advantages, pulsating combustors may be developed for practical applications.

CHAPTER 9

Summary

9. Summary

The effect on convective heat transfer of resonant, longitudinal oscillations superimposed on a turbulent mean flow in a pipe has been investigated relative to the equivalent steady flow.

For the defined range of pulsation parameters, it is shown theoretically that the effect of acoustic streaming velocities is negligible, but that the oscillating velocity can generate changes in the time-mean diffusivity. The mean flow diffusivity can be predicted if quasi-steady pulsations are assumed. Local heat transfer coefficients for the mean flow can be evaluated from a solution of the Energy equation, for fully established conditions, assuming quasi-steady oscillations. It is shown from a comparison of acoustic frequency to eddy frequency that the practical heat transfer is related to the quasi-steady predictions by a function of Strouhal number.

Local heat transfer was measured experimentally for a constant heat flux supply to an oscillating air flow in a pipe. The range of major parameters was

Dimensionless pulsation velocity,	B	: 0.3 - 5.0
Strouhal number	S	: 0.5 - 10.0
Reynolds number	$\overline{R_{e_d}}$	: 14,300 - 31,250 defined at bulk air temperature of 15°C

From a comparison of the experimental heat transfer coefficients to the corresponding quasi-steady predictions for fully established flow, a frequency correction factor was derived - the factor was a function of Strouhal number only. It was shown that the changes in heat transfer were due to changes in the mean diffusivity generated by the acoustic velocity.

For a defined range of variables, a method has been derived to predict local heat transfer, under fully developed conditions, for a pulsating flow i.e. from the theoretical quasi-steady predictions using the empirically defined frequency correction factor.

References

REFERENCES

1. General survey of pulse combustion

   A.A. Putnam

   1st Int. Symposium on Pulsating Combustion, University of Sheffield. Sept. 1971

2. The pulsations and energy transfers in a double-orifice pulsating combustor

   C.K. Beale

   Ph.d Thesis, University of Durham 1974 (to be published)

3. Pulsating combustion - the collected works of F.H. Reynst

   ed. M. Thring

   Pergamon Press 1961

4. Non-steady flame propagation

   ed G.H. Markstein

   Pergamon Press 1964

5. Combustion-driven oscillations in industry

   A.A. Putnam

   American Elsevier 1971

6. Heat transfer from acoustically resonating gas flames in a cylindrical burner

   W. Zartman, S.W. Churchill

   A.I.Ch.E. Journal, Dec. 1961. Pg. 588-592

7. Heat transfer from pre-mixed gas flames in a cooled tube

   D. Sundstrom, S.W. Churchill

   Chemical Engineering Progress Symposium Series No. 30 Vol. 56, Pg. 65-73

8. A study of gas-fired pulsating combustors for industrial applications

   W. Francis et al

   Journal of Institute of Gas Engineers 1963, No. 3, Pg. 301-323

9. Convective heat transfer in a gas-fired pulsating combustor

   V. Hanby

   Trans. A.S.M.E. 1968. Paper No. 68-WA/FU-1 Pg. 1-5

10. The effect of vibration on heat transfer by free convection from a horizontal cylinder

R.C. Martinelli, L.M.K. Boelter

Proceedings 5th Int. Congress of Applied Mechanics 1938 Pg. 578

11. Flow near a heated solid body in a standing acoustic field

P.N. Kubanskii

LAL, N.A.C.A. Oct. 1955

12. Effect of vibration on natural convective heat transfer

R. Lemlich

Industrial Eng. Chem. Vol. 47, No. 6 1955, Pg. 1175-1180

13. Mechanism of sound field effects on heat transfer

J.P. Holman

Trans. A.S.M.E.-Journal of Heat Transfer Vol. 82 1960 Pg. 393-396

14. Acoustic streaming in the vicinity of a cylinder

W.P. Raney et al

Journal of Acoustical Society of America. Vol. 26, No. 6 1954, Pg. 26-39

15. Mechanism of interaction between vibrations and heat transfer

R.M. Fand

Journal of Acoustical Society of America. Vol. 34, No. 12 1962

16. Effect of sound vibrations on heat transfer

P.D. Richardson

Applied Mechanics Review. Vol. 20, No. 3, 1967

17. Heat transfer to a fluid flowing periodically at low frequencies in a vertical pipe

R. Martinelli et al

Trans. A.S.M.E. Vol. 65, 1943, Pg. 789-798

18. Effect of pulsations on heat transfer

F. West, A. Taylor

Chemical Engineering Progress. Vol. 48, No. 1, 1952 Pg. 39-43

19. Heat transfer to liquids in intermittent flow

G.B. Darling

Petroleum, May 1959, Pg. 177-180

20. Vibration and pulsation boost heat transfer

R. Lemlich

Chemical Engineering, May 15, 1961, Pg. 171-174

21. The effect of vibration and pulsation on heat transfer

P.G. Morgan

Engineering and Boiler House Review. April 1963, Pg. 128-129

22. Heat transfer in pulsed turbulent flow

M.H.I. Baird

Chemical Engineering Science. Vol. 21, 1966, Pg. 197-199

23. Studies for a new hot air engine

H. Havemann et al

Journal of Indian Institute of Science. Vol. 38B, 1956 Pg. 172-202

24. Heat transfer in pulsating flow

H. Havemann

Nature No. 4418, July 3, 1954, Pg. 41

25. Heat transfer characteristics of periodically pulsating turbulent pipe flow

W. Mueller

Thesis, University of Illinois, 1956

26. Heat transfer to fluids flowing with velocity pulsations in pipes

F. Romie

Thesis, University of California, 1956

27. Effect of longitudinal pulsations on heat transfer

V. Chalitbtan

Thesis, University of Texas, 1959

28. The effect of acoustic vibration on forced convective heat transfer

R. Lemlich, C.K. Hwu

A.I.Ch.E. Journal. March 1961, Pg. 102-106

29. Free convection, forced convection and acoustic vibrations in a constant temperature vertical tube

T.W. Jackson et al

Trans. A.S.M.E. - Journal of Heat Transfer, Vol. 81 February 1959, Pg. 68-74

30. Effects of resonant acoustic vibrations on local and overall heat transfer coefficients for air flowing through an isothermal tube

T.W. Jackson et al

U.S.A.F. Aeronautical Res. Labs. ARL 60-322, October 1960

31. Heat transfer threshold values for resonant acoustic vibrations in a horizontal tube

T.W. Jackson et al

U.S.A.F. Aeronautical Res. Labs. ARL 62-326, 1962

32. Viscous fluid flow under the influence of resonant acoustic field

T.W. Jackson, K. Purdy

Trans. A.S.M.E. - Journal of Heat Transfer, Feb. 1964 Pg. 97-106

33. Effect of a resonant acoustic field on laminar flow in a circular tube

T.W. Jackson, K. Purdy

U.S.A.F. Aerospace Res. Labs. ARL 65-96, May 1965

34. Resonant pulsating flow and convective heat transfer

T.W. Jackson, K. Purdy

Trans. A.S.M.E. - Journal of Heat Transfer, November 1965 Pg. 507-512

35. Laminar forced convection under the influence of a resonant acoustic field

T.W. Jackson, K. Purdy

Proceedings of Heat Transfer and Fluid Mechanics Institute Stanford University 1967.

36. Investigation of the effect of acoustic vibration on convective heat transfer

T.W. Jackson

U.S.A.F. Aerospace Res. Labs. ARL 65-97

37. Heat transfer in oscillating flow

D.T. Harrje, E. Croke

Aero. Eng. Rep. No. 483, Princeton University, Oct. 1959

38. Heat transfer in oscillating flow

D.T. Harrje

Aero. Eng. Rep. No. 483b, Princeton University, Sept. 1960

39. Heat transfer in oscillating flow

D.T. Harrje

Aero. Eng. Rep. No. 483c, Princeton University, Sept. 1961

40. Heat transfer in oscillating flow

R. Saunders, D.T. Harrje

Aero. Eng. Rep. No. 483d, Princeton University, July 1963

41. Heat transfer in oscillating flow

J. Marec, D.T. Harrje

Aero. Eng. Rep. No. 483e, Princeton University, July 1963

42. A study of the mechanisms of heat transfer in oscillating flow

D. Bogdanoff, D.T. Harrje

Aero. Eng. Rep. No. 483f, Princeton University, Sept. 1967

43. Heat transfer in oscillating flow

D.T. Harrje

Aero. Eng. Rep. No. 483g, Princeton University, Oct. 1967

44. Convective heat transfer for a flow in a pipe fluctuating about the 1st resonant harmonic

B.M. Galitseyskiy et al

Heat Transfer - Soviet Research, Vol. 1, No. 2 March 1969

45. Effect of resonant fluctuations of coolant pressure on convective heat transfer in pipes

B.M. Galitseyskiy et al

Heat Transfer - Soviet Research, Vol. 1, No. 2, March 1969

46. Effect of the variable volume of a reservoir on the resonant frequency and on the convective heat transfer in a pulsating flow in a tube

B.M. Galitseyskiy et al

Heat Transfer - Soviet Research, Vol. 1, No. 5, Sept. 1969

47. Experimental study of the effect of non-resonance coolant pressure fluctuations on the heat transfer in a pipe

B.M. Galitseyskiy et al

Heat Transfer - Soviet Research, Vol. 2, No. 4, July 1970

48. The effect of flow pulsations on heat transfer by forced convection from a flat plate

F.J. Bayley et al

Int. Heat Transfer Conf. Aug. 28 - Sept. 1, 1961

49. Effect of large amplitude oscillations on heat transfer

C. Feiler, E. Yeager

N.A.S.A. Tech. Report R-142, 1962

50. Experimental heat transfer and boundary layer behaviour with 100 Hz flow oscillations

C. Feiler

N.A.S.A. TND-2521, Dec. 1964

51. Heat transfer in the oscillating turbulent boundary layer

J. Miller

Trans. A.S.M.E. 69-GT-34

52. Influence of sound on heat transfer in separated flows

P.D. Richardson

Chemical Engineering Science, Vol. 21, 1966, Pg. 609-610

53. Dynamics and thermodynamics of compressible fluid flow

A.H. Shapiro

Vol. I and II, Ronald Press Co. 1954

54. Physical Acoustics Vol. II, Part B

Non-linear Acoustics

R. Beyer

Academic Press 1965

55. Theory of Sound Vol. I and II
Lord Rayleigh
MacMillan and Co. 1896

56. Textbook of Sound
A.B. Wood
G. Bell and Sons Ltd. 1932

57. Sound propagation in a combustion can with axial temperature and density gradient
A. Kapur et al
Journal of Sound and Vibration, Vol. 25, No. 1, 1972

58. Introduction to numerical analysis
C.E. Fröberg
Addson-Wesley Pub. Co. Ltd. 1964

59. Viscous fluid flow under the influence of a resonant acoustic field
K.R. Purdy et al
Journal of Heat Transfer. Trans. A.S.M.E., Feb. 1964 Pg. 97

60. A photomultiplier-schlieren for acoustic measurements and some investigations of the Kundt's tube
J.V. Sanders
Dissertation Abs., February 1962

61. Motion in the boundary layer with a rapidly oscillating external flow
C.C. Lin
9th Int. Congress of App. Mech. University of Brussels, Belgium. Vol. 4, September 1956, Pg. 155

62. Heat Transfer
F. Bayley et al
Nelson 1972

63. On the interaction of intense acoustic fields and viscous fluid flows
A.E. Hirbar and K.R. Purdy
Journal of Basic Eng., Trans. A.S.M.E. March 1969, Pg. 74.

64. Theorie de l'ecoulement tourbillant
J. Boussinesq
Mem. proc. Acad. Sci. 1877 XXIII, Pg. 46

65. Über die ausgebildet Turbulenz
L. Prandtl
Zamm 1925, 5, Pg. 136

66. Convective heat and mass transfer
W.M. Kays
McGraw-Hill Co. Ltd. 1966

67. Probability theory and its applications
W. Feller
Vol. 1, Wiley

68. Boundary layer theory
H. Schlichting
Pergamon 1955

69. Turbulence Phenomena
J.T. Davies
Academic Press 1972

70. A 50 H.P. siren
R. Jones
J. of Ac.Soc. of America, Vol. 18, No. 2, Pg. 371-387, 1946

71. Siren design for producing controlled waveforms at high intensities
C.H. Allen, B.G. Watters
J. of Ac.Soc. of America, Vol. 31, No. 2, Pg. 177-185, 1959

72. Siren design for producing controlled waveforms with amplitude modulation
C.H. Allen, B.G. Watters
J. of Ac.Soc. of America, Vol. 31, No. 4, Pg. 463-469, 1959

73. Acoustic siren for generating wide band-noise
J. Cole et al
J. of Ac. Soc. of America, Vol. 35, No. 2, Pg. 173-191, 1963

74. Evaluation of the acoustic response of an air/water siren
W. Mitchell, D. Muster
J. of Ac.Soc. of America, Vol. 45, No. 1, Pg. 83-91, 1968

75. Testing and performance of a wide-band underwater liquid communicator

W. Mitchell, D. Muster

J. of Ac.Soc. of America, Vol. 45, No. 3, Pg. 733-741, 1968

76. Suppression of burner oscillations by acoustical dampers

A.A. Putnam, W.R. Dennis

Trans. A.S.M.E. 1955, Pg. 875

77. Oscillatory combustion in tunnel burners

J.K. Kilham et al

10th International Symp. on Combustion, 1965

78. Theoretical and experimental investigation of mufflers with comments on engine-exhaust muffler design

D. Davies et al

NACA Rep. 1192, 1954

79. Calibration graphs - Copper/Constantan thermocouples

B.S. 1828 : 1961

80. Thermodynamic and transport properties of fluids

arranged by T.R. Mayhew, G.F.C. Rogers

Oxford 1967

81. Dealing with data

A.J. Lyon

Pergamon Press, 1970

82. Experimental methods for engineers

J.P. Holman

McGraw-Hill, 1971

Appendices

Appendix I

Basic Quasi-steady Theory

For fully developed turbulent flow in a pipe, it has been shown experimentally that

$$\text{Nusselt number, } N_{u_d} \approx 0.02 \, (R_{e_d})^{0.8}$$

for R_{e_d}, Reynolds number

(66)

For a pulsating flow let the instantaneous bulk velocity, $U_{m(t)}$, be given at a point by

$$U_{m(t)} = \overline{U}_m + \hat{U} \sin(\omega t)$$

for $\overline{U}_m$, mean flow bulk velocity

$\hat{U}$, velocity amplitude at that point

ω, angular frequency of oscillations

$$\therefore \quad U_{m(t)} = \overline{U}_m \, (1 + B \sin(\omega t))$$

where Dimensionless pulsation velocity, $B = \hat{U}/\overline{U}_m$

Define Instantaneous Reynolds number, $R_{e_{d(t)}} = \frac{d}{\nu} U_{m(t)}$

It is assumed that, at any instance of the cycle, the steady flow relationship is valid

i.e. Instantaneous Nusselt number, $N_{u_{d(t)}} \approx 0.02 \, (R_{e_{d(t)}})^{0.8}$

with $R_{e_{d(t)}} = \frac{d}{\nu} \overline{U}_m \, (1 + B \sin(\omega t))$

If $B > 1$, flow reversal occurs, and it is assumed that the Nusselt number is dependant on the modulus of the velocity.

i.e. $N_{u_{d(t)}} = 0.02 \, (\frac{d}{\nu} \overline{U}_m \, |1 + B \sin(\omega t)|)^{0.8}$

Time mean Nusselt number is defined by

$$\overline{N_{u_d}} = \frac{1}{2\pi} \int_0^{2\pi} N_{u_{d(t)}} \, d\omega t$$

Let the Improvement ratio, $R_A = \dfrac{\overline{N_{u_d}}}{N_{u_{d_e}}}$

where $N_{u_{d_e}}$ is the Nusselt number for the equivalent steady flowrate

i.e. $N_{u_{d_e}} \approx 0.02 \left(\frac{d}{\bar{v}} \bar{U}_m\right)^{0.8}$

$$\therefore \quad R_A = \frac{1}{2\pi} \int_0^{2\pi} \left(1 + B \sin(\omega t)\right)^{0.8} d\omega t$$

The integral can be solved numerically - the change in heat transfer with respect to the Dimensionless pulsation velocity is shown graphically.

Figure 1A Page 123

It is shown that there is an initial decrease in Improvement ratio until flow reversal occurs (B = 1). As Dimensionless pulsation velocity increases beyond this point, an almost linear increase is predicted. The changes in heat transfer are independant of the frequency of oscillation.

Fig. 1A Basic Quasi-steady theory

- Improvement Ratio against Dimensionless Pulsation velocity

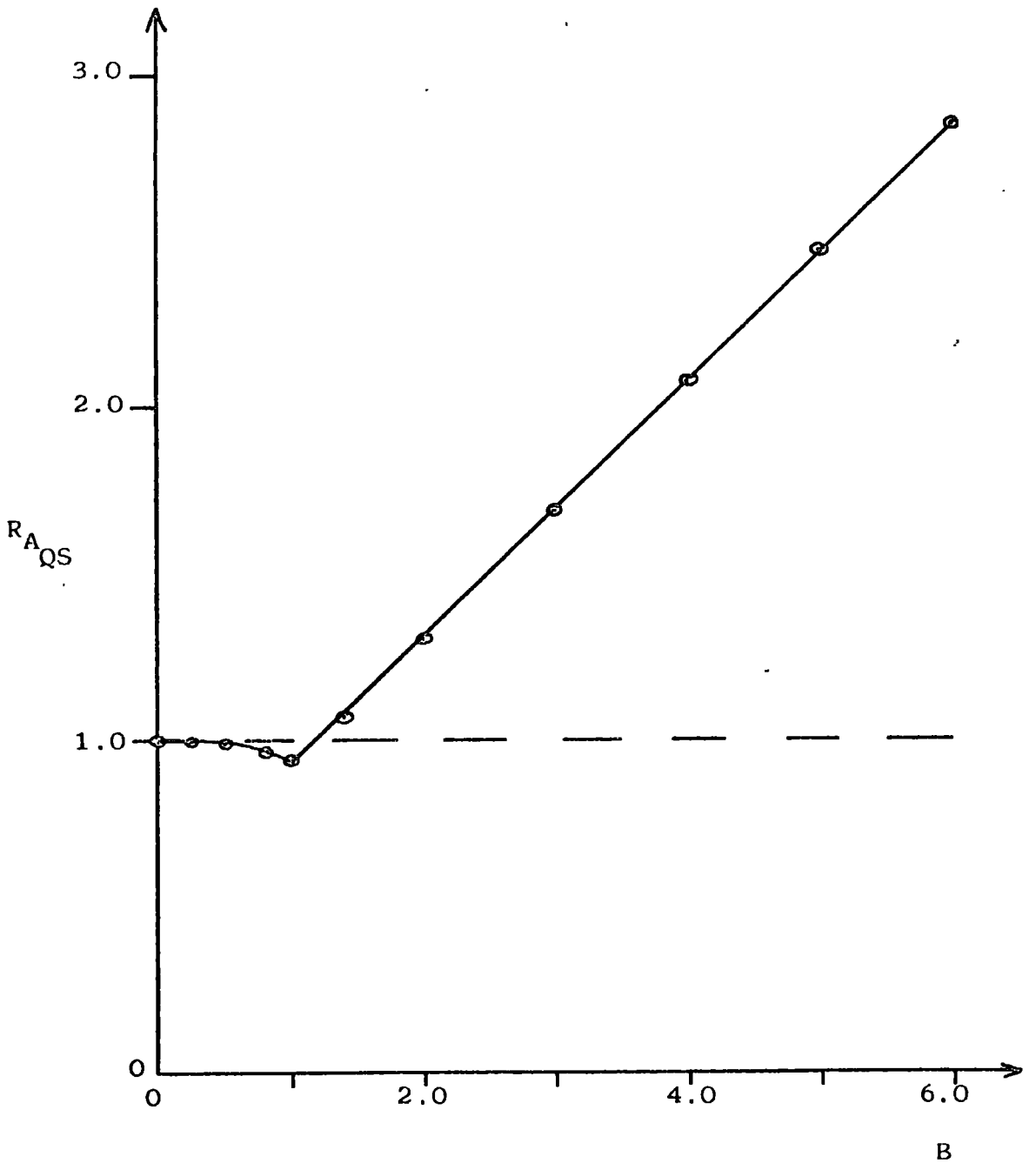

Appendix II

Wave propagation in a stratified medium

To solve equation

$$\frac{\partial^2 u_1}{\partial t^2} = (Mx + N)^2 \frac{\partial^2 u_1}{\partial x^2}$$

..... 1

Define $z = z(x)$ such that $u_1 = f(t, z)$

$$\therefore \quad \frac{\partial u_1}{\partial x} = \frac{\partial u_1}{\partial z} \cdot \frac{dz}{dx}$$

$$\frac{\partial^2 u_1}{\partial x^2} = \frac{\partial u_1}{\partial z} \cdot \left(\frac{d^2 z}{dx^2}\right) + \frac{\partial^2 u_1}{\partial z^2} \left(\frac{dz}{dx}\right)^2$$

Let $\frac{dz}{dx} = \frac{1}{Mx + N}$

$$\therefore \quad \frac{d^2 z}{dx^2} = \frac{-M}{(Mx + N)^2} = -M \left(\frac{dz}{dx}\right)^2$$

Substitute into 1

$$\frac{\partial^2 u_1}{\partial t^2} = -M \frac{\partial u_1}{\partial z} + \frac{\partial^2 u_1}{\partial z^2}$$

This equation has constant coefficients and can be solved by the method of separation of variables

$$u_1 = e^{Mz/2} \left(A e^{ibz} + B e^{-ibz} \right) \cos(\omega t)$$

assuming sine wave generation at $x = 0$

Where A, B are constants

$$b = \frac{1}{2} \sqrt{(4\omega^2 - M^2)}$$

$$z = \frac{1}{M} \log_e \left(\frac{M}{N} x + 1 \right)$$

$$i = \sqrt{(-1)}$$

Assume $4w^2 > M^2$

$$\therefore \quad u = e^{\frac{Mz}{2}} (D \cos(bz) + C \sin(bz)) \cos(\omega t)$$

where C, D are constants

Boundary condition

$$u_1 = 0 \text{ at } x = 0$$

$$\therefore \quad u_1 = \hat{U}_c e^{\frac{Mz}{2}} \sin(bz) \cos(\omega t)$$

where $\hat{U}_c$ is a velocity amplitude constant

But $$\frac{\partial p_1}{\partial t} = - \bar{c}^2 \bar{\rho} \frac{\partial u_1}{\partial x}$$

By substitution and integration

$$p_1 = - \bar{\rho} \frac{\bar{c}}{\omega} \hat{U}_c e^{Mz/2} \left(\frac{M}{2} \sin(bz) + b \cos(bz) \right) \sin(\omega t) + I_c$$

where I_c is an integration constant

Boundary condition

$$p_1 = 0 \quad \text{at } x = L_A$$

$$\therefore \quad I_c = 0 \text{ and } \left(\frac{M}{2} \sin(Bz_L) + b \cos(bz_L)\right) = 0$$

Resonant frequencies are defined by

$$\frac{M}{2} \sin(bz_L) + b \cos(bz_L) = 0$$

where $Z_L = \frac{1}{M} \log_e \left(\frac{M}{N} \cdot L_A + 1\right)$

Let pressure amplitude at x = 0 be P0

$$\therefore \quad \hat{U}_c = \frac{\omega}{b} \cdot \frac{N}{\gamma P} \cdot P0$$

Governing equations for resonance

Resonant frequencies are given by

$$\frac{M}{2}\sin(bz_L) + b\cos(bz_L) = 0$$

Velocity amplitude distribution

$$u_1 = -\frac{\omega}{b}\cdot\frac{N}{\gamma\bar{p}}\cdot PO\cdot e^{Mz/2}\cdot \sin(bz)\cdot\cos(\omega t)$$

Pressure amplitude distribution

$$p_1 = \frac{N}{b}\cdot\frac{1}{(Mx+N)}\cdot PO\cdot e^{Mz/2}\left(\frac{M}{2}\sin(bz) + b\cos(bz)\right)\sin(\omega t)$$

Appendix III

Experimental heat transfer - flow independant Nusselt number against position in heat exchanger (Figure 2A)

The following graphs show the majority of experimental heat transfer results for the following range of parameters.

Mean air flowrate $\bar{\dot{m}}$ -Kg/s	Reynolds number R_{e_d}
0.0080	14300
0.0145	25900
0.0175	31250
	at Bulk air temperature 15°C

Results are shown for five frequencies

f = 25, 75, 125, 175, 225 Hz

for different pressure amplitudes relative to the equivalent steady flow (compared to the fully-developed flow independant Nusselt number).

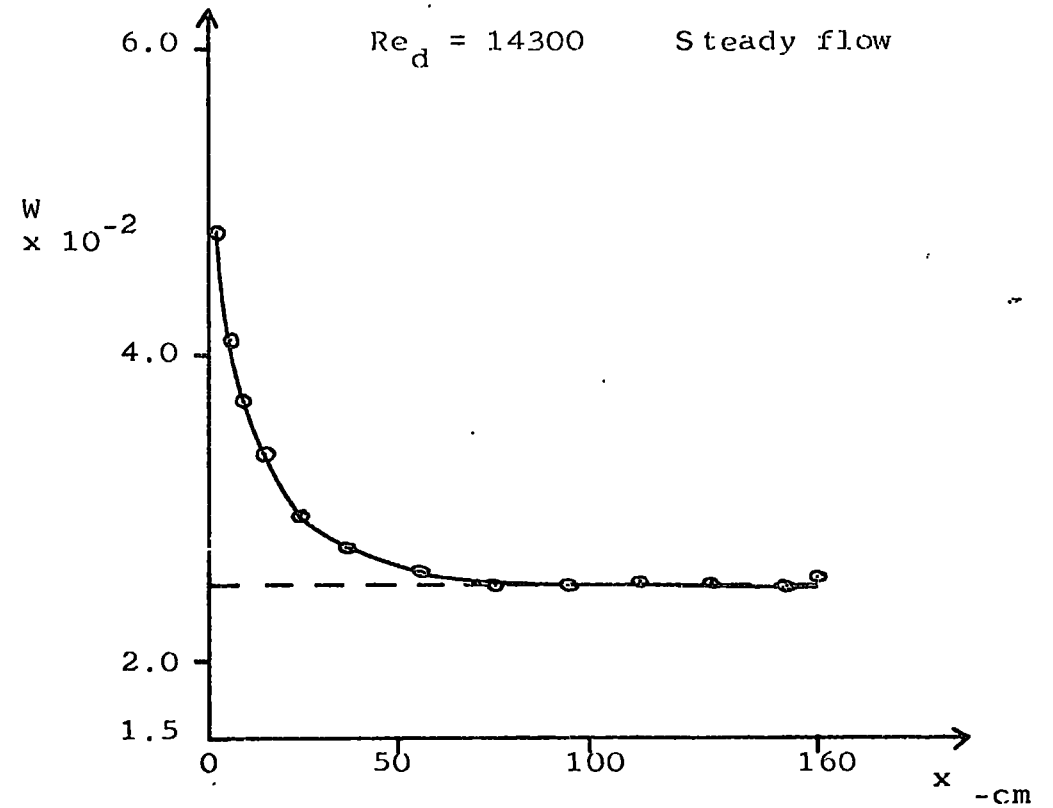
Re_d = 14300 Steady flow
W
x 10^{-2}
6.0
4.0
2.0
1.5
0
50
100
160
x
-cm

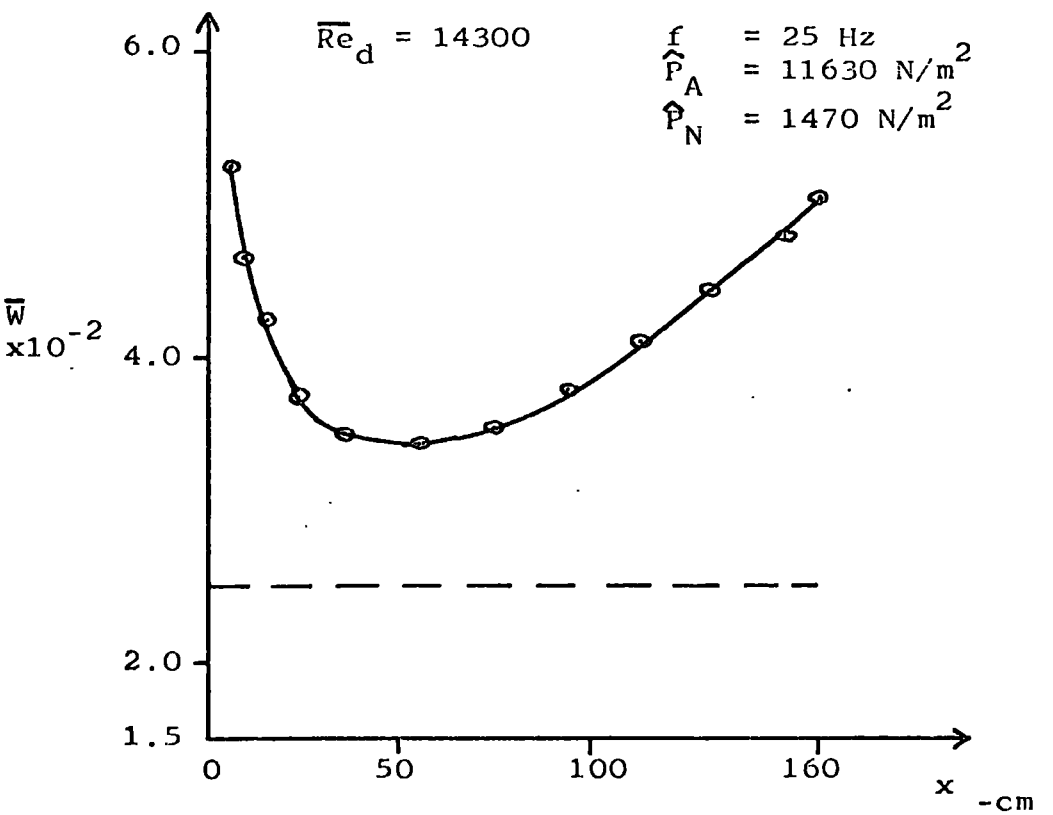
$\overline{Re}_d$ = 14300
f = 25 Hz
$\hat{P}_A$ = 11630 N/m^2
$\hat{P}_N$ = 1470 N/m^2
$\overline{W}$
x10^{-2}
6.0
4.0
2.0
1.5
0
50
100
160
x
-cm

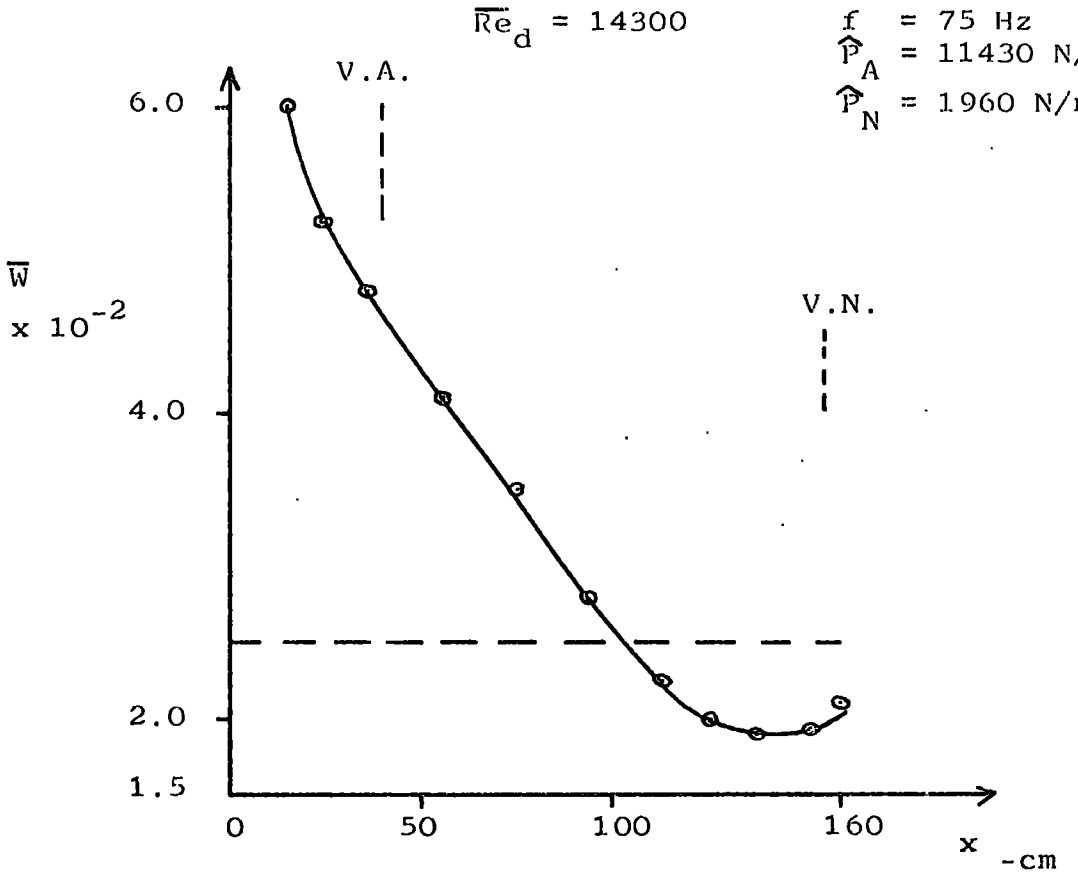
$\overline{Re}_d$ = 14300
f = 75 Hz
$\hat{P}_A$ = 11430 N/m^2
$\hat{P}_N$ = 1960 N/m^2
V.A.
V.N.
$\overline{W}$ x 10^{-2}
6.0
4.0
2.0
1.5
0
50
100
160
x -cm

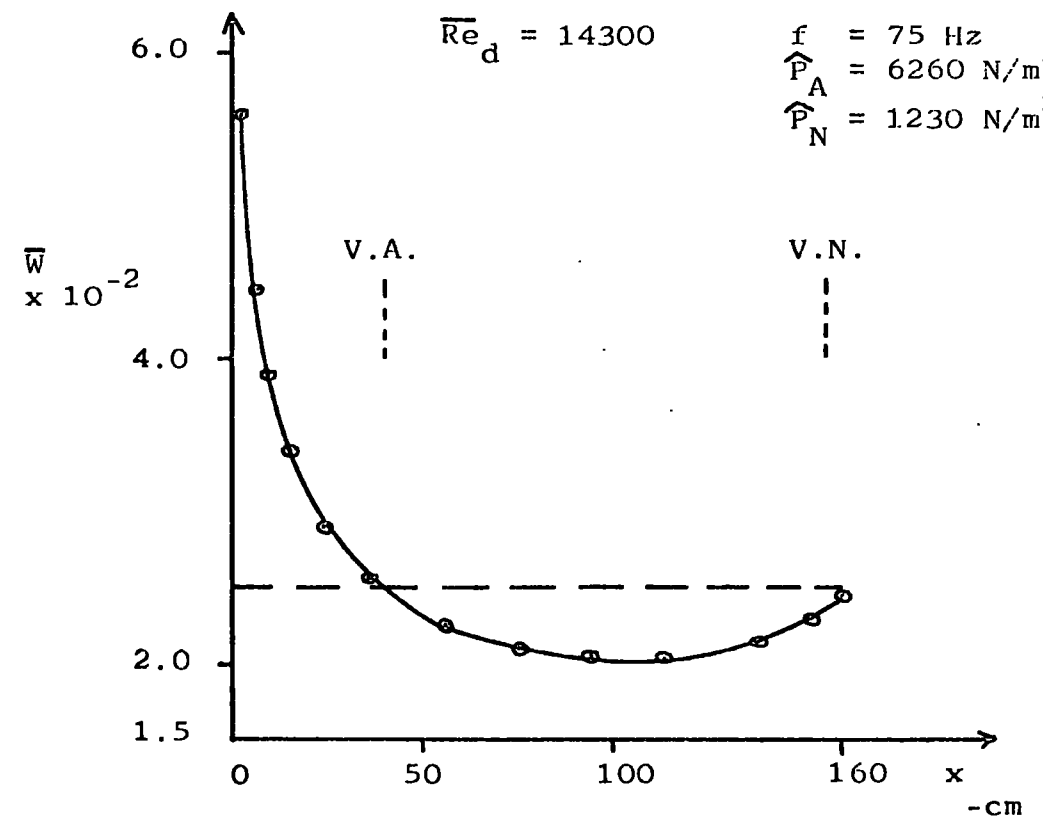
$\overline{Re}_d$ = 14300
f = 75 Hz
$\hat{P}_A$ = 6260 N/m^2
$\hat{P}_N$ = 1230 N/m^2
V.A.
V.N.
$\overline{W}$ x 10^{-2}
6.0
4.0
2.0
1.5
0
50
100
160
x -cm

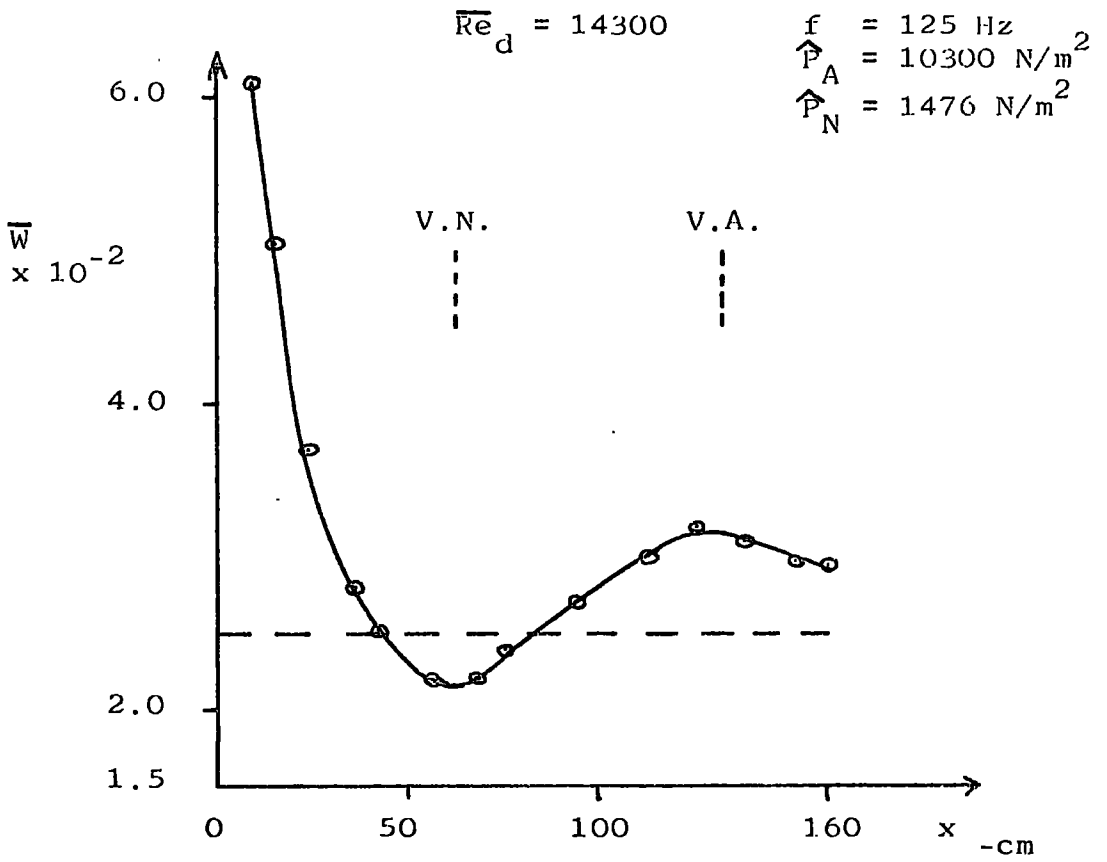
$\overline{Re}_d$ = 14300
f = 125 Hz
$\hat{P}_A$ = 10300 N/m^2
$\hat{P}_N$ = 1476 N/m^2
$\overline{W}$ x 10^{-2}
6.0
4.0
2.0
1.5
V.N.
V.A.
0
50
100
160
x -cm

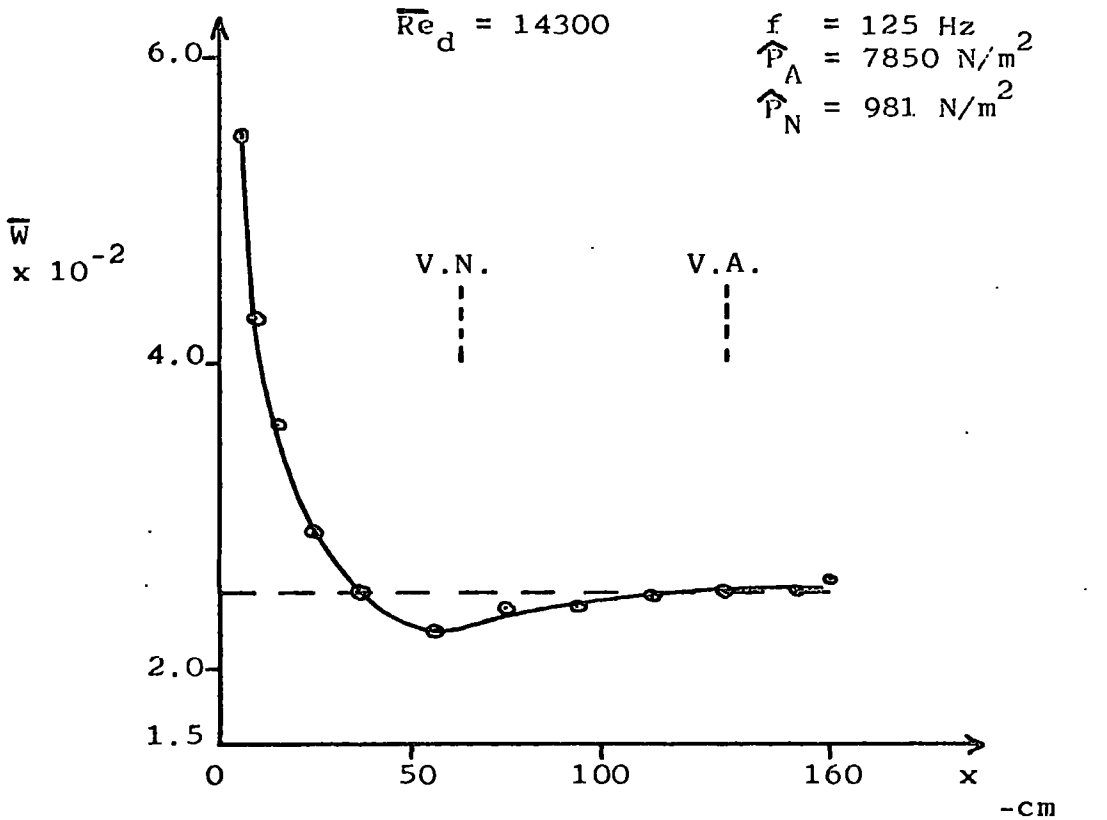
$\overline{Re}_d$ = 14300
f = 125 Hz
$\hat{P}_A$ = 7850 N/m^2
$\hat{P}_N$ = 981 N/m^2
$\overline{W}$ x 10^{-2}
6.0
4.0
2.0
1.5
V.N.
V.A.
0
50
100
160
x -cm

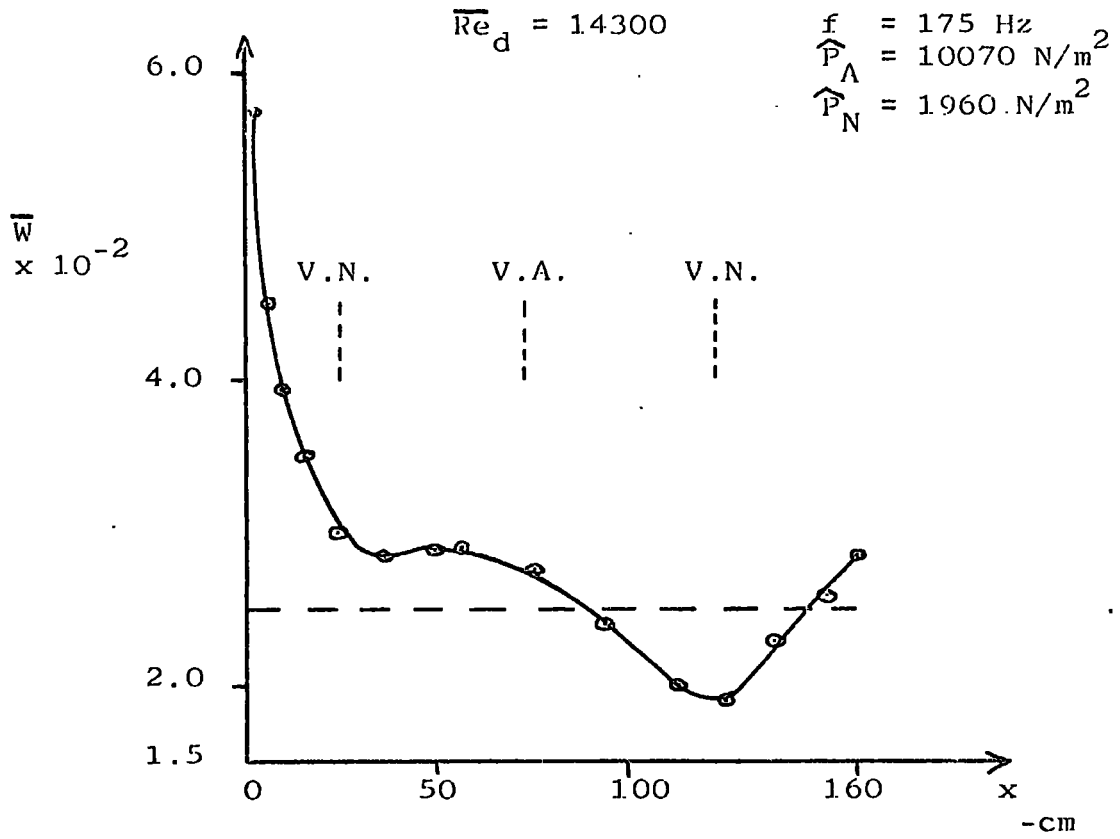
$\overline{Re}_d$ = 14300
f = 175 Hz
$\hat{P}_A$ = 10070 N/m^2
$\hat{P}_N$ = 1960 N/m^2
$\overline{W}$ x 10^{-2}
6.0
4.0
2.0
1.5
V.N.
V.A.
V.N.
0
50
100
160
x
-cm

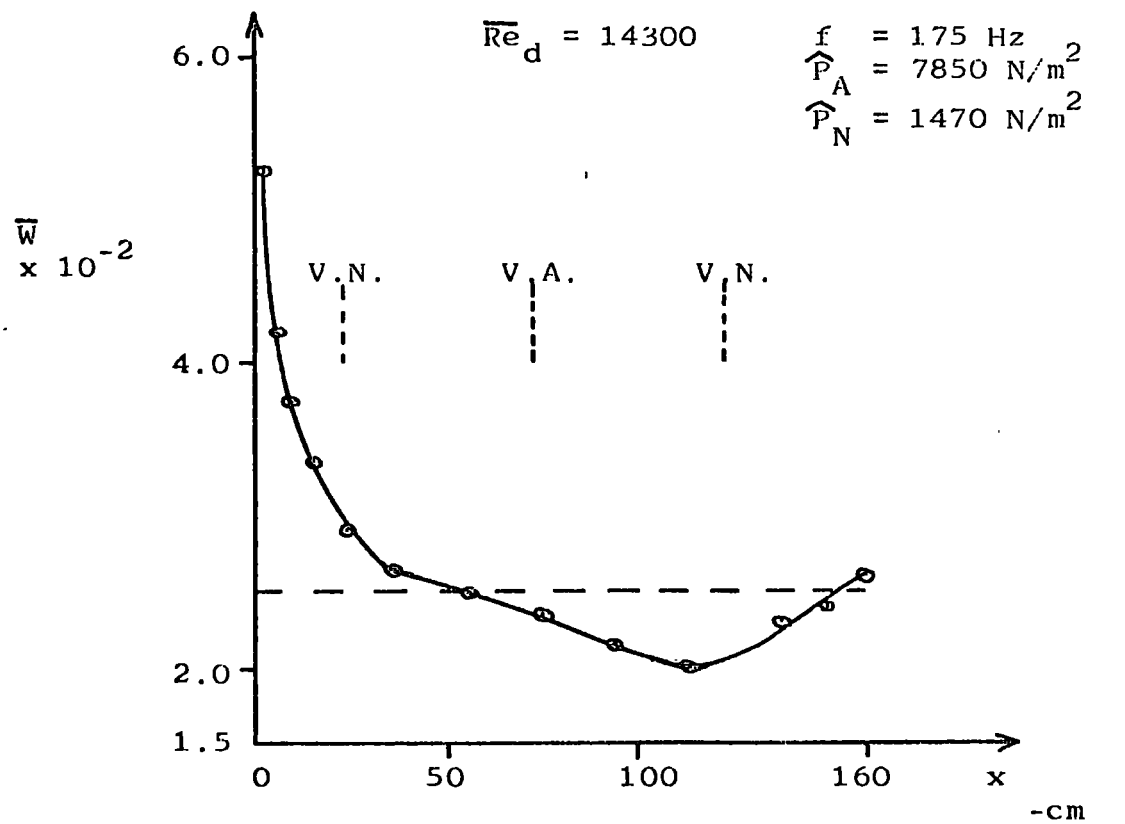
$\overline{Re}_d$ = 14300
f = 175 Hz
$\hat{P}_A$ = 7850 N/m^2
$\hat{P}_N$ = 1470 N/m^2
$\overline{W}$ x 10^{-2}
6.0
4.0
2.0
1.5
V.N.
V.A.
V.N.
0
50
100
160
x
-cm

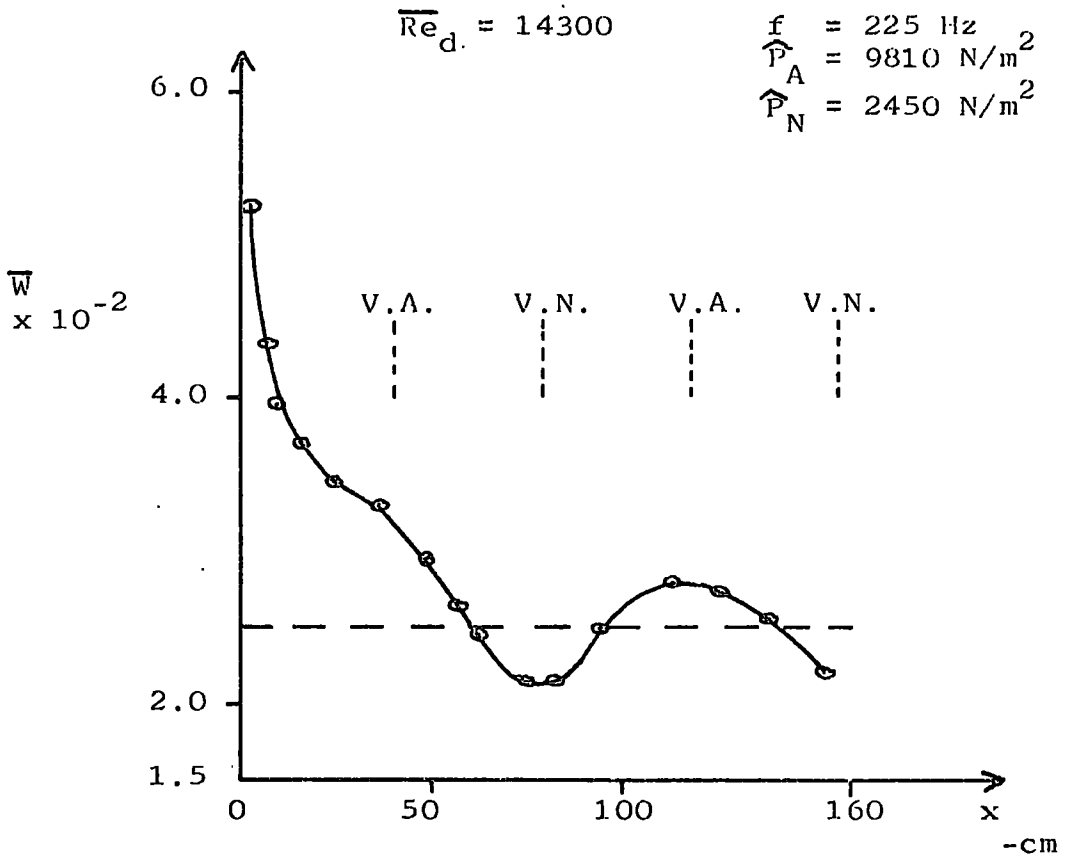
$\overline{Re}_d$ = 14300
f = 225 Hz
$\hat{P}_A$ = 9810 N/m^2
$\hat{P}_N$ = 2450 N/m^2
$\overline{W}$ x 10^{-2}
6.0
4.0
2.0
1.5
V.A.
V.N.
V.A.
V.N.
0
50
100
160
x
-cm

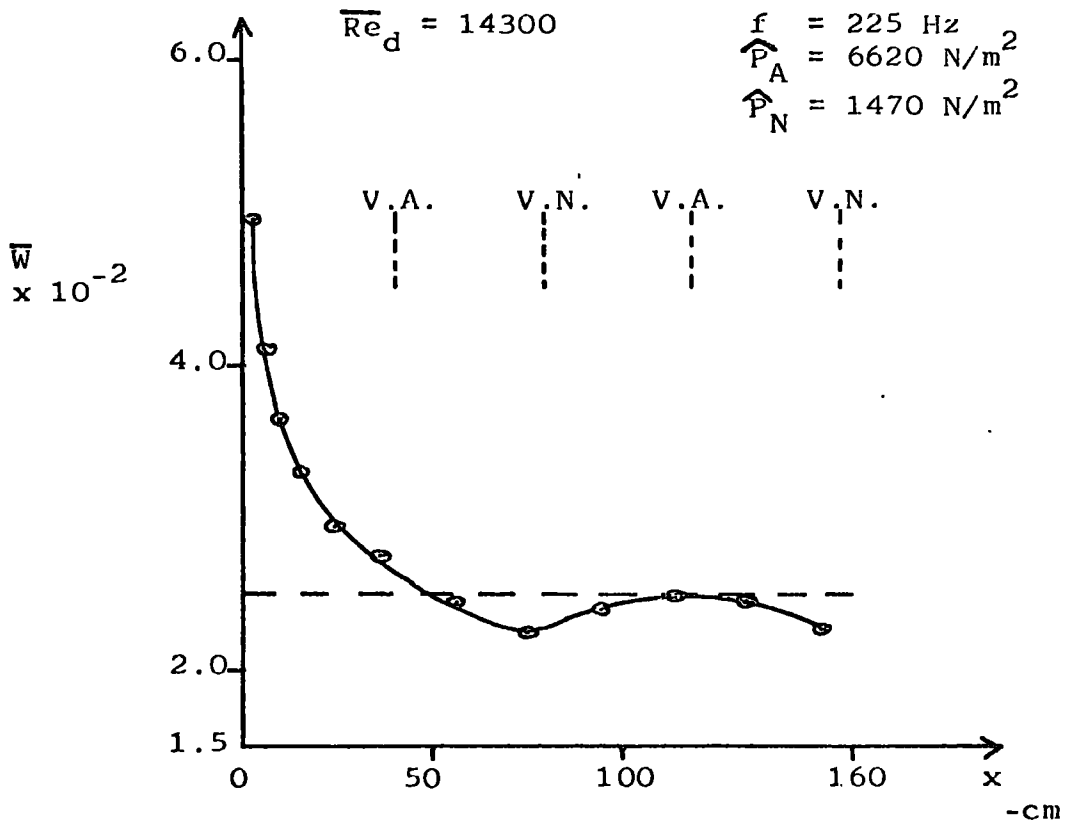
$\overline{Re}_d$ = 14300
f = 225 Hz
$\hat{P}_A$ = 6620 N/m^2
$\hat{P}_N$ = 1470 N/m^2
$\overline{W}$ x 10^{-2}
6.0
4.0
2.0
1.5
V.A.
V.N.
V.A.
V.N.
0
50
100
160
x
-cm

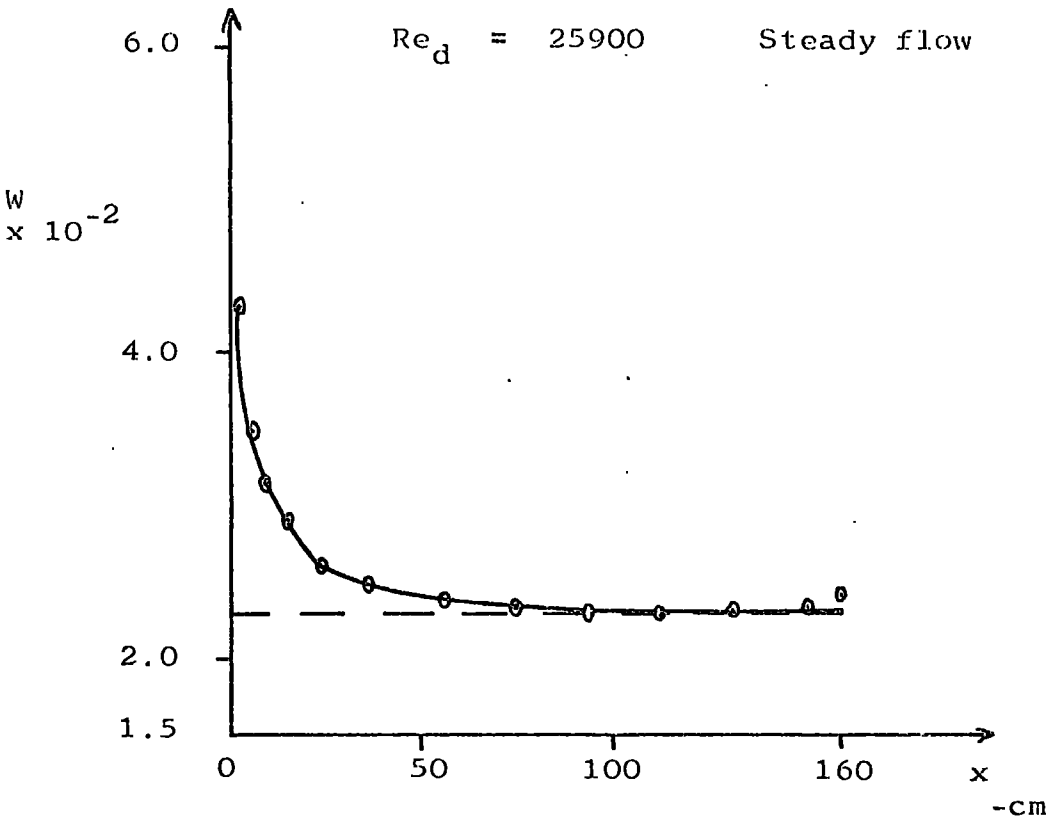
6.0
Re_d = 25900
Steady flow
W
x 10^{-2}
4.0
2.0
1.5
0
50
100
160
x
-cm

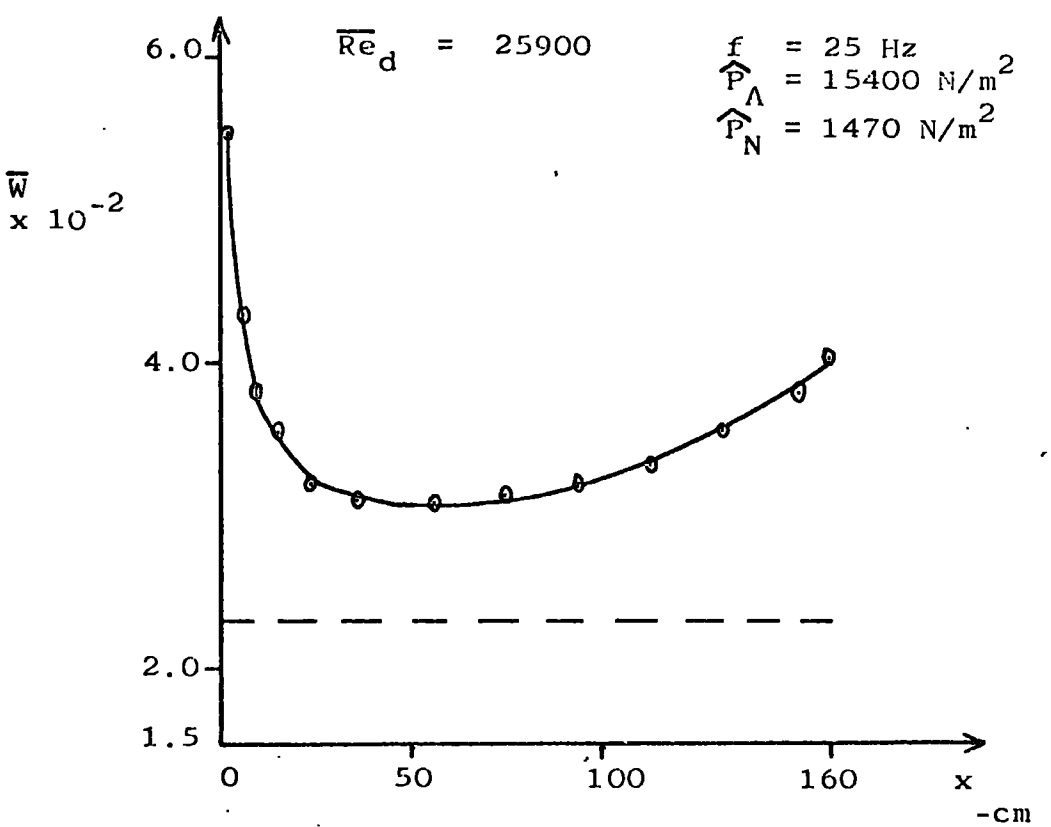
6.0
$\overline{Re}_d$ = 25900
f = 25 Hz
$\hat{P}_\Lambda$ = 15400 N/m^2
$\hat{P}_N$ = 1470 N/m^2
$\overline{W}$
x 10^{-2}
4.0
2.0
1.5
0
50
100
160
x
-cm

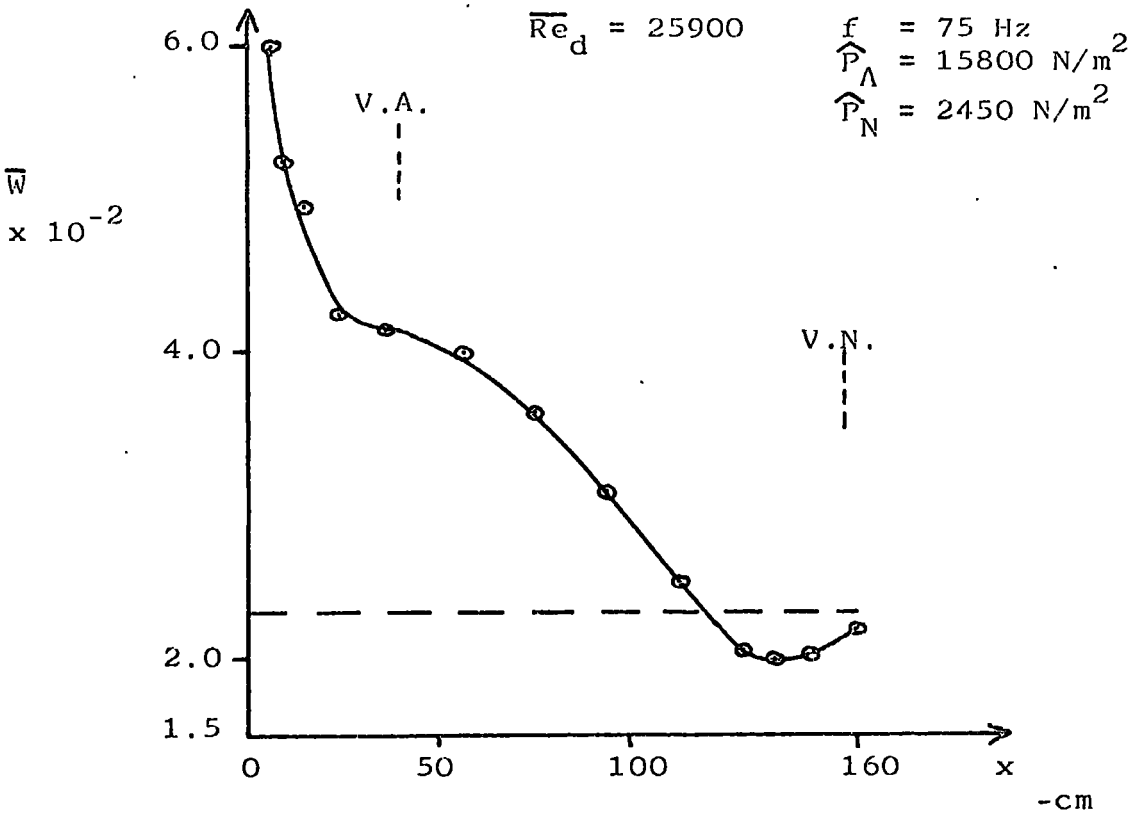
$\overline{Re}_d$ = 25900
f = 75 Hz
$\hat{P}_A$ = 15800 N/m^2
$\hat{P}_N$ = 2450 N/m^2
$\overline{W}$ x 10^{-2}
6.0
4.0
2.0
1.5
V.A.
V.N.
0
50
100
160
x
-cm

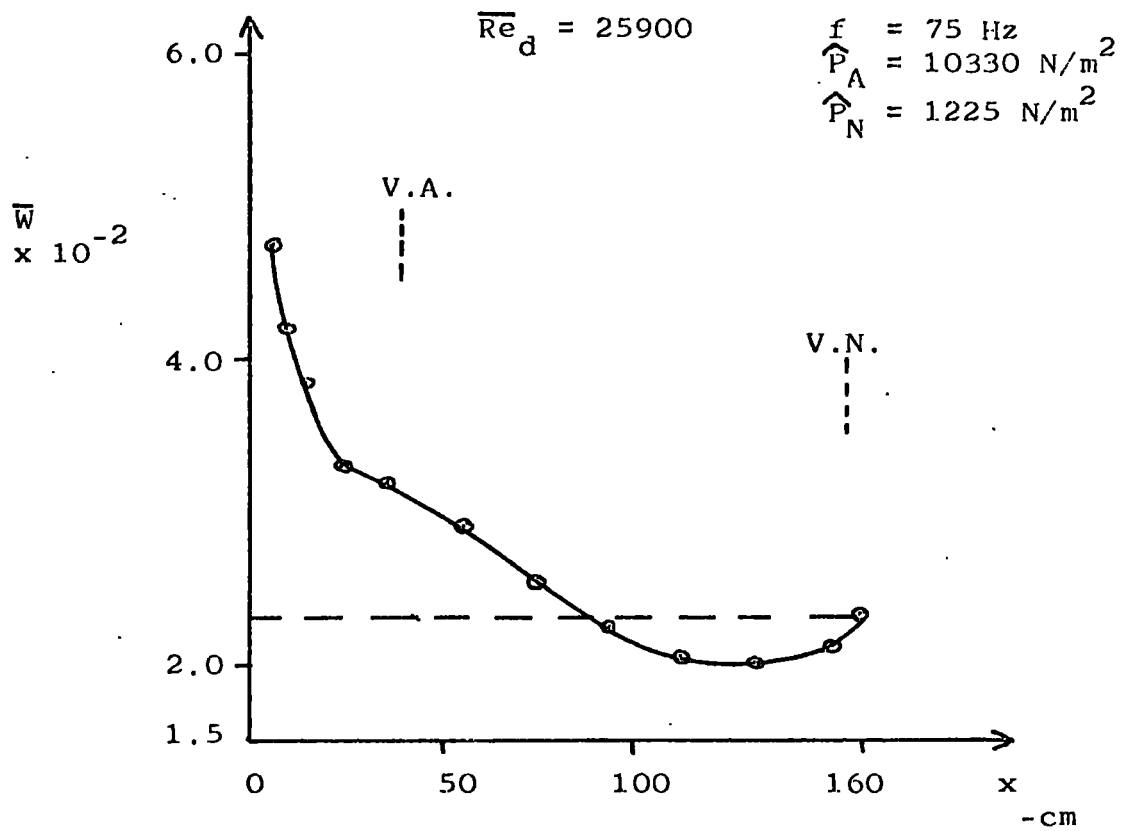
$\overline{Re}_d$ = 25900
f = 75 Hz
$\hat{P}_A$ = 10330 N/m^2
$\hat{P}_N$ = 1225 N/m^2
$\overline{W}$ x 10^{-2}
6.0
4.0
2.0
1.5
V.A.
V.N.
0
50
100
160
x
-cm

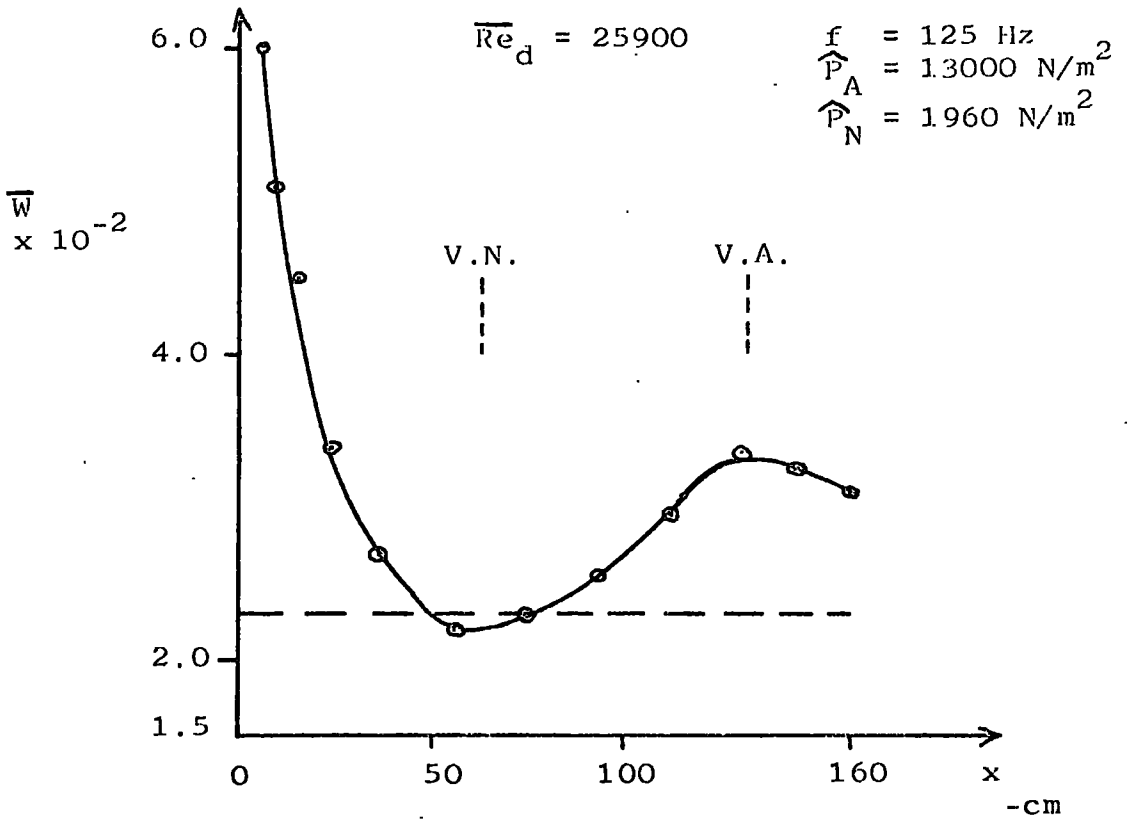
$\overline{Re}_d$ = 25900
f = 125 Hz
$\hat{P}_A$ = 1.3000 N/m^2
$\hat{P}_N$ = 1.960 N/m^2
$\overline{W}$ x 10^{-2}
6.0
4.0
2.0
1.5
V.N.
V.A.
0
50
100
160
x
-cm

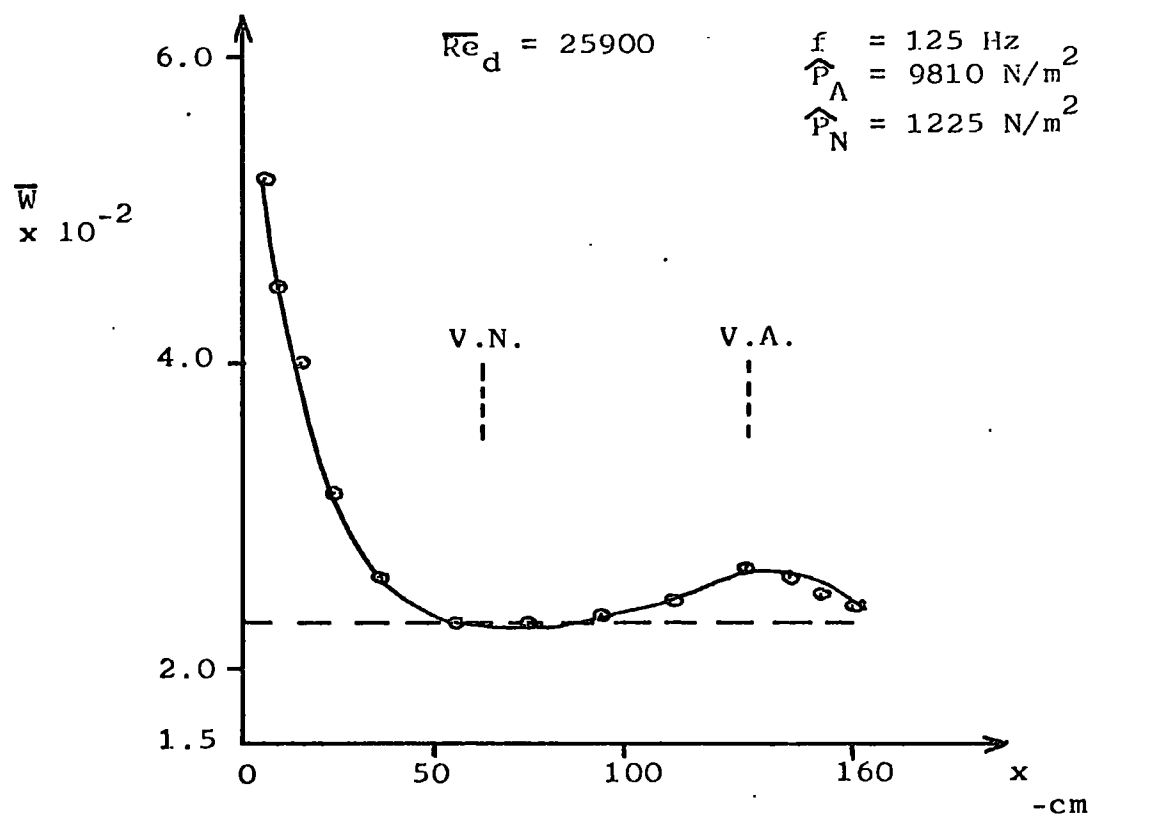
$\overline{Re}_d$ = 25900
f = 125 Hz
$\hat{P}_A$ = 9810 N/m^2
$\hat{P}_N$ = 1225 N/m^2
$\overline{W}$ x 10^{-2}
6.0
4.0
2.0
1.5
V.N.
V.A.
0
50
100
160
x
-cm

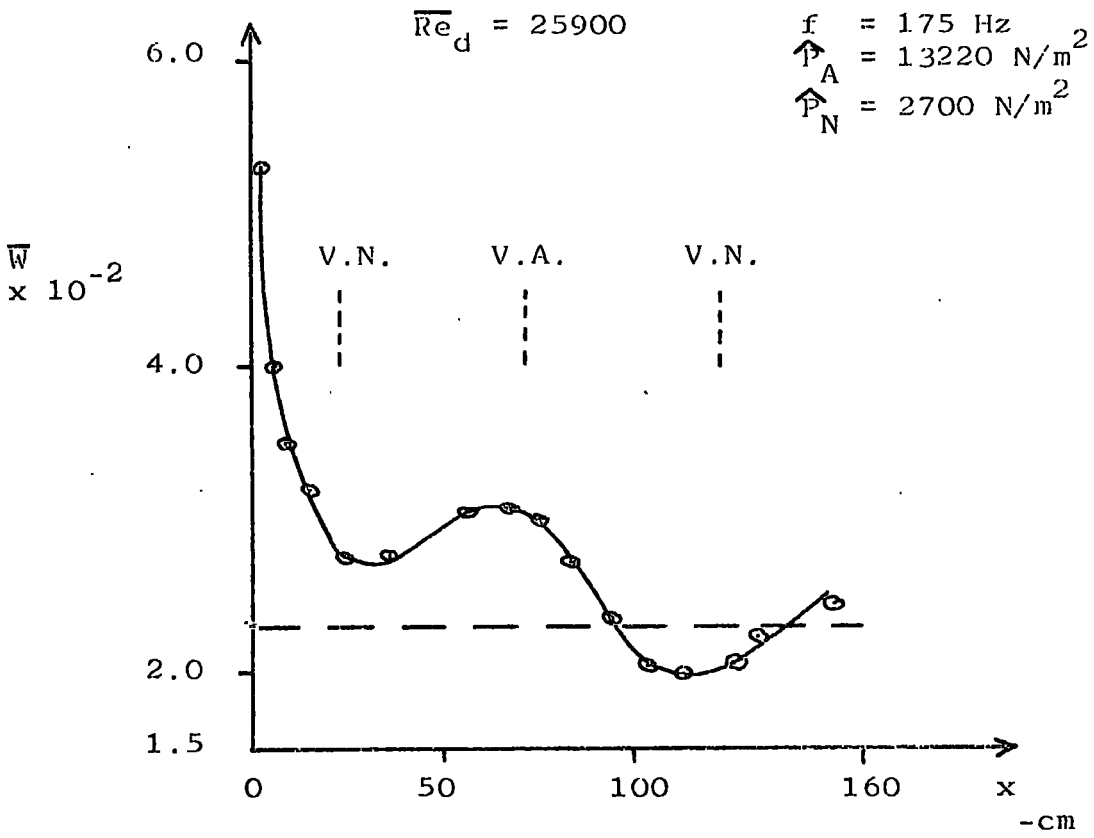
$\overline{Re}_d$ = 25900
f = 175 Hz
$\hat{P}_A$ = 13220 N/m^2
$\hat{P}_N$ = 2700 N/m^2
$\overline{W}$ x 10^{-2}
6.0
4.0
2.0
1.5
V.N.
V.A.
V.N.
0
50
100
160
x
-cm

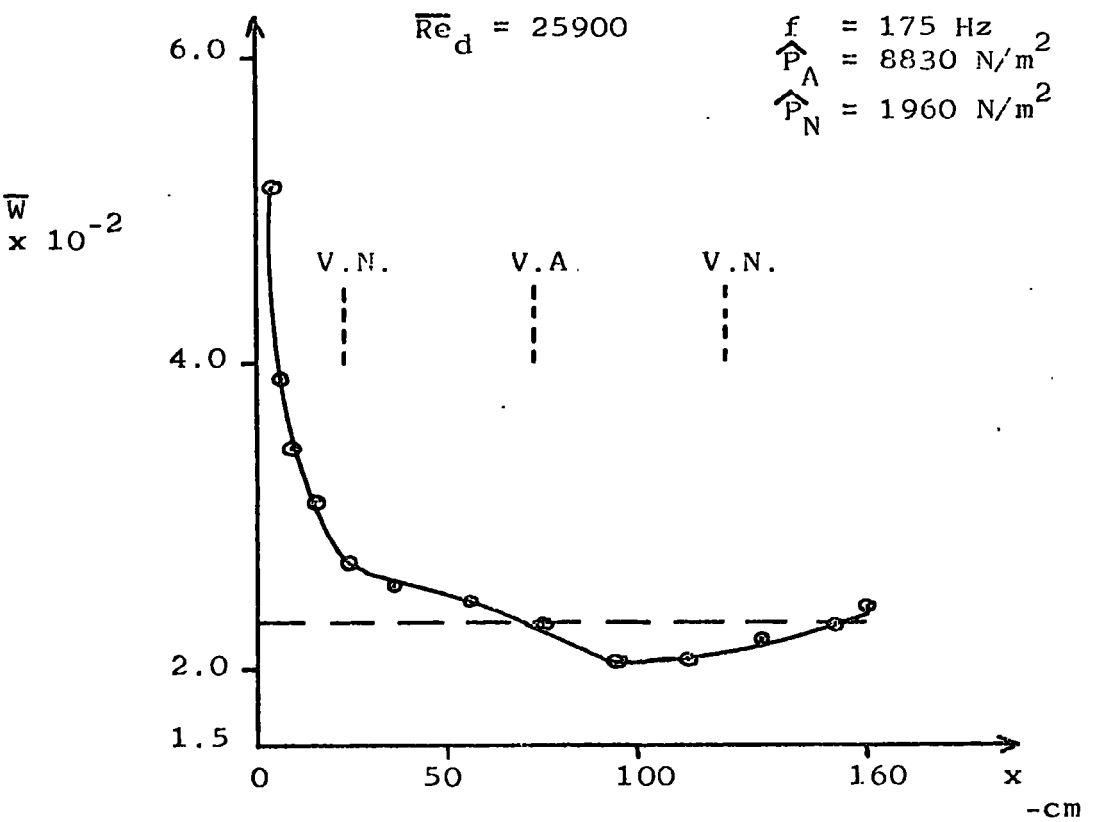
$\overline{Re}_d$ = 25900
f = 175 Hz
$\hat{P}_A$ = 8830 N/m^2
$\hat{P}_N$ = 1960 N/m^2
$\overline{W}$ x 10^{-2}
6.0
4.0
2.0
1.5
V.N.
V.A.
V.N.
0
50
100
160
x
-cm

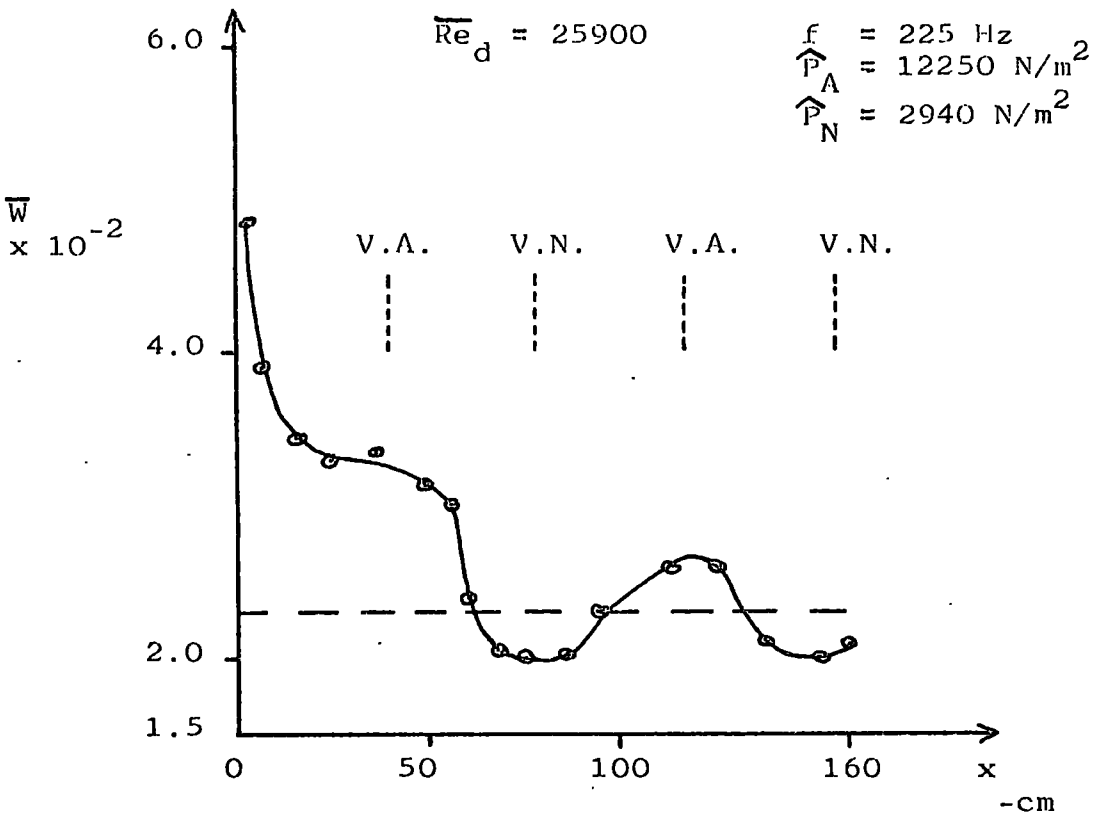
$\overline{Re}_d$ = 25900
f = 225 Hz
$\hat{P}_A$ = 12250 N/m^2
$\hat{P}_N$ = 2940 N/m^2
$\overline{W}$ x 10^{-2}
V.A.
V.N.
V.A.
V.N.
6.0
4.0
2.0
1.5
0
50
100
160
x
-cm

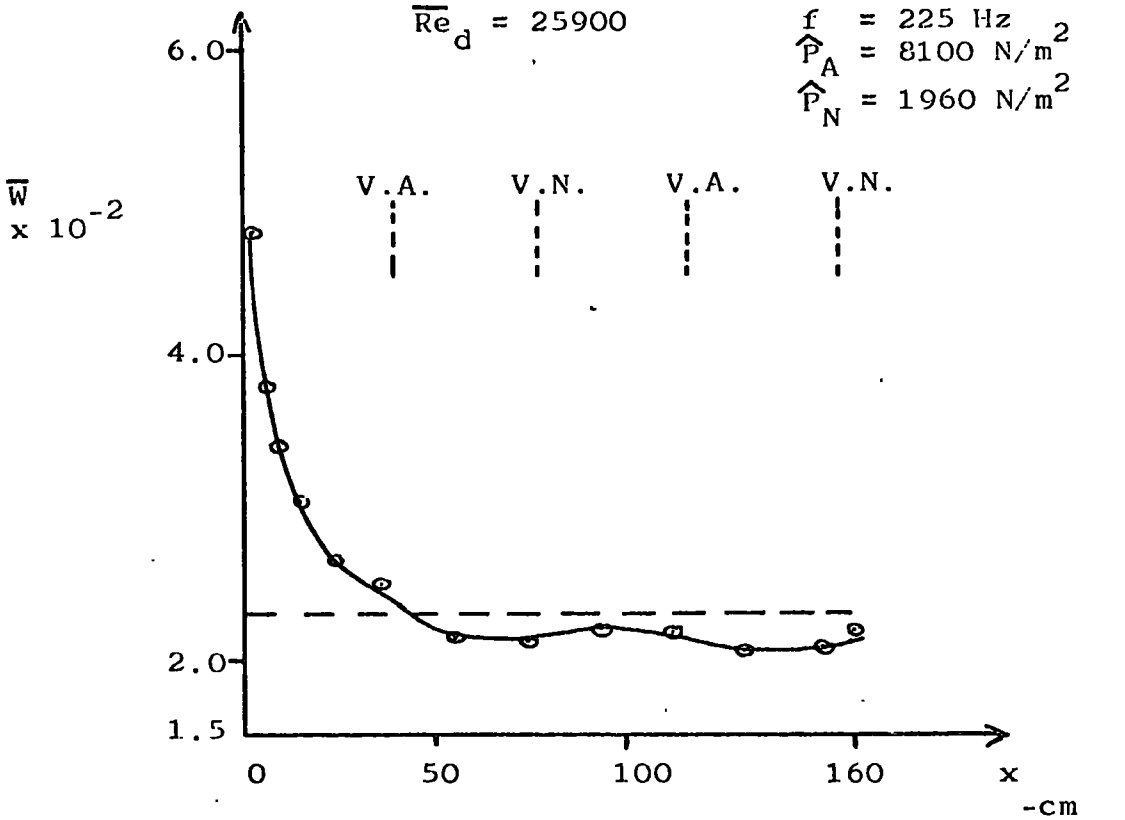
$\overline{Re}_d$ = 25900
f = 225 Hz
$\hat{P}_A$ = 8100 N/m^2
$\hat{P}_N$ = 1960 N/m^2
$\overline{W}$ x 10^{-2}
V.A.
V.N.
V.A.
V.N.
6.0
4.0
2.0
1.5
0
50
100
160
x
-cm

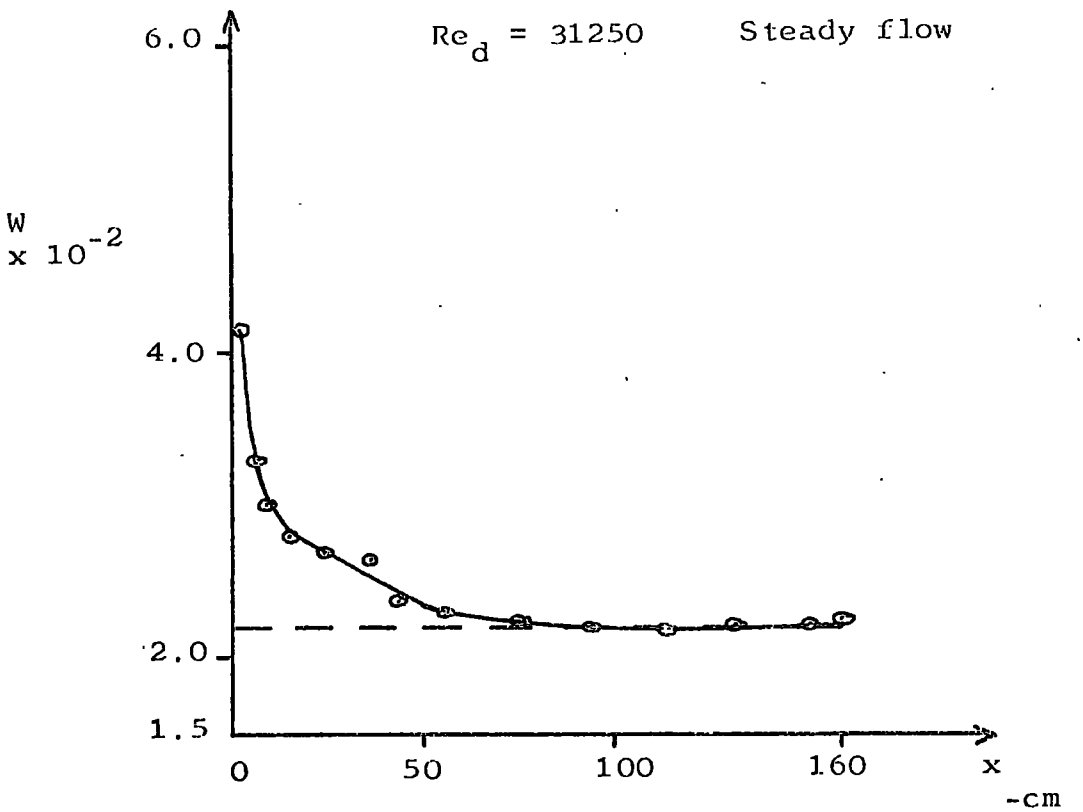
6.0
4.0
2.0
1.5
W
x 10^-2
Re_d = 31250
Steady flow
0
50
100
160
x
-cm

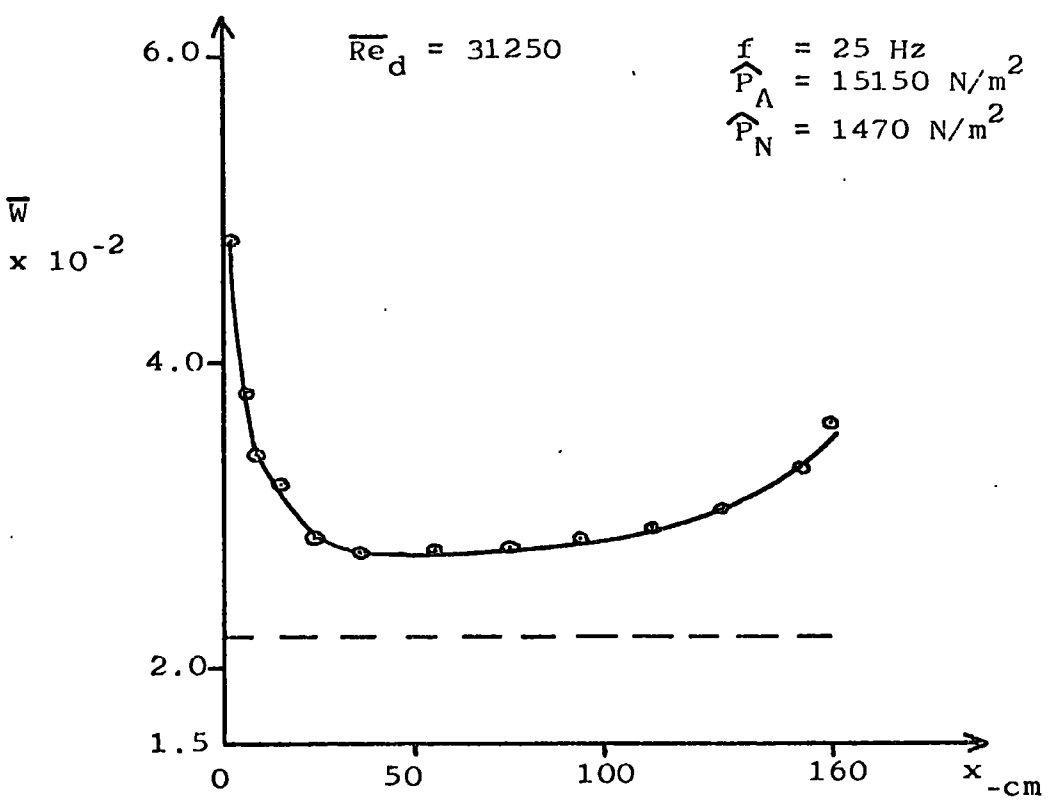
6.0
4.0
2.0
1.5
W̄
x 10^-2
Re_d = 31250
f = 25 Hz
P̂_A = 15150 N/m^2
P̂_N = 1470 N/m^2
0
50
100
160
x
-cm

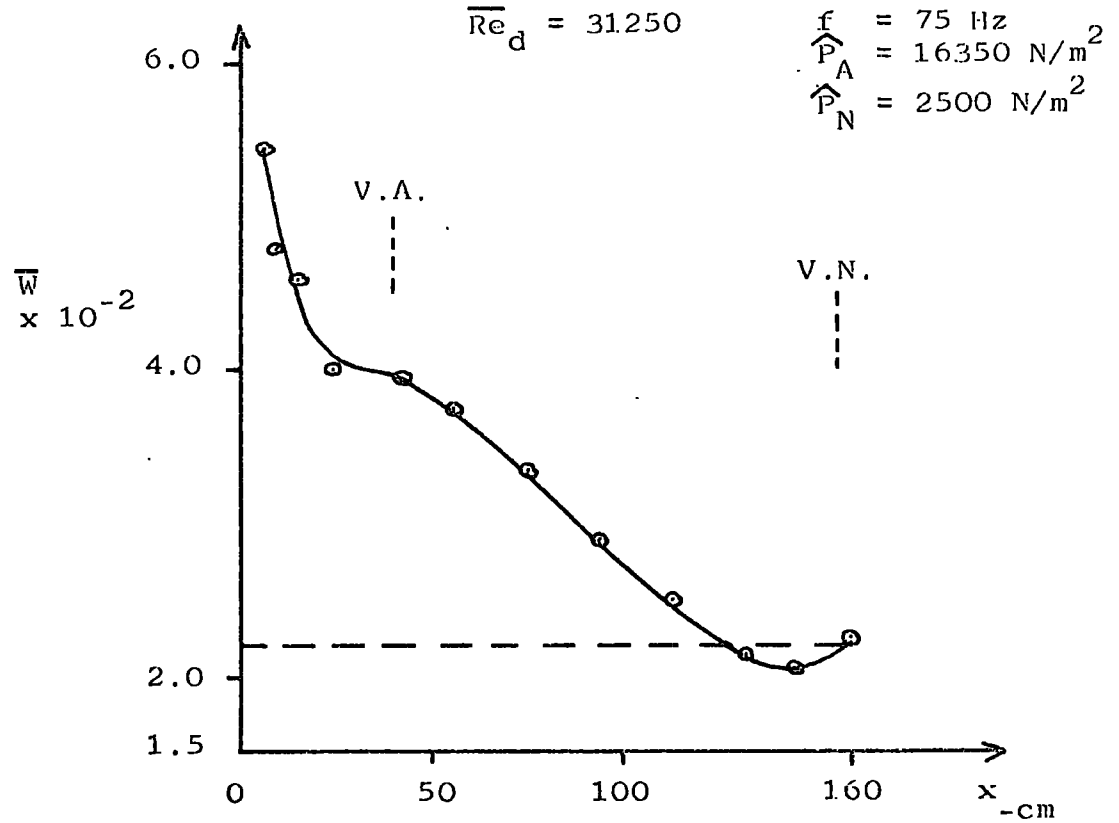
$\overline{Re}_d$ = 31250
f = 75 Hz
$\hat{P}_A$ = 16350 N/m^2
$\hat{P}_N$ = 2500 N/m^2
V.A.
V.N.
$\overline{W}$ x 10^{-2}
6.0
4.0
2.0
1.5
0
50
100
160
x -cm

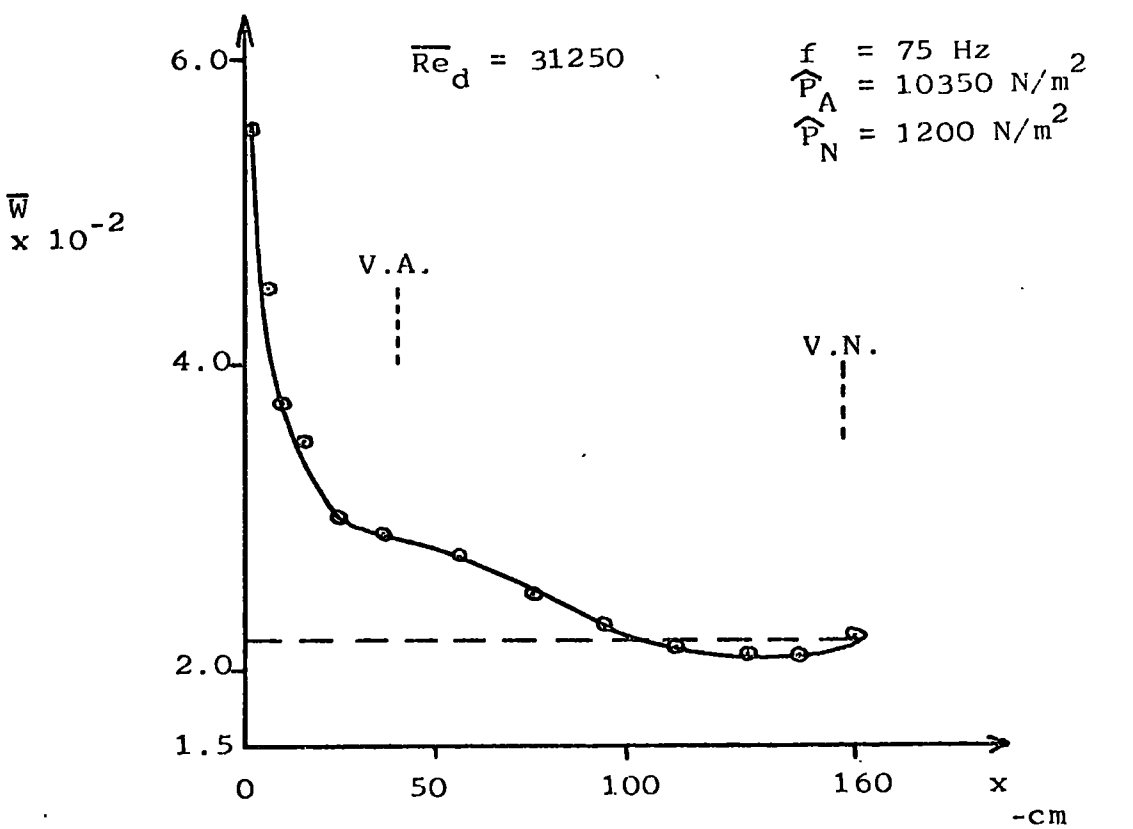
$\overline{Re}_d$ = 31250
f = 75 Hz
$\hat{P}_A$ = 10350 N/m^2
$\hat{P}_N$ = 1200 N/m^2
V.A.
V.N.
$\overline{W}$ x 10^{-2}
6.0
4.0
2.0
1.5
0
50
100
160
x -cm

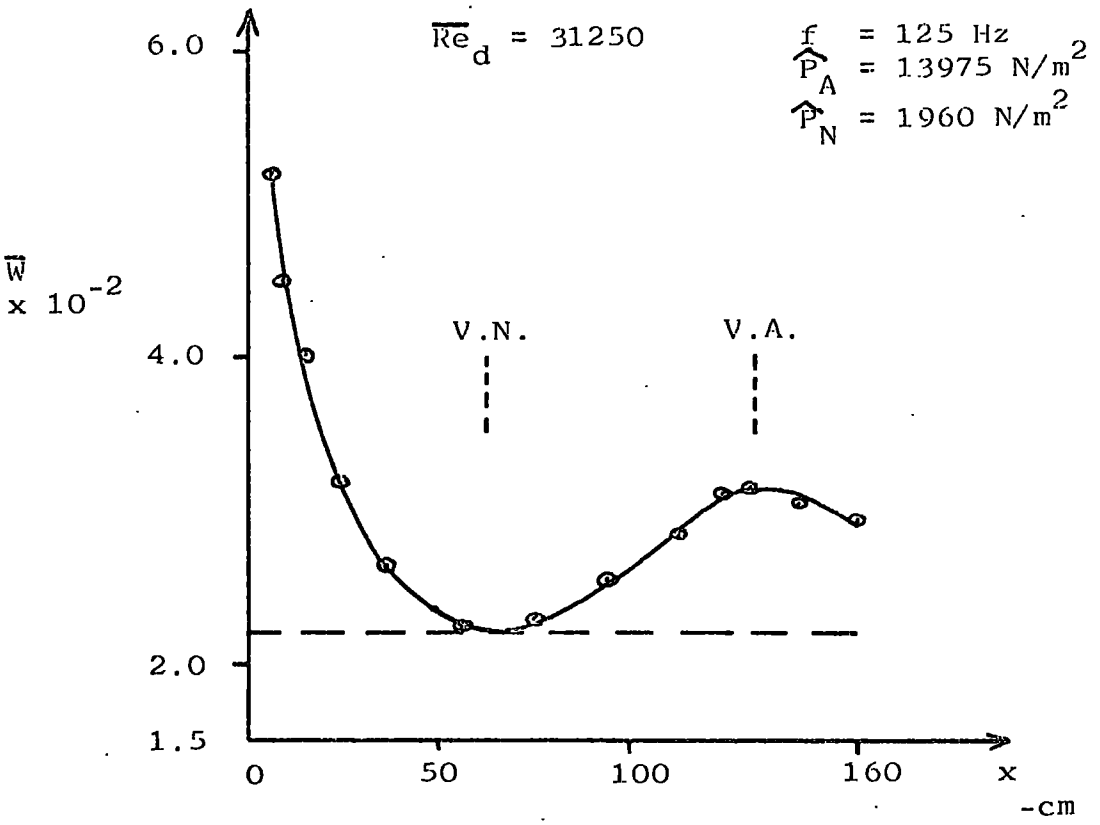
$\overline{Re}_d$ = 31250
f = 125 Hz
$\hat{P}_A$ = 13975 N/m^2
$\hat{P}_N$ = 1960 N/m^2
$\overline{W}$ x 10^{-2}
6.0
4.0
2.0
1.5
V.N.
V.A.
0
50
100
160
x
-cm

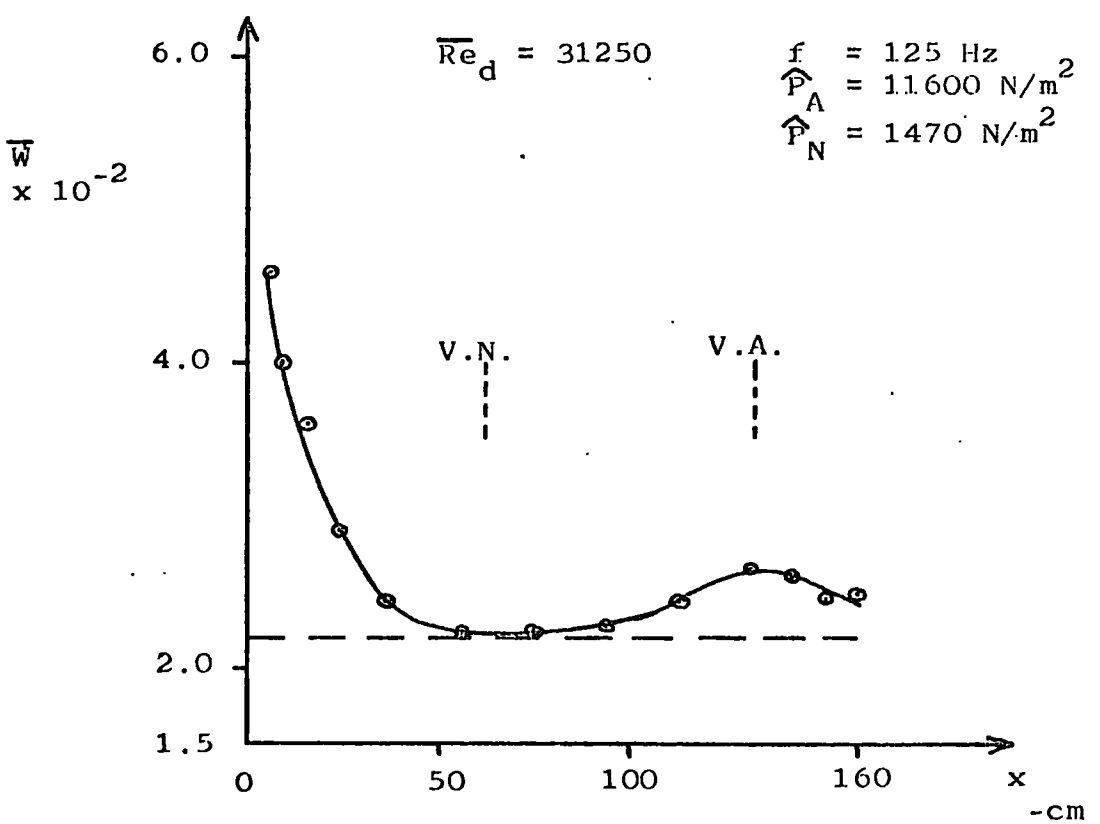
$\overline{Re}_d$ = 31250
f = 125 Hz
$\hat{P}_A$ = 11600 N/m^2
$\hat{P}_N$ = 1470 N/m^2
$\overline{W}$ x 10^{-2}
6.0
4.0
2.0
1.5
V.N.
V.A.
0
50
100
160
x
-cm

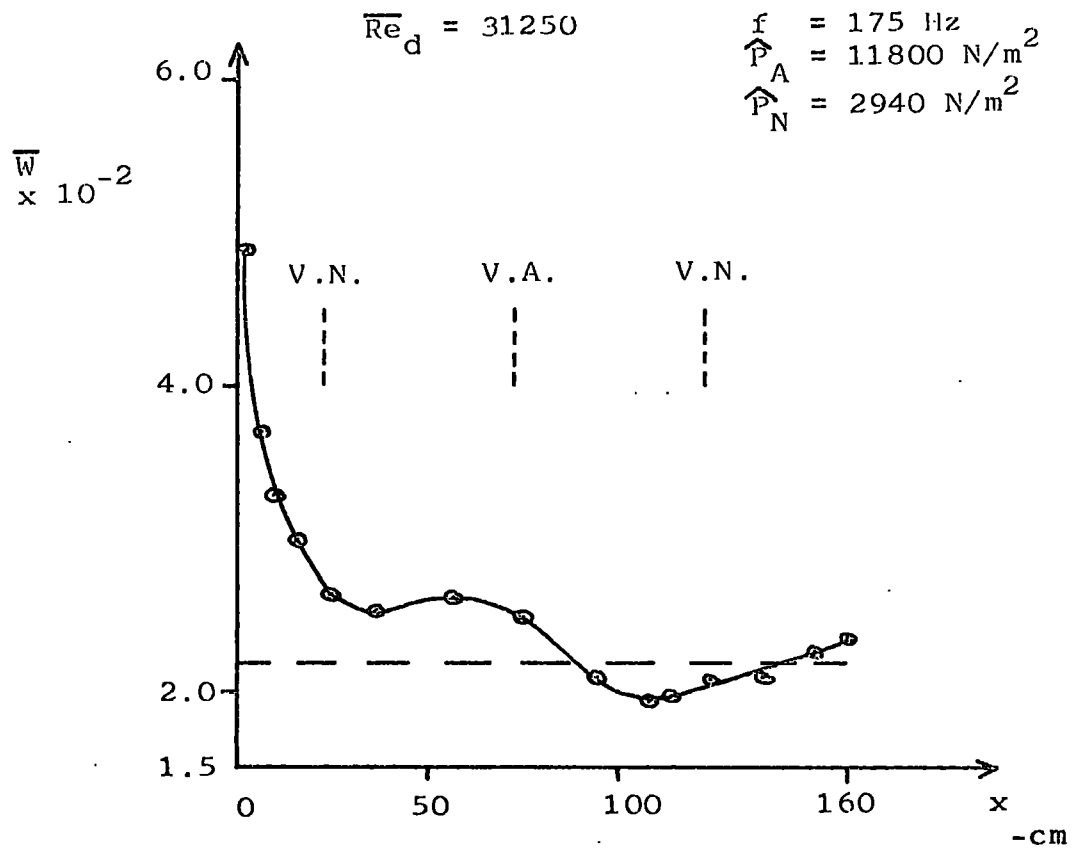
$\overline{Re}_d$ = 31250
f = 175 Hz
$\hat{P}_A$ = 11800 N/m^2
$\hat{P}_N$ = 2940 N/m^2
$\overline{W}$ x 10^{-2}
6.0
4.0
2.0
1.5
V.N.
V.A.
V.N.
0
50
100
160
x
-cm

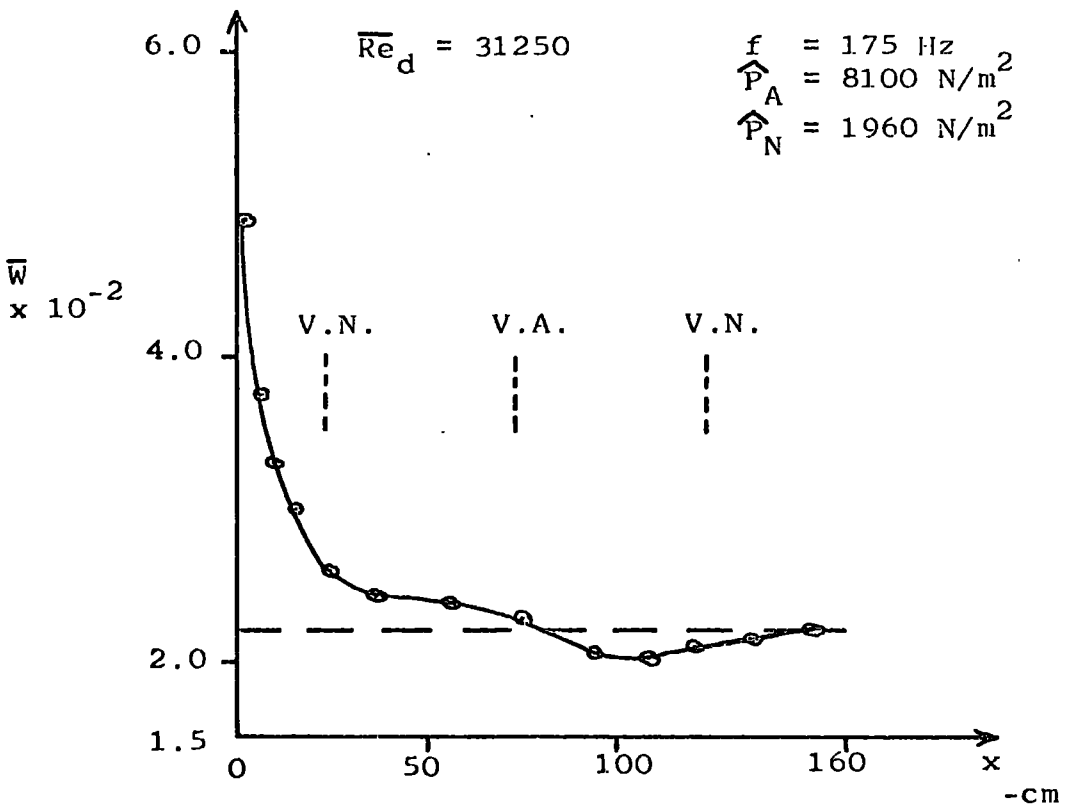
$\overline{Re}_d$ = 31250
f = 175 Hz
$\hat{P}_A$ = 8100 N/m^2
$\hat{P}_N$ = 1960 N/m^2
$\overline{W}$ x 10^{-2}
6.0
4.0
2.0
1.5
V.N.
V.A.
V.N.
0
50
100
160
x
-cm

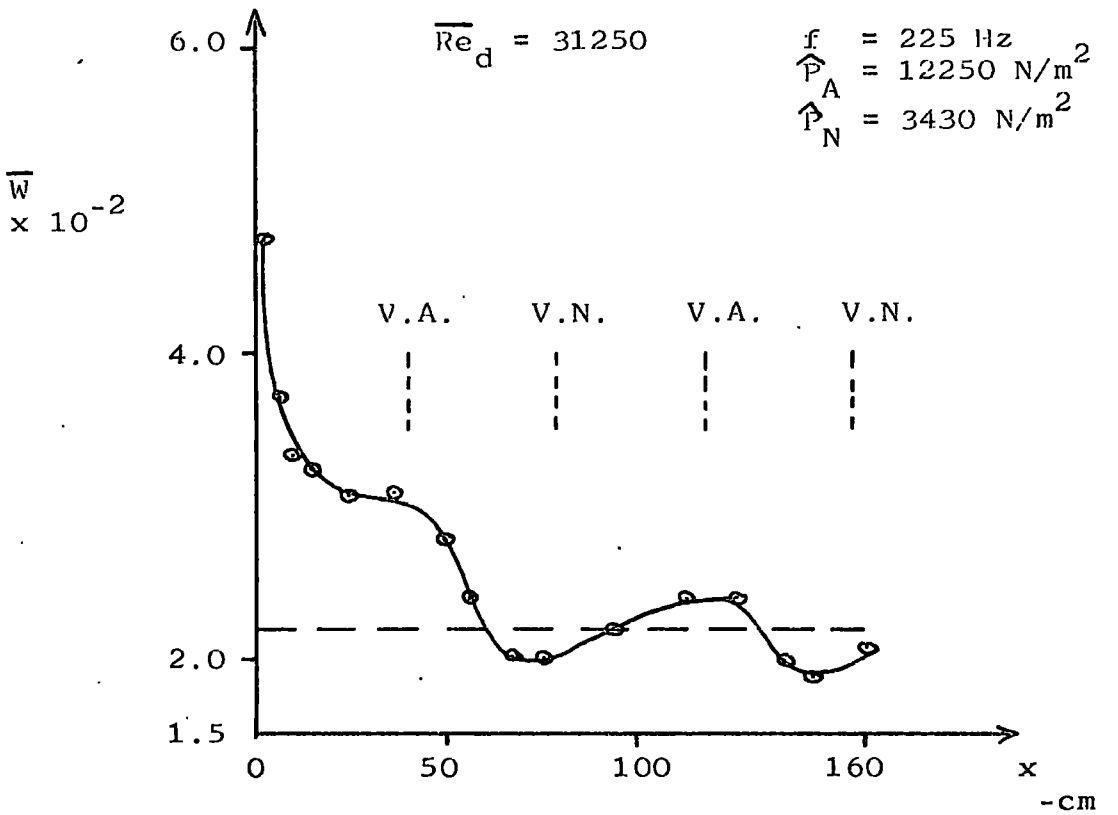
$\overline{Re}_d$ = 31250
f = 225 Hz
$\hat{P}_A$ = 12250 N/m^2
$\hat{P}_N$ = 3430 N/m^2
$\overline{W}$ x 10^{-2}
6.0
4.0
2.0
1.5
V.A.
V.N.
V.A.
V.N.
0
50
100
160
x
-cm

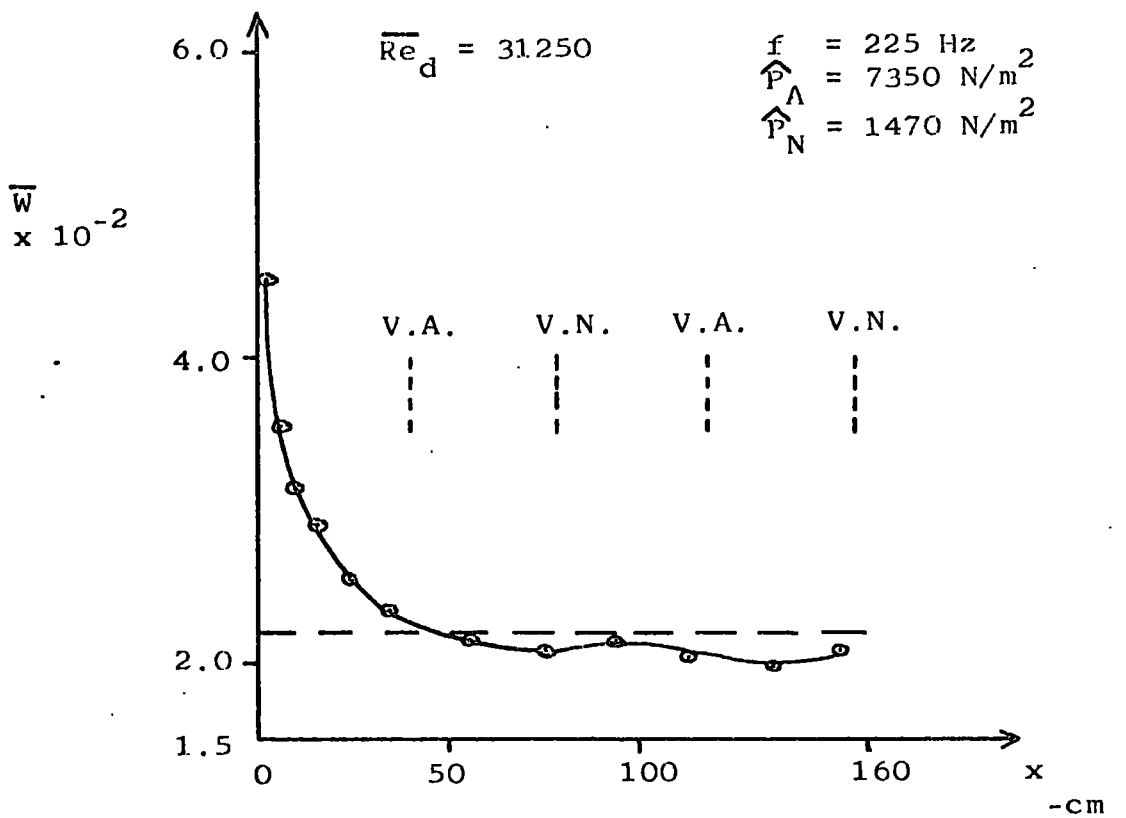
$\overline{Re}_d$ = 31250
f = 225 Hz
$\hat{P}_A$ = 7350 N/m^2
$\hat{P}_N$ = 1470 N/m^2
$\overline{W}$ x 10^{-2}
6.0
4.0
2.0
1.5
V.A.
V.N.
V.A.
V.N.
0
50
100
160
x
-cm

Appendix IV

Correlation of Improvement ratio for fully developed flow against the corresponding local Dimensionless Pulsation velocity (Figure 3A)

The following graphs show the relationship of local Improvement ratio for fully established flow against the corresponding local Dimensionless Pulsation velocity - the experimental results are analysed for each frequency of each flowrate.

Mean air flowrate $\bar{\dot{m}}$ -Kg/s	Reynolds number Re_d
0.0080	14300
0.0145	25900
0.0175	31250
	at Bulk air temperature 15°C

The experimental data is shown in comparison to the equivalent quasi-steady predictions.

×, Δ Experimental

⊙ Quasi-steady

Mean air flowrate $\overline{\dot{m}}$ = 0.008 Kg/s

Reynolds number, $\overline{Re}_d$ = 14300
at bulk air temperature 15°C

Frequency -Hz	Strouhal Number S
25	1.13
75	3.36
125	5.54
175	7.65
225	10.05

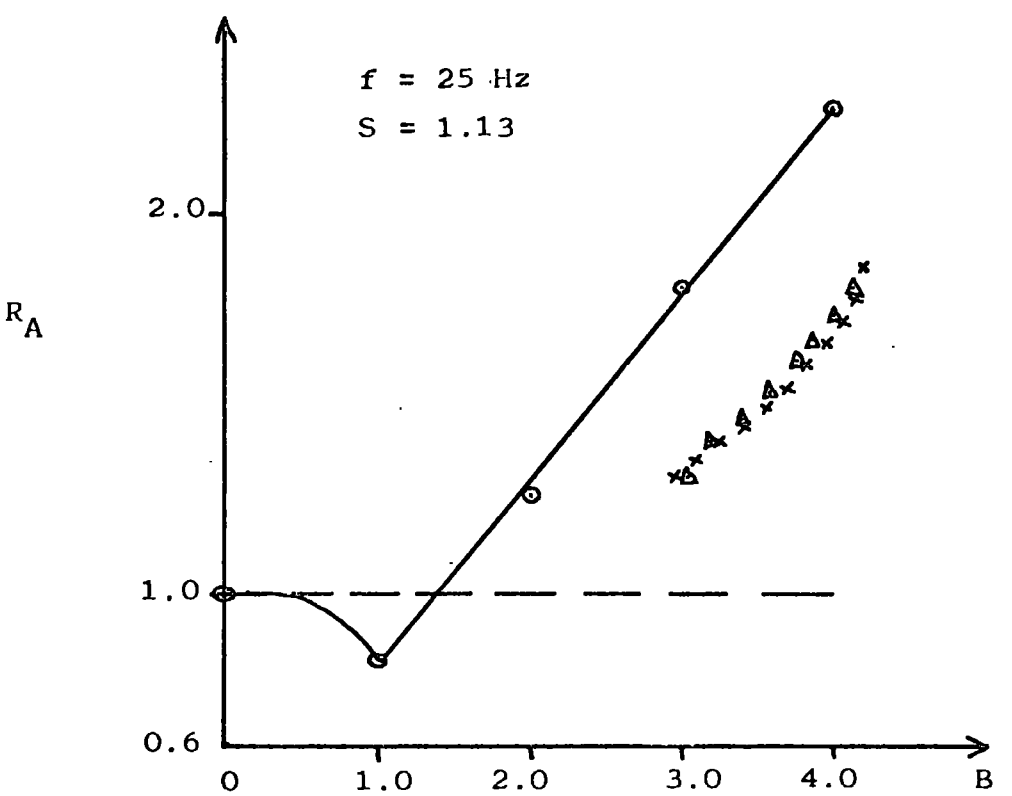

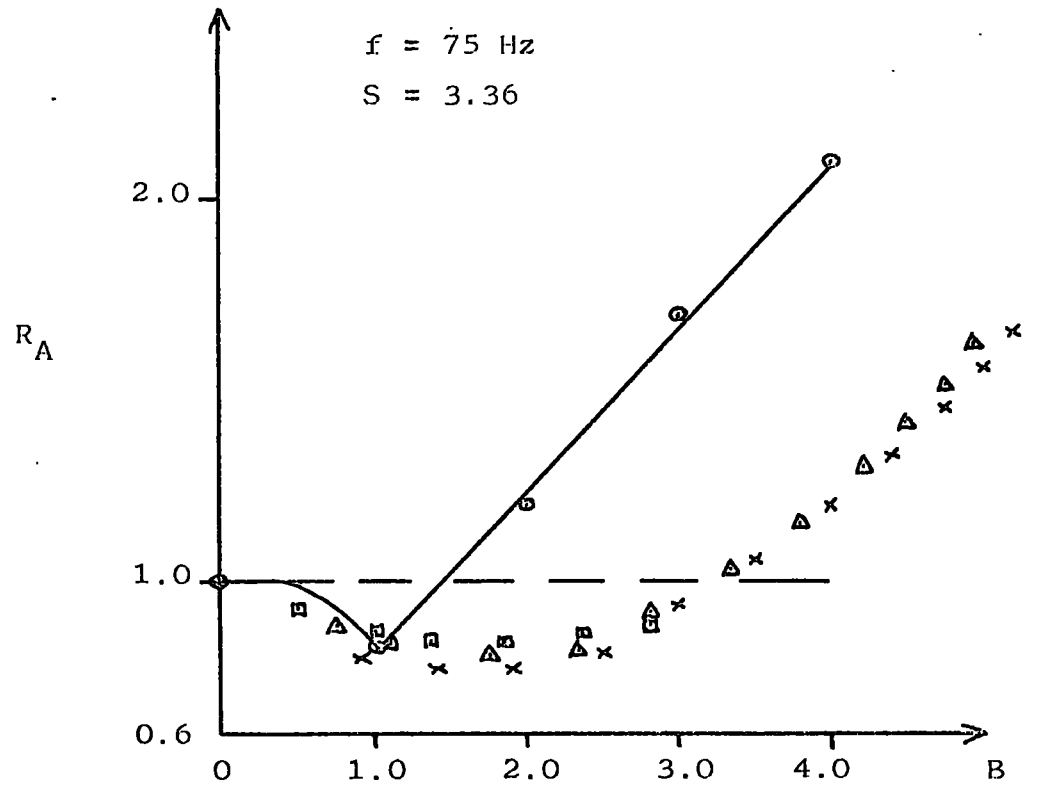
f = 75 Hz
S = 3.36
R_A
2.0
1.0
0.6
0
1.0
2.0
3.0
4.0
B

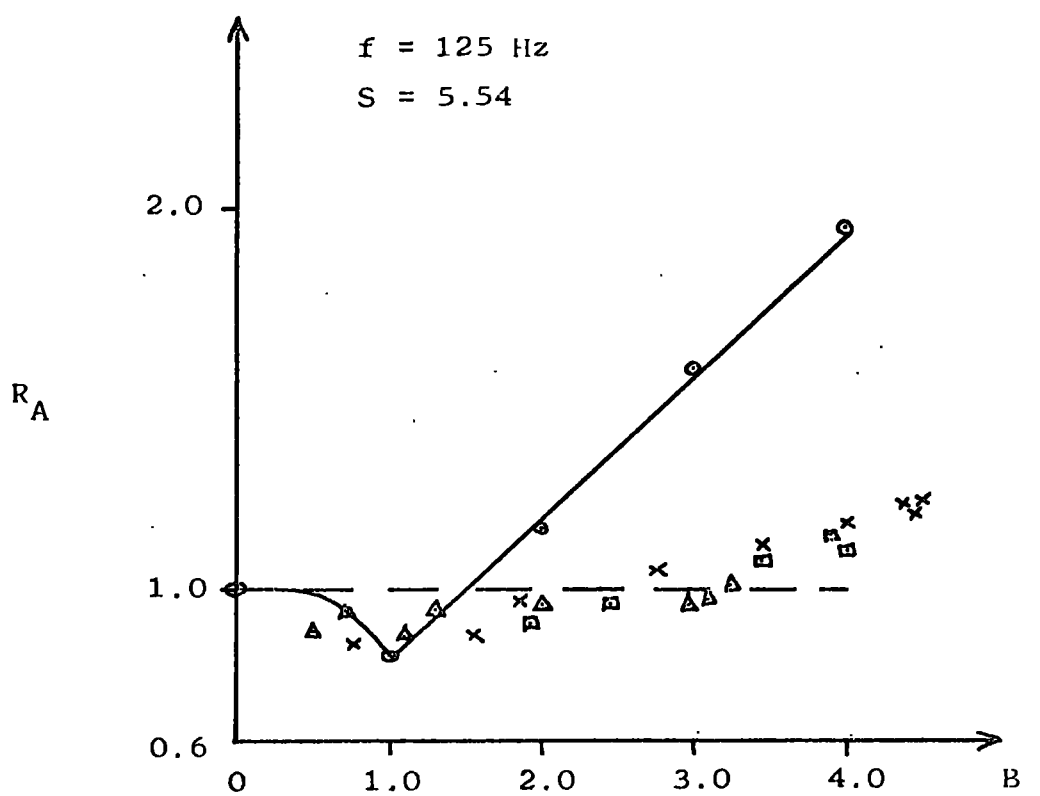
f = 125 Hz
S = 5.54
R_A
2.0
1.0
0.6
0
1.0
2.0
3.0
4.0
B

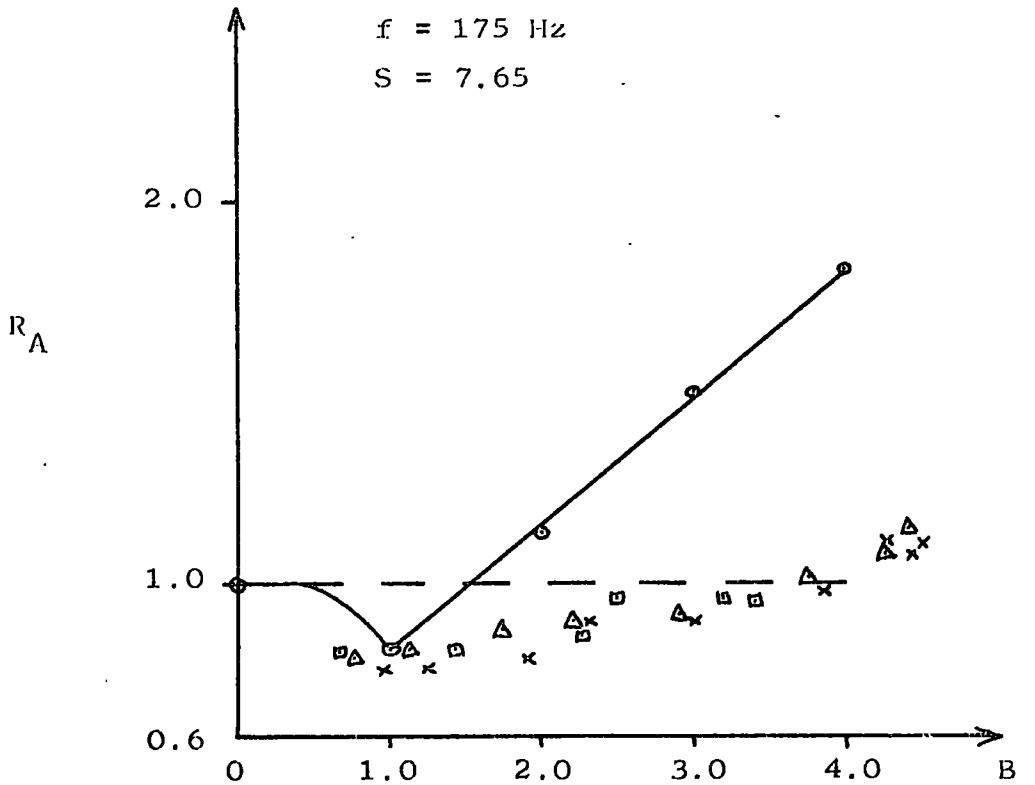
f = 175 Hz
S = 7.65
2.0
1.0
0.6
R_A
0
1.0
2.0
3.0
4.0
B

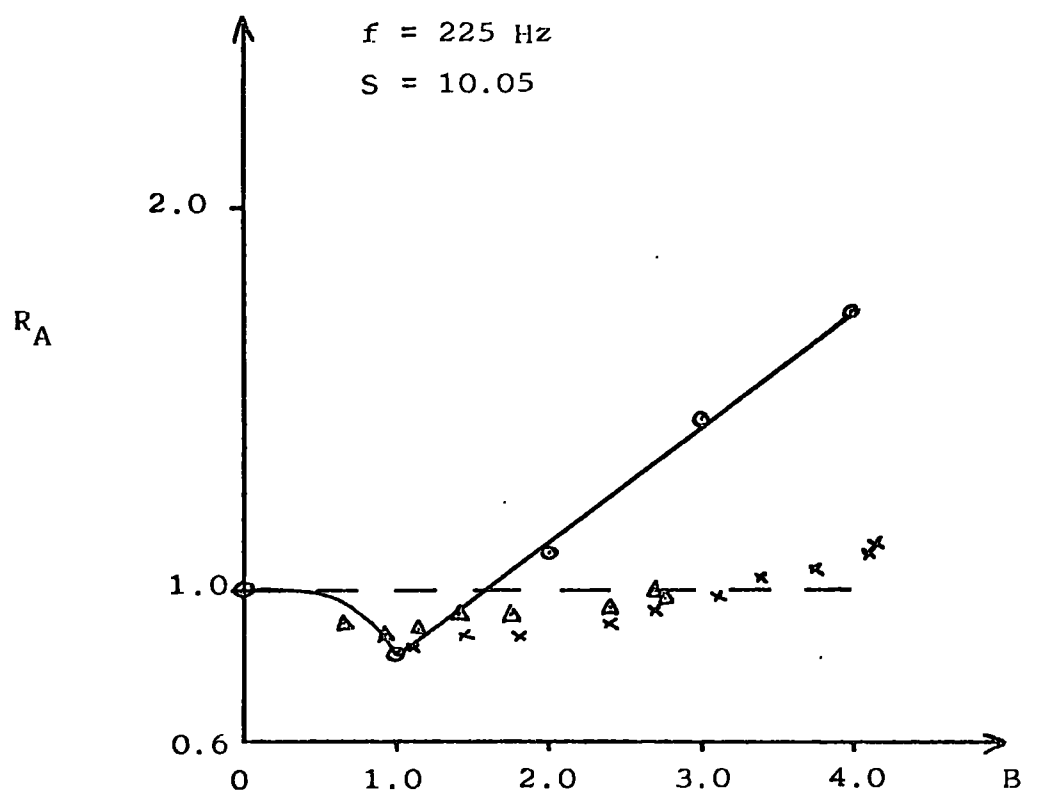
f = 225 Hz
S = 10.05
2.0
1.0
0.6
R_A
0
1.0
2.0
3.0
4.0
B

Mean air flowrate $\overline{\dot{m}}$ = 0.0145 Kg/s

Reynolds Number, $\overline{Re}_d$ = 25900
at bulk air temperature 15°C

Frequency -Hz	Strouhal number S
25	0.63
75	1.87
125	3.11
175	4.34
225	5.56

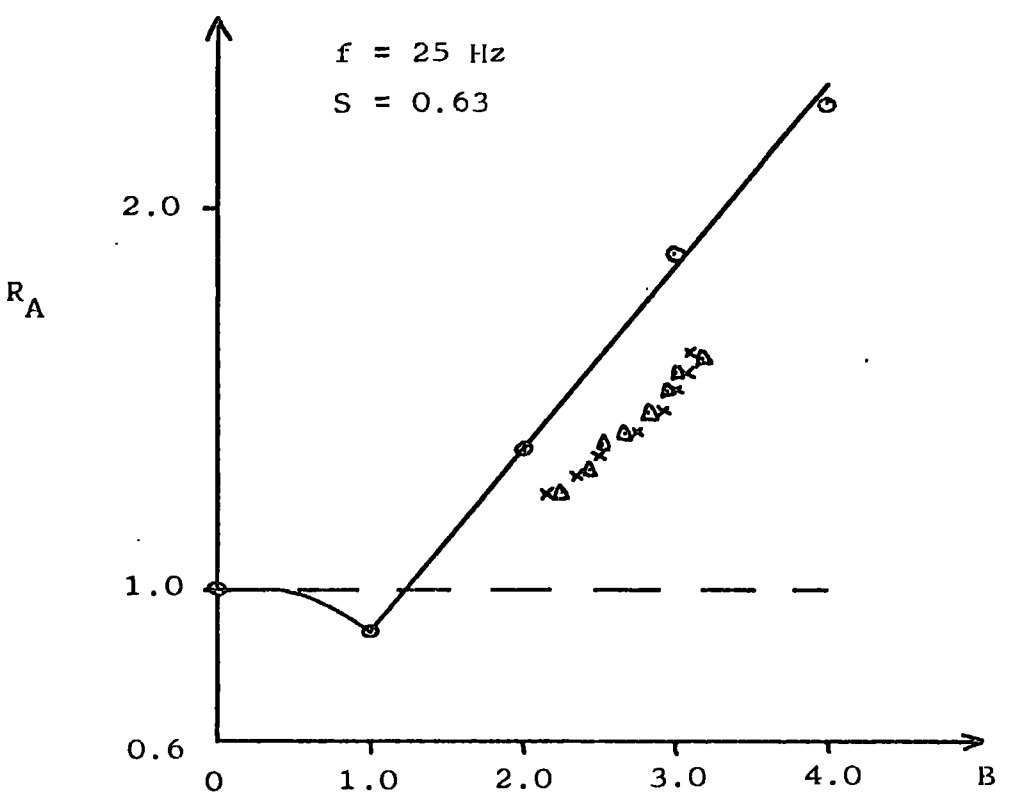

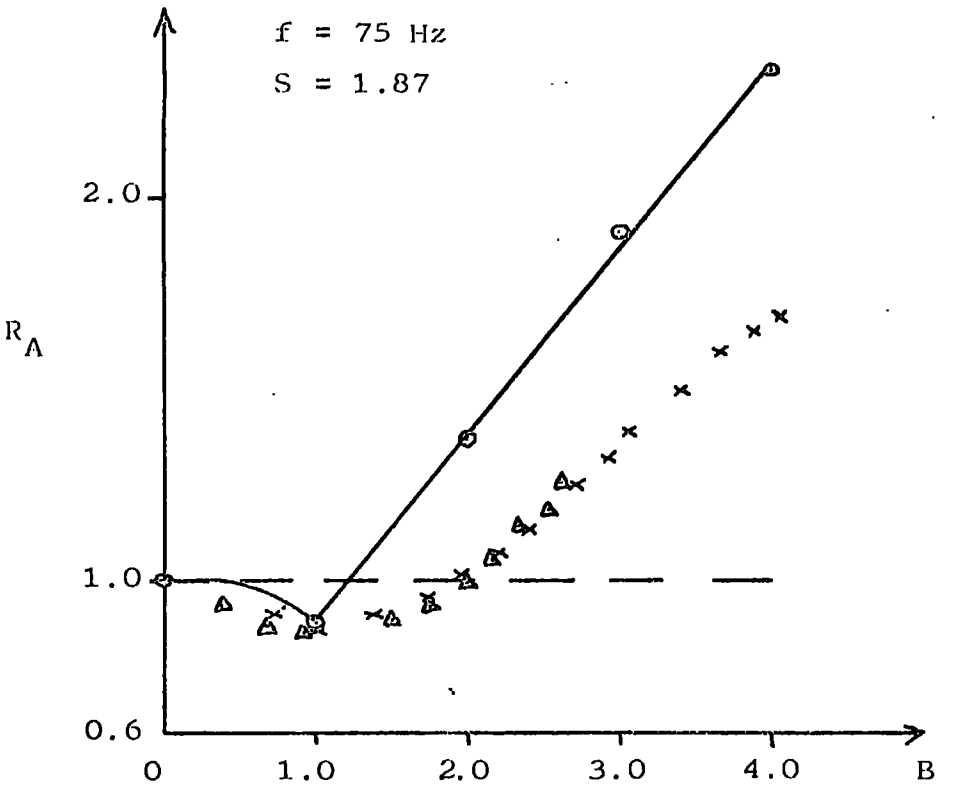
f = 75 Hz
S = 1.87
2.0
1.0
0.6
R_A
0
1.0
2.0
3.0
4.0
B

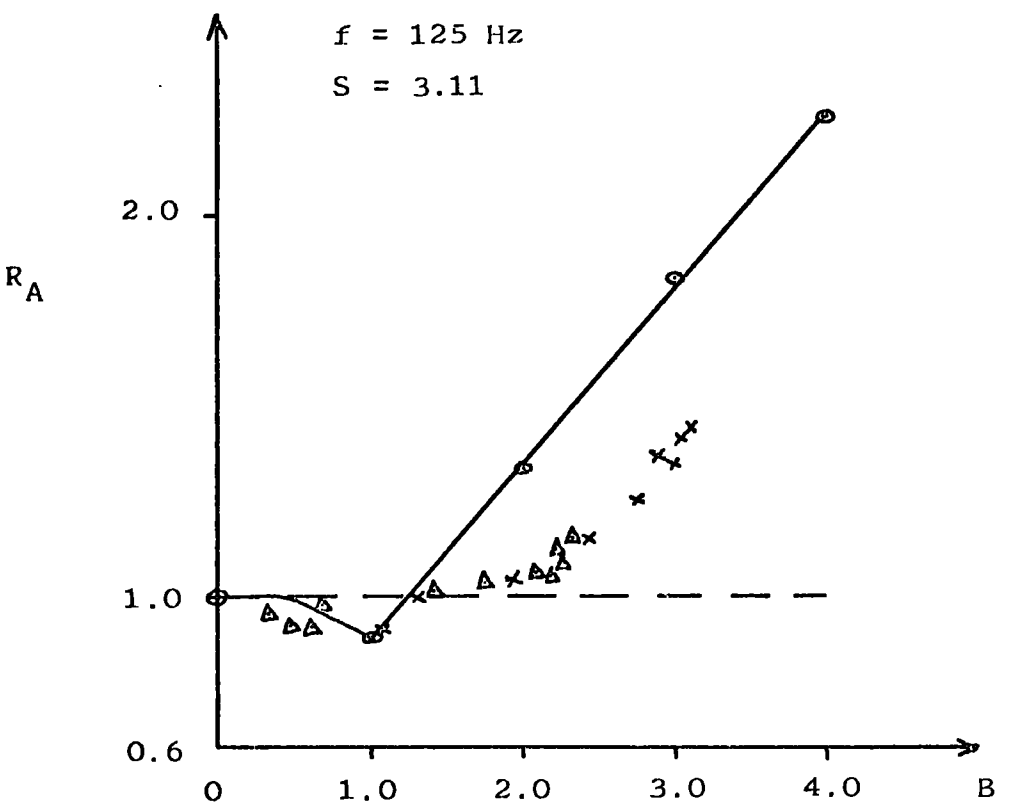
f = 125 Hz
S = 3.11
2.0
1.0
0.6
R_A
0
1.0
2.0
3.0
4.0
B

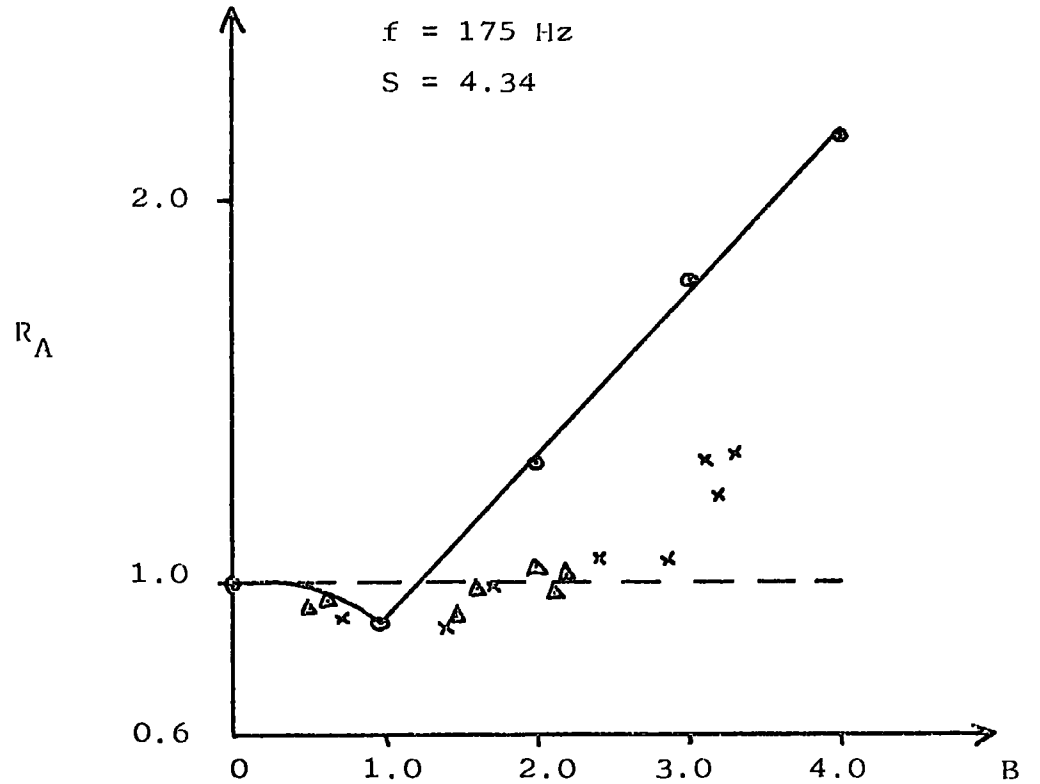
f = 175 Hz
S = 4.34
2.0
1.0
0.6
R_A
0
1.0
2.0
3.0
4.0
B

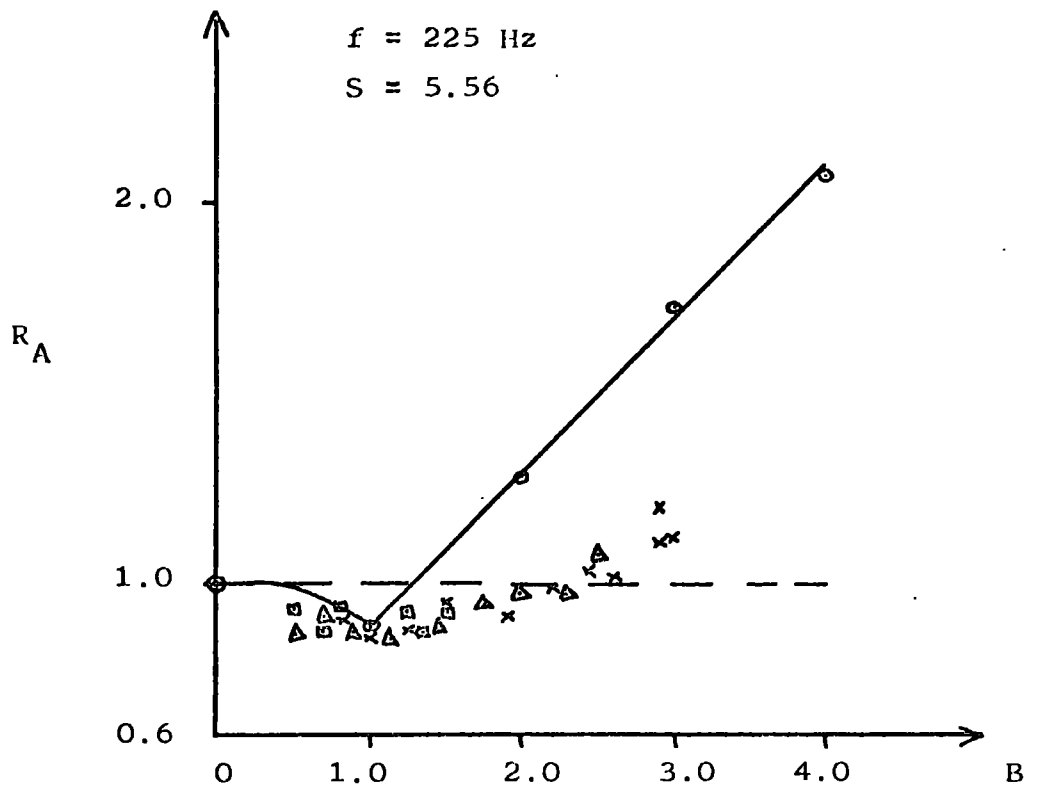
f = 225 Hz
S = 5.56
2.0
1.0
0.6
R_A
0
1.0
2.0
3.0
4.0
B

Mean air flowrate $\overline{\dot{m}}$ = 0.0175 Kg/s

Reynolds number, $\overline{Re}_d$ = 31250
at bulk air temperature 15°C

Frequency -Hz	Strouhal number S
25	0.51
75	1.52
125	2.51
175	3.52
225	4.49

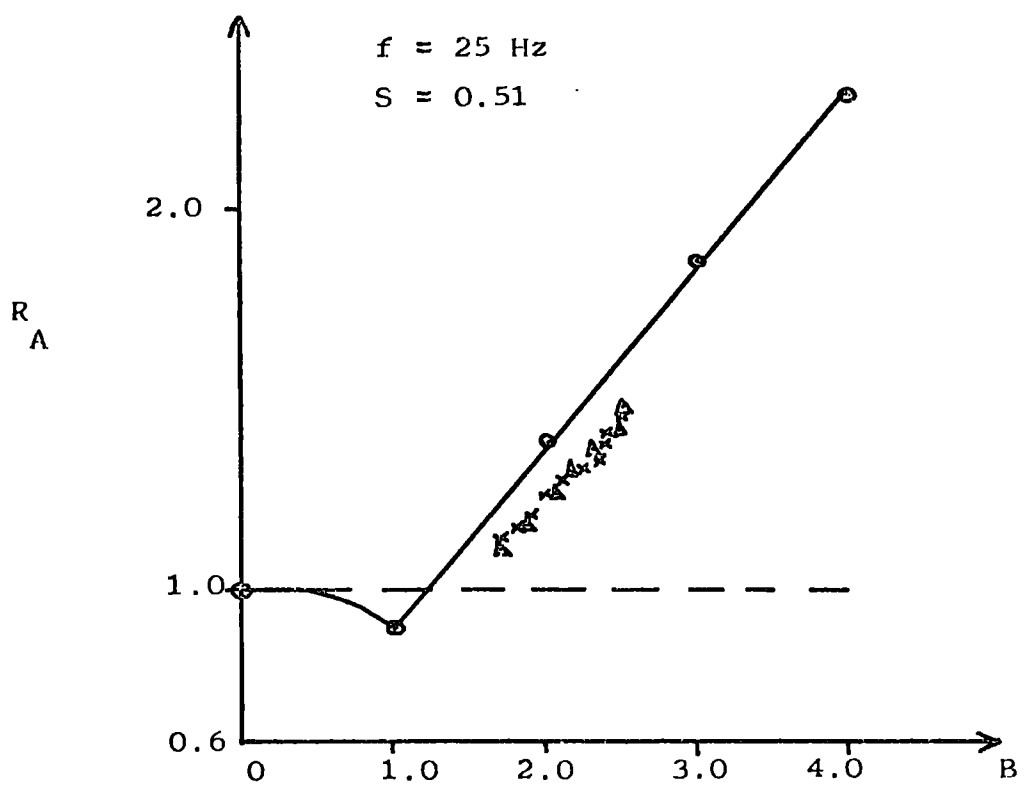

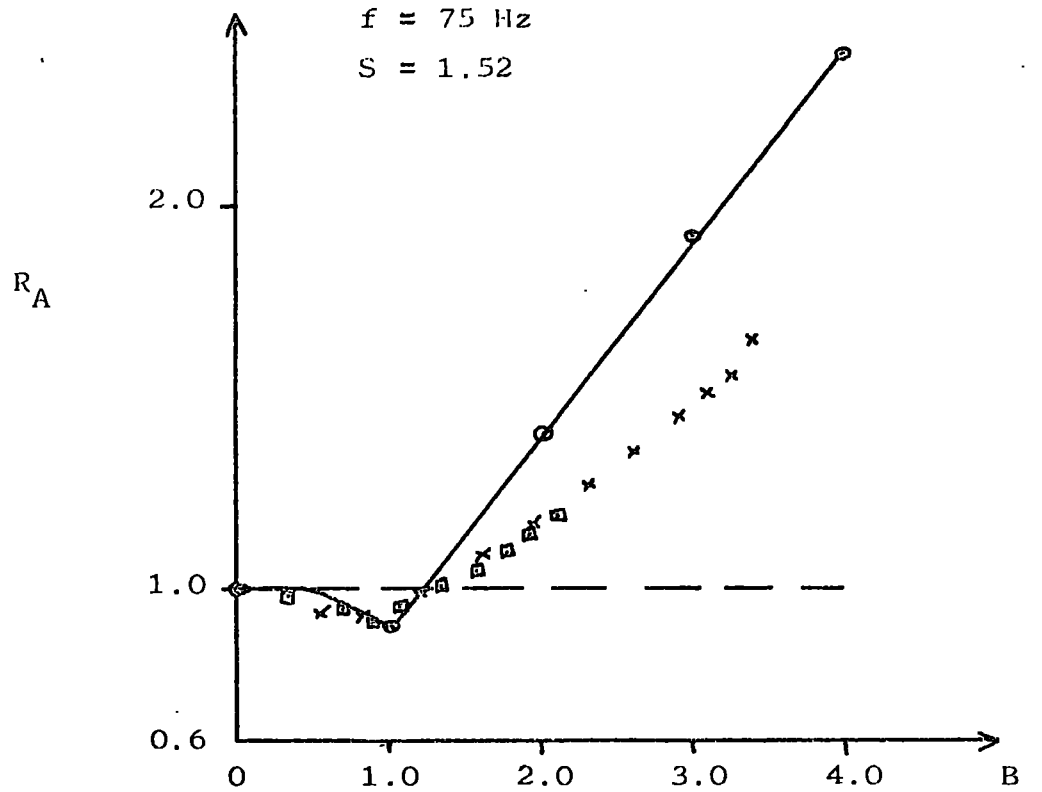
f = 75 Hz
S = 1.52
R_A
2.0
1.0
0.6
0
1.0
2.0
3.0
4.0
B

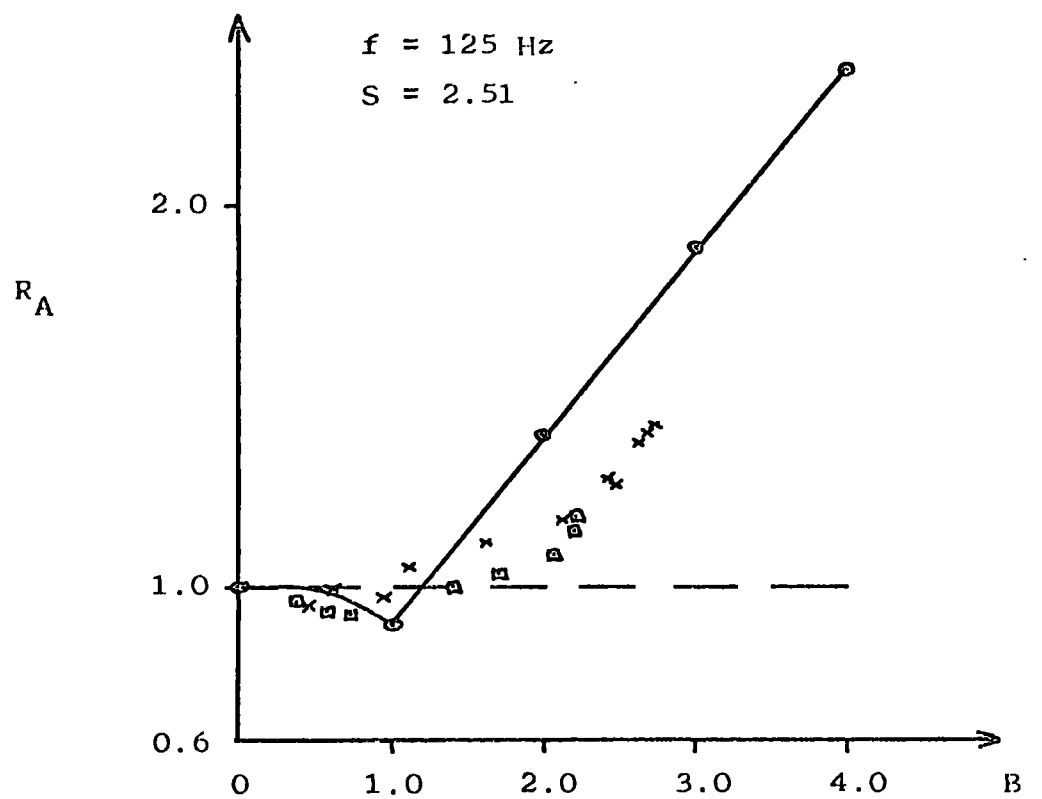
f = 125 Hz
S = 2.51
R_A
2.0
1.0
0.6
0
1.0
2.0
3.0
4.0
B

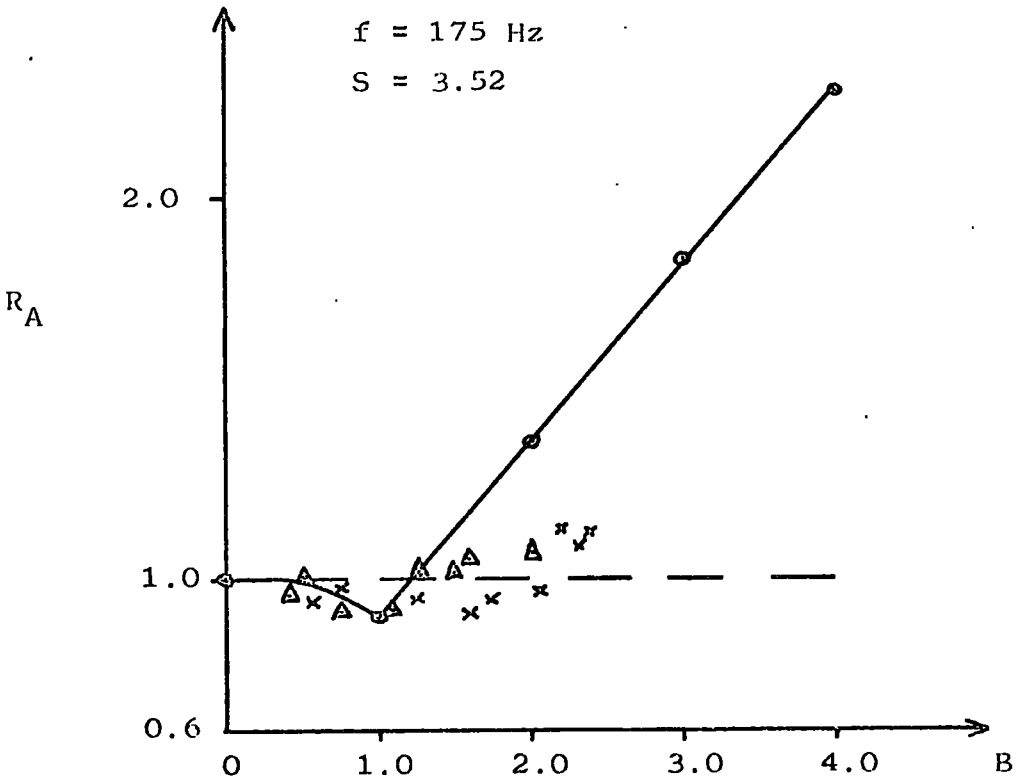
f = 175 Hz
S = 3.52
R_A
2.0
1.0
0.6
0
1.0
2.0
3.0
4.0
B

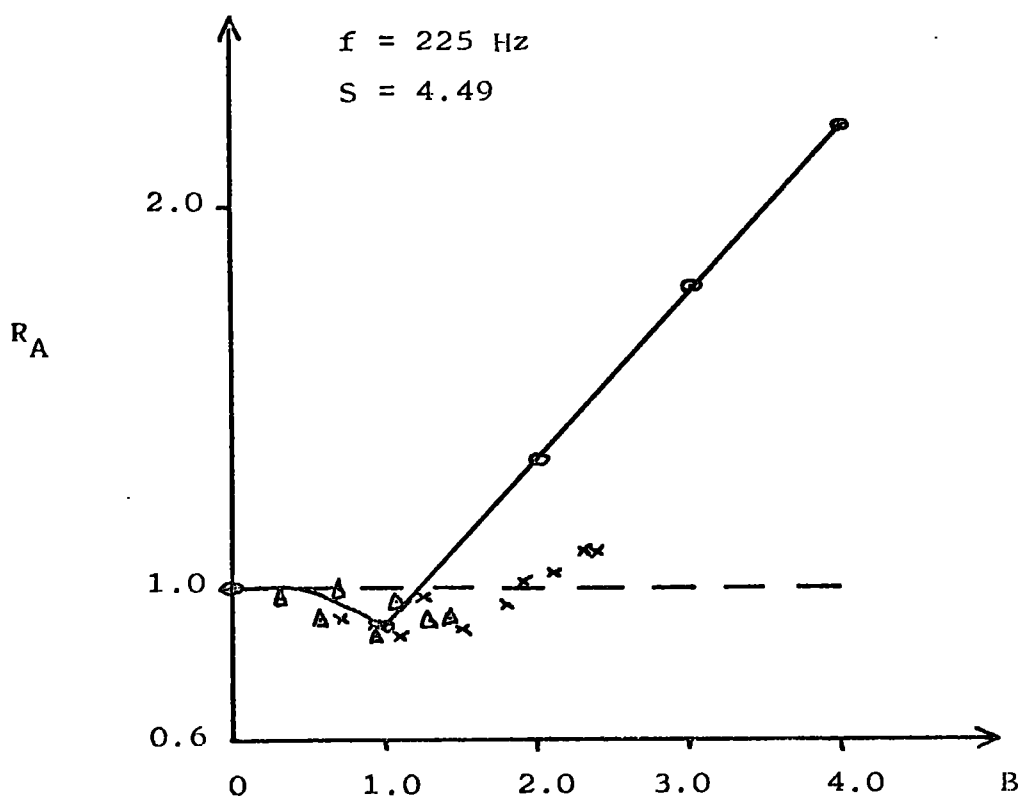
f = 225 Hz
S = 4.49
R_A
2.0
1.0
0.6
0
1.0
2.0
3.0
4.0
B

Bibliography

BIBLIOGRAPHY

1. Effect of sound waves on heat transfer

P.J. Westervelt

Journal of Acoustical Society of America, Vol. 32, No. 3
March 1960, Pg. 337-338

2. On the effect of sound waves on heat transfer

J.P. Holman

Journal of Acoustical Society of America, Vol. 32, 1960
Pg. 407

3. Effect of sound on heat transfer from a horizontal circular cylinder at large wavelengths

B.H. Lee, P.D. Richardson

Journal of Mechanical Eng. Science, Vol. 7, No. 2 1965
Pg. 127-130

4. Local details of influence of a vertical sound field on heat transfer from a circular cylinder

P.D. Richardson

Proceedings 3rd Int. Heat Transfer Conference, Vol. 3, 1966
Pg. 71

5. Critical sound pressures for heat and mass transfer stimulated by acoustic oscillations

Y. Bornov

Soviet Physics - Acoustics, Oct./Dec. 1968, Vol. 14, No. 2
Pg. 155/157

6. Local effects of horizontal and vertical sound field on natural convection from a horizontal cylinder

P.D. Richardson

Journal of Sound and Vibration, Vol. 10, No. 1, July 1969
Pg. 32-42

7. Heat transfer from a vibrating circular cylinder

B.J. Davidson

Int. Journal of Heat and Mass Transfer, Vol. 16, 1973
Pg. 1703-1727

8. Heat transfer from a circular cylinder by acoustic streaming

P.D. Richardson

Journal of Fluid Mechanics, Vol. 30, 1967, Pg. 337-355

9. Effect of transverse vibrations on heat transfer by natural convection from a horizontal plate

T.S. Sarma

Indian Journal of Technology, Vol. 8(12), 1970, Pg. 439-442

10. Heat transfer by free convection from a longitudinally vibrating vertical plate

K.K. Pravad

International Journal of Heat and Mass Transfer, Vol. 15(6) 1972, Pg. 1213-1223

11. Instantaneous measurement of heat transfer from an oscillating wire in free convection

W. Schaetzle

Journal of Heat Transfer - A.S.M.E., Vol. 92, Aug. 1970, Pg. 439-446

12. Vibration effect on convective heat transfer in enclosures

C. Carley

Journal of Heat Transfer - A.S.M.E., Vol. 92, Aug. 1970 Pg. 429-439

13. Effect of vibration on heat transfer from spheres

C. Basi, A. Ramachandran

Journal of Heat Transfer - A.S.M.E., Aug. 1969, Pg. 37

14. Oscillatory viscous flows - review and extension

N. Riley

Journal of Institute of Mathematics, Vol. 3, 1967 Pg. 419-434.

15. Natural convection in a sound field giving large streaming Reynolds number

G. De Vahl Davis, P.D. Richardson

International Journal of Heat and Mass Transfer, Vol. 16 June 1973, Pg. 1245-1265

16. Analogy of heat, mass and momentum transfer to a pulsating flow from an inner tube wall

T. Shirotouka et al

Kagaku Kikai, Vol. 21, 1957, Pg. 638-644

17. Heat transfer to water in turbulent flow in internally heated annuli Part 2 - Pulsating flow

I. Shai, Z. Rotem

A.S.M.E. Preprint, No. 60-HT-21, 1960

18. Heat transfer in turbulent flow in channels under pulsating flow conditions

Z. Rotem

DECH Monograph, Vol. 47, 1962, Pg. 219-231

19. Effect of vibration on heat transfer from a wire to air in parallel flow

R. Anantanarayan, A. Ramachandran

Trans. A.S.M.E., Vol. 80, 1958, Pg. 1426-1432

20. Sonic effect on convective heat and mass transfer rates between air and a transverse cylinder

L. Fussell, C. Tao

Chemical Engineering Progress Series, No. 41, Vol. 59, 1963

21. Influence of sound on heat transfer from a cylinder in cross-flow

R. Fand, P. Cheng

International Journal of Heat and Mass Transfer, Vol. 6 1963, Pg. 571-596

22. Effect of oscillation on instantaneous local heat transfer in forced convection from a cylinder

Y. Mori, S. Tokuda

Proceedings 3rd International Heat Transfer Conf. Vol. 3, 1966, Pg. 49

23. Effect of vibration on heat transfer for flow normal to a cylinder

J. Faircloth, W. Schaetzle

Journal of Heat Transfer - A.S.M.E., Feb. 1969, Pg. 140

24. Vibrations and Pulsations

M.H.I. Baird

British Chemical Engineering, Vol. 11, No. 1, Jan. 1966 Pg. 20-25

25. Flow separation and acoustic effects

H. McManus, E. Soehngen

Trans. A.S.M.E. - Journal of Heat Transfer, Aug. 1960

26. Unsteady boundary layer and heat transfer pheonomena - a literature survey

R. Wick

California Institute Technology, Technical Report 20-279, 1955

27. Vibration - its effect on heat transfer

W. Mason, L. Boelter

Power Plant Engineering, June 1940, Pg. 43

28. An empirical method for calculating heat trasnfer rates in resonating gaseous pipe flow

G. Morell

Jet Propulsion, Dec. 1958, Pg. 829-831

29. Periodic heat transfer at small pressure fluctuations

H. Pfriem

N.A.C.A. TM 1048, 1943

30. Heat transfer for pulsating laminar duct flow

R. Siegel, M. Per mutter

Trans. A.S.M.E. - Journal of Heat Transfer, May 1962, Pg. 111-123

31. Effects of ultrasonic vibrations on heat transfer to liquid by natural convection and by boiling

S. Wong, W. Chon

Chemical Engineering, Vol. 15, No. 2, March 1969, Pg. 281-288

32. Effects of ultrasonics on heat transfer by convection

G. Robinson et al

Ceramic Bulletin, Vol. 37, No. 9, 1958, Pg. 399-404

33. Effect of sonic pulsation on forced convective heat transfer to air and on film condensation of isopropanol

W. Mattewson, J. Smith

Chemical Engineering Symposium Series, 1967, Pg. 173-179

34. A musical heat exchanger

R. Lemlich

Trans. A.S.M.E. - Journal of Heat Transfer, Aug. 1961
Pg. 385-386

35. The effect of periodic shock-fronted pressure waves on instantaneous heat flux rates

R. Goluba, G. Borman

International Journal of Heat and Mass Transfer, Vol. 12
1969, Pg. 1281-1293

36. Effect of vibration on condensation heat transfer to a horizontal tube

J. Dent

Institute of Mechanical Eng. Proc. 1969/70, Vol 184,
Part 1, No. 5

37. Ultrasonics boosts heatless drying

R. Boucher

Chemical Engineering, Sept. 21 1959, Pg. 151-154

38. The influence of flow vibrations on forced convection heat transfer

A.E. Bergles

Trans. A.S.M.E. - Journal of Heat Transfer, Nov. 1964
Pg. 559-560

39. A study of the effect of ultrasonic vibrations on convective heat transfer to liquid

M. Larson

A.S.M.E. Paper No. 62-HT-44, 5th National Heat Transfer
Conference, Houston 1962

40. Influence of ultrasonic vibrations on heat transfer to water flowing in annuli

A. Bergles, P. Newell Jr.

International Journal of Heat and Mass Transfer, Vol. 8
Sept. 1965, Pg. 1273

41. Calculations of heat transfer coefficient for condensation of steam on a vibrating vertical tube

J. Dent

International Journal of Heat and Mass Transfer, Vol. 12
September 1969, Pg. 991-996

42. A survey study of the effect of vibration, sound fields and pulsations on heat and mass transfer from flat plates, cylinders and ducts

M. Rao

U.S.A.F. Aerospace Labs. ARL 65-217, 1965

43. Unsteady convective heat transfer and hydrodynamics in channels

E.K. Kalinin, G.A. Dreister

Advances in Heat Transfer 1970

44. An analysis of convective heat transfer for pulsating flow in a tube

D. Barnett, R. Vachon

Heat Transfer 1970, Vol. 3, Paper FC 3.1

45. Unsteady heat transfer with laminar fluid flow in a cylindrical tube

V.D. Vilensky

Heat Transfer 1970, Vol. 2, Paper CF 4.6

46. Investigation of unsteady convective heat transfer in tubes

Yu. N. Kuznetzov

Heat Transfer 1970, Vol. 2, Paper CF 4.3

47. Effect of sound on separated flows

J.A. Peterka, P. Richardson

Journal of Fluid Mechanics 1969, Vol. 37(2), Pg. 265-287

48. The theory of steady rotational flow generated by a sound field

P.J. Westervelt

Journal of Acoustical Society of America, Vol. 25, 1953

Pg. 60-67

49. On the circulation of air observed in Kundt's tube and some allied acoustical problems

Lord Rayleigh

Philosophical Trans., Royal Society, Vol. 175, Part I 1883

50. The response of laminar skin friction and heat transfer to fluctuations of the stream velocity

M.J. Lighthill

Proceedings of Royal Society, Series A, Vol. 224, No. 1156
June 1954

51. On the circulations caused by the vibration of air in a tube

E.N. da C. Andrade

Proceedings of Royal Society, Series A, Vol. 134, 1932

52. Transition phenomena in oscillating boundary layer flows

J. Millar, A. Fejer

Journal of Fluid Mechanics, Vol. 18, 1974, Pg. 438

53. An unsteady turbulent boundary layer

S. Karlsson

Journal of Fluid Mechanics, Vol. 5, 1959, Pg. 622

54. Effects of a sound wave on the compressible boundary layer on a flat plate

C. Illingworth

Journal of Fluid Mechanics, Vol. 3, 1958, Pg. 471

55. Small amplitude frequency behaviour of fluid lines with turbulent flow

F.T. Brown et al

Journal of Basic Engineering, Dec. 1969, Pg. 678

56. Developments of a periodic flow in a rigid tube

P.J. Florio, W. Mueller

Journal of Basic Engineering, Sept. 1968, Pg. 395

57. Experimental determination of critical Reynolds number for pulsating flow

T. Sarpkaya

Journal of Basic Engineering, Vol. 88, No. 3, Sept. 1966, Pg. 5-9

58. An experimental investigation of pulsating turbulent water flow in a tube

J.H. Gerrard

Journal of Fluid Mechanics, Vol. 46, Part 1, 1971, Pg. 43-64

59. Friction factors in a pulsed turbulent flow

M.H. Baird et al

Canadian Journal of Chemical Engineering, Vol. 49, April 1971 Pg. 220-223

Reference Books

REFERENCE BOOKS

Vibration and Sound
P.M. Morse
McGraw Hill 1948

Fundamentals of Acoustics
L.E. Kinsler, A.R. Frey
Wiley 1962

Vibrations and Waves
R.V. Sharman
Butterworth 1963

Theoretical Acoustics
P.M. Morse, K.U. Ingard
McGraw Hill 1968

Viscous Flow Theory
I. Pai
Van Nostrand 1956

Gas Dynamics
A. Cambel, B.H. Jennings
McGraw Hill 1958

Elements of Compressible Flow
F. Cheers
Wiley 1963

A First Course in Turbulence
H. Tennekas, J.L. Lumley
MIT Press 1972

Mathematical Models of Turbulence
B. Launder, D.B. Spalding
Academic Press 1972

An Introduction to Heat Transfer
A.J. Ede
Pergamon Press 1967

Heat Transfer

F. Holland et al

Heinemann 1970

Heat Transfer

B. Gebhart

McGraw Hill 1971

Fundamentals of Temperature, Pressure and Flow Measurements

R.P. Benedict

Wiley 1969

Measurement of Air Flow

E. Owen, R.C. Pankhurst

Pergamon 1966

Survey of Applicable Mathematics

C. Rektorys

Iliffe 1969

Applied Mathematics for Engineers and Physicists

L.A. Pipes, L.R. Harvill

McGraw Hill 1970